



UFS·UV

UNIVERSITY OF THE FREE STATE
UNIVERSITEIT VAN DIE VRYSTAAT
YUNIVESITHI YA FREISTATA

**STRUCTURAL-STRATIGRAPHIC INVESTIGATION
OF AN AREA NEAR KAKAMAS AND ENVIRONS,
NAMAQUA MOBILE BELT, SOUTH AFRICA**

Hendrik Lukas Marthinus Mathee

Submitted in fulfilment of the requirements for the degree of
Magister Scientiae

In the

Faculty of Science

Department of Geology

University of the Free State, Bloemfontein

Supervisor: Prof. W.P. Colliston

July 2017

Declaration

I, Hendrik Lukas Marthinus Mathee, as a student at the University of the Free State, ID number 9108095329804, declare that this is my own work and that no script with the same content of this script has been submitted for any degree or examination in any other university or tertiary institution. I also declare that all the sources I have used to cite or quote my work have been indicated and acknowledged by making use of complete references.



Marthinus Mathee

04/07/2017
Date

Abstract

The study area is near Kakamas in the Northwest Cape and is located in the tectonostratigraphic Grünau Terrane - an accreted crustal fragment associated with the Mesoproterozoic Namaqua Province. The mapping campaign covered an area of some 6,500 km² comprising of highly deformed and metamorphosed pre-tectonic supracrustals and syntectonic sheet intrusives emplaced and tectonised during the 1.2 to 1 Ga Namaqua Orogeny. The granulite grade Grünau Terrane is juxtaposed against the amphibolite facies Bladgrond Terrane and transported south-westwards along the inter-terrane Hartbees River Thrust (HBRT).

The study area incorporates the north-western section of the Riemvasmaak-Kenhardt Mega Sheath Fold (RK-MS) which contains a series of sheath fold complexes divided into five structural domains. Macroscopic sheath folds have been recognised and documented in the western Namaqua Province for both the ~2Ga Pofadder Terrane and the ~1.6Ga Aggeneys Terrane: this study reports for the first time, the details of large scale sheath fold complexes in the Eastern Namaqua sector. In the Aggeneys Terrane the Aggeneys Mountain consist of a series of stacked sheath folds and Gamsberg Mountain represents a single macroscopic sheath fold formed under a compressive simple shear regime associated with south-west accretion of terranes.

The dominant stratigraphic features are suites of sheeted granitoids interdigitating pre-tectonic supracrustals that consist of metasedimentary and volcanoclastic rocks. The oldest of the supracrustals is the Blouputs Formation with a provenance age of c.1800 Ma. The intrusives are a combination of leucocratic to granodioritic granites and the product of kilometre scale anatexis. Both the supracrustal and intrusive rocks are confined to the five structural domains. The Vaaldrift sheath fold is the only structure (Domain 4) that does not have an inter-sheeted granite associated with the supracrustals. The intrusive rocks has an intrusive age distribution ranging from the oldest, Eendoorn gneiss (1200 Ma) to the youngest, Friersdale charnockite (1080 ±13 Ma).

The sheath fold complexes are bounded by intra-terrane thrusts along which thrust sheets (both supracrustals and granites) are cut out. The boundary of the RK-MS is defined by the Waterval thrust which is the sole thrust to the intra-terrane thrust system. The macroscopic sheath folds which are mapped during this study contains co-linear L-fabrics consisting of meso- and macroscopic fold axes of various fold phases and mineral stretching lineations plunging towards the north-north-east, which indicates a south-south-westerly tectonic transport direction. Three main fabrics are defined during this study, namely: S0 (compositional banding), S1 and the regional S2; both foliations are caused by shear processes and are also recognisable in the sheeted intrusives (e.g. Rooipad, Eendoorn and Harpersputs). The foliation and axial planes of the macroscopic sheath folds have a co-planar relationship and trend north-west. On a mesoscopic scale, two types of folds have been defined as model 1 and model 2 folds, which formed simultaneously during a flow perturbation process. North-west trending shear zones are mapped as the last stage of deformation during which the intra-terrane thrust was reactivated as sub-vertical shear zones.

A progressive shear deformation model is proposed for the structures in the study area. Four deformation phases were recognised with the first of them having two separate sub-phases

(D1a and D1b). The initial phase of the first event (D1a) resulted in the mesoscopic model 1 and model 2 folds during terrane assembly. The main deformation event was the second D1 event (D1b), characterised by macroscopic scale sheath folds (F1) formed during flow perturbation under general shear. The D1(b) event consisted of two phases of sheath folds (F1 and F2), the F2 being localised refolding of the F1 structures during a similar process. The D1(b)F1 structures are characterised by folded S0/S1 with S2 as an axial planar cleavage. Two metamorphic events are recorded by previous authors for the area: the first event was during terrane amalgamation at ~1200Ma and the second event during the last stages of deformation (1018±11 to 1024±14Ma; D4 north-west shear event).

The second deformation phase (D2) is characterised by the intrusion of the Oranjekom Complex (~1100Ma) which is simultaneously deformed into a sheath fold; it defined the end of a progressive shear model which initiated at D1a. The Grünau Terrane underwent two phases of kilometre scale anatectic melting producing two of the most prominent lithological units, namely: Eendoorn gneiss (~1200Ma) and Witwater gneiss (~1123±6).

The third deformation phase (D3) resulted in the intrusion of the Friersdale Charnockite into pre-existing macroscopic D1(b)F1 and F2 sheath fold hinge zones. This emplacement resulted in the D3 folds which are associated with D4 shearing. The D4 shear event caused reactivation of intra-terrane thrusts as sub-vertical shear zones and shears such as the Cnydas, Neusberg and Duiwelsnek shear zones along the limbs of the macroscopic sheath folds. The D4 shear zones trend north-westerly with an associated oblique movement resulting in both a lateral and vertical displacement of strata and structures. The dominant lateral displacement is predominantly sinistral with East-up; the sigmoidal rotation (on km-scale) of F1 axial traces of the macroscopic sheath folds are prominent features of this late shear event.

It is concluded that a dynamic model combining progressive shear deformation during flow perturbation (layer-normal differential and layer-parallel shear) from a mesoscopic to a macroscopic scale resulted in the intricate structures mentioned above.

Table of Contents

1. Introduction	1
1.2 Regional Geology	2
1.3 Previous Work	4
1.4 Problems encountered with previous research methodologies.....	6
1.5 Purpose of this study	6
2. Stratigraphy	9
2.2 Supracrustals	11
2.2.1 Supracrustals of the RK-MS.....	12
2.2.2 Supracrustals – Grünau Terrane.....	34
2.2.3 Supracrustals – Bladgrond Terrane (Driekop Group)	37
2.3 Plutonic Rocks	39
2.3.1 Plutonic Rocks – RK-MS.....	39
2.3.2 Plutonic Rocks – Grünau Terrane	55
2.3.3 Undifferentiated rocks of the Grünau Terrane	63
2.3.4 Plutonic Rocks – Bladgrond Terrane.....	64
2.3.5 Undifferentiated rocks of the Bladgrond Terrane.....	67
3 Structural divisions description	68
3.1 Domain 1: Bladgrond Terrane	69
3.1.1 Stratigraphy	69
3.1.2 Domain boundaries.....	72
3.1.3 Regional Foliation	72
3.1.4 Macroscopic structures	73
3.2 Domain 2: Grünau Terrane	73
3.2.1 Stratigraphy	73
3.2.2 Domain boundaries.....	74
3.2.3 Regional Foliation	76
3.2.4 Regional Lineation	77
3.2.5 Macroscopic Structures	78

3.2.6	Mesoscopic Structures.....	81
3.2.7	Discussion and summary of domain 2: Grünau Terrane	84
3.3	Domain 3: Augrabies Sheath Fold	85
3.3.1	Stratigraphy	85
3.3.2	Domain boundaries.....	86
3.3.3	Regional foliation	89
3.3.4	Regional lineations	90
3.3.5	Macroscopic Structures	91
3.3.6	Mesoscopic Structures.....	97
3.3.7	Summary of Domain 3: Augrabies Sheath Fold	105
3.4	Domain 4: Vaaldrift Sheath Fold	107
3.4.1	Stratigraphy	107
3.4.2	Domain boundaries.....	109
3.4.3	Regional foliation	109
3.4.4	Regional lineation	110
3.4.5	Macroscopic Structures	111
3.4.6	Mesoscopic Structures.....	114
3.4.7	Summary and discussion of Domain 3: Vaaldrift Sheath Fold	117
3.5	Domain 5: Puntsit/ Goede Hoop Domain with special reference to Harpersputs gneiss.....	121
3.5.1	Domain boundaries.....	121
3.5.2	Stratigraphy	123
3.5.3	Regional foliation	123
3.5.4	Regional lineation	124
3.5.5	Macroscopic Structures	125
3.5.6	Mesoscopic Structures.....	128
3.5.7	Strain analysis of the Puntsit/Goede Hoop Domain.....	133
3.5.8	Summary of domain 5: Puntsit/Goede Hoop Domain with special reference to Harpersputs gneiss	133
4	Discussion.....	135

4.1	Comparison of domains	135
4.2	Sheath fold criteria.....	140
4.2.1	Vaaldrift sheath fold is used as an example of listed criteria (section 4.2)	143
4.3	Tectonic Framework of Domains 2 to 5.....	146
4.3.1	D1.....	146
4.3.2	D2.....	147
4.3.3	Terrane stitching.....	148
4.3.4	D3.....	148
4.3.5	D4.....	149
5	Summary and conclusion	151
6	Acknowledgements	153
7	References	154
8	Appendices	163

List of Figures

Figure 1-1: Regional map of the Namaqua Province with a detailed insert of the megastructures in the Grünau Terrane. The locality of the study area is demarcated by the grey square. (Modified from Colliston, et al., 2015). 3

Figure 1-2: Reference map of the previous research in the study area..... 5

Figure 2-1: The stratigraphic nomenclature used during this study is based on Praekelt (1984), Colliston et al. (2015) and Moen (2007). Where a new stratigraphic unit is mapped a relevant geographic name is provided. 10

Figure 2-2: Stratigraphic profile of the study area, the distribution of the lithologies are structurally controlled. The map displays the outline of the supracrustals located between intrusive rocks. Legend is not to scale..... 11

Figure 2-3: Stratigraphic distribution of the Koekoepkop Formation..... 12

Figure 2-4: Type section for the Koekoepkop Formation (station 6, Figure 3) where the lithologies are subdivided into four main units from top to bottom: Upper, Middle, Lower and Basal Units. Numbers on the left side of the stratigraphic profile represent stratigraphic placement of the photographs (1-14). Ruler scale = 15 cm, block scale = 10 cm. Refer to

Appendix A for the geographic coordinates of the type section. 1. Quartz-feldspar-augen biotite-hornblende gneiss (Upper Unit) with randomly orientated mafic clasts on decimetre scale, interpreted as pyroclastic bombs. The regional metamorphic fabric is sub-parallel to the compositional banding (S0) and cross cuts the mafic clasts. 2. 30-100mm thick feldspar-quartz bands (yellow stippled line in the stratigraphic profile) interbanded within the fine banded quartz-feldspar-augen biotite-hornblende gneiss of the Upper Unit. Both contacts are sharp with the lower undulating and upper one planar. 3. Banding in the Middle Unit (feldspathic-quartzite): the decrease in thickness and frequency of banding towards the top defines an upward fining cycle on decametre scale. 4. Sharp undulating contact between a thicker amphibolite layer and quartz-feldspar gneiss within the Basal Unit. 5. 500mm thick leucocratic band with oval shaped quartz-plagioclase clasts on the contact between the Lower and Middle Units. 6. Hornblende gneiss of the Lower Unit displaying discontinuous thin leucocratic bands and quartz-plagioclase clasts. 7. Sharp contact between a thin quartz-eye amphibolite and fine-grained quartz-feldspar gneiss; a highly weathered component of the quartz-feldspar gneiss lies beneath the scale. 8. Laminated feldspathic-quartzite of the Middle Unit containing 20mm thick monomineralic bands of hornblende (blue stippled line in the stratigraphic profile), which are discontinuous throughout the Middle Unit. 9. Medium-banded feldspathic-quartzite of the Middle Unit. 10. A sharp contact between amphibolite and overlying quartz-feldspar gneiss (Basal Unit). 11. Homogeneous feldspathic-quartzite with lenticular leucocratic bands (Basal Unit). 12. Biotite gneiss (Basal Unit) exhibiting a sharp contact with the Eendoorn gneiss (footwall thrust). 13. Quartz-feldspar-augen biotite-hornblende gneiss (Upper Unit) with two distinctive felsic bands (30mm) with interbanded oval shaped lithic clasts (1-10mm). 14. Laminated hornblende gneiss with discontinuous quartz bands (Lower Unit)..... 17

Figure 2-5: Stratigraphic outline of the Omdraai Formation. Refer to Figure 2-6 for detailed stratigraphic profiles at point X (28°36'7.85"S, 20°26'0.57"E), Figure 2-7 for cross sections A-A' (28°34'41.16"S, 20°23'58.02"E) and B-B'(28°37'34.46"S, 20°28'49.45"E) and Figure 2-13 for cross section C-C' (28°47'26.52"S, 20°42'55.35"E)..... 20

Figure 2-6: Stratigraphic profile of the Omdraai Formation at point X (Figure 2-5). The regional profile (A) containing the 6 sequences and two intra-terrane thrusts is not to scale. Stratigraphic profiles B and C are detailed profiles (to scale) of the first sequence and contact zone between the first and second sequence at point X on the map (Figure 2-5)..... 21

Figure 2-7: NE section (A-A', B-B') across the Omdraai Formation, which indicates the stratigraphic and structural relationships between the 6 sequences (refer to section lines on **Figure 2-5**). The Omdraai Formation overlies the Rooipad gneiss (RP) and is separated by the

Kliprug thrust (KRT). The first (#1) and second (#2) sequences cuts out long the Harpersputs thrust (HPT) and forms branch points (BP) in depth. The third (#3) sequence contains a thrust sheet consisting of volcanic rocks (V). The fourth (#4) sequence is an enclosed lithology and forms the core of the Vaaldrift sheath fold. The Harpersputs gneiss (HPG) overlies the Vaaldrift sheath fold. The sixth (#6) sequence forms part of a separate sheath folds which is enveloped within the Harpersputs gneiss. 22

Figure 2-8: First sequence of the Omdraai Formation. A: Agglomerate of the volcanic unit between the first and second sequences. B: Various grain sizes in the quartzites (graded bedding) indicate a fining upward sequence; the fining upwards feature is also indicated by beds varying in thickness (from thick to thin-bedded/laminated)..... 23

Figure 2-9: A: Quartzites of the second sequence. B: 5m thick agglomerate zone within the quartzites of #2; note the mafic clasts representing pyroclastic material..... 24

Figure 2-10: Third sequence of the Omdraai Formation. A: General outcrop of the quartzfeldspar-biotite gneiss. B: The well-banded, quartzites. C: Biotite nodules in the quartzfeldspar-biotite gneiss. D: Upward fining cycle in the quartzites. 25

Figure 2-11: The distribution of the fifth sequence along the Duiwelsnek shear zone. The fifth sequence is interpreted as a thrust sheet..... 26

Figure 2-12: Stacked imbricates of ODF (#6) and Harpersputs gneiss (HPG) along the Harpersputs thrust. 27

Figure 2-13: Cross section (C-C'; Figure 2-5) in the south-eastern portion of the Omdraai Formation where the stratigraphy of the sixth sequence (#6) overlies the rest of the ODF sequences (1-3, 5); the contact is defined by the Harpersputs thrust (HPT). Section line is 1.87km long. 27

Figure 2-14: A: Renosterkop's southern face (photograph looks towards the north). B: Rooipad gneiss (RP) intrudes the Renosterkop Rocks (RR) in a lit-par-lit fashion giving rise to an interbanding between the gneiss and Renosterkop Rocks. 28

Figure 2-15: Stratigraphic distribution of the Goede Hoop Formation. Best visible outcrop is at point X (28°43'51.71"S 20°42'30.13"E) and point, Y (28°26'14.78"S 20°34'2.46"E). Refer to Figure 2-16 for details on point Z..... 29

Figure 2-16: Quartzites of the Goede Hoop Formation. A: Flattened quartz pebbles in a fine grained quartz-muscovite matrix. B: Upward fining cycles in the quartzites (C= coarse-grain, F= fine-grain; point “Z” in Figure 2-15).....	31
Figure 2-17: Stratigraphic distribution of the Puntsit Formation. A north-east cross section (black line) across the Puntsit Formation is shown in Figure 2-18.	31
Figure 2-18: North-east section over the isoclinal Neusberg sheath fold indicating the structural relationship between the Puntsit and Goede Hoop Formations (refer to section line on Figure 2-17) Harpersputs gneiss (HPG) underlies the Goede Hoop (GHF) and Puntsit (PSF) Formations; the contact is defined as the Neusberg shear zone (NSZ), which is a re-activated intra-terrane thrust (see section 3.5.5).	32
Figure 2-19: Puntsit formation. A: boudin of a pyroclastic bomb in the volcanoclastic sequence. B: Low strain zone with preserved angular pyroclastic clasts.	33
Figure 2-20: Stratigraphic distribution of the Blouputs Formation.....	34
Figure 2-21: Blouputs Formation and the relationship with the neighbouring lithologies. A: Witwater gneiss (1123 Ma) intrudes the migmatitic Blouputs Formation (28°47'49.91"S 20°29'13.36"E; same locality for C). B: Metatexites of the Blouputs Formation; the Blouputs Formation (1800 Ma) underwent two stages of anatectic melting (28°29'4.10"S 20°15'26.81"E). C: Lit-par-lit intrusive relationship between the Witwater gneiss and an amphibolite of the Blouputs Formation. D: Large xenolith of Blouputs Formation in the Eendoorn gneiss (1200 Ma; dark lenticular shape body in the centre of the photograph. 28°31'34.13"S 20°11'26.44"E).....	36
Figure 2-22: Stratigraphic distribution of the amphibolite sequence –HBRT.	37
Figure 2-23: Stratigraphic distribution of the Driekop Group.	38
Figure 2-24: Structurally controlled stratigraphic profile of the study area. The map displays the outline and distribution of the plutonic rocks. Profile is not to scale.	39
Figure 2-25: Stratigraphic distribution of the Augrabies gneiss.	40
Figure 2-26: Moonrock; an example of an exfoliation dome in the Augrabies Falls National Park (28°35'51.60"S 20°18'59.86"E)	40
Figure 2-27: Augrabies gneiss. A: Schlieren structures in the gneiss range from millimetres to meter. B: Wavy foliations formed by late shear zones (D4). C: Elliptical shaped fine-grained	

quartz-feldspar-biotite gneiss xenolith (arrow); xenoliths come in a variety of shapes and sizes, with composition mostly of quartz-feldspar-biotite and hornblende. D: Schlieren structures pre-dates the D4 shearing (shear zone indicated by dashed line). 41

Figure 2-28: *Stratigraphic distribution of the Rooipad gneiss*. 43

Figure 2-29: Rooipad gneiss. A: metre scale feldspathic gneiss xenolith in the Rooipad gneiss (flat-lying regional foliation). B/C: Incipient melting of Rooipad gneiss with quartz-feldspar porphyroblasts growing across biotite-amphibole gneiss xenolith. D: lit-par-lit intrusive relationship between the Augrabies gneiss (AUG) and Rooipad gneisses (RP); a tongue of Rooipad gneiss intruded into the Augrabies gneiss, indicating that the Rooipad gneiss is younger than Augrabies gneiss. 45

Figure 2-30: Stratigraphic distribution of the Harpersputs gneiss. 46

Figure 2-31: A: fine-grained quartz-feldspar-biotite gneiss xenolith within Harpersputs gneiss (below the quartz vein- qv), the xenolith is orientated at an angle to the regional foliation, which is transected by the Harpersputs gneiss foliation. B: lenticular shaped xenolith of fine grained quartz-feldspar-biotite gneiss within the foliation of Harpersputs gneiss. Both xenoliths (A and B) are overprinted by the regional foliation in the Harpersputs gneiss. 47

Figure 2-32: Stratigraphic distribution of the Brabees gneiss. 48

Figure 2-33: Brabees gneiss. A: hornblende nodules in the matrix; the nodules are equidimensional and orientated within the regional foliation. B: 100 x 1.5m feldspathic quartzite xenolith in situated within the regional foliation along strike of the Brabees gneiss; the foliation within the xenolith is co-planar with the regional foliation. C: sharp contact between Brabees gneiss (BB; upper) and Rooipad gneiss (RP; lower). 49

Figure 2-34: *Stratigraphic distribution of the Seekoeisteeek gneiss*. 50

Figure 2-35: Seekoeisteeek gneiss. A: migmatitic banding (2mm to 100mm) in Seekoeisteeek gneiss is orientated co-planar to the regional foliation. B: quartzite xenolith in the Seekoeisteeek gneiss. 51

Figure 2-36: Stratigraphic distribution of the Oranjekom Complex. 52

Figure 2-37: Metagabbro of Oranjekom Complex. A: Deformed leucocratic bands in the metagabbro indicates that the Oranjekom Complex underwent a period of anatexic melting. B: quartzite xenolith within the metagabbro. 53

Figure 2-38: Stratigraphic distribution of the Friersdale Charnockite.....	54
Figure 2-39: Stratigraphic distribution of the Eendoorn gneiss.....	56
Figure 2-40: Features of the Eendoorn gneiss. A: General texture illustrated by the regional foliation on the yz plane (looking north –down dip), large (2 – 50mm) megacrysts situated with intermediate axis parallel to the strike of the foliation. The shape of the megacrysts indicates high strain and later shear (sigmoidal shape, dextral shear with top to the east). The foliation is defined by the alignment of biotite and megacrysts. B: The north dipping sharp contact between the Koekoepkop Formation (KKP) and Eendoorn gneiss (ED). The sharp contact is defined as the Waterval Thrust and represents a decollemént. C/D: Sheets of Witwater gneiss intruding the Eendoorn gneiss during the second stage of kilometre scale anatexis melting of the Grünau Terrane (late sub-vertical north-west shear zone). E: Fine-grained quartz-feldspar-biotite gneiss xenolith with a pre-Eendoorn foliation, which is at an angle to the foliation in the Eendoorn gneiss. F: lit-par-lit intrusive relationship between Eendoorn gneiss and the Blouputs Formation (quartz-feldspar-biotite gneiss) with co-planar foliation relationships. ..	58
Figure 2-41: Stratigraphic distribution of the Witwater gneiss.	59
Figure 2-42: Witwater gneiss. A: large veins and melt sheets of Witwater gneiss intruding the Blouputs Formation; the dark patches represents paleosome of Blouputs Formation after the Grünau Terrane melted for the second time forming an anatexis melt (Witwater gneiss). B: A road cutting on the Blouputs Road shows a sheet of Witwater gneiss intruding the Blouputs Formation (biotite-amphibole-garnet gneiss) along the regional foliation with pinch-and-swell structure.....	61
Figure 2-43: Stratigraphic distribution of the Nelshoop gneiss.	61
Figure 2-44: Nelshoop Gneiss with a lenticular shaped feldspathic quartzite xenoliths situated sub-parallel to the regional foliation in the host gneiss.	62
Figure 2-45: Stratigraphic distribution of the undifferentiated gneisses.....	63
Figure 2-46: Undifferentiated augen gneiss of the Grünau Terrane	64
Figure 2-47: <i>Stratigraphic distribution of the Putsies Migmatite Complex.</i>	64
Figure 2-48: Interbanded Metatexites and diatexites in the Putsies Migmatite Complex deformed by late north-west shears (D4).	66
Figure 2-49: Stratigraphic distribution of the Karama'am Augen gneiss.....	66

Figure 3-1: Structural map of domain1: Bladgrond Terrane..... 71

Figure 3-2: Structural map of domain 2: Grünau Terrane. Numbers, 1 to 7, represents D1(b)F1 macroscopic sheath folds in the Grünau Terrane; 1-4 and 7 consist of Nelshoop gneiss, whereas 5 and 6 contains Blouputs Formation. 8a and 8b represent the synforms and antiforms associated with the D4F2 folding..... 75

Figure 3-3: Stereonets representing the regional foliation (S20 in the western and eastern sub-domains (Figure 3-2). A: the regional foliation of the western Grünau Terrane (with late rotation to the north) with a mean foliation orientation of 03246 (n=104). B: eastern part of the Grünau Terrane with a mean foliation of 04046 (n=169). Dots represents the poles to foliation. 76

Figure 3-4: Stereonets of the regional stretching lineations (L1; mineral and augen) for the western and eastern sub-domains of Domain 2 (Figure 3-2). A: The lineations in the western part forms a girdle with point maximum of 00838 (n=38). B In the eastern part form a girdle with point maximum at 01637 (n=63). The girdle distribution of lineations is probably caused by the rotation of the strata by late north-west shear zones (D4). In compensation for late rotation, the lineations for both the western and eastern sub-domains indicates that the tectonic transport direction during ductile thrusting was towards the south-south-west. 78

Figure 3-5: Stereonets of the macroscopic sheath folds (D1(b)F1) for the western sub-domain of Domain 2 (Figure 3-2). A. Nelshoop sheath fold closures; 00544 for sheath fold 3 and 35535 for sheath fold 4. Note that the fold hinges plots within the cluster of mineral stretching lineations. B. Two well exposed closures of the Blouputs Formation sheath fold (sheath fold 5) in the west have fold hinge orientation of 01460 and 01061. The steep plunges of the closures indicates that the sheath fold were deformed by the later transpressional shear system (D4) which rotated the hinges towards the vertical. The fold axes of the sheath folds are co-linear with the stretching lineations and indicate a tectonic transport direction to the south-south-west (compensating for D4 shear rotation. 80

Figure 3-6: Stereonets of the D4F2 folds for the western sub-domain of Domain 2 (Figure 3-2). The synclinal and anticlinal fold axes (respectively 02634 and 02737) are co-linear with the mineral stretching lineations (n=16; poles, poles to S2, n=35)..... 81

Figure 3-7: Mesoscopic structures of the western (A) and eastern sub-domains (B, C) in domain 2 (Figure 3-2). A. A D1(a) intrafolial S-fold in the Eendoorn gneiss with fold axis plunging towards the north-north-west (33634). B. A metre scale sheath fold in the Witwater gneiss on the farm Boesmansrivier. It contains transposed hinges and an axial planar S2

cleavage co-planar to the regional foliation. C. S-c cleavages associated with the dextral sense of D4 shear along the reactivated HRBT; the intersection of C' and S2/S1 indicates that there is an oblique sense of shear with north up. 83

Figure 3-8: map of domain 3 (Augrabies Sheath Fold). Domain 3 is sub-divided into three sub-domains (A-C). The red squares (a-g) are sub-areas of associated folds and are referred to in the text. The inset are a schematic representation of the rotation of the D1(b)F1 axial trace (sigmoidal shape) of the AF-N which suggests kilometre scale sinistral shear during D4. ... 87

Figure 3-9: Thrust model adapted after McClay, 1991 for the Waterval thrust system (Figure 3-8). Koekoepkop thrust sheet (KKP) and the Seekoeisteek thrust sheet (SKS) are two imbricates overlying the footwall Eendoorn gneiss (ED), along the Waterval thrust (sole thrust). The two thrust sheets wedge out along strike (B1 and B2) and in depth (B1* and B2*) at branch points (B) against the sole thrust. The internal thrust separating the thrust sheets is represented by branch lines (BL). The Waterval imbricates are overlain by the Rooipad thrust which forms a roof thrust sheet and is defined by Rooipad gneiss (RP). 89

Figure 3-10: Stereonets showing the sigmoidal rotated distribution of the regional (S2) foliation in Domain 3 (Figure 3-8). A. Western part with a mean S of 05466 (n=196). B. Central part with a mean S of 01533 (n=419), and C: eastern part with a mean S of 06644 (n=473). 90

Figure 3-11: Stereonets showing the distribution of the regional stretching (L1) lineation in Domain 3 (Figure 3-8). A. the western part has a mean mineral stretching lineation of 35037 (n=117). B. The central part is defined by a mean lineation of 01232 (n=180). C. In the eastern part of the domain the mean lineation has an orientation of 06042 (n=189). The girdle at C, is caused by rotation due to dextral shear of the Duiwelsnek shear zone (D4). 91

Figure 3-12: Stereonet presenting the fold axes for the D2F2 folds in sub-areas a-d, that form part of the tight Z-fold of sub-domain A (Figure 3-8). The mean lineations for the area is 01956. A: stereonet of the D4F2 isoclinal closure of sub-area a, the fold axis have an orientation of 00972. B: represents the geometrical data for the antiform in sub-area b with a fold axis orientation of 35138. C. Stereonets representing the orientation of the two synforms in sub-area b (02753) and sub area c (02548), respectively. D. Stereonet indicating the geometrical orientation of the antiformal fold hinge in sub-area d with fold axis orientation of 05660. 92

Figure 3-13: Transposition process of the isoclinal Eendoorn gneiss hinge in sub-area b (Figure 3-8). The original hinge contains a folded S0/S1 foliation with an inner Eendoorn gneiss (ED; core) and an outer Rooipad gneiss (RP). The closure is then transposed by shear zones developing sub-parallel to the axial trace of the original fold. The shears zones displace

the lithologies (S0) and rotates the S1 foliation which causes the transposition and develops a new foliation (axial planar S2 foliation) which are co-planar to S0/S1 along the limbs of the macroscopic isoclinal fold. The displacement causes ED and RP to be placed side by side – creating an apparent lit-par-lit contact relationship. 93

Figure 3-14: Structural map of the Oranjekom Complex sheath fold (OKC). The OKC is defined shape-wise by its closed elliptical lithological traces in the east and “omega” shaped folds in the west; the end isoclinal closure in the west is completely transposed. Geometrically the fold axes are sub-parallel with a mean trend and plunge of 08866. The D1(b)F1 axial trace of the Augrabies gneiss (core of the AF-N) is folded by the D2F1 fold of the Oranjekom Complex. This indicates that within one domain or structure multiple fold phases (ages) can exist and even refold each other. This is the type of effect associated with progressive deformation. 95

Figure 3-15: Stereographic projection of large S-fold (D4F1) on the southern limb of the Augrabies sheath fold (Figure 3-8). Fold axes symbols for the D4F1 folds are: synform (blue triangle), antiform (red dots), parasitic z (green), parasitic s (pink); L1 regional lineations (blue), poles to the regional S2 fabric (black). 96

Figure 3-16: Stereonets presenting the structural features and geometries of the Swartpad and Duiwelsnek closures (sub areas “g” and “f”, respectively; Figure 3-8). The orientation of fold axes for the Swartpad (A) and Duiwelsnek (B) closures are 09533 and 09946, respectively. The easterly plunges of the hinge zones are the result of the D4F2 open fold that is produced by the regional shear events. 97

Figure 3-17: Schematic illustration of the model 1 folds (D1(a)F1) formed by layer-normal shear during the flow perturbation process. The fold axes are co-linear with the stretching lineation or tectonic transport direction (<45° to the flow direction). In this case the transport direction is out of the page (parallel to the co-linear linear fabrics). 98

Figure 3-18: Schematic illustration of the model 2 folds (D1(a)F1') formed by layer-parallel shear during flow perturbation. Fold axes is at a high angle (>45°) to the flow direction/transport direction/ mineral stretching lineations. 99

Figure 3-19: General shear models of flow cells and related layer-parallel and layer-normal shear processes (modified from Alsop and Holdsworth, 1993, 2007). A: Schematic plan view of a flow cell in non-coaxial flow. The grey ellipse represents the flow cell, and the length of the open arrows within in the flow cell indicates the relative flow velocities. In areas “c” and “d” differential sinistral and dextral shear, respectively, are caused by the retardation in flow

(indicated by half, open arrows). Strain ellipsoids are represented by the blue (shortening sector) and yellow (stretching sector) ellipsoids. Areas “c” and d falls within the shortening sectors (blue) of the strain ellipsoid and results in S- (“c”) and Z- fold (“d”) symmetries – the model 1 folds of this study. Z-folds will have a fold axis sub-parallel or clockwise sense of obliquity to the flow direction; S-fold fold axes will be sub-parallel or they will have an anticlockwise sense of obliquity to the flow direction. At area “a” layer-parallel shear will form folds at high angle to the flow direction (model 2 folds), verging in the direction of flow. Area “b” represents an area of elongation and stretching. B: Shear strains associated with layer-parallel shearing develop at the frontal tips (“a” in A) to thrusts and shear zones, resulting in folding at a high angle to transport, i.e. Model 2 folds. The layering (S0) and S1 foliation lie approximately parallel to the base of the cube. C: Differential shear strains associated with layer-normal shearing develop at lateral ramps to thrusts and shears, resulting in asymmetric buckle folds with axes oblique or even sub-parallel to the direction of flow, i.e. Model 1 folds.
 100

Figure 3-20: Mesoscopic structures of Domain 3 relating to the D1(a/b) deformation events. A: A single outcrop containing both model 1 and model 2 folds; the folds formed simultaneously. B. Model 1 S-fold in the Koekoepkop Formation with S2 as an axial planar cleavage. C. Centimetre scale model 2 S-fold also having transposed hinges and an S2 axial planar cleavage. D. Sheath fold in the Koekoepkop Formation, the long axis plunges towards the north-east which is sub-parallel to the regional stretching lineation. The axial plane of the sheath fold is co-planar to the regional S2 foliation (xy-plane of the strain ellipsoid). 102

Figure 3-21: Structural interpretation of D4 shears in the Augrabies gneiss. A shows a 500mm high cross section measured in the Augrabies gneiss, the planes above the section are measured in dip direction and dip. B. The increase in dips of foliation are interpreted to represent sheared fabric between the shear planes. The foliation (S1//S2) with the shallower dips presents the foliation outside of the shear zones, they rotate to the vertical in close proximity of the shear planes. C. The three dimensional block diagram displays the relationship of the north-south shear zones with the north-west south-east shear zones, the latter being the youngest..... 103

Figure 3-22: Mesoscopic structures associated with the D4 late shearing. A. Cross cutting metre scale shear zones in the Augrabies gneiss. Two sets of shears, older (larger) north trending shear zone is cut by a younger (smaller, red) south-east trending shear zone. B and C are associated with the sinistral shearing along the Waterval thrust after when the thrust was reactivated as a shear zone during D4. B. S-c’ cleavages indicates sinistral shearing. C. Mylonitic bands in the Eendoorn gneiss contains boudin structures due to the shearing.

Present in the mylonitic band is the primary S1 fabric which is rotated anticlockwise, indicating sinistral shearing. Elsewhere S1 and S2 is co-planar in the gneiss. The shearing has also rotated the megacrysts. D is an xz plane of the later dextral shearing along the Waterval thrust; it contains boudins and grain tail complexes indicating dextral shear. 105

Figure 3-23: Structural map of domain 4: Vaaldrift Sheath Fold. Domain 4 is sub-divided into a western, central and eastern sub-domains. The western sub-domain contains fold hinges A to D associated with the D1(b)F1 and D1(b)F2 sheath folding events. The area between B, C and D is classified as a culmination zone whereas the central and eastern sub-domains are depression zones. The N-VSF is the northern Vaaldrift sheath fold and contains the sixth sequence of the Omdraai Formation. The S-fabrics in the N-VSF is co-planar to the regional VSF S-fabric and the L-fabrics are co-linear. 108

Figure 3-24: Stereonets of the regional foliation (S2) in the three sub-domains and Northern-Vaaldrift sheath fold (N-VSF) of Domain 4 (Figure 3-23). The poles to the S2 foliation shows a distribution around the great circle for the western and eastern sub-domains; the central approximates a point maximum: the variable distribution of pols are due to late D4 regional shearing effects on mesoscopic folds and limbs. A. Western sub-domain with a mean S of 04530 (n=343). B. The long limb of the VSF (central sub-domain) have an average S2 foliation of 04029 (n=67). C. The eastern sub-domain has a mean S2 foliation of 08242 (n=82), the rotation being the result of the D4F2 open fold. D. For the N-VSF the S2 foliation is generally co-planar to the S2 foliations in the underlying VSF, 04631 (n=102). 110

Figure 3-25: Stereonets showing the distribution of the regional stretching lineation (L1) in the VSF. A. Western VSF with a mean orientation of 02935 (n=68). B. Central VSF with a mean orientation of 03927 (n= 47), C. Eastern VSF with a mean lineation orientation of 03931 (n=23). D. N-VSF with a mean lineation orientation of 03128 (n=92), which is co-linear to the regional lineation in the underlying VSF. 111

Figure 3-26: Combined linear elements (fold axes and stretching lineations) of the Vaaldrift sheath fold (Figure 3-23). Western sub-domain fold axes for closures: D = 05828, C = 04346, B = 09912, north-western core hinge = 03938, south-eastern = 07329. Central sub-domain fold axes: north-western hinge of N-VSF = 01129, D4F2 hinge = 02829. Eastern sub-domain fold axes: A = 03543, B = 04433 and C = 03233 (after Van Bever Donker, 1980). 114

Figure 3-27: Mesoscopic structures associated with Domain 4, Vaaldrift sheath fold (VSF; Figure 3-23). A. centimetre scale model 1 S and Z folds (D1(a)F1) in the quartzites of the Omdraai Formation. The S1 axial traces of model 1 folds are rotated by a centimetre scale

dextral shear zone (D1b) giving rise to a S2 foliation (regional). B. D1(a)F1 sheath fold and model 1 folds in the Omdraai Formation with transposed hinges and axial planar foliation (S1). The x-axis of the sheath fold and the fold axes of the model 1 folds are co-linear. The D1b shear also rotated the axial traces (S1) of the D1(a)F1 model 1 fold. C. Kilometre scale subsidiary shear zone associated with the larger Duiwelsnek shear zone (D4); the interpretation of the sigmoidal rotation of lithologies indicate west up. With sinistral shear. D. A series of metre scale model 1 Z folds with centimetre scale parasitic folds. The hinges of the folds are transposed forming the S1 axial planar cleavage..... 116

Figure 3-28: Synthesis stereographic projection of planar and linear fabrics of Domain 4 (Vaaldrift sheath fold; VSF Figure 3-23). The LS fabrics are deformed by the late D4 regional shear event and are not restored on this data projection. Note the large angle between D1(a)F1 and D1(a)F1' folds (model 1 and model 2, respectively) is still retained (c.f. section 3.3.6). 118

Figure 3-29: Flow diagram illustrating the processes associated with the production of macroscopic D1(b)F1 and F2 folds during regional progressive general shear. 119

Figure 3-30: Model and mechanism for the formation of the Vaaldrift Sheath Fold. A: Flow cell model for the Omdraai Formation overlying the Kliprug thrust which service as detachment. Flow direction is from left to right (tectonic transport direction, open arrows in B, C and D). The section A-A' is illustrated in figure C. B: The main processes involved in the formation of the Vaaldrift Sheath fold are layer-normal shear (LNS) and layer-parallel shear (LPS); a combination of the two shear processes results in double-verging fold. C. The section A-A' represents the yz plane of the first phase of D1(b)F1 regional sheath folds, formed by the process of layer-parallel shear. The core (containing the # four stratigraphic sequence) developed as part of a culmination zone. The VSF at this phase already shows a reversal in fold facing. D. 3D schematic yz profile of the current VSF. Localised layer-normal differential shear (LNS) causes the D1(b)F1 axial trace to be folded by the D1(b)F2 folds resulting in a semi-omega shape structure. The "Z" folds defining the semi-omega has a reversal in fold facing; the semi-omega structure is situated in a culmination zone of the shear regime.... 120

Figure 3-31: Structural map of domain 5 (Puntsit/Goede Hoop Stratigraphic Domain). Domain 5 is sub-divided into a northern Cnydas sub-domain and a southern Neusberg sub-domains. The Cnydas sub-domain contains a series of sheath fold complexes (1-5, Biesje Poort and Rondekop sheath folds). The Neusberg sub-domain contains the Neusberg sheath fold and the Warm Sand structure. 122

Figure 3-32: Stereonet illustrating the orientation of the regional foliation (S2) in the Neusberg sub-domain. The regional foliation is defined by co-planar S1 and S2 (dark greater circle). The mean orientations of the S2 foliation is 04336 (n=240). The penetrative cleavage (S3) that is superimposed across the north-western isoclinal closure of the Neusberg sheath fold have an average orientation of 026026 (grey greater circle) and is associated with the regional D4 shear event. The intersection of 34220 between the regional S2 foliation and the penetrative cleavage indicates oblique shear movement and has a sense of shear similar to Neusberg shear zone (section 3.5.5.1)..... 124

Figure 3-33: Stereonet illustrating the regional stretching lineation (L1) orientation for Neusberg sub-domain; 01031 (n=122). The lineations are defined by mica-fish and long axes of quartz pebbles in the Goede Hoop Formation and by amphibole, sillimanite and quartz-feldspar aggregates in the Puntsit Formation. 125

Figure 3-34: Stereonet presenting the stretching lineation and D2F1 fold axes of the north-western isoclinal closures of Neusberg sheath fold (03826). The two inner closures have hinges that plunges (32° and 44°, respectively) towards 077. The blue dots represents the northern (32329) and southern (10029) fold hinges of the Warm Sand dome structure (D2F1; data from Van Bever Donker, 1980)..... 126

Figure 3-35: Cnydas sub-domain (Figure 3-31). A. Sheath fold 1's north-western and south-eastern D1(b)F1 closures fold axes orientations are 35021 and 01933, respectively. B. The geometries of sheath fold 2: north-western and south-eastern closures has fold axes orientations of 00238 and 35426, respectively. The D1(b)F1 fold axes o 128

Figure 3-36: Mesoscopic structures of the Neusberg sub-domain (Figure 3-31). A. D1(a)F2 intrafolial Z-fold in the Harpersputs gneiss; the fold is defined by folded S1 with S0 as an axial planar cleavage. S1 and S2 are co-planar elsewhere and fold axes co-linear. B. Metre scale model 1 Z-fold (D1(a)F1) which is flattened, steepened and boudined due to the D4 Neusberg shear zone; both S0, S1 and S2 are co-planar, whereas the fold axes and stretching lineations are co-linear. C. S-c cleavages associated with the Neusberg shear zone, indicating an oblique sense of direction with dextral sense of shear and east-up. D. Boudins in the Goede Hoop Formation with long axis plunging in the xy plane indicates an oblique sense of shear for the Neusberg shear zone. E. Cross bedding defined by S0 in the quartzites has a younging direction towards the west which indicates that the quartzites on the eastern limb of the Neusberg sheath fold are overturned. 130

Figure 3-37: Mesoscopic structures in the Cnydas sub-domain (Figure 3-31). A. yz-plane indicating strain partitioning on a metre scale in the Goede Hoop Formation. The highly folded and contorted zones are associated with low strain zones, containing D1(a)F1 folds and S1 axial planar cleavage, separated by zones of high strain where the S-fabrics (S0, S1 and S2) are all co-planar and L-fabrics (L1,-stretching lineations and D1(a)F1 fold axes) co-linear. B. More detail on strain partitioning in A, showing Ramsay Type 3 interference folds. C. Centimetre scale sheath folds are also associated with the low strain zones. D. Intrafolial D1(a) model 1 S-fold in the Puntsit Formation with S1 as axial planar cleavage. 132

Figure 3-38: Hsu diagrams for the Neusberg sub-domain (quartz-pebbles) and the Cnydas sub-domain (gneissic-pebbles). Both areas plotted in the oblate strain sector of the Hsu plot indicating that domain 5 is dominated by flattening strain. Sample locations indicated on Figure 3-31. 133

Figure 4-1: Synthesis stereonet combining the regional S (S0, S1 and S2) and L (macroscopic fold axes and mineral stretching lineations) fabrics across Domains 2 (black; 00838, n= 101), Domain 3 (red; 01132, n= 180), Domain 4 (blue; 03429, n= 122), Domain 5 (green; 01031, n= 122). The dots represents the regional mineral stretching lineations and the lines the regional S2 foliation. The squares represents the macroscopic D1(b)F1 and F2 fold axes orientations (steeper plunges are due to D4 shearing). The effects of the D4F2 fold is eliminated. There is a strong co-planar and co-linear relationship between the S and L fabrics across the 4 domains. 137

Figure 4-2: Modelled shape of a schematic sheath fold (modified after Alsop and Holdsworth (2004b); the front face of the model represents the yz plane of the strain ellipsoid, with the stretching direction, “x” into the plane of the page (8). The shape of the sheath fold is referred to as an omega (Ω) type. The numbers 1-11 (red; see text) represents the sheath fold criteria needed to classify a structure as a sheath fold. 1. Minor S and Z-folds have a reversal in asymmetry across the strike after crossing major fold axial traces. 2. The eyes of the structure are bound by double-vergence geometries. 3. Symmetrical arrangement of lithologies (elliptical shapes). 4. Displacement and tectonic sliding along pre-existing structural discontinuities. 5. Localized reversal in fold obliquity (rotation in horizontal). 6. Large scale sheath folds may be compose of several smaller subsidiary sheath folds. 7. Cannot be displayed on this model. 8. Sheath folds show elongation in the same direction (co-linear x-axis). 9. Sheath folds will have non-continuous axial planes. 10. The core or eye structures are situated in culmination zones. 11. Thickness of the sheath folds limb indicate flow direction and overturned limb. 143

Figure 4-3: Vaaldrift sheath fold as an example for the 10 point sheath fold criteria. Numbers (1-10) relates to the 10 points discussed in the previous section. 1. Minor S and Z-folds displays a reversal in asymmetry along strike of the D1(b)F1 axial trace of the Vaaldrift sheath fold. 2. The core of the VSF contains an elliptically shaped lithological unit with a reversal in facing along strike. 3. Symmetrical arrangement of the first, second, third and fourth stratigraphic sequences. 4. Displacement and tectonic sliding along the Harpersputs (HPT) and Kliprug (KRT) thrusts (tectonic transport to south-west). 5. Localized reversal in fold obliquity of the minor folds. 6. The VSF consist of a single core and then the supplementary northern (N-VSF) co-planar sheath fold. 7. The VSF is a synformal sheath fold, with closure in depth (northwards). 8. All of the subsidiary sheath folds have co-linear long axes parallel to the stretching direction of the regional strain ellipsoid (x-direction) and sub-parallel to the south-south-westerly tectonic transport direction. 9. All of the above mentioned subsidiary sheath folds have non-continuous axial planes that are co-planar to the regional S-fabrics. 10. The elliptical core of the VSF is situated in a culmination zone between doubly verging folds, whereas the long limb represents a depression zone. 11. The north-eastern limb of the VSF is thinner than the south-western limb (length of blue arrows indicates limb thickness). The different thickness indicates that the north-eastern limb is the overturned limb and the VSF closes in depth (synformal sheath fold), refer to the insert for a schematic model from an observer's point of view..... 145

List of Tables

Table 3-1: Structural framework for Domain 2: Grünau Terrane.....	84
Table 3-2: Structural framework for Domain 3: Augrabies sheath fold.	106
Table 3-3: Structural framework for Domain 4: Vaaldrift sheath fold.	119
Table 3-4: Structural framework for Domain 5.....	134
Table 4-1: Comparison of structural features present across the 5 domains (DSZ: Duiwelsnek, CSZ: Cnydas, NSZ: Neusberg shear zones).....	140
Table 4-2: Structural framework for Domain 2 to 5.....	149
Table 4-3: Tectonic Framework of the study area (GT: Grünau Terrane, HBRT: Hartbees River Thrust, WVT: Waterval, NBT: Neusberg, KRT: Kliprug, HPT: Harpersputs thrusts). Ages: a: Colliston et al. (2015); b: Kruger et al. (2000); c: Cornell et al. (2012); d: Diener et al. (2014); e: Bial et al. (2016).....	150

List of Appendices

Appendix A: Geographic coordinates of relative figures.....	163
Appendix B: Topographic map of the study area superimposed on the geological map. Refer to text box (lower left corner) for place names used in the text.....	164
Appendix C: Stratigraphic nomenclature of previous research conducted in the study area	165
Appendix D: Regional study of the Blouputs Formation (BPF).....	166
Appendix E: Regional study of the Eendoorn gneiss (ED).....	167
Appendix F: Regional study of the Witwater gneiss (WW).....	169

List of Abbreviations

Terranes

BdT- Bladgrond Terrane

GT- Grünau Terrane

Structures

HBRT- Hartbees River Thrust

WVT- Waterval thrust

KRT – Kliprug thrust

HPT- Harpersputs thrust

RK-MS- Riemvasmaak-Kenhardt Mega Sheath Fold

AF-N- Augrabies Sheath fold

VSF- Vaaldrift sheath fold

N-VSF- Northern Vaaldrift sheath fold

CSZ- Cnydas shear zone

DSZ- Duiwelsnek shear zone

NSZ- Neusberg shear zone

Stratigraphy

KKP- Koekoepkop Formation

DKG- Driekop Group

ODF- Omdraai Formation (#1 to #6 refers to the six sequences)

RR- Renosterkop Rocks

PSF- Puntsit Formation

GHF- Goede Hoop Formation

BPF- Blouputs Formation
BSF- Bysteeek Formation
WKF- Witklip Formation
SWF- Saamwerk Formation
PMC- Putsies Migmatite complex
NH- Nelshoop gneiss
WW- Witwater gneiss
ED- Eendoorn gneiss
Augrabies gneiss- Augrabies gneiss
SKS- Seekoeisteeek gneiss
BB- Brabees gneiss
RP- Rooipad gneiss
OKC- Oranjekom Complex
HPG- Harpersputs gneiss
FC- Friersdale Charnockite

1. Introduction

The study area is situated within the Grünau Terrane and forms part of the 2820 C map coordinate area (Figure 1-1). The town of Kakamas lies in the centre of the study area, with Keimoes to the east and Augrabies towards the north-west. The area of 6530km², stretches south-east (20° 55'00"E, 29°00'00"S) to north-west (20°00'00"E, 28°20'00"S) of Kakamas. The Augrabies Falls National park covers a large part of the area along the north-western border. The northern border of the study area is the crossover from Namaqua Province aged geology to the Neoproterozoic Nama Group. The north-west trending Orange River surrounded by hectares of vineyards cuts through the centre of the mapped area. Topographically the area can be classified as a moderate mountainous area with high rising peaks forming continuous outcrop; towards the south and south-east the area becomes more flat lying with dominant grasslands and sub-outcrops of gneiss. The highest peak is the Neusberg Mountain at 967m and the lowest point lies within the Orange River valley at 450m above sea level.

The study area is situated in a part of the Grünau Terrane, which is dominated by macroscopic, different size, elliptically shaped structures, which will be defined as sheath fold complexes. The elliptically shaped structures form part of a series of macroscopic stacked structures situated within the Riemvasmaak-Kenhardt Mega Sheath Fold (RK-MS) as defined by Colliston, et al. (2015) and Mathee et al. (2016). The RK-MS has outcrop dimensions of 110 km x 35 km. The sheath folds have a north-westerly trend and plunge towards the north-east. Two tectonostratigraphic terranes form part of the study, namely: Bladgrond Terrane in the south which occupies a quarter (south-west quadrant) of the area with the rest being Grünau Terrane. The Grünau Terrane overthrusts the Bladgrond Terrane during the initial stages of terrane accretion (Colliston, et al., 2015). The region under investigation has a unique stratigraphy comprised of supracrustals and plutonic rocks, and is situated in kilometre scale sheath fold complexes with the RK-MS.

Project statistics:

- Days in the field: 170 field days (excluding weekends and admin/office days)
- Average distance per day: ~10km
- Total distance covered: >1500km
- Study area: 653 000ha / 6 530km²

1.2 Regional Geology

The Mesoproterozoic Namaqua Province (Figure 1-1) is a metamorphic complex on the western flank of the Archaean Kaapvaal Craton (Tankard, et al., 1982; Cornell, et al., 2006); consisting of 8 major tectono-stratigraphic terranes juxtaposed on top of each other during the 1.2-1.0 Ga Namaquan (Grenvillian) Orogeny (Blignault, et al., 1983; Colliston, et al., 2014). The boundary zone between the Namaqua Province and the Kaapvaal Craton is defined as a major north-west-striking linear zone and referred to as the Namaqua Front (Blignault, et al., 1983). The Namaqua Province, Kheiss and Kaapvaal Craton form part of the Kalahari Craton (Jacobs, et al., 2008), which is a concept developed by Hartnady, et al. (1985).

The Complex has been subdivided into an eastern Namaqua Province (Gordonia Subprovince) and a western Namaqua Province (Bushmanland Subprovince; Stowe, et al., 1984, Hartnady, et al., 1985). The Gordonia Subprovince consists of Archaean and Proterozoic rocks characterised by northwest trending bifurcating shear zones deformed against the margins of the Kaapvaal Craton and Kheis Belt (Stowe, 1983). The Bushmanland Subprovince consists of easterly trending Proterozoic lithologies overprinted by the Pan African Orogeny (Gariiep Belt in the west; Blignault, et al., 1983). The Namaqua Province forms part of the Kibaran system of mobile belts and reflects two orogenies at ~1.8-1.6 Ga (Orange River Orogeny correlated with the Eburnian) and 1.2-0.8 Ga (Namaqua Orogeny correlated with the Grenville), with the latter overprinting the older orogeny (Blignault et al., 1983; Joubert, 1986; Stowe, 1983, 1986). Subsequent regional structural and stratigraphic studies have indicated the tectonostratigraphic nature of the Namaqua Province and subsequently the formation of terranes (*sensu* Coney et al., 1980 as “suspect terranes”); and summarised in Thomas et al. (1994); Cornell et al. (2006); Colliston and Schoch (2013); Colliston et al. (2014).

Isotopic ages for many of the supracrustals and intrusives are summarised e.g. in Eglinton (2006) and references therein; Moen and Armstrong (2008); Cornell et al. (2012); Colliston et al. (2015). It has been suggested by Colliston and Schoch (2000, 2002), that the tectonostratigraphic terranes of the Namaqua Province presented major thrust sheets formed during mid-crustal conditions in a sub-horizontal shear regime. The main effects of the sub-horizontal ductile shear at mid-crustal conditions is evident throughout the Namaqua Province in the form of high-grade metamorphism, a thermal event and magmatism giving rise to the universal 1100-1 200 Ma radiometric ages, a penetrative gneissosity and a dominant (east-west striking, gently northerly dipping) LS-tectonite fabric (Colliston, et al., 1991; Colliston & Schoch, 2000; Colliston, et al., 2014; Blignault, et al., 1983). The majority of the terranes were intruded by voluminous sheets of silicic magma during the Namaqua Orogeny; the regional metamorphic zonation (greenschist-amphibolite-granulite/migmatite facies) is ascribed to the

voluminous felsic magmas providing the advective heat transfer for the P-T evolution (e.g. Stowe, 1983; Waters, 1986). The peak metamorphic assemblage equilibrated for the Grünau Terrane (Gordonia Subprovince) at 800-850°C at 4.0-4.5 kbar (Bial, et al., 2016) and for the Aggeneys Terrane (Bushmanland Subprovince) at 650± 20°C and 5±1 kbar (Diener, 2014).

The supracrustal sequences in the terranes of the eastern Namaqua Province are represented by an interbanded clastic-volcanic sequence in the 1.8 Ga Olifantshoek Terrane; interbanded quartzite and schist in the 2.1-1.8 Ga Kaaien Terrane; sequence of amphibolite, metavolcanites, metacarbonates and VMS deposits in the ~1.3 Ga Upington Terrane; the ~1.8 Ga granulite Grünau Terrane is comprised of kinzigites, calc-silicates, mafic gneiss, interbanded with carbonate-rich rocks and pyroclastics (revised lithostratigraphy after Tankard et al., 1982; Moen, 2007; Cornell et al., 2006). Thrusts and sheath folds are characteristic structures that typify the deformation at granulite to amphibolite facies, in the eastern part of the Grenvillian age Namaqua Province (Colliston, et al., 2015; Mathee, et al., 2016).

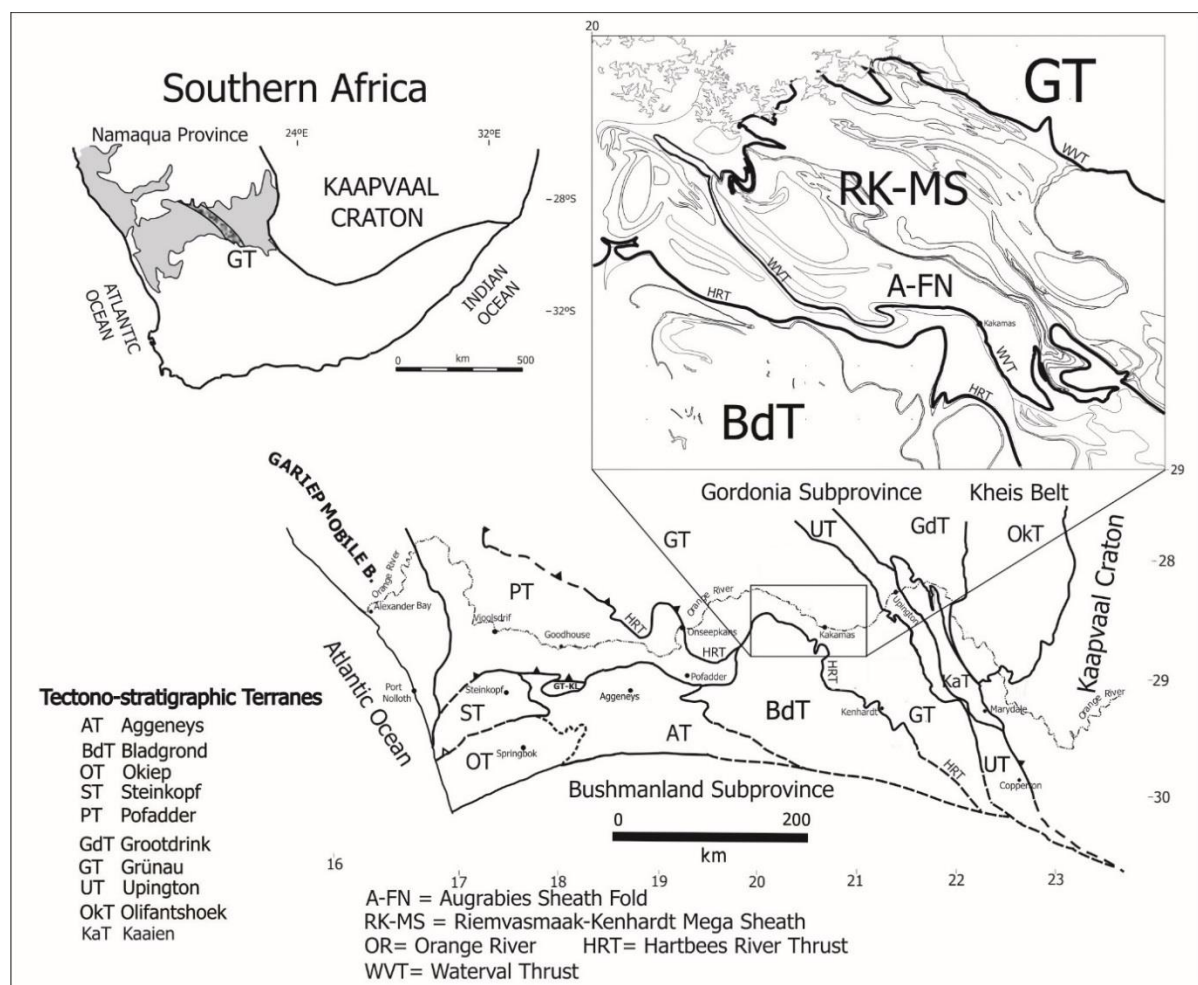


Figure 1-1: Regional map of the Namaqua Province with a detailed insert of the megastructures in the Grünau Terrane. The locality of the study area is demarcated by the grey square. (Modified from Colliston, et al., 2015).

1.3 Previous Work

The past five decades have seen structural, stratigraphic and geochemical studies over the area (Figure 1-2). The first regional map was published by Von Backström (1964) on 1:125 000 scale, who focussed on the area around Keimoes with detailed studies on the Friersdale Charnockite, classified then as the Phacoliths of Charnockitic Adamellites-porphyry. Von Backström (1967) also completed a detailed study on the mineral deposits in the Riemvasmaak area. The northern part of the current study area was mapped in detail by Geringer (1973), who published a 1:100 000 map; the study concentrated on the occurrence and origin of the various granites. The first research that focused primarily on the metamorphism and structures of the area was by Van Bever Donker (1980); the area forms the south-eastern section of the current project. Van Bever Donker (op.cit) published a 1:100 000 map of his study area when he was part of the National Geodynamics Project. His map was incorporated within the 1:250 000 “Upington Geotraverse” map of Stowe (1983).

The 1:100 000 geological map by Praekelt (1984) forms the central and largest part of the current study area; his project primary focus was to provide details on the stratigraphy of the area. It was during this study that the first thrust faults were recognised and described for the Namaqua Province (Praekelt, 1984, Praekelt, et al., 1986). Jankowitz (1986) continued the work by Geringer (op.cit) in the northern part of the current research area, however he focused more on the petrography of the Cnydas Batholith (Grünau Terrane). A 1:250 000 geological map was compiled from previous maps in 1988 by the Council of Geoscience; the sheet description was published later (Moen, 2007).

The regional mapping of the area was then completed and more detailed studies started to become of more importance. A regional study about the crust fragments in the current study area was done by Praekelt, et al., (1986). Saad (1987) did a petrological study on the tin-tungsten deposit at Renosterkop hosted by the Rooipad Gneiss. Geringer, et al., (1990) published the details of the Oranjekom Complex and described it as a layered metamorphosed anorthosite-gabbro suite. This was followed by Havenga (1992) who completed a detailed petrological and geochemical study of the Oranjekom Complex.

During the last decade detailed geochronological and geochemical studies were undertaken by various researchers. Pettersson (2008) did a regional study on the Mesoproterozoic crustal evolution and published isotope analysis on the Rooipad gneiss. Cornell, et al. (2012) focused on the crustal residence and emplacement ages of various granites in the eastern Namaqua Province, with special reference to the Friersdale Charnockite. Colliston, et al. (2015)

published geochronological data of specific granites of the Augrabies Sheath Fold and proposed new insights in the formation of the Mesoproterozoic Namaqua Province.

Sheath folds across the Namaqua Province have been noted and described by a number of researches with most of the work being done in the west (Blignault, et al., 1983; Strydom & Visser, 1986; Colliston, et al., 1991; Colliston & Schoch, 2002; Dewey, et al., 2006; Miller, 2012; Colliston, et al., 2012; Colliston & Schoch, 2013; Colliston, et al., 2015), but smaller sheath folds have also been reported in the east (Coward & Potgieter, 1983). Blignault, et al. (op.cit) and Colliston and Schoch (2002) reported that the long axis of the sheath folds are sub-parallel to the extensional lineations of the specific areas. Colliston and Schoch (1991) explain that the sheath folds in the Aggeneys area of western Namaqua Province formed as the result of rotation due to increasing shear, with the long axes of the sheaths parallel to the transport direction.

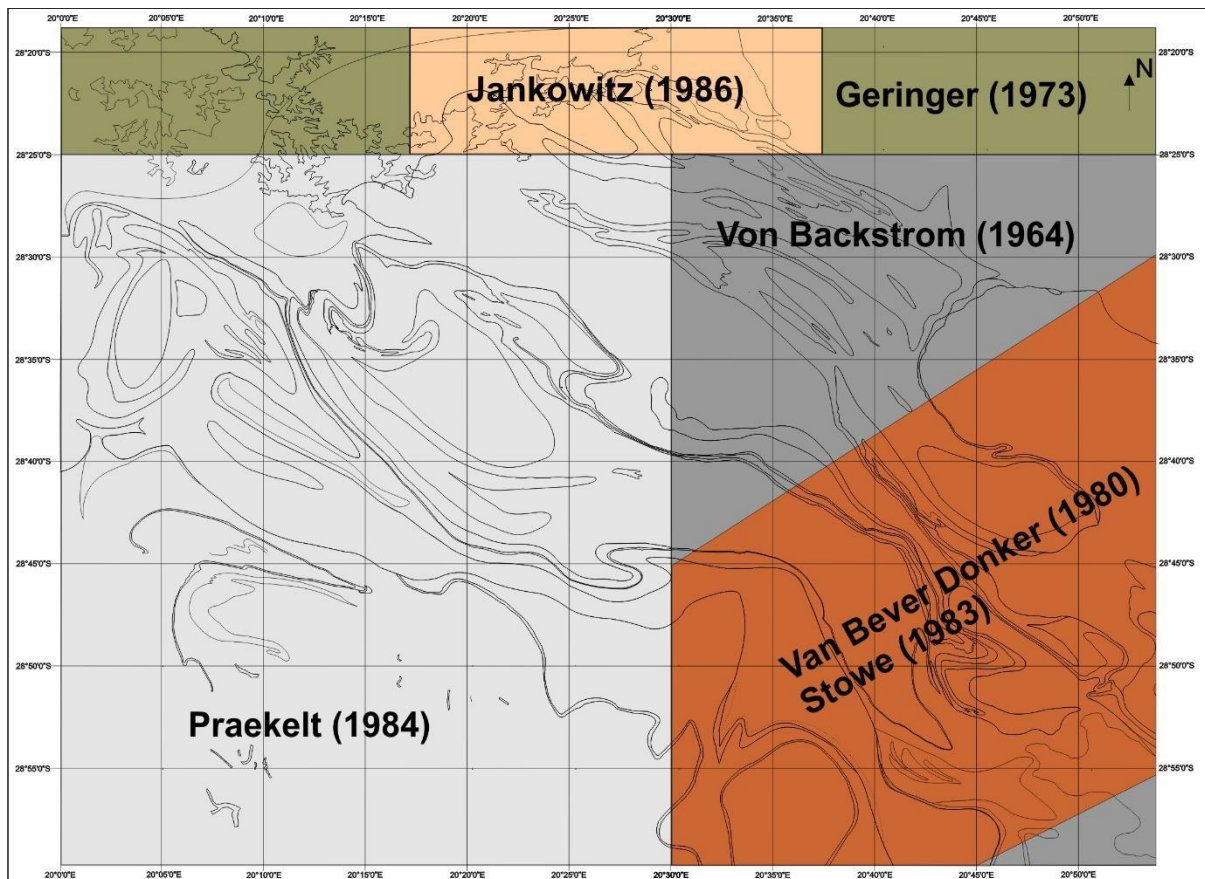


Figure 1-2: Reference map of the previous research in the study area.

1.4 Problems encountered with previous research methodologies

Previously the area was mapped by researchers from different institutions and geological backgrounds, which made correlating the geology between the areas rather difficult. This led to problems such as:

- Mega structures overlapping numerous study areas in the past were never described as complete structures (e.g. the Augrabies sheath fold was never mapped or analysed as a complete structure, as it was split into two research areas).
- Published explanations for the formation and understanding of structures were found to be inadequate due to a lack of understanding of the regional geology.
- Inaccurate structural frameworks due to the limitations of the previous two points.
- Incoherent stratigraphic classifications: this is a function of the different styles of mapping and geological understanding; researchers either “lumped” units together that differed compositionally and structurally or discriminated between origin (rocks subdivided into intrusive, extrusive and sedimentary types) and structure (e.g. the effects of strain on granitoids: a gneiss affected by high strain does not become “another” gneissic unit).

To solve the above mentioned problems, Praekelt's (1984) map and stratigraphy was used as a reference and areas were remapped in order to holistically correlate structures and stratigraphy regionally. The area was mapped on 1:20 000 scale and with the help of ArcGIS (9.3) software a geological map on 1:100 000 scale could be compiled (Map 1). Several types of ductile structures were investigated on various scales which included interference folds, sheath folds, an inter-terrane thrust, intra-terrane thrusts and shear zones. All of the structures being related through the progressive shear deformation process. After the mapping was completed a structural framework and models were proposed for the deformation history in this part of the Grünau Terrane. The Augrabies Falls National Park, farms and town references can be found on the topographic map (Appendix B). The map was constructed using 1:50 000 topographic maps of the study area superimposed on the geological map using ArcGIS 9.3.

1.5 Purpose of this study

The aim of the study was to:

- Contribute towards the understanding of the stratigraphic and structural development of macro to mesoscopic structures within a high grade metamorphic terrane.

- Describe the controls and processes of producing folds in ductile shear zones.
- Correctly identify and describe macroscopic structures.
- Mapping and structural analysis of deformation mechanisms in the severely deformed Grünau Terrane.
- Provide criteria which can be used to define macroscopic sheath folds in deformed metamorphic terrains.
- Establish a detailed structural framework and fold models for the Grünau Terrane.

A table (Table 4-3) illustrating the major conclusions is added here to facilitate ease of reading and correlation of events; it is discussed in detail in section 4.3. (pp. 146).

Table 4-3: Tectonic Framework of the study area (GT: Grünau Terrane, HBRT: Hartbees River Thrust, WVT: Waterval, NBT: Neusberg, KRT: Kliprug, HPT: Harpersputs thrusts). Ages: a: Colliston et al. (2015); b: Kruger et al. (2000); c: Cornell et al. (2012); d: Diener et al. (2014); e: Bial et al. (2016).

Deformation Event	Published event	Age (Ma)	Characteristic	Magmatism (Emplacement)	Metamorphism	Structures	Fabric	Progressive shear
D1(a)	D1	~1200	Terrane amalgamation	1st melting of GT; emplacement of Eendoorn gneiss	^d First: 800-850°C at 4-4,5kbar	Inter-terrane thrust (HBRT), Model 1 and 2 folds		Activation of progressive shear model
D1(b)	D2	1168±6 ^a to 1155±7 ^a	Sheet intrusives D1(b)F1/F2 sheath folds	Emplacement of all the sheet intrusives		Intra-terrane thrust (WVT, NBT, KRT, HPT)	S1= shear fabric S2= regional fabric	Progressive flow perturbation continuing
D2	D3	1155±7 to 1100 ^b	Localised refolding of D1(b) folds together with the 2 nd series of sheath folds.	2nd melting of GT; Witwater gneiss emplaced at 1123±6 Ma. Oranjekom Complex(1100Ma)		D2F1 sheath folds, D2F2 folds		Peak of the progressive shear model
Terrane stitching	The Karama'am Augen gneiss intruded the HBRT at 1107±6 Ma and stitches the Bladgrond and Grünau Terranes together.							
D3	D4	1080 ±13 ^c	Friersdale charnockite	Friersdale charnockite into pre-existing (D1b) fold hinges			Folds all pre-existing S fabrics	Progressive shear model terminated
D4	D5/6	1018 ± 11 ^a to 1024 ± 14 ^a	NW shear zones, D4F1 S-fold, D4F2 open folds		^e Isobaric cooling: 580-660 at 5,8±0,5kbar	Reactivation of thrust (intra and inter), formation of NW-trending sub-vertical shear zones	Deforms all pre-existing structures	Activation of transpressional shear model

2. Stratigraphy

The Namaqua Province in the Kakamas district, consist of two tectono-stratigraphic terranes, namely the Bladgrond and Grünau Terranes (Colliston & Schoch, 2013; Colliston, et al., 2014), separated by the Hartbees River Thrust (Steyn, 1988; Lower Fish River Thrust of Blignault et al., 1983). The distribution of stratigraphy in the terranes is structurally controlled (Figure 2-2). In the Grünau Terrane, the supracrustal and plutonic suites are contained within a mega sheath fold – RK-MS. Other stratigraphic units occur around the RK-MS and define the remainder of various lithological sequences in the Grünau Terrane. As the main study lies within the Grünau Terrane, only a broad discussion of the lithologies in the Bladgrond Terrane near its contact (Hartbees River Thrust; HBRT) with the Grünau Terrane will be given.

The high grade Grünau Terrane is characterized by distinctive supracrustal cordierite-biotite-sillimanite garnet gneiss, calc-silicates, quartzites and schist's; intruded by megacrystic granite gneisses, migmatites with quartz-feldspar-garnet leucosomes and amphibolites (Colliston & Schoch, 2006; Colliston, et al., 2014). The amphibolite grade Bladgrond Terrane consists of a migmatite complex (Putsies migmatites; Kalpakiotis, 2016), quartzites, calcsilicate rocks and meta-arkose intruded by syn-late tectonic granites (Colliston, et al., 2015).

The stratigraphy in the two terranes will be discussed as follows: supracrustal sequences of the Grünau Terrane within the RK-MS (section 2.2.1) and surrounding the RK-MS (section 2.2.2), followed by a short discussion on the supracrustals of the Bladgrond Terrane (section 2.2.3). This is followed by a description of the plutonic rocks in the Grünau and Bladgrond Terranes (sections 2.3.1, 2.3.2 and 2.3.4). In this study a combination of stratigraphic nomenclature from Praekelt (1984), Moen (2007) and Colliston et al. (2015) will be used. Where a new stratigraphic unit is mapped a relevant geographic name is provided. The subdivisions of the pre-tectonic lithologies and plutonites are illustrated in Figure 2-1 and Appendix C.

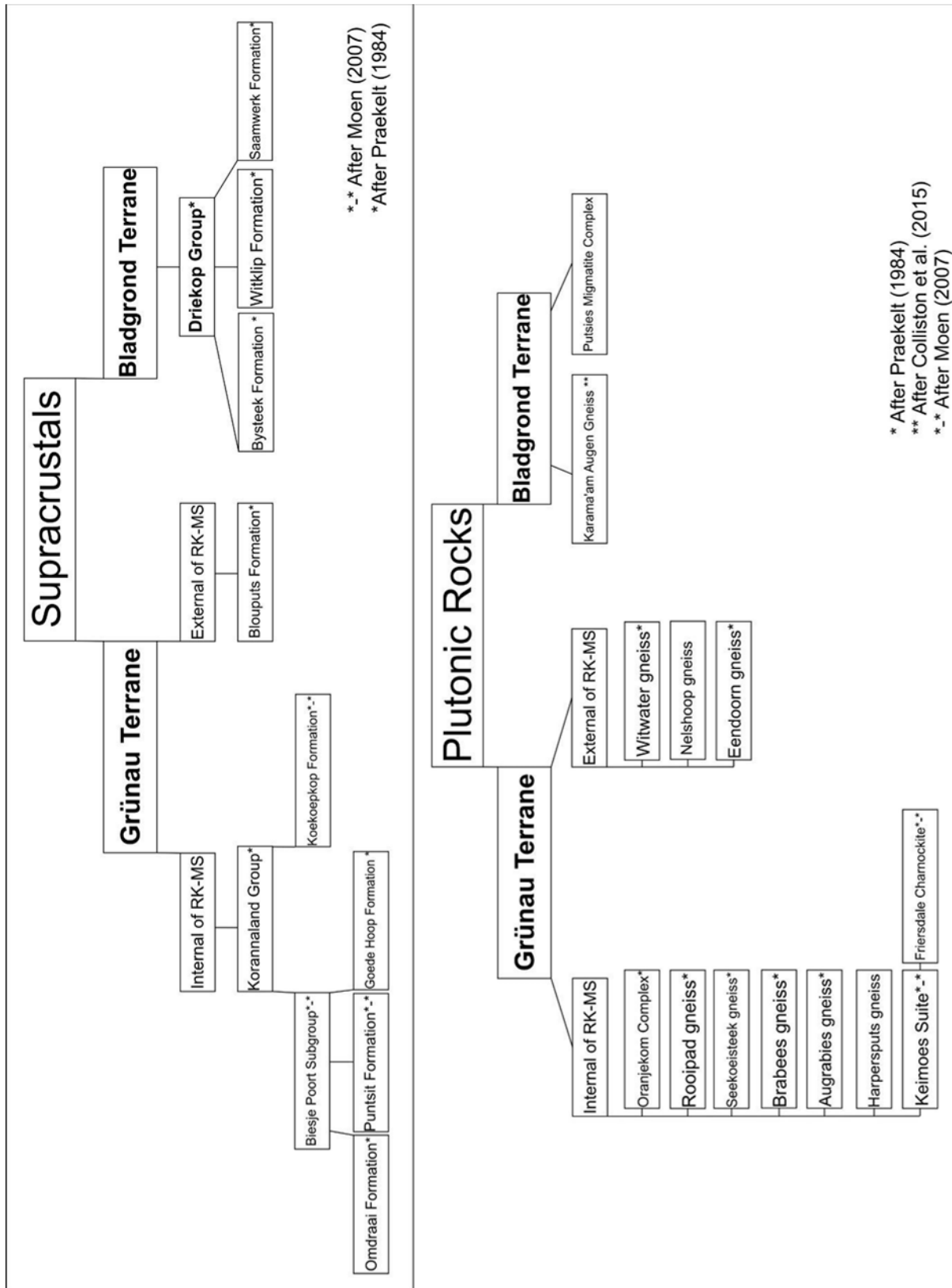


Figure 2-1: The stratigraphic nomenclature used during this study is based on Praekelt (1984), Colliston et al. (2015) and Moen (2007). Where a new stratigraphic unit is mapped a relevant geographic name is provided.

2.2 Supracrustals

The supracrustal formations of the Grünau Terrane consist of the Korannaland Group (supracrustals within the RK-MS) and the Blouputs Formation (Praekelt, 1984; Moen, 2007; Figure 2-1). The Korannaland Group is restricted to the Grünau Terrane and comprises of a variety of metamorphosed psammitic and semipelitic rocks (Moen, 2007). A sub-division of the Korannaland Group is the Biesje Poort Subgroup, consisting of the Omdraai Formation, Goede Hoop Formation and the Puntsit Formation. The Blouputs Formation is associated directly with the Grünau Terrane (Figure 2-1, Figure 2-2). The Bladgrond Terrane consist of the Driekop Group sub-divided into the Saamwerk, Bysteeck and Witlip Formations (Praekelt, 1984; Figure 2-1, Figure 2-2).

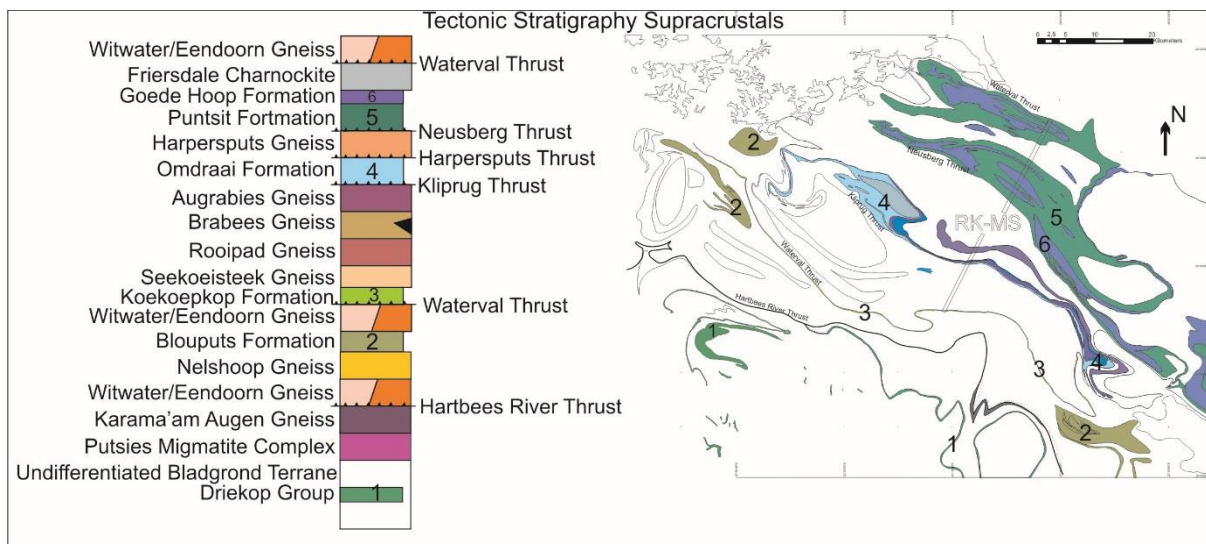


Figure 2-2: Stratigraphic profile of the study area, the distribution of the lithologies are structurally controlled. The map displays the outline of the supracrustals located between intrusive rocks. Legend is not to scale.

2.2.1 Supracrustals of the RK-MS

2.2.1.1 Koekoepkop Formation

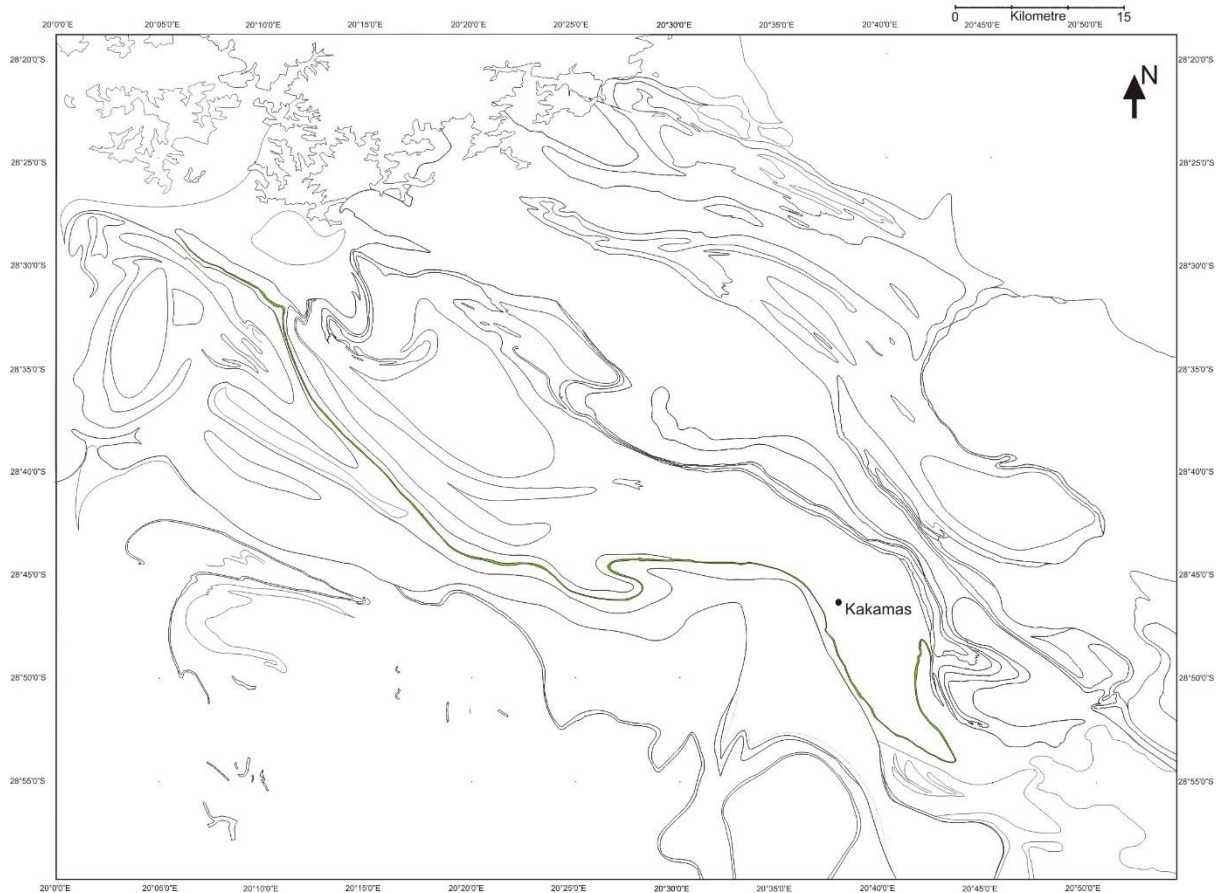


Figure 2-3: Stratigraphic distribution of the Koekoepkop Formation.

The Koekoepkop Formation defines the southern boundary of the Augrabies sheath fold (AFN) and forms the hangingwall sequence of a decollement (Waterval Thrust; Praekelt, 1984) along the highly strained Eendoorn gneiss. The KKP represents a thrust sheet (~25km²) sandwiched between granite-gneiss sheets. The formation has been structurally mapped over a strike-length of 106 km and is stratigraphically divided into four main units (Basal, Lower, Middle, and Upper) of which the Upper and Middle Units could be traced out laterally across the full extent of the thrust sheet. The four units represent an interbanded sequence of mafic and felsic gneisses, and quartzofeldspathic gneisses, with an unduplicated maximum thickness of 57 m.

In the study area the sequence of lithologies has been described as “Marais River Amphibolite” (Van Bever Donker, 1980), “Marais River Formation” (Stowe, 1983; Praekelt, 1984) and “dark-weathering quartz-rich granulite” (Von Backström, 1964); and also as the Koekoepkop Formation (Moen, 2007). During recent regional mapping, it became apparent that the use of the term “Marais River Formation” (e.g. Stowe, 1983, 1986) represents a general nondescript sequence of lithologies (collection of feldspathic quartzites and amphibolites), having

ambiguous regional stratigraphic relationships and positions. Moen (2007) described the lithologies as calc-silicates of the Koekoepkop Formation; however Table 2.10 (data from Praekelt, 1984 in Moen, 2007) indicates no identification of calc-silicate minerals, such as e.g. calcite, diopside, Ca-amphiboles and epidote-group minerals. The modal compositions reflected in the above mentioned table are representative of feldspathic quartzites \pm hornblende/biotite.

It became necessary therefore to find an alternative and more appropriate geographic place-name associated with the distribution of this unique feldspathic quartzite – amphibolite and mafic/quartzofeldspathic gneiss sequence. Moen (2007) renamed the “Marais River Formation” of Praekelt (1984) to represent a new lithological subdivision known as the Koekoepkop Formation (KKP). During this study the latter formation name has been adopted to describe this lithological sequence which is more extensively distributed than in the area mapped by Praekelt (1984). Praekelt (1984) states that the KKP (his Marais River Formation) consists of a prominent sequence of cataclasites consisting of feldspathic-amphibole-quartzites. Extensive structural-stratigraphic mapping leads to the understanding that the KKP is much more complex than what other authors considered it to be.

The units will be described from the footwall thrust (WVT; Eendoorn gneiss décollement) upwards towards the roof thrust (RST; Rooipad gneiss décollement). The basement to the KKP is equivocal and reflects the general problem of identifying basement in the Namaqua Metamorphic Province (Colliston et al., 2012). The units are described according to IUGSSCMR nomenclature (Schmid, et al., 2007) and the lithostratigraphic classification used by the Council of Geoscience in their sheet descriptions of the area (Upington sheet 2820; Moen, 2007).

2.2.1.1.1 Basal Unit

The Basal Unit forms the lowermost sequence to the KKP and can be sub-divided into lower, middle and upper sub-units - all with diagnostic members (Figure 2-4). The thickness variation observed laterally in the sub-units is ascribed to wedging, where large percentages of lithologies are cut out along strike of the Waterval Thrust. The lower and middle sub-units are the most persistent along strike.

2.2.1.1.1.1 Lower sub-unit

The sub-unit consists of a 5 m thick fine to medium-grained banded biotite gneiss and has a sharp upper contact with the lower amphibolite member of the middle sub-unit. The biotite gneiss mainly consists of biotite, quartz and feldspar (Figure 2-4; photograph 12). Three types

of banding are apparent in the biotite gneiss: the first type is defined by biotite-feldspar laminae, the second by discontinuous nonparallel leucocratic feldspar-quartz bands on 5 to 10 mm scale, which gives the gneiss a thinly banded to thickly laminated appearance: the third by discontinuous stretched quartz-feldspar clasts. The flattened clasts with anastomosing biotite laminae, range in size from a few millimetres to 15 mm; the long axes are obliquely aligned within the foliation plane. In lower strain zones the clasts have a well-defined semi-elliptical shape.

2.2.1.1.1.2 Middle sub-unit

The middle sub-unit is 5 m thick and is characterised by the interbanding of five members namely, three amphibolite and two quartz-feldspar gneiss lithologies. The upper and lower contacts of all these members are sharp-undulating (Figure 2-4, photograph 7, 4). The lowermost and uppermost amphibolite members are 500 mm and 200 mm thick respectively and both are thinly banded having a discontinuous, wavy and parallel shape. The bands consist of alternating hornblende-feldspar-quartz and feldspar-quartz laminae; they also contain oval shaped feldspar-quartz aggregates (“quartz-eyes”; 1-5 mm in diameter).

The middle amphibolite member (1 m thick) has a higher proportion of leucocratic minerals and is also distinguished from the upper and lower amphibolite members by a lighter colour. It has a well-developed mafic banding defined by fine-grained hornblende laminae in a fine-grained mesocratic matrix of hornblende-feldspar-quartz (Figure 2-4; photograph 4, 10). These bands are continuous, even and parallel of nature and never exceed 5 mm in thickness. The upper contact with the quartz-feldspar gneiss member is separated by a 3 cm thick amphibolite band. Oval to lenticular shaped mafic clasts having a variable size range (always less than 50 mm), are scattered throughout the amphibolite member.

The interbanded quartz-feldspar gneiss members have thicknesses of 3 m and 1 m respectively (Figure 2-4; photograph 7). The members consist mainly of quartz and feldspar and small amounts of biotite. Thin coarser-grained leucocratic bands of quartz and feldspar (10-30 mm) alternate with laminae of biotite in a fine-grained leucocratic matrix with scattered biotite; both the banding and laminae are discontinuous, wavy, and parallel.

2.2.1.1.1.3 Upper sub-unit

A 5 m thick, homogeneous thick-banded feldspathic-quartzite defines the top of the Basal Unit and contains alternating thin (10-30 mm), fine-grained quartz-plagioclase bands and mesocratic bands (Figure 2-4; photograph 11). The banding can be described as uneven, non-parallel and discontinuous. The basal contact with the upper quartz-eye amphibolite

member of the middle sub-unit as well as the upper contact with the hornblende gneiss (Lower Unit) is sharp. The feldspathic-quartzite has a massive textural appearance notwithstanding its banded nature. An interbanded amphibolite (300 mm thick) occurs 300 mm from the basal contact with the middle sub-unit.

2.2.1.1.2 Lower Unit

The Lower Unit is a 7 m thick hornblende gneiss having a sharp upper contact with the Middle Unit and consist of pyroxene, biotite, hornblende feldspar and quartz (Figure 2-4; photograph 14). Compositional banding is defined by quartz-feldspar and quartz-feldspar-amphibole dominated layers. They occur as laminates to thin bands, discontinuous (wavy and nonparallel) on meter scale within a matrix of hornblende-biotite-quartz-K-feldspar-plagioclase. Another type of banding is defined by flattened quartz-feldspar clasts that are discontinuous on centimetre scale (Figure 2-4; photograph 6).

The sharp contact between the Lower and Middle Unit is defined by a fine-grained thick to thinly laminated leucocratic layer (~500 mm thick) (Figure 2-4; photograph 5). The layer consists of alternating laminae of quartz and feldspar. Oval shaped quartz-feldspar porphyroblasts (5-20 mm) are scattered throughout. This basal lithology is only apparent in the type section; elsewhere the contact between the Lower and Middle Units remains sharp.

2.2.1.1.3 Middle Unit

The Middle Unit is a 12 m thick, fine-grained, well-banded quartzite and consists of quartz-feldspar-biotite-amphibole with accessory garnet (Figure 2-4; photographs 3, 9). The unit has a characteristic composite banding of quartz-plagioclase rich bands alternating with biotite-amphibole-plagioclase bands. Three zones are defined on the basis of compositional banding and its variable thickness: thick (>300 mm), medium (30-300 mm) and thin-banded (10-30 mm) to laminate (<10 mm). The compositional banding in any one zone is defined by the systematic alternation of dark (more mesocratic) and light (more leucocratic) bands; band thickness changes proportionally towards the Upper Unit (Figure 2-4; photograph 3). This change in band thickness from 300 mm to <10 mm occurs over a vertical distance of 9 m and indicates one macroscopic upwards fining cycle containing two mesoscopic upward fining sequences of 7,5 m and 2,5 m respectively (Figure 2-4). Some of the characteristic features of the Middle Unit are: monomineralic bands of amphibole up to 20 mm in thickness (discontinuous and randomly spread throughout the lithologies; Figure 2-4; photograph 8); mixed oval clasts of mafic (hornblende) and felsic composition of random distribution; the mafic clasts vary in size from 15 - 5 mm with felsic clasts less than 5 mm.

A “brecciated” mafic lens (2000 x 300 mm) is situated within the contact zone between the medium and thin-banded feldspathic-quartzite. The zone consists of coarse amphibole, quartz and epidote, and is boudinaged, and discontinuous along strike.

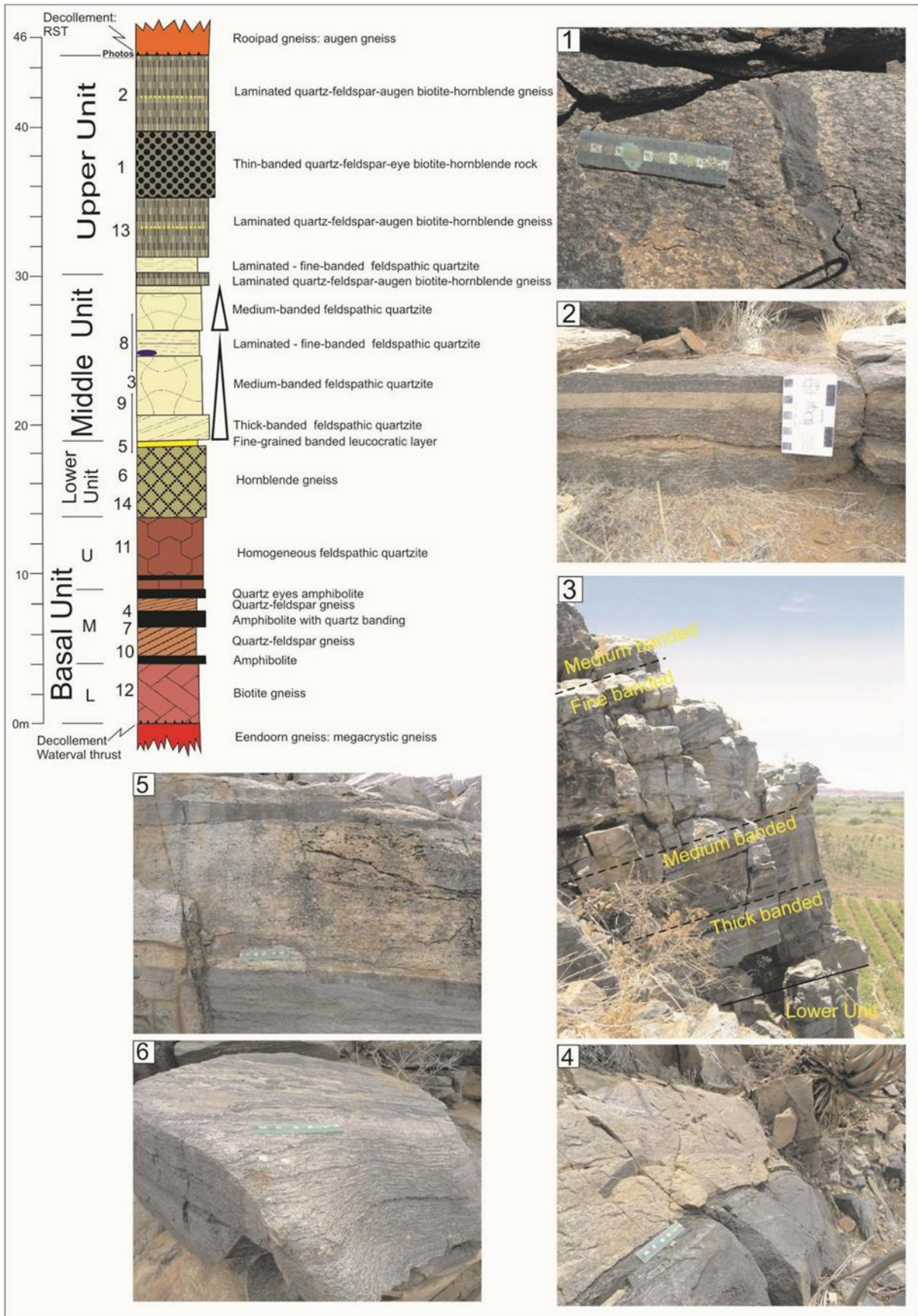
2.2.1.1.4 Upper Unit

The laminated to banded feldspathic-quartzite of the Middle Unit forms a 3 m wide interbanded contact with the mafic gneiss of the Upper Unit. The Upper Unit of the KKP has a maximum thickness of 15 m and is defined as a biotite-hornblende augen gneiss (augen composed of aggregates of quartz and feldspar) and is sub-divided into three lithological members namely, a lower laminated, a middle thin banded and an upper laminated (Figure 2-4; photograph 13). The contact between all the members is sharp. All members contain laminations that are discontinuous, wavy and parallel; they are 1-3 mm thick and consist of quartz and feldspar in a fine-grained matrix of biotite-amphibole-quartz-K-feldspar-plagioclase. A second type of banding consists of hornblende-biotite laminae that are lenticular over a few centimetres.

All three members contain medium-banded (20-100 mm) felsic layers that are continuous on decametre scale. The layers are defined by very fine-grained quartz and feldspar with scattered flattened oval clasts (Figure 2-4; photograph 13, 2). The flattened oval shaped quartz-feldspar augens (lithic clasts) range from 1 mm to 5 mm in size in all members and are distributed throughout the matrix as well as the leucocratic banding. Fine-grained mafic clasts (10-200 mm) of hornblende and biotite occur sporadically throughout the Upper Unit (Figure 2-4; photograph 1). The mafic clasts are often rounded or elliptically shaped but larger clasts with angular shapes also occur. The lower contact of the felsic layer with the host rock is undulating and sharp; the upper contact is planar and sharp.

Figure 2-4: Type section for the Koekoepkop Formation (station 6, Figure 3) where the lithologies are subdivided into four main units from top to bottom: Upper, Middle, Lower and Basal Units. Numbers on the left side of the stratigraphic profile represent stratigraphic placement of the photographs (1-14). Ruler scale = 15 cm, block scale = 10 cm. Refer to Appendix A for the geographic coordinates of the type section.

1. Quartz-feldspar-augen biotite-hornblende gneiss (Upper Unit) with randomly orientated mafic clasts on decimetre scale, interpreted as pyroclastic bombs. The regional metamorphic fabric is sub-parallel to the compositional banding (S0) and cross cuts the mafic clasts.
2. 30-100mm thick feldspar-quartz bands (yellow stippled line in the stratigraphic profile) interbanded within the fine banded quartz-feldspar-augen biotite-hornblende gneiss of the Upper Unit. Both contacts are sharp with the lower undulating and upper one planar.
3. Banding in the Middle Unit (feldspathic-quartzite): the decrease in thickness and frequency of banding towards the top defines an upward fining cycle on decametre scale.
4. Sharp undulating contact between a thicker amphibolite layer and quartz-feldspar gneiss within the Basal Unit.
5. 500mm thick leucocratic band with oval shaped quartz-plagioclase clasts on the contact between the Lower and Middle Units.
6. Hornblende gneiss of the Lower Unit displaying discontinuous thin leucocratic bands and quartz-plagioclase clasts.
7. Sharp contact between a thin quartz-eye amphibolite and fine-grained quartz-feldspar gneiss; a highly weathered component of the quartz-feldspar gneiss lies beneath the scale.
8. Laminated feldspathic-quartzite of the Middle Unit containing 20mm thick monomineralic bands of hornblende (blue stippled line in the stratigraphic profile), which are discontinuous throughout the Middle Unit.
9. Medium-banded feldspathic-quartzite of the Middle Unit.
10. A sharp contact between amphibolite and overlying quartz-feldspar gneiss (Basal Unit).
11. Homogeneous feldspathic-quartzite with lenticular leucocratic bands (Basal Unit).
12. Biotite gneiss (Basal Unit) exhibiting a sharp contact with the Eendoorn gneiss (footwall thrust).
13. Quartz-feldspar-augen biotite-hornblende gneiss (Upper Unit) with two distinctive felsic bands (30mm) with interbanded oval shaped lithic clasts (1-10mm).
14. Laminated hornblende gneiss with discontinuous quartz bands (Lower Unit).





2.2.1.2 Omdraai Formation

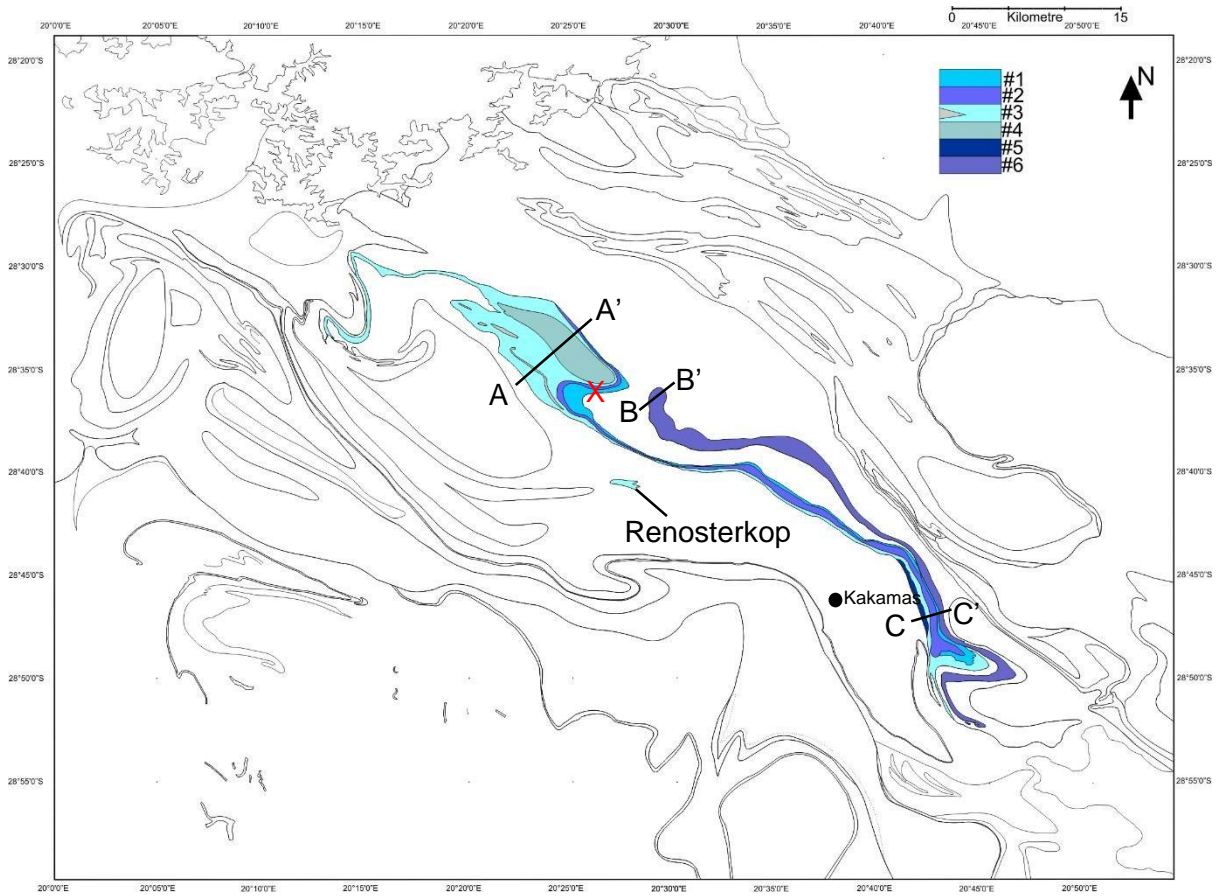


Figure 2-5: Stratigraphic outline of the Omdraai Formation. Refer to Figure 2-6 for detailed stratigraphic profiles at point X (28°36'7.85"S, 20°26'0.57"E), Figure 2-7 for cross sections A-A' (28°34'41.16"S, 20°23'58.02"E) and B-B' (28°37'34.46"S, 20°28'49.45"E) and Figure 2-13 for cross section C-C' (28°47'26.52"S, 20°42'55.35"E).

The Omdraai Formation is a series of metamorphosed and deformed volcano-sedimentary and fluvial sediments containing a sequence of quartzites, quartzofeldspathic gneisses, volcanic sequences and bands of schist's (Figure 2-5). It was previously referred to as the Marais River Amphibolite and Micaceous Quartz Feldspar Schist (Van Bever Donker, 1980), and the Quartz-plagioclase Schist and Quartz-Tourmaline Schist's of the Kaaien Series (Von Backström, 1964). According to Moen (2007), the Omdraai Formation consist of schistose, leucocratic, often well-bedded semi-pelitic metasediments. The formation is named after the farm Omdraai, north of the Orange River which contains most of the stratigraphy of the Omdraai Formation (Praekelt, 1984). According to Praekelt (op.cit) the formation consist of fine to medium-grained leucocratic quartz-feldspar gneiss with interbanded massive (fine-grained magnetite and hornblende bearing) quartzites, biotite schist and amphibolites.

The Marias River Amphibolite described by Van Bever Donker (1980) is related to the Marias River/Koekoepkop Formation (Praekelt 1984, Moen 2007, respectively) on the Waterval Thrust and not the Omdraai Formation. During the current stratigraphic mapping it was concluded that the Koekoepkop Formation and the Omdraai Formation are not related and both are allochthonous units with different source regions.

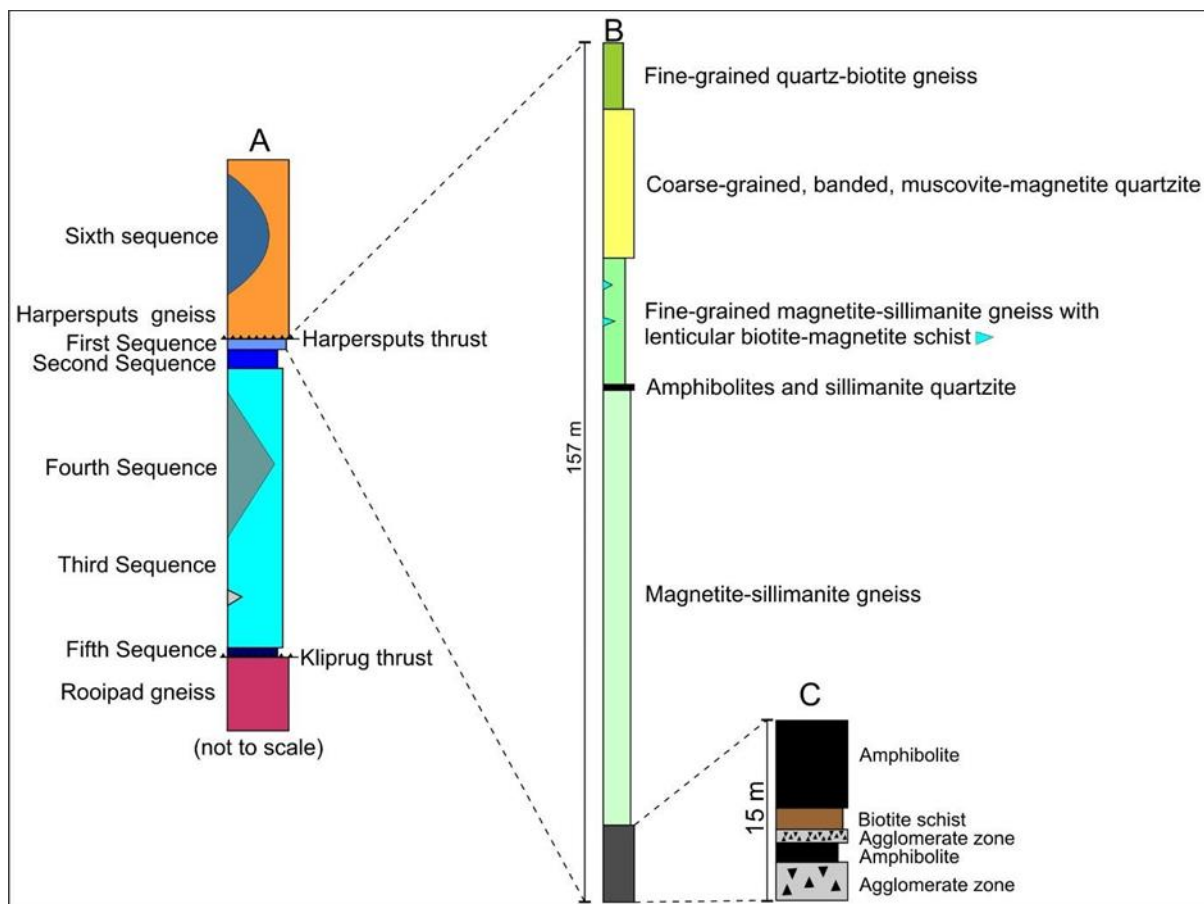


Figure 2-6: Stratigraphic profile of the Omdraai Formation at point X (Figure 2-5). The regional profile (A) containing the 6 sequences and two intra-terrane thrusts is not to scale. Stratigraphic profiles B and C are detailed profiles (to scale) of the first sequence and contact zone between the first and second sequence at point X on the map (Figure 2-5).

During the stratigraphic mapping of the current study it was established that the Omdraai Formation is a complex series of lithologies that could be sub-divided into 6 stratigraphic sequences (Figure 2-7); each sequence is separated by unique micro and mesoscopic features. Von Backström (1964) have noted that the plagioclase-quartz schist he mapped (as Omdraai Formation) contains lithologies with various characteristics (different mineral composition, textures and colours), this observation could be interpreted as the distinguishing characteristics between the 6 sequences.

The complete stratigraphy of the Omdraai Formation is situated within the Vaaldrift sheath fold (VSF) which is sandwiched between two granite gneisses separated by a roof thrust (Harpersputs thrust, HPT) and a footwall thrust (Kliprug thrust) overlying the Rooipad gneiss; Augrabies sheath fold (Figure 2-7). The six sequences of the Omdraai Formation are found as discontinuous units throughout the VSF; the only continuous sequences is the third (#3) sequence, which is distributed over the total length of the VSF. The discontinuity of the sequences can be ascribe to wedging out of units during thrusting; lithologies are cut off against decollement planes, either on a macro (wedging out of sequences against major thrust planes) or mesoscopic scale (wedging out of lithologies within a sequence) (refer to section 3.1.2 and 3.3.2 for the detail on wedging and thrust faults).

Primary sedimentary cycles and graded beds are still preserved in some of the units of the Omdraai Formation. Along the short limb of the large Z-fold on the western VSF, graded beds indicated fining towards the north (inside of structure, point X in Figure 2-5).

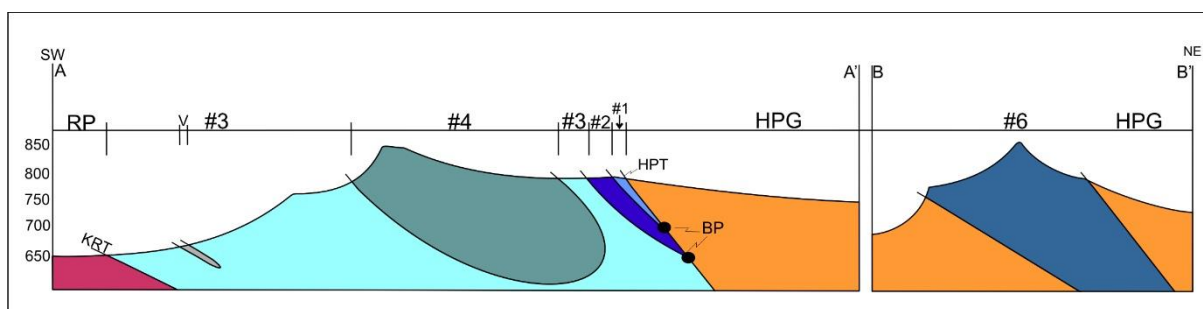


Figure 2-7: NE section (A-A', B-B') across the Omdraai Formation, which indicates the stratigraphic and structural relationships between the 6 sequences (refer to section lines on Figure 2-5). The Omdraai Formation overlies the Rooipad gneiss (RP) and is separated by the Kliprug thrust (KRT). The first (#1) and second (#2) sequences cuts out long the Harpersputs thrust (HPT) and forms branch points (BP) in depth. The third (#3) sequence contains a thrust sheet consisting of volcanic rocks (V). The fourth (#4) sequence is an enclosed lithology and forms the core of the Vaaldrift sheath fold. The Harpersputs gneiss (HPG) overlies the Vaaldrift sheath fold. The sixth (#6) sequence forms part of a separate sheath folds which is enveloped within the Harpersputs gneiss.

2.2.1.2.1 First Sequence

The first sequence (#1) is the uppermost stratigraphic sequence of the Omdraai Formation and forms a lit-par-lit contact with the Harpersputs gneiss. The lithologies of #1 have been mapped as a package due to the sillimanite and magnetite-rich gneisses as well as quartzites that provide sufficient markers for stratigraphic mapping. The following lithologies characterise the first sequence (157 m thick): fine-grained biotite-quartz gneiss (12 m), coarse grained banded magnetite- muscovite quartzite (27 m), fine grained sillimanite-magnetite-biotite-feldspar-quartz gneiss (23 m) which is interbanded on a metre scale with magnetite- biotite

schist (epidote-rich), amphibolite, calc-silicates, sillimanite-quartzite (1 m) and a sillimanite-magnetite-biotite-feldspar-quartz gneiss (79 m; Figure 2-6C).

The contact between #1 and #2 is demarcated by a 15 m thick volcanoclastic zone consisting of amphibolite (7 m), biotite schist (1.7 m), agglomerate zone (1 m), and hornblende-biotite gneiss (1.5 m), amphibolite (65 cm) and another 3m thick agglomerate zone (Stratigraphic profile C in Figure 2-6, Figure 2-8A). The agglomerates consist of various sizes mafic pyroclastic bombs and tuffaceous bands (Figure 2-8). The lithologies of #1 are discontinuous bodies along strike and vary in thicknesses. The first sequence cuts out along the roof thrust (Harpersputs thrust) in the north-west and south-east (Figure 2-5).

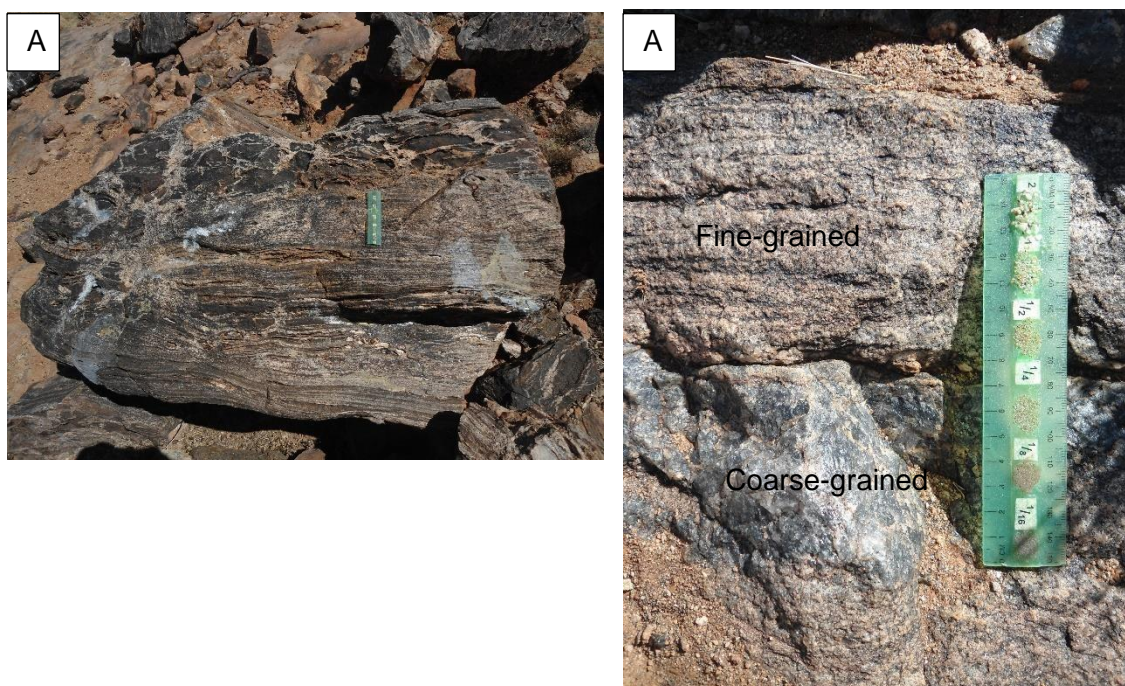


Figure 2-8: First sequence of the Omdraai Formation. A: Agglomerate of the volcanic unit between the first and second sequences. B: Various grain sizes in the quartzites (graded bedding) indicate a fining upward sequence; the fining upwards feature is also indicated by beds varying in thickness (from thick to thin-bedded/laminated).

2.2.1.2.2 Second Sequence

The second sequence (#2) is characterized by a thick fine-grained quartzite with a well-defined pink banding of K-feldspar (<5cm; Figure 2-9A); its maximum thickness in the VSF is 250m. The quartzite contains high concentrations of magnetite and biotite in the matrix, giving rise to a smoky colour. It has interbanded lenticular units of fine grained biotite-feldspar-quartz gneiss with a maximum thickness of 1m and locally forms a 5m thick agglomerate zone (Figure 2-9B). Towards the southern part of the Omdraai Formation a homogeneous dark quartzite (magnetite-rich) is situated within #2. The #2 stratigraphy overlies the third sequence and is

marked by a sharp contact; towards the north-west and south-east it wedges out along the roof thrust of the Omdraai Formation (Harpersputs thrust).

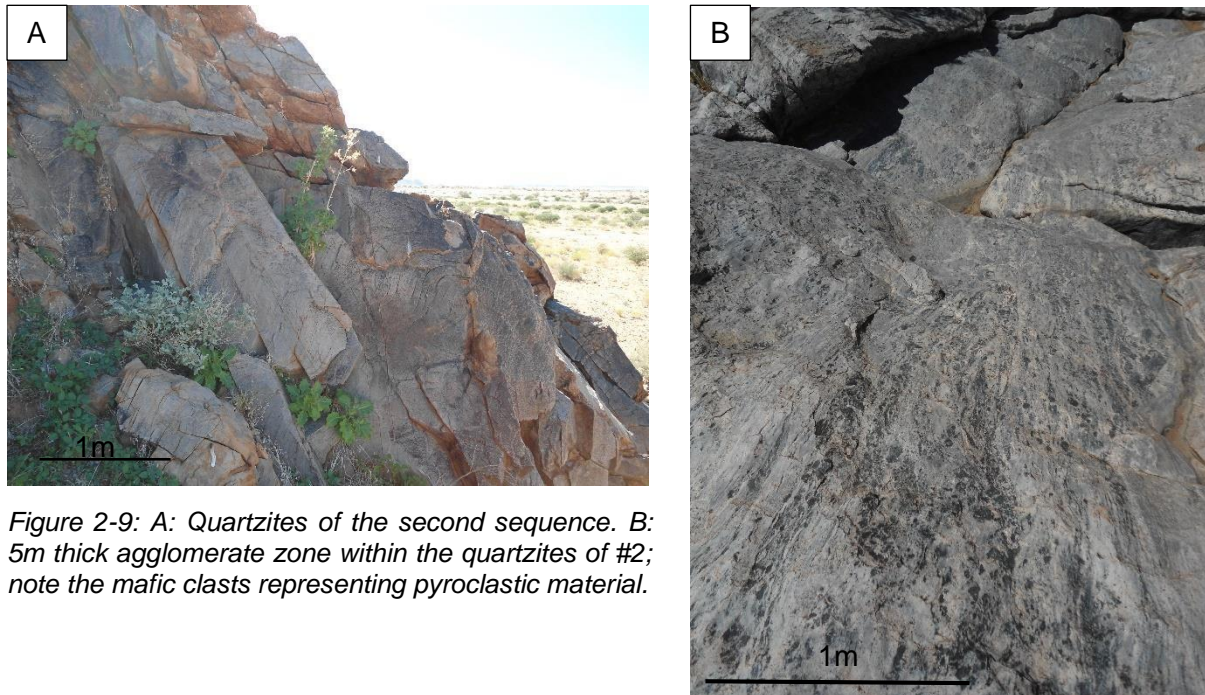


Figure 2-9: A: Quartzites of the second sequence. B: 5m thick agglomerate zone within the quartzites of #2; note the mafic clasts representing pyroclastic material.

2.2.1.2.3 Third sequence

The internal stratigraphy of the third sequence (#3) consist of two biotite-feldspar-quartz gneiss members and massive banded quartzite (Figure 2-10A, B). The two gneissic members are distinguished from each other by grain size; the coarser grained member contains sporadic 10mm-50mm biotite nodules (Figure 2-10C). The fine grained member contains interbanded coarser quartz bands on a centimetre scale.

No sharp contact exists between the two members, with the matrix of both being the same composition. The coarser and fine grained members grade into each other: it is for this reason that they are difficult to show on a regional mapping scale. Along strike the two members' grade into one another, but normal to the strike the two members are separated by a sharp contact; Von Backström (1964) notes that across strike the changes can be sudden and sharply defined.

Another part of the internal stratigraphy of #3 are the large well banded magnetite-quartzites (Figure 2-10B). The highly deformed quartzites can be up to 30m thick. The third sequence also incorporates a number of volcanic sequences with unique lithologies compared to the rest of the Omdraai Formation. The volcanic sequences are discontinuous bodies that pinch out along strike. Their internal stratigraphy is made up of: amphibolites, quartz-feldspar rocks,

amphibole-biotite rocks with mafic clasts and laminated quartz-feldspar rocks. The third sequence is the most widely distributed sequence of the entire Omdraai Formation; it stretches

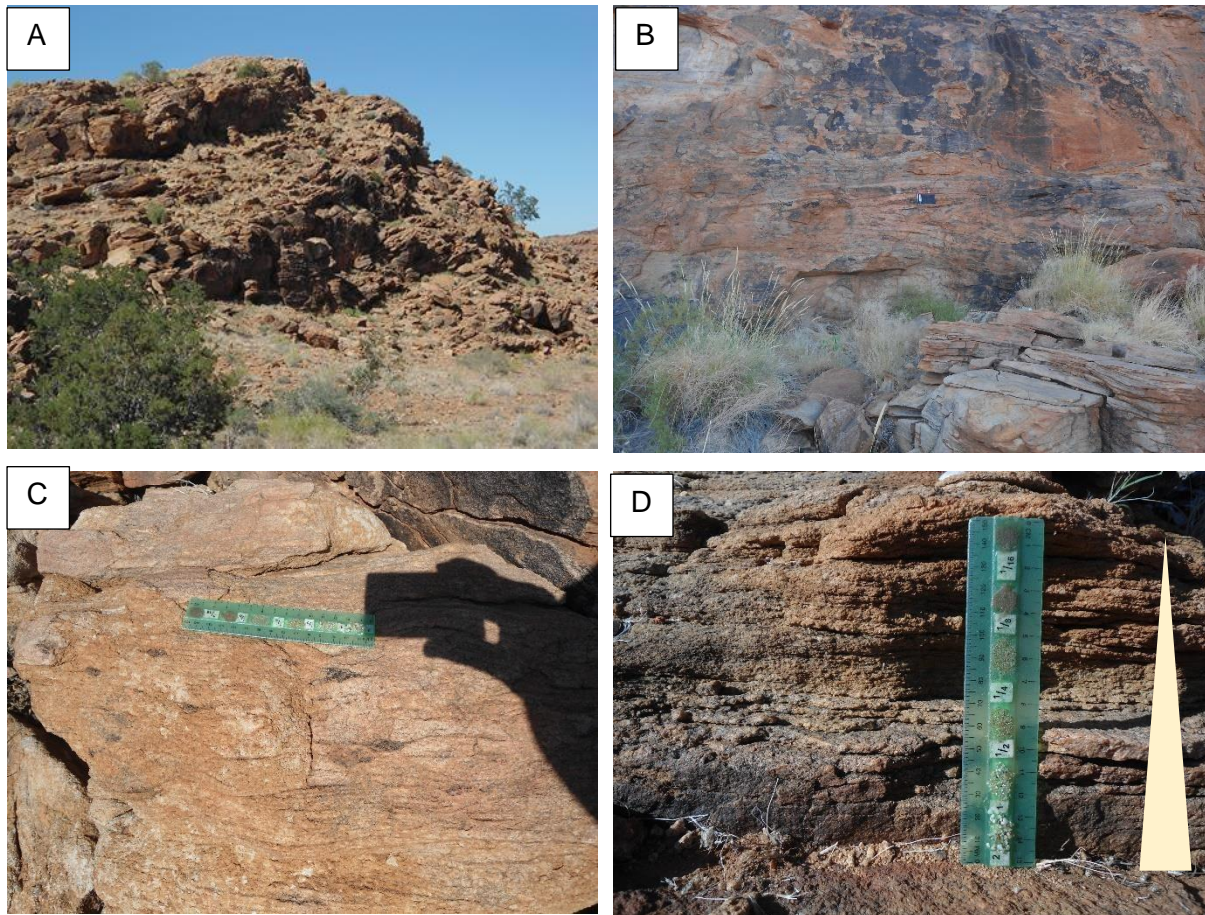


Figure 2-10: Third sequence of the Omdraai Formation. A: General outcrop of the quartz-feldspar-biotite gneiss. B: The well-banded, quartzites. C: Biotite nodules in the quartz-feldspar-biotite gneiss. D: Upward fining cycle in the quartzites.

the full extent of the VSF where it ends as a fold closure in the north-west and cut out against the Kliprug thrust in the south-east (Figure 2-5). The contact with Rooipad gneiss is characterised by a 100m wide imbricate zone.

2.2.1.2.4 Fourth sequence

The fourth sequence (#4) is characterized by a homogenous fine grained plagioclase-biotite-quartz-feldspar gneiss with a well-defined compositional banding alternating between quartz-feldspar bands and plagioclase bands (centimetre scale). Moen (2007) interpreted the lithology as a pink weathering granite-gneiss by Moen (2007), while Von Backström (1967) referred to it as a Pink Gneiss. In some localities there is a grain size variation in the gneiss. #4 is contained within the centre (eye) of the Vaaldrift sheath fold and does not occur anywhere else in the structure.

2.2.1.2.5 Fifth sequence

The fifth sequence (#5) underlies the third sequence and has a limited strike length; the contact with the underlying Rooipad gneiss is sharp. The sharp contact with the underlying Rooipad gneiss represents a structural decollement referred to as the Kliprug thrust. #5 consists of a fine grained quartzite with interbanded medium-fine grained leucocratic quartz-feldspar gneiss. A gradational contact exists between #5 and #3; where #5 extends for 8km in a north-south direction. The lithologies decrease in thickness towards the end points (north and south) after which they wedge out along the footwall thrust (Kliprug thrust; Figure 2-11).

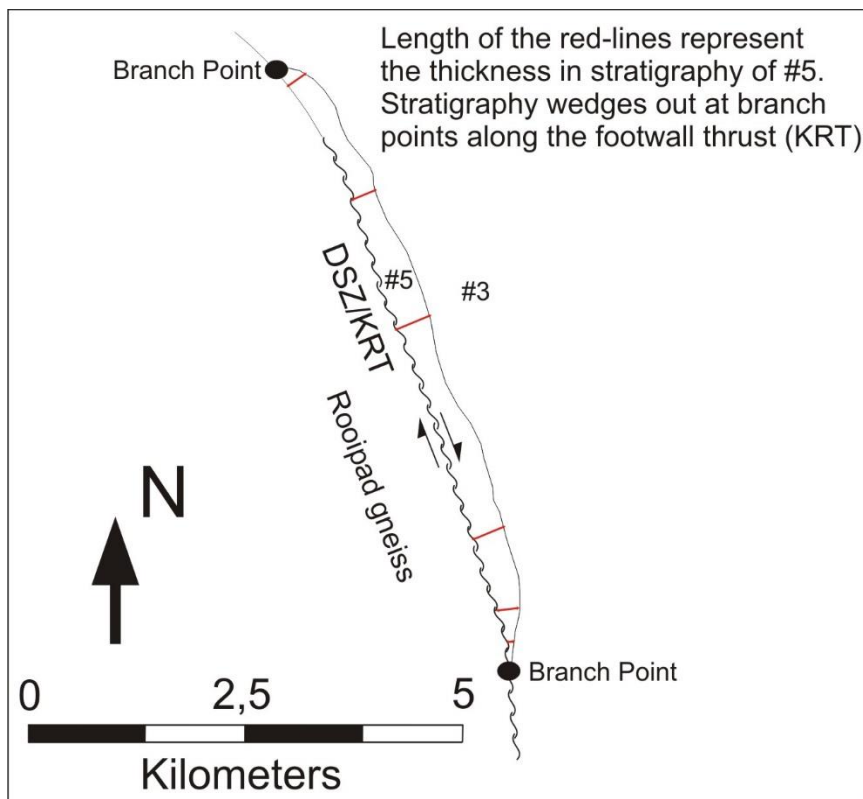


Figure 2-11: The distribution of the fifth sequence along the Duiwelsnek shear zone. The fifth sequence is interpreted as a thrust sheet.

2.2.1.2.6 Sixth Sequence

The sixth sequence (#6) is a volcano-sedimentary sequence and occurs in the northern VSF (N-VSF). In the southern part of the VSF, #6 overlies the first sequence and underlies the Harpersputs thrust (Harpersputs gneiss in the hanging wall). The contact in general along strike is sharp, but locally (e.g. Neuseiland) forms a series of stacked lenses of alternating Omdraai Formation (#6) and Harpersputs gneiss (Figure 2-12).

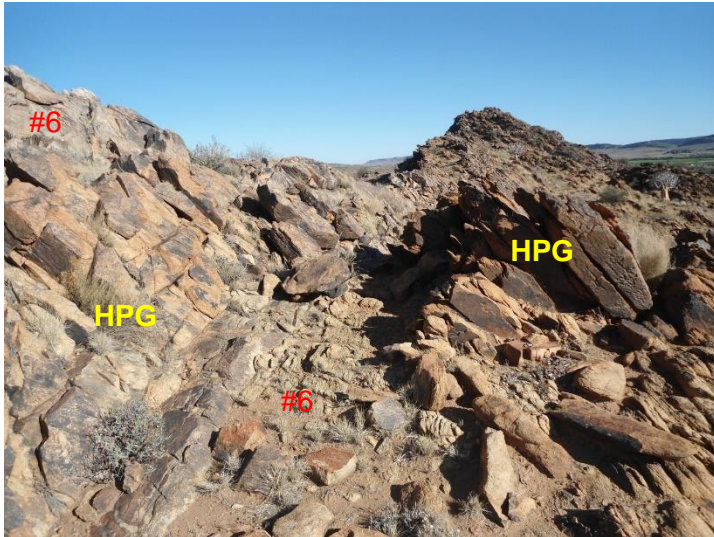


Figure 2-12: Stacked imbricates of ODF (#6) and Harpersputs gneiss (HPG) along the Harpersputs thrust.

The lithologies west of the Harpersputs gneiss contact consist of a feldspathic gneiss, biotite-feldspar-quartz gneiss with bands of mafic clasts (pyroclastic bombs), and amphibole gneisses. Towards the base of #6 a fine grained quartzites (smoky colour), calc-silicate, biotite gneiss, garnet-biotite gneiss and quartz-biotite-rich rocks with interbanded breccias are found (Figure 2-13). #6 are highly sheared and the lithologies are rarely thick packages. In the north-west and south-east the lithologies of #6 fold out, in the central area of the N-VSF the lithologies are wedged out along the intra-terrane thrust (hangingwall thrust of VSF).

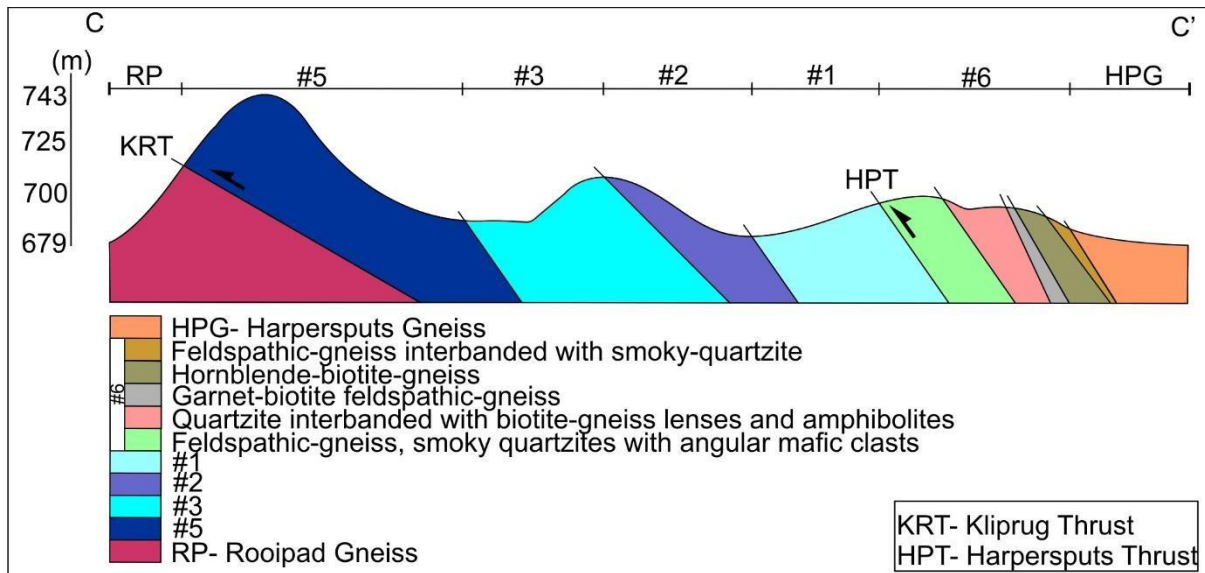


Figure 2-13: Cross section (C-C'; Figure 2-5) in the south-eastern portion of the Omdraai Formation where the stratigraphy of the sixth sequence (#6) overlies the rest of the ODF sequences (1-3, 5); the contact is defined by the Harpersputs thrust (HPT). Section line is 1.87km long.

2.2.1.2.7 Renosterkop Rocks

The Omdraai Formation forms an enclave (2,2km x 0,3km) in the Rooipad gneiss to the south of the Vaaldrift sheath fold and it outcrops as a prominent “koppie” known as Renosterkop (Figure 2-5, Figure 2-14A). The RR was first mapped by Praekelt (1984) as Topaz-bearing rocks; he described the outcrop as quartzites and granite with abundant topaz throughout which formed due to the process of pneumatolysis (intrusion of gas and fluids).

Saad (1987) did a geochemical study of the Renosterkop gneiss and described it as a large low grade tin- tungsten- zinc deposit, with the mineralization hosted by shallow-dipping sheet greisen bodies surrounded by the host granite (Rooipad gneiss). The mineralised bodies consist of quartz, biotite and topaz with minor amounts of fluorite and accessory opaque minerals, zircon and secondary chlorite (Saad, op.cit). Saad (op.cit) described the contact between the mineralised zone and the Rooipad gneiss as a 2m wide transition zone. Rooipad gneiss intrudes the quartzite body in a lit-par-lit (Figure 2-14B). The quartzites and the Rooipad gneiss share the same fabric orientation. The compositional banding in the quartzites is defined by alternating grain size biotite and quartz. Scattered throughout the quartzite are lenses of unmineralised Rooipad gneiss, which would suggest that the mineralization was prior to the intrusion of Rooipad gneiss.

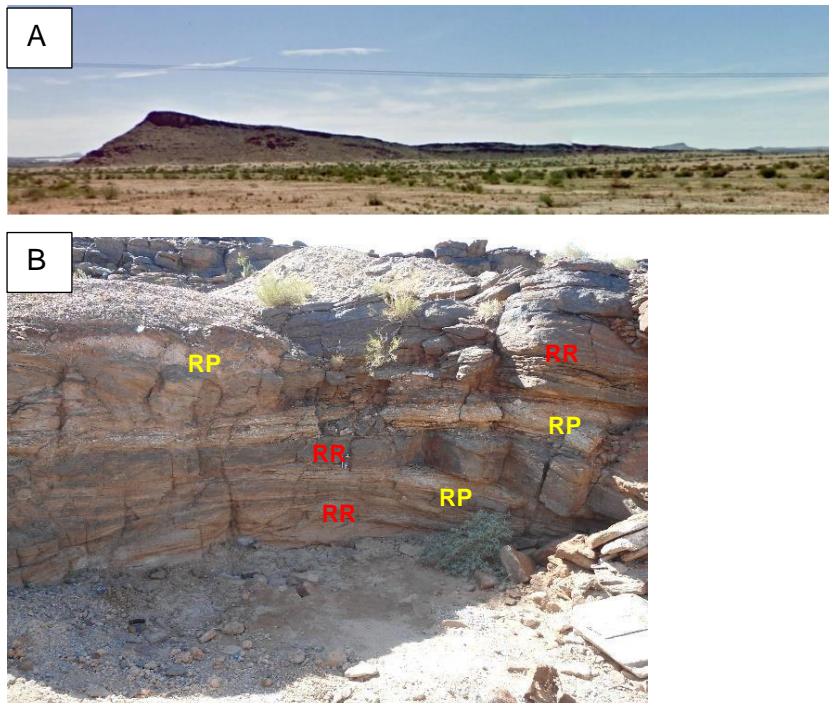


Figure 2-14: A: Renosterkop's southern face (photograph looks towards the north). B: Rooipad gneiss (RP) intrudes the Renosterkop Rocks (RR) in a lit-par-lit fashion giving rise to an interbanding between the gneiss and Renosterkop Rocks.

2.2.1.3 Goede Hoop Formation

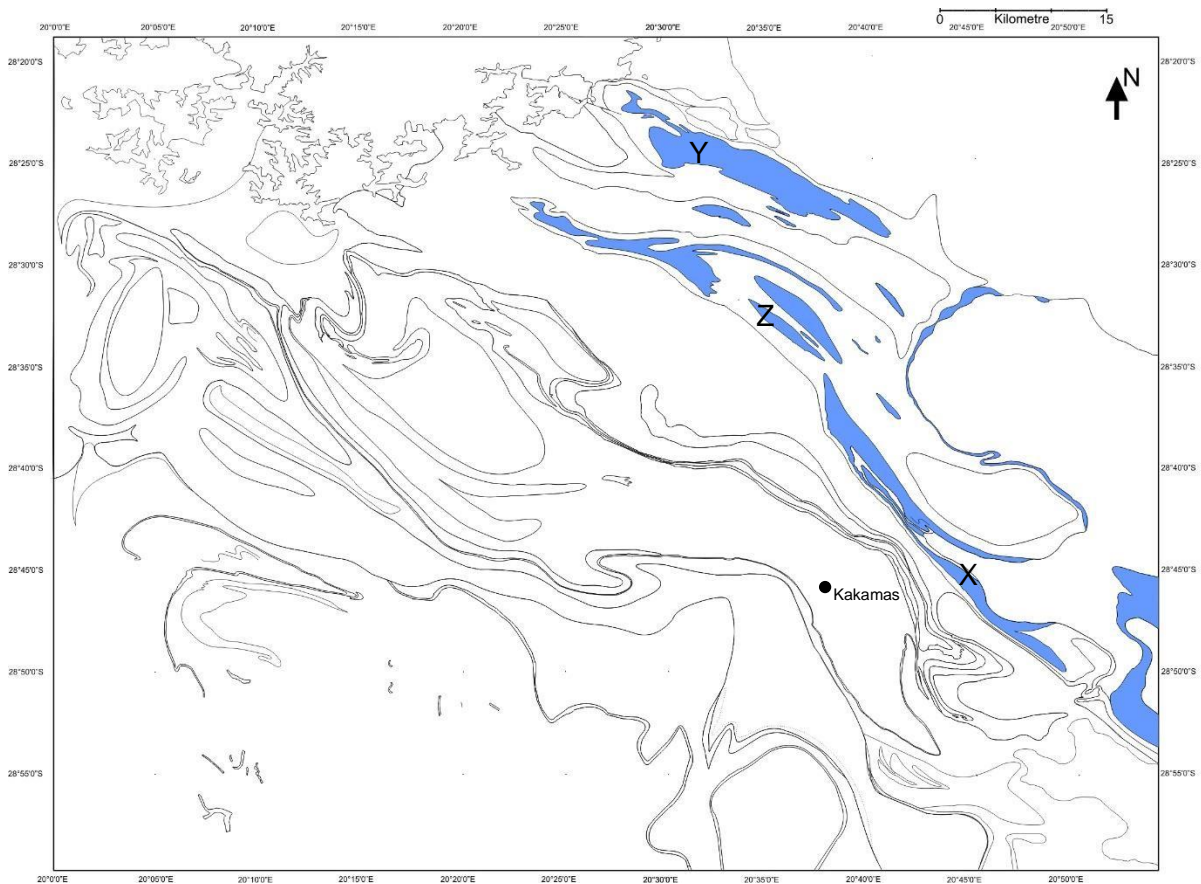


Figure 2-15: Stratigraphic distribution of the Goede Hoop Formation. Best visible outcrop is at point X (28°43'51.71"S 20°42'30.13"E) and point, Y (28°26'14.78"S 20°34'2.46"E). Refer to Figure 2-16 for details on point Z.

The Goede Hoop Formation weathers positively giving rise to a prominent hilly landscape in low lying areas (e.g. Komsberg, Gifberg, Rondekop and Neusberg; Figure 2-15, Appendix B). It is named after the farm Goede Hoop which is about 10km south of the town Ludzputz (Geringer, 1973). According to Geringer (1973) the Goede Hoop Formation is one of the oldest metasediments in the Namaqua Mobile Belt west of Upington and it consists mainly of a quartz-muscovite-schist with minor biotite-schist, amphibolite and sillimanite-schist. Von Backström (1964) mapped the Goede Hoop Formation as a quartzite and quartz-sericite schist (occasionally containing bands of metamorphosed conglomerate) with cross-bedding and ripple marks still present in the quartzites and not removed by metamorphic recrystallization. Moen (2007) also describes the Goede Hoop Formation as a muscovite-quartzites. Van Bever Donker (1980) divided the Goede Hoop Formation into two end members namely the Neuspoort Member and the Zwart Boois Berg Member. The Neuspoort Member is a platy quartz-mica schist with conspicuous flakes of mica on the cleavage planes which preserved graded bedding in some areas. The Zwart Boois Berg Member of Van Bever Donker (1980)

is a feldspathic quartzite and it overlies the platy quartz-mica schist. Both end-members can be seen in the Neusberg Mountain range. Praekelt (1984) only mentions that a sericite-quartzite of the Goede Hoop Formation exists in the north-eastern corner of his study area. The best possible outcrops of the Goede Hoop Formation can be seen along the N14 road cutting through Neusberg (Figure 2-15, point X; 28°43'51.71"S 20°42'30.13"E) or along the Kakamas-Ludzputs dirt road (Figure 2-15, point Y; 28°26'14.78"S 20°34'2.46"E).

In this study the Goede Hoop formation has been mapped as a sequence of muscovite-quartzites, and it is not regarded as a "schist" like the previous authors; the sediments are quartz dominant with minor muscovite. The sediments of the Goede Hoop Formation are in contact with volcanic sequences of the Puntsit/Biesje Poort Formations and the Friersdale charnockite; all the contacts are sharp.

Discontinuous zones of scattered flattened oval shaped quartz grains (5 mm – 100 mm) are found sporadically throughout the quartzites; the quartz grains are interpreted as deformed primary pebbles and represents a matrix-supported conglomerate horizon. Due to the sporadic development of the conglomerate zones no clearly defined stratigraphic relationship could be established with the quartzites. Moen (2007) however claims that the pebbly layers are generally located near the base of the Goede Hoop Formation. The pebbles in the quartzites are flattened and stretched with the long axis (parallel to long axis of strain ellipsoid) parallel to the regional stretched mineral lineations. The quartz-pebbles are orientated with their intermediated axis parallel to the penetrative cleavage of the Goede Hoop Quartzites which is at an angle to the compositional banding (Figure 2-16A). Von Backström (1964, p.27) also interpreted zones with high concentration of pebbly horizons as conglomerate.

Primary sedimentary structures (e.g. graded beds and cross bedding) were also recognized by Von Backström (1964, p.23), Van Bever Donker (1980, p.32) and Geringer (1973, p.25). Van Bever Donker (op.cit) interpreted the Goede Hoop Formation containing primary structures as trough-crossbedded sand deposits. In this study graded beds, indicates a younging direction to the north-east, is defined by upwards fining cycles (centimetre scale); they are illustrated by grain and pebble size variation in the vertical on north-east dipping beds (Figure 2-16B). This type of cycle and the composition of the quartzites is an indication that the quartzites of the Goede Hoop Formation are most likely to represent beach deposits (Reineck & Singh, 1980). Primary bedding in the road-cutting on the N14 indicated remnants of cross bedding, also showing north-east to east younging. A metamorphic fabric, defined by orientated muscovite is co-planar to the bedding. Detrital zircon Pb/Pb age spectrum for the Goede Hoop Formation (Moen, op.cit.) suggests a depositional age between 1.8 and 1.6 Ga.

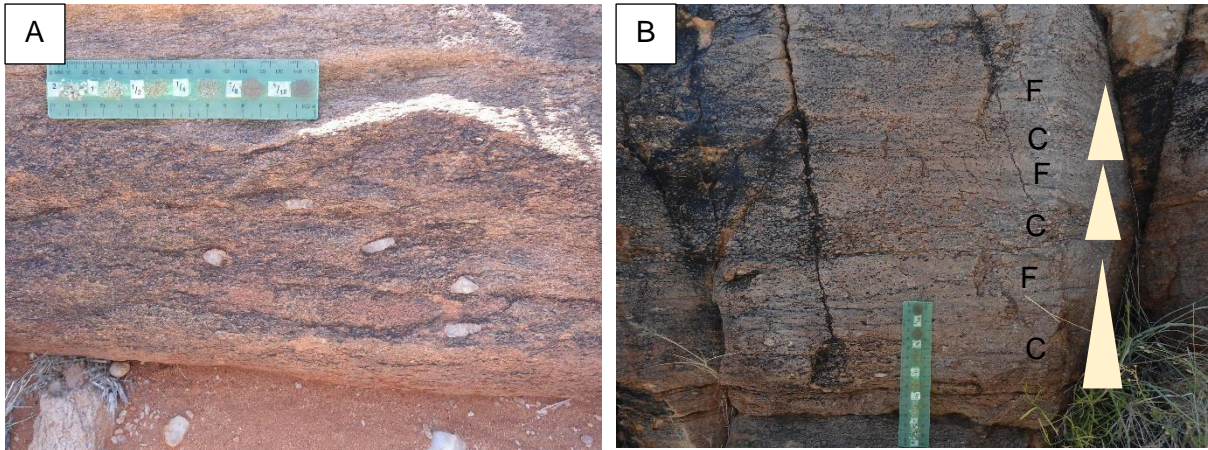


Figure 2-16: Quartzites of the Goede Hoop Formation. A: Flattened quartz pebbles in a fine grained quartz-muscovite matrix. B: Upward fining cycles in the quartzites (C= coarse-grain, F= fine-grain; point “Z” in Figure 2-15).

2.2.1.4 Puntsit Formation

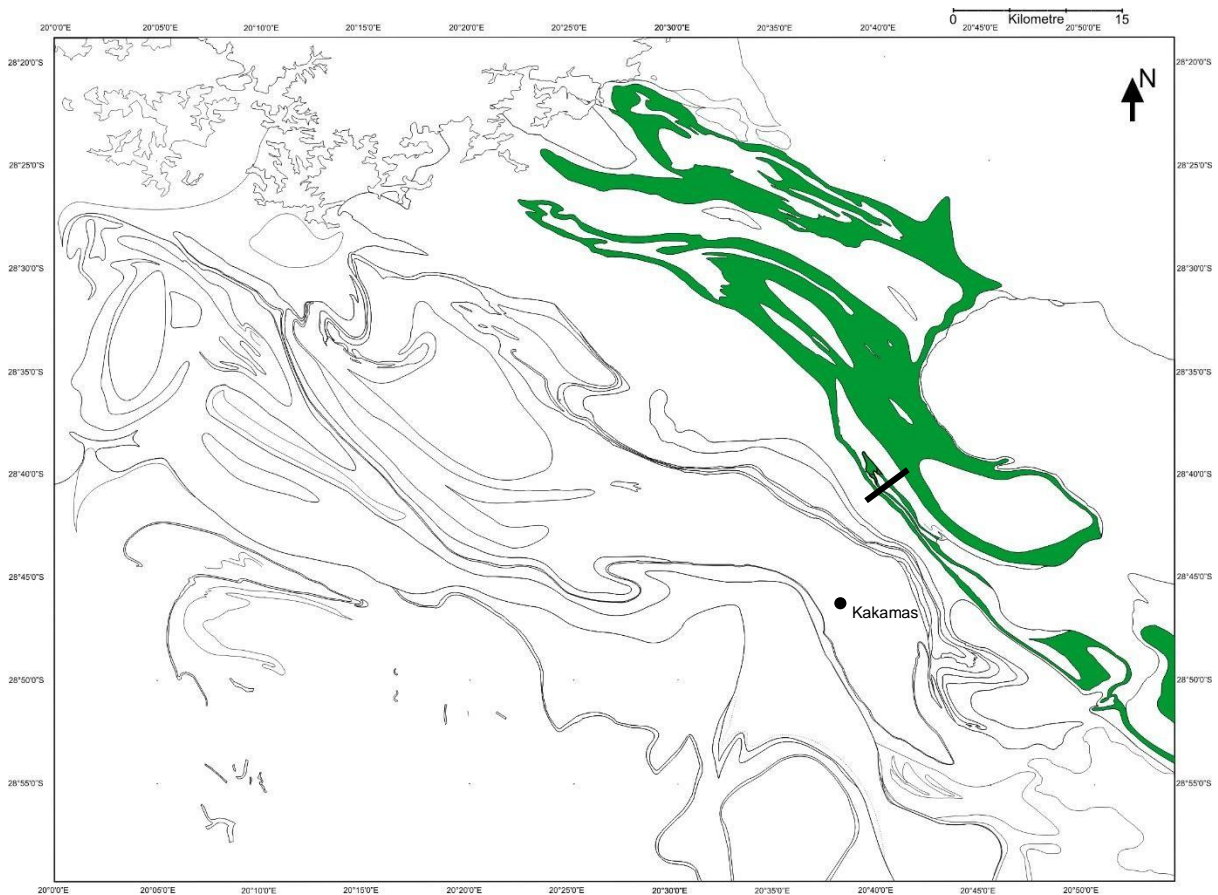


Figure 2-17: Stratigraphic distribution of the Puntsit Formation. A north-east cross section (black line) across the Puntsit Formation is shown in Figure 2-18.

Moen (2007) suggests that the Puntsit Formation underlies the Goede Hoop Formation. The Puntsit Formation is the most widely distributed supracrustal sequence in the study area; it hosts a number of lithologies and underlies the entire Goede Hoop Formation (Figure 2-17,

Figure 2-18). According to Moen (2007), the Puntsit Formation is part of the Biesje Poort Group of sediments incorporating the Omdraai Formation; no correlation between the Puntsit Formation and the Omdraai Formation could be established. The Puntsit Formation was previously referred to as the Baviaanskrantz calc-silicate rich quartzite (Van Bever Donker, 1980), granulite containing lenses of calc-silicate rocks (Von Backström, 1964), and Biesje Poort Formation (Geringer, 1973). Van Bever Donker (op.cit.) sub-divided the Puntsit Formation into two end members (Zwart Boois Berg and Warm Zand members) with respect to the amount of amphibolite. Moen (op.cit.) describes the Puntsit Formation as dark weathering calc-silicate rocks with layers of marble and amphibolite. Von Backström (1964) who used the Puntsit Formation as a marker unit and described the granulite calc-silicates as dense fine-grained rocks having a light-grey, pink or white colour and accessory mafic minerals. Geringer (1973) suggests that the Puntsit Formation consist of heterogeneous zones of calc-silicates with minor granulites, marble and amphibolites.

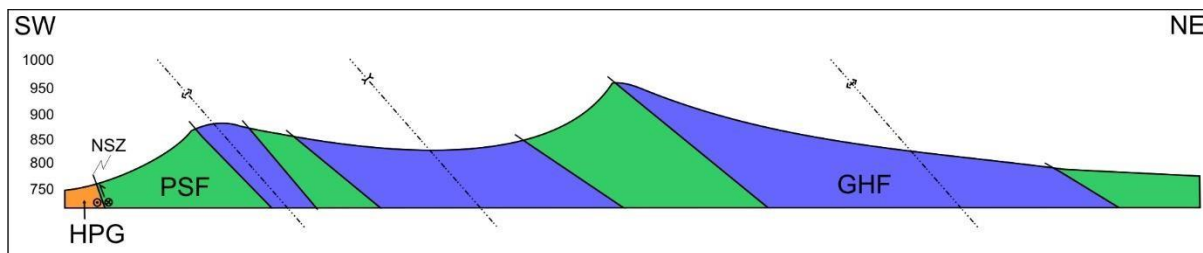


Figure 2-18: North-east section over the isoclinal Neusberg sheath fold indicating the structural relationship between the Puntsit and Goede Hoop Formations (refer to section line on Figure 2-17) Harpersputs gneiss (HPG) underlies the Goede Hoop (GHF) and Puntsit (PSF) Formations; the contact is defined as the Neusberg shear zone (NSZ), which is a re-activated intra-terrane thrust (see section 3.5.5).

In this study the lithologies hosted by the Puntsit Formation are as follows: calc-silicates (sediments referred by Geringer, 1973), biotite-gneisses with lenses of biotite-schist (1m x 500mm), biotite-gneisses with sillimanite nodules, amphibolites, garnet bearing amphibole gneiss, muscovite-quartz-feldspar-quartzite and pyroclastic- rich rocks. All the various lithologies have sharp contact relationships with each other. There are areas where lenses and/or bands of amphibolite contains epidote enrichment, the bands are inferred to be a later enrichment. Moen (2007) claims that these epidote bands could be on decametre to kilometre scale, however these size bands were not observed, bands are normally discontinuous on a centimetre scale. During this study no marbles were found in association with the Puntsit Formation, as suggested by previous authors. Felsic pyroclastic breccias represent high explosive felsic lava flows (Figure 2-19B) and are preserved in low strain areas. The pyroclastic clasts are angular and randomly orientated (Figure 2-19A).

The Puntsit Formation stretches beyond the limits of this study; in the south-east it continues beyond the mapped area while in the north-west the Puntsit Formation becomes part of a series of kilometre scale isoclinal fold closures as part of the Rondekop and Biesje Poort sheath folds. Not all of the above mentioned lithologies of the Puntsit Formation are present throughout its distribution; some lithologies are more dominant in specific areas. A sharp contact separates the Puntsit Formation from the overlying Goede Hoop Formation; the basal contact of the Puntsit Formation is separated from the Harpersputs gneiss by the Neusberg shear zone (structural contact).

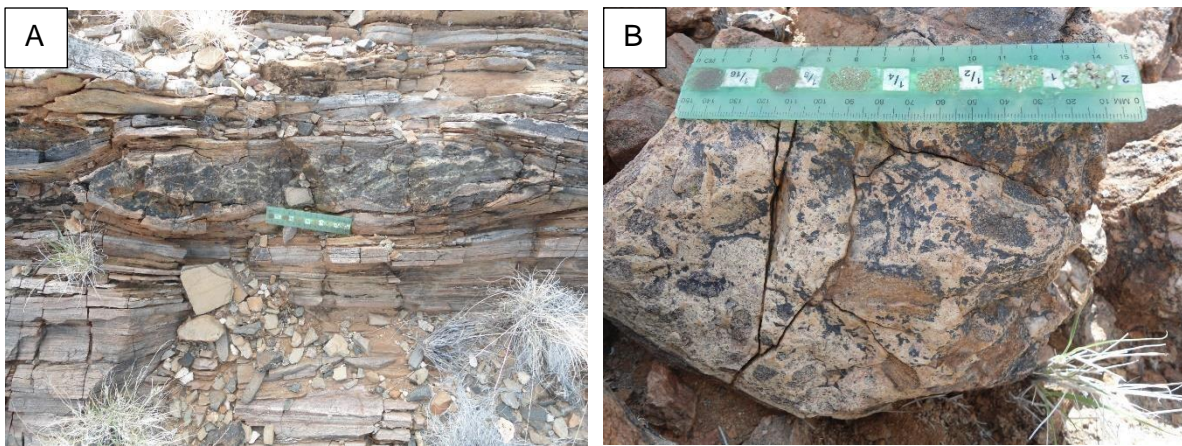


Figure 2-19: Puntsit formation. A: boudin of a pyroclastic bomb in the volcanoclastic sequence. B: Low strain zone with preserved angular pyroclastic clasts.

2.2.2 Supracrustals – Grünau Terrane

2.2.2.1 Blouputs Formation

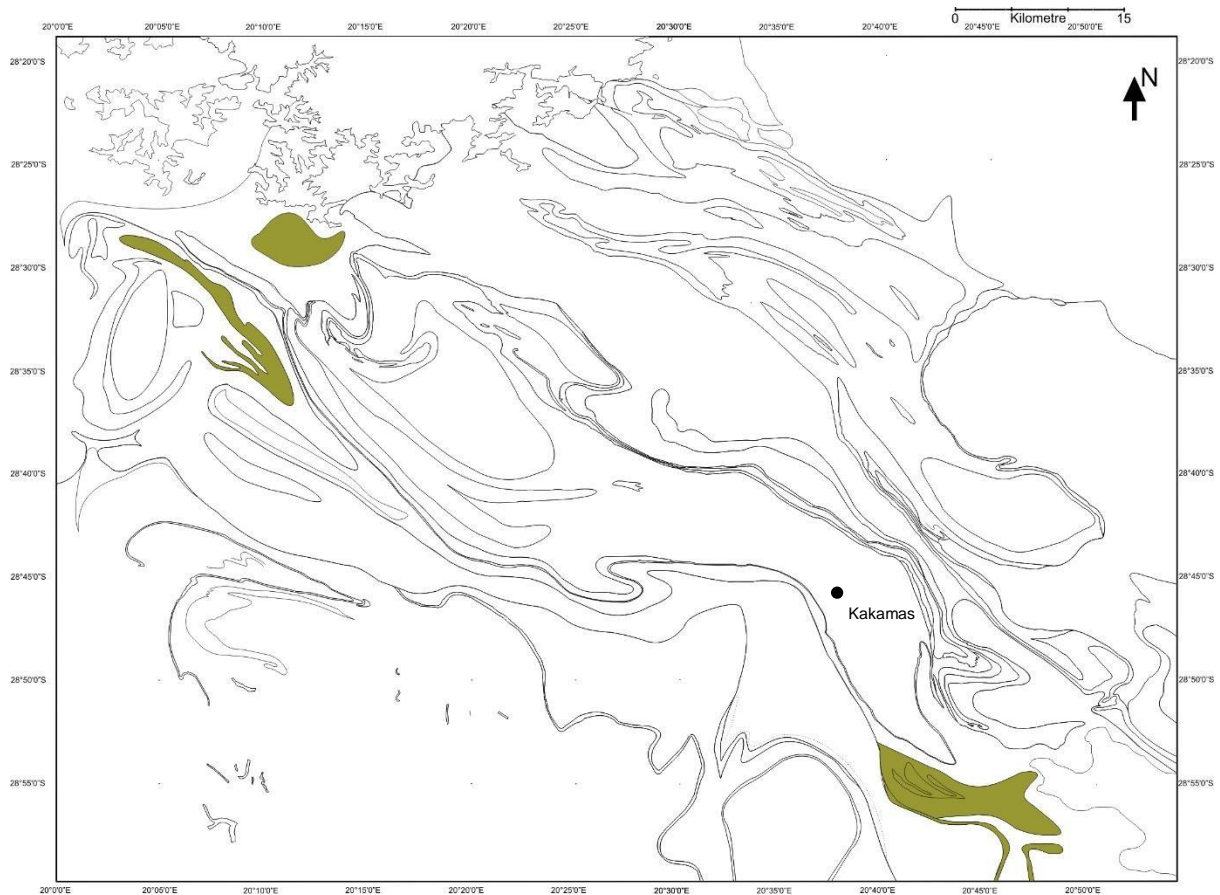


Figure 2-20: Stratigraphic distribution of the Blouputs Formation.

The Blouputs Formation represents the meta-sediments (Praekelt, 1984) and metavolcanites (Colliston, et al., 2015) of the Grünau Terrane (Figure 2-20; Appendix D). The Blouputs Formation is named after the farm Blouputs 10 by Praekelt (1984); various other authors described the formation, both in South-Africa and Namibia. Moen (2007) refers to the Blouputs Formation as the Vyfbeker Metamorphic Suite and the Kourop Migmatites, which consists of a migmatitic leucogneiss, biotite gneisses (garnetiferous in places) and an amphibole gneiss. The Blouputs Formation is described as migmatitic gneiss and consist of a lit-par-lit gneiss by Von Backström (1967). Geringer (1973) included the meta-sediments of the Grünau Terrane with the garnet-bearing sillimanite-cordierite-biotite gneisses of the Toeslaan Formation. The Blouputs Formation was mapped as an aluminous gneiss consisting of garnet-sillimanite-cordierite gneisses, a biotite gneiss and thin (centimetre scale) meta-quartzites, and calcsilicate bands by Blignault (1977) and Nordin (2009). In the Aus area of Namibia the Garub Sequence consists of various aluminous gneisses and granulites (Diener, et al., 2013) and is the equivalent of the Blouputs Formation. The Blouputs Formation is divided into two separate formations by Beukes (1973) namely: Arus Formation and Umeis Formations, both formations

consisting of garnet-rich sillimanite-cordierite gneisses. West of the current study area the Blouputs Formation is referred to as the Narries Formation by Du Plessis (1979) which refers to the Arus Formation of Beukes (op.cit.). Praekelt (1984) did not distinguish the Blouputs Formation from the neighbouring Witwater gneiss due to the close association between the two lithologies. Enclaves of the meta-sediments are found within the Witwater gneiss and Eendoorn gneiss, xenoliths of up to 50 m width are described by Praekelt (1984).

During this study it was concluded that the Blouputs Formation consists of an interbanded series of biotite-gneiss, biotite schist, amphibolite, quartzite, garnet-hornblende gneiss, sillimanite-cordierite-garnet-biotite gneiss, feldspathic gneisses and garnetiferous granulite's (Figure 2-21). The garnetiferous granulite consists of quartz (26%), plagioclase (5%), K-feldspar (7%), biotite (6%), garnet (31%) and hornblende (24%). The various lithologies display evidence of anatectic melting during a later phase; leucosomes are found frequently throughout the rocks. Where the leucosome vein networks connect, large leucocratic melt sheets resemble the Witwater gneiss: this characteristic feature was also noted by Praekelt (1984) and Moen (2007).

Isotopic analysis by Samskog (2009) suggests that the Blouputs Formation has a provenance age of ~1.8Ga. A number of previous researchers working on lithologies of the Blouputs Formation have done detailed metamorphic studies; results have indicated that the Blouputs Formation underwent amphibolite to granulite metamorphism (5.3-7Kbar at 620-650°C; Du Plessis, 1979). Peak metamorphism occurred at 8Kbar, 760-825°C, this event is recorded at 1204±13Ma (Du Plessis, 1979; Nordin, 2009; Diener, et al., 2013), which coincides with the terrane assembly stage (Colliston, et al., 2015).

The largest continuous body of the Blouputs Formation is situated in a kilometre scale sheath fold within the western part of the Augrabies National Park; the close association of Witwater gneiss, Blouputs Formation and Eendoorn gneiss can be seen in this area (Figure 2-21; A-D). Blouputs Formation occurs as xenoliths in the Witwater gneiss and in the Eendoorn gneiss. The fabric in the Blouputs Formation is co-planar with the weakly developed fabric of the Witwater gneiss.

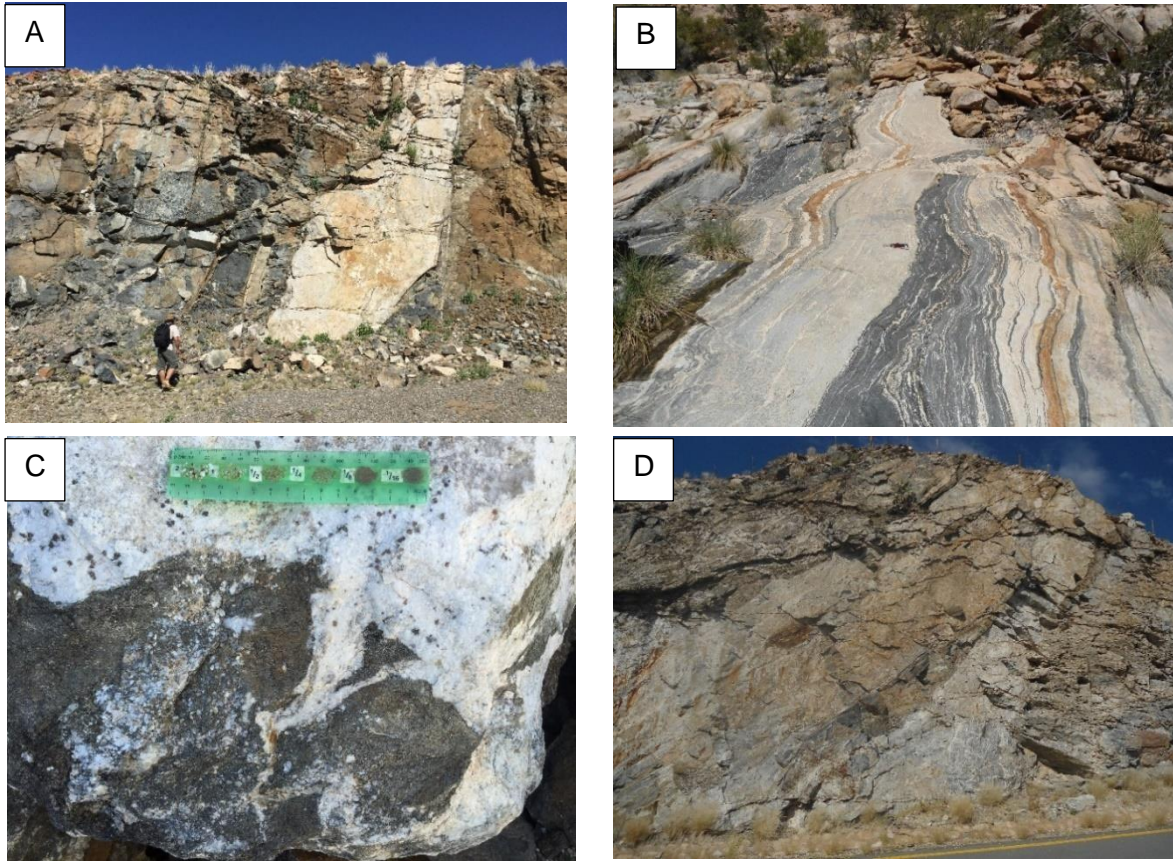


Figure 2-21: Blouputs Formation and the relationship with the neighbouring lithologies. A: Witwater gneiss (1123 Ma) intrudes the migmatitic Blouputs Formation (28°47'49.91"S 20°29'13.36"E; same locality for C). B: Metatexites of the Blouputs Formation; the Blouputs Formation (1800 Ma) underwent two stages of anatectic melting (28°29'4.10"S 20°15'26.81"E). C: Lit-par-lit intrusive relationship between the Witwater gneiss and an amphibolite of the Blouputs Formation. D: Large xenolith of Blouputs Formation in the Eendoorn gneiss (1200 Ma; dark lenticular shape body in the centre of the photograph. 28°31'34.13"S 20°11'26.44"E).

2.2.2.2 Amphibolite Sequence-HBRT

A large amphibolite sequence of well-foliated amphibolites with interbanded biotite schist and calc-silicates are situated along the HBRT (Figure 2-22), and forms a prominent ridge that trends east-west. The sequence is referred to as a mafic intrusion by Moen (2007), Marais River Amphibolite (Van Bever Donker, 1980) and dark-weathering quartz-rich granulite (Von Backström, 1964). The amphibolites have a distinctive compositional banding that is co-planar with the regional fabric. Along strike the amphibolites change composition, banding and grain sizes. Towards the west the amphibolites contain porphyroblasts of 10mm in a fine grained hornblende dominated matrix without a compositional banding.

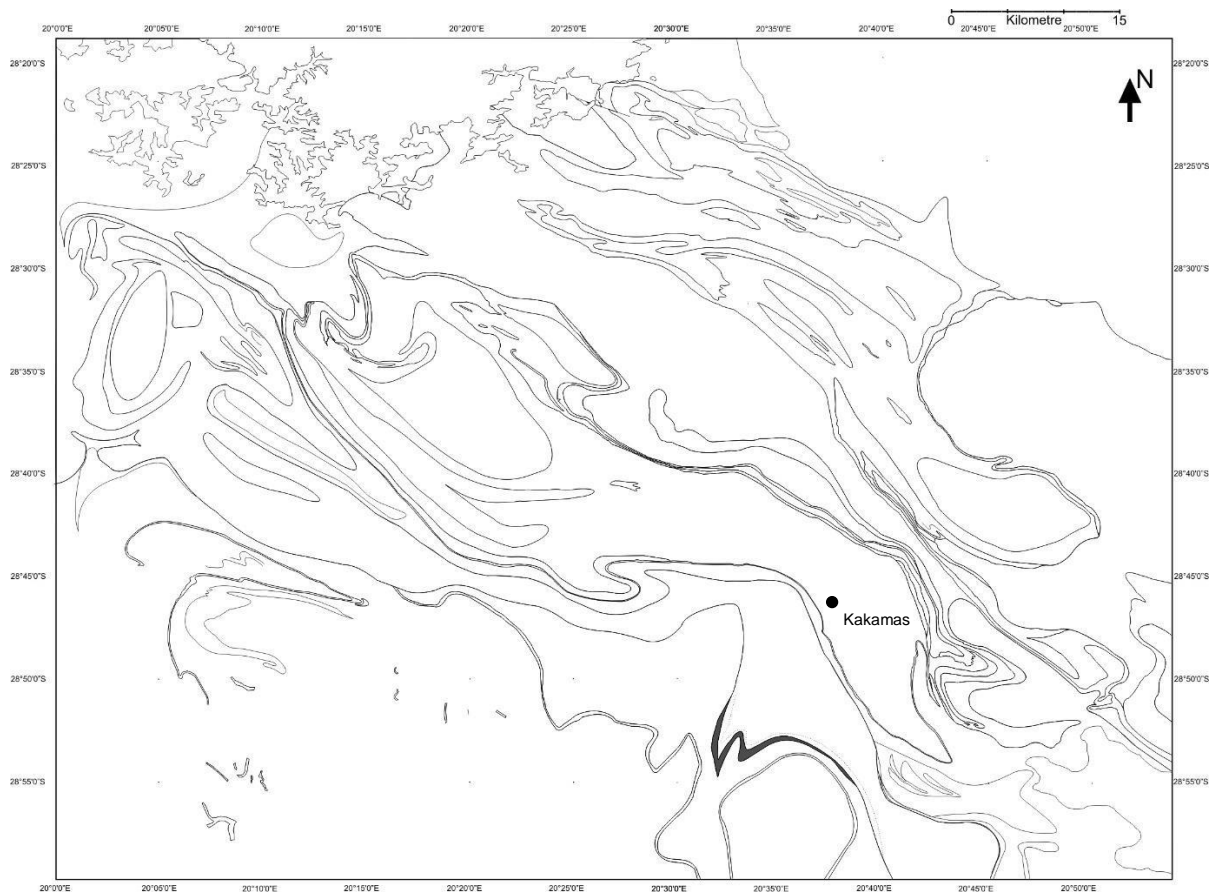


Figure 2-22: Stratigraphic distribution of the amphibolite sequence –HBRT.

The more banded fine-grained amphibolites contain lenses of biotite schist; the banding is defined by the compositional alternation on millimetre scale of hornblende and quartz-feldspar bands. Along strike in low strain areas, the original depositional nature of the rocks, such as lavas and tuffs, are still recognisable; the tuffs containing angular pyroclastic clasts (lithic clasts) in low strain areas. Pyroclastic clasts/bombs in the amphibolites are an indication that the unit has a volcanic origin. The amphibolite sequence with a maximum thickness of ~750m, wedges out along strike against the HBRT. The amphibolite sequence represents a thrust sheet (imbricate) of the Hartbees River Thrust System (HBRT).

2.2.3 Supracrustals – Bladgrond Terrane (Driekop Group)

The Bladgrond Terrane consists of a large variety of supracrustal rocks but poor outcrop makes for difficult stratigraphic divisions (Figure 2-2, Figure 2-23). The Bladgrond Terrane is not covered in detail through this thesis and a short summary of the lithologies will be discussed with reference to the descriptions of Praekelt (1984). The prominent lithologies of the Bladgrond Terrane form part of the Driekop Group and can be sub-divided into three formations: Bysteeek Formation (BSF), Witklip Formation (WKF) and the Saamwerk Formation (SWF) (Praekelt, 1984). Moen (2007) divided the Driekop Group into the Droëboom Group

and Arribees Group and was dated in the Onseepkans area at ~1.9 Ga (Moen & Toogood, 2007).

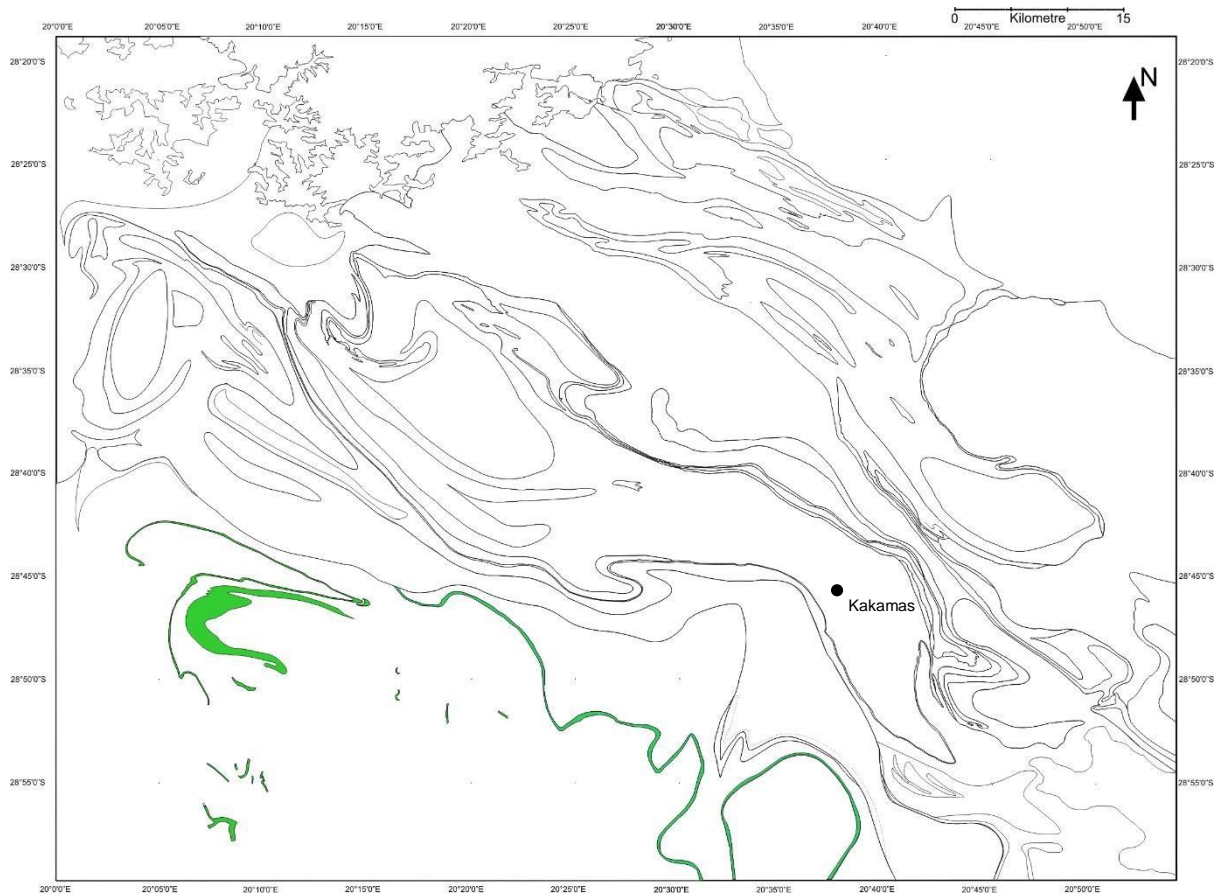


Figure 2-23: Stratigraphic distribution of the Driekop Group.

2.2.3.1 Bysteeek Formation

The Bysteeek Formation consist of a basal quartz-rich calc-silicate that is interbanded with hornblende-quartzite, feldspathic quartzite, marble and amphibolite. The basal unit is overlain by feldspathic quartzite with lenses of calc-silicates. The BSF is overlain by the Witklip Formation and SWF. Conglomerates are also associated with the Bysteeek Formation.

2.2.3.2 Witklip Formation

The Witklip Formation consists of a massive quartzite, leucocratic nodular feldspar-quartz gneiss and sillimanite-biotite schist. The formation has a minimum thickness of 200 m. The most notable outcrop of the Witklip Formation is the large isoclinal fold, known as Africa Berg; it strikes sub-parallel to the HBRT. It is overlain by the SWF. The nodular gneiss and the massive quartzites alternate so that the lithologies appears to be stacked, with gradational contacts (decrease in feldspar concentrations towards the quartzites). The darker components

of the quartzites contain magnetite within a quartz-rich matrix. Biotite-sillimanite schist occurs as lenses in the nodular gneiss and can be up to 10m thick.

2.2.3.3 Saamwerk Formation

This formation has the same distribution as the Bysteeek Formation and consist of similar lithologies - the difference being the occurrence of mafic gneisses and amphibolites. The mafic rocks are fine to medium-grained, and a weakly developed fabric is defined by the alignment of mafic minerals (hornblende). The mafic sequence consist of a series of hornblende-biotite gneiss, garnet-hornblende gneiss and biotite-amphibolites.

2.3 Plutonic Rocks

The Grünau Terrane consists of 10 different meta-plutonic suites, whereas the Bladgrond Terrane consist of only 2 in the study area (Figure 2-1, Figure 2-24). Praekelt (1984) describes that the sediments of the Driekop Group “float in a sea” of intrusive rocks.

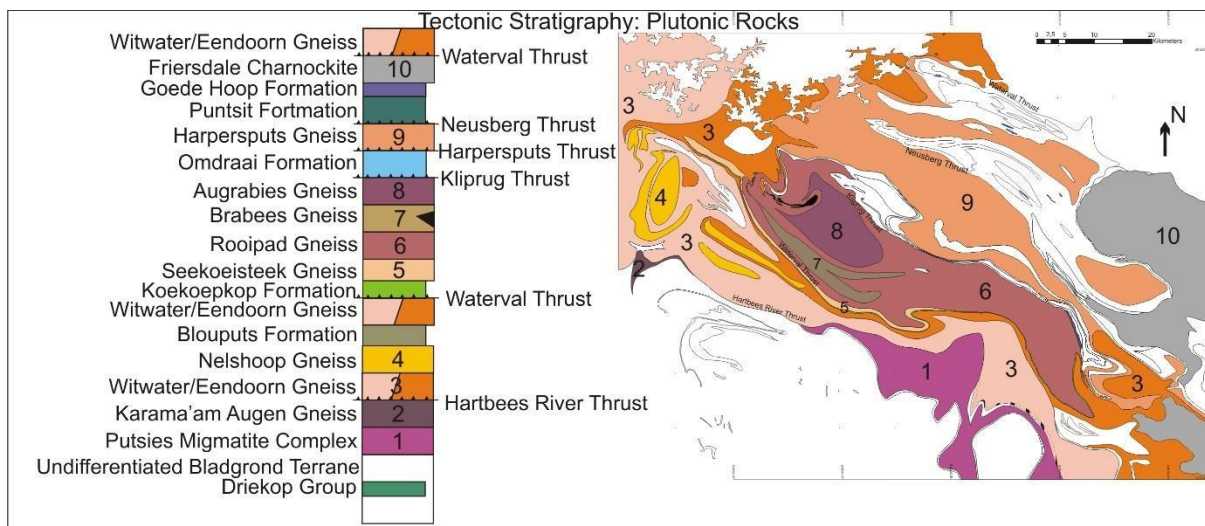


Figure 2-24: Structurally controlled stratigraphic profile of the study area. The map displays the outline and distribution of the plutonic rocks. Profile is not to scale.

2.3.1 Plutonic Rocks – RK-MS

2.3.1.1 Augrabies Gneiss

The Augrabies gneiss (Figure 2-25) is the most prominent (and well known) sheet-intrusive in the Augrabies area due to the large exfoliation domes that extrude from the flat surrounding areas (Figure 2-26). The Augrabies gneiss is referred to as the Pink Gneiss by Von Backström (1964), but was first mapped as a separate granitic body by Praekelt (1984).

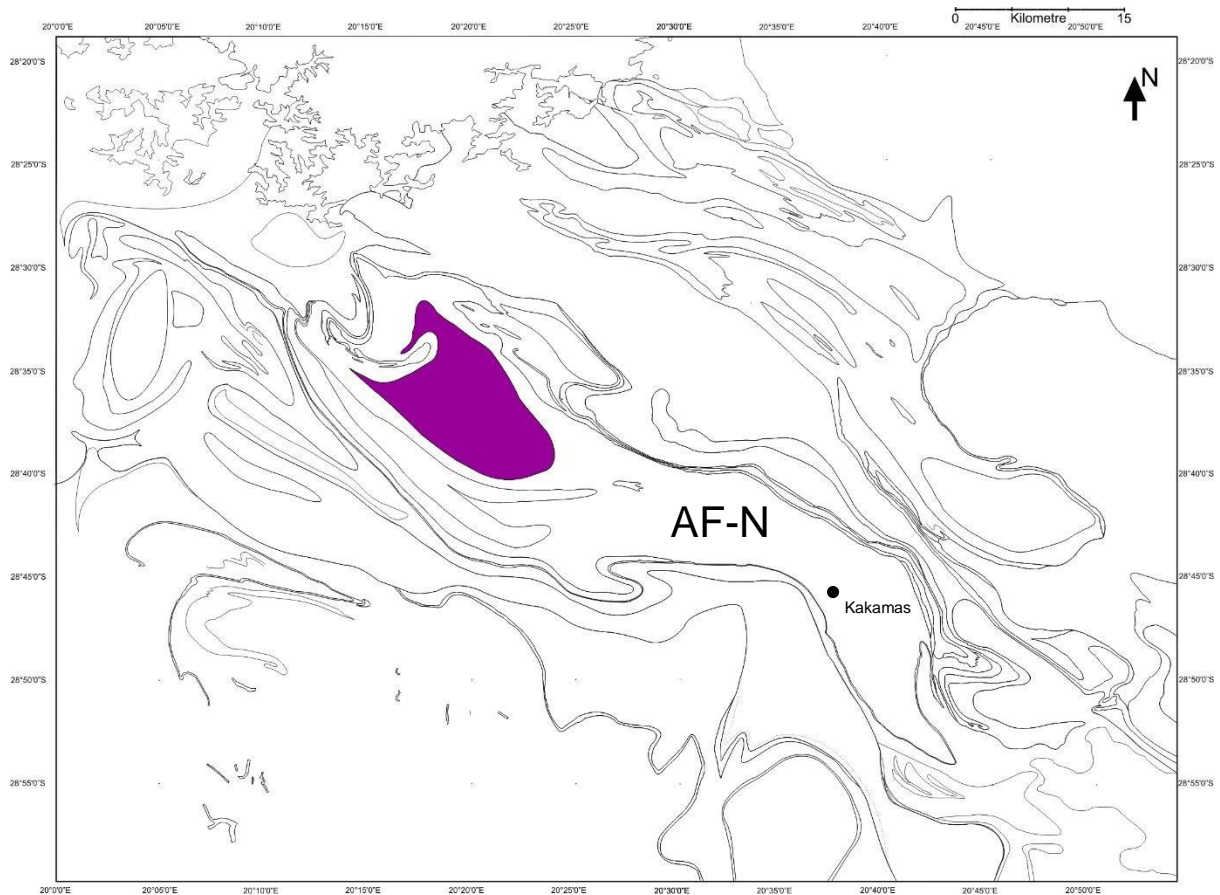


Figure 2-25: Stratigraphic distribution of the Augrabies gneiss.

Augrabies gneiss has a limited distribution and can only be found in the centre of the Augrabies Sheath Fold as a deformed thrust sheet (Figure 2-25), it is totally enveloped by the Rooipad gneiss with a lit-par-lit contact relationship between the two plutonic lithologies. The Augrabies gneiss has an emplacement age of 1168 ± 6 Ma (Colliston, et al., 2015).



Figure 2-26: Moonrock; an example of an exfoliation dome in the Augrabies Falls National Park ($28^{\circ}35'51.60''S$ $20^{\circ}18'59.86''E$)

Augrabies gneiss is a medium to coarse-grained, foliated, biotite (2%) - hornblende (12%) - plagioclase (18%) - quartz (29%) - K-feldspar (36%) gneiss (Colliston, et al., 2015). The gneiss often displays schlieren (Figure 2-27) ranging from centimetre to metre scale. The schlieren structures are concentrated mafic minerals, dominantly hornblende (Figure 2-27A, D). A “wavy” foliation in the Augrabies gneiss is defined by the alignment of amphibole and minor biotite. The “wavy” effect seen in the foliations is caused by two sets of conjugate shear zones (Figure 2-27B. Refer to section 3.3.6 for details on crosscutting shear zones). Moen (2007) states exfoliation domes are as a result of the wavy fabric.

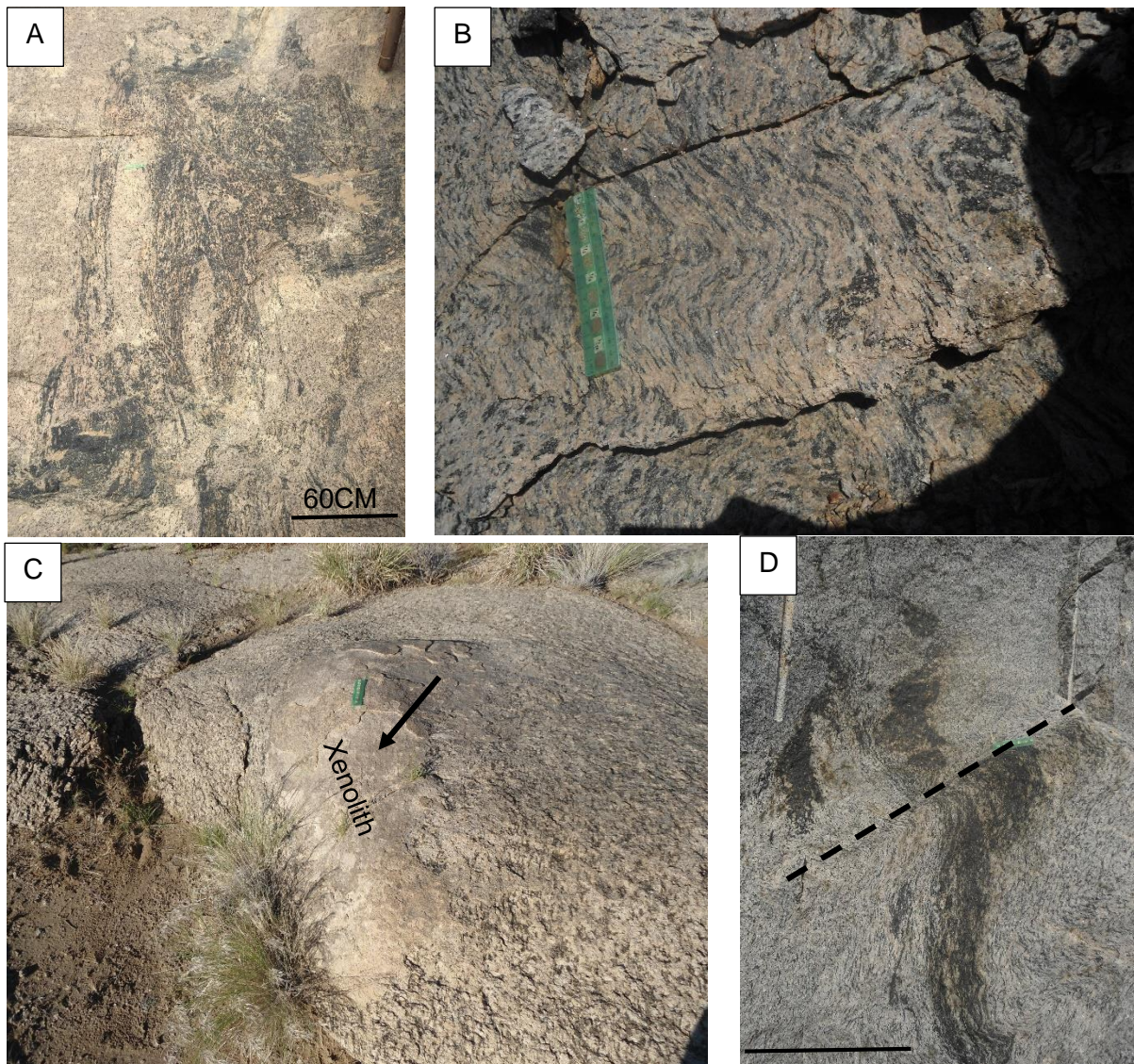


Figure 2-27: Augrabies gneiss. A: Schlieren structures in the gneiss range from millimetres to meter. B: Wavy foliations formed by late shear zones (D4). C: Elliptical shaped fine-grained quartz-feldspar-biotite gneiss xenolith (arrow); xenoliths come in a variety of shapes and sizes, with composition mostly of quartz-feldspar-biotite and hornblende. D: Schlieren structures pre-dates the D4 shearing (shear zone indicated by dashed line).

Xenoliths with various composition are found sporadically throughout the gneiss, the most common xenoliths are rounded to elliptical shaped fine-grained amphibole-biotite-feldspar-quartz gneiss (Figure 2-27C). Praekelt (1984) notes that enclaves of 100-500m are found within the Augrabies gneiss, but during the current study only xenoliths on metre scale were observed. The contact between xenoliths and host gneiss are defined by a concentration in mafic minerals and can rather be interpreted as a transitional zone (<1cm to 3cm wide) between xenolith and host. The concentration of mafic minerals is ascribed to the process of assimilation during regional metamorphism. The origin of the xenoliths are unknown but they do provide evidence for an intrusive origin.

2.3.1.2 Rooipad Gneiss and Harpersputs Gneiss

The two largest granitic lithologies within the RK-MS are for the first time separated and mapped as individual granites, namely the Rooipad gneiss and Harpersputs gneiss. In previous literature the two granites were inferred to be one lithology with compositional variations. The gneiss was termed the Wolfkop Gneiss by Van Bever Donker (1980) who did not define an origin for the gneiss, but mentions a compositional and textural difference. Praekelt (1984) called the gneiss the Rooipad Granite and states that it has a plutonic origin; Moen (2007) gave the term Riemvasmaak Gneiss and explains that it can either be a pre-tectonic or a syntectonic granitoid. Other authors regarded the two granite gneisses to have a sedimentary origin; it was termed Pink Gneiss by Von Backström (1964) who considered it to be sediments of the Kaaie Series. Geringer (1973) called the gneiss the Riemvasmaak Formation and interpreted it to be metasediments of the Namaqua Mobile Belt.

In this study, the the Rooipad and Harpersputs gneisses are separated due to the following reasons: Rooipad gneiss is defined by an augen texture with augens less than 30mm; whereas Harpersputs gneiss only carries the development of augen locally with the coarse K-feldspar augen up to 80mm. The Harpersputs gneiss is also coarser-grained and often displays pencil weathering. The ratio of mafic to felsic minerals is less for Harpersputs gneiss than for Rooipad gneiss, making Harpersputs gneiss more of a leucocratic granite (1-3%). The two gneisses are never in contact, they are separated by two intra-terrane thrusts and the Vaaldrift Sheath Fold. Their distribution through the RK-MS is different and represents two individual thrust sheets. The intrusive nature of the two gneisses has been defined by the ubiquitous display of xenoliths both locally and regionally. It is however deduced that the two sheets intruded more or less at the same time.

2.3.1.2.1 Rooipad Gneiss

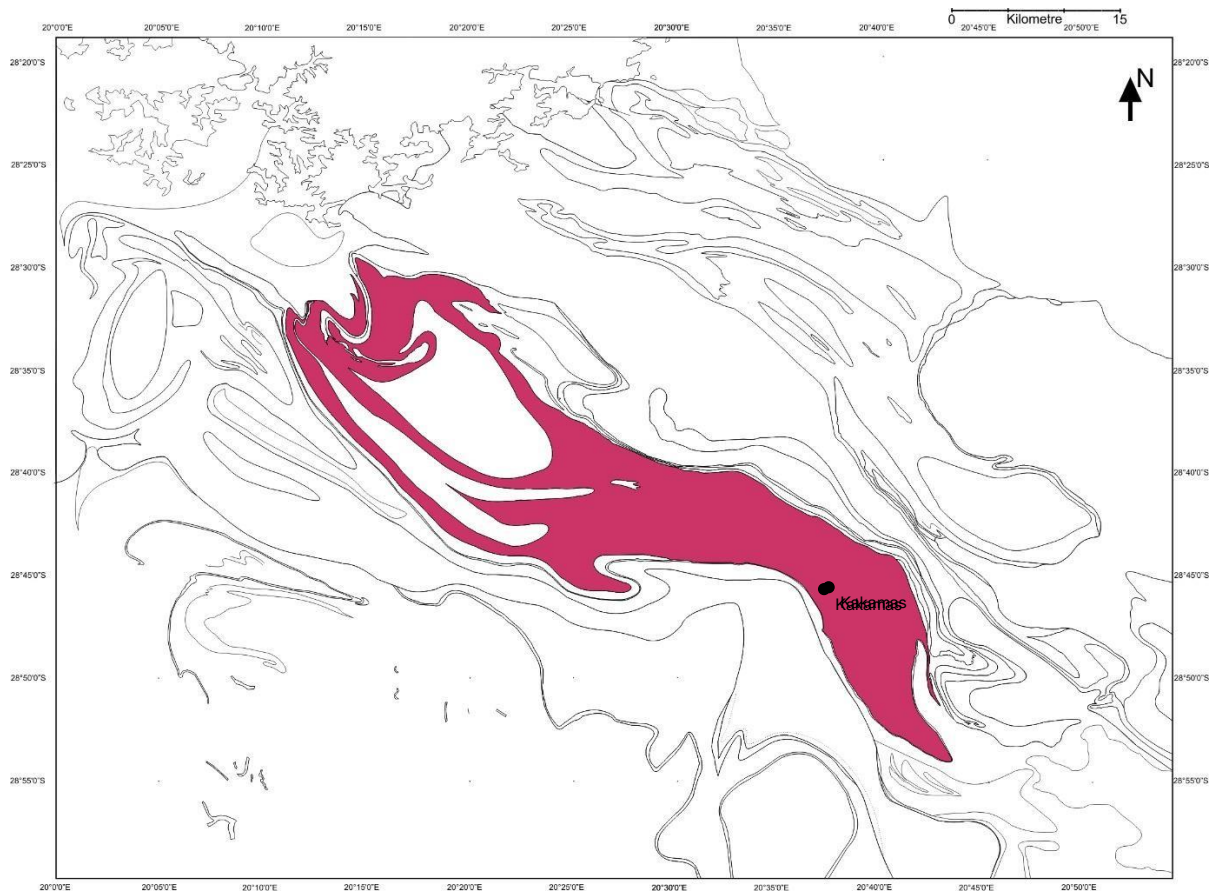


Figure 2-28: Stratigraphic distribution of the Rooipad gneiss.

The Rooipad gneiss can be classified as well foliated, medium to coarse-grained hornblende-plagioclase-biotite-feldspar-quartz augen gneiss. The augen consist of K-feldspar and lie within the foliation and range from 3mm to 30mm in width. The foliation is defined by the alignment of mafic minerals and the intermediate axes of augens; the long axis of the augen lies within the foliation plane or obliquely to it. The elliptical shaped augens are stretched and flattened in areas of high oblate dominated strain.

Lens and lenticular shaped xenoliths of feldspathic gneiss, biotite gneiss and amphibole-biotite gneiss are scattered throughout Rooipad gneiss, the xenoliths can range from centimetre to decametre scale. The origin of these medium to fine-grained gneisses is unknown. One xenolith with a tabular shape (10 x 1.5m) is interpreted to represent the quartzites of the 3# stratigraphy from the Omdraai Formation, Praekelt (1984) also suggests xenoliths originated from the Omdraai Formation. The lenticular shaped xenoliths are orientated parallel to the regional foliation whereas some of the lens/oval shaped xenoliths are orientated at an angle to the regional fabric but the fabric cuts through the xenolith. (Figure 2-29A) Assimilation during

metamorphism caused gradational contacts between Rooipad gneiss and xenoliths as well as the concentration of dark minerals. Small pockets of concentrated mafic minerals suggest that the Rooipad gneiss underwent melting (Figure 2-29B, C), but the augens were not affected by the partial melting. In other localities two phases of leucosomes cuts across the Rooipad gneiss.

The distribution of Rooipad gneiss is controlled by the shape and the size of the Augrabies Sheath Fold (Figure 2-28). Enveloped within the western portion of Rooipad gneiss is the kilometre scale mushroom structure consisting of Brabees gneiss and the smaller Oranjekom Complex sheath fold. Along the south-western margin the Rooipad is overlying the Seekoeisteeek gneiss as well as the Koekoepkop Formation, along the north-eastern margin it is overlain by Vaaldrift Sheath Fold (#3 of Omdraai Formation). The above mentioned contact zones along the margins of Rooipad gneiss are sharp tectonic decollements but an intrusive relationship exists between the Augrabies gneiss and Rooipad gneiss where “tongues” of Rooipad gneiss intruded into the Augrabies gneiss (Figure 2-29D). This intrusive relationship indicates that Rooipad gneiss is younger than Augrabies gneiss; this structural age relationship is supported by the isotopic work Colliston et al. (2015) which resulted in emplacement ages for the Rooipad gneiss at 1155 ± 7 Ma and the Augrabies gneiss at 1168 ± 6 Ma (Peterson, 2008 dated the Riemvasmaak gneiss at 1151 ± 14 Ma and according to the coordinate position the sample was taken in the Rooipad gneiss and not Harpersputs gneiss). The xenoliths and intrusive relationships characterise the Rooipad gneiss as a having an intrusive origin.

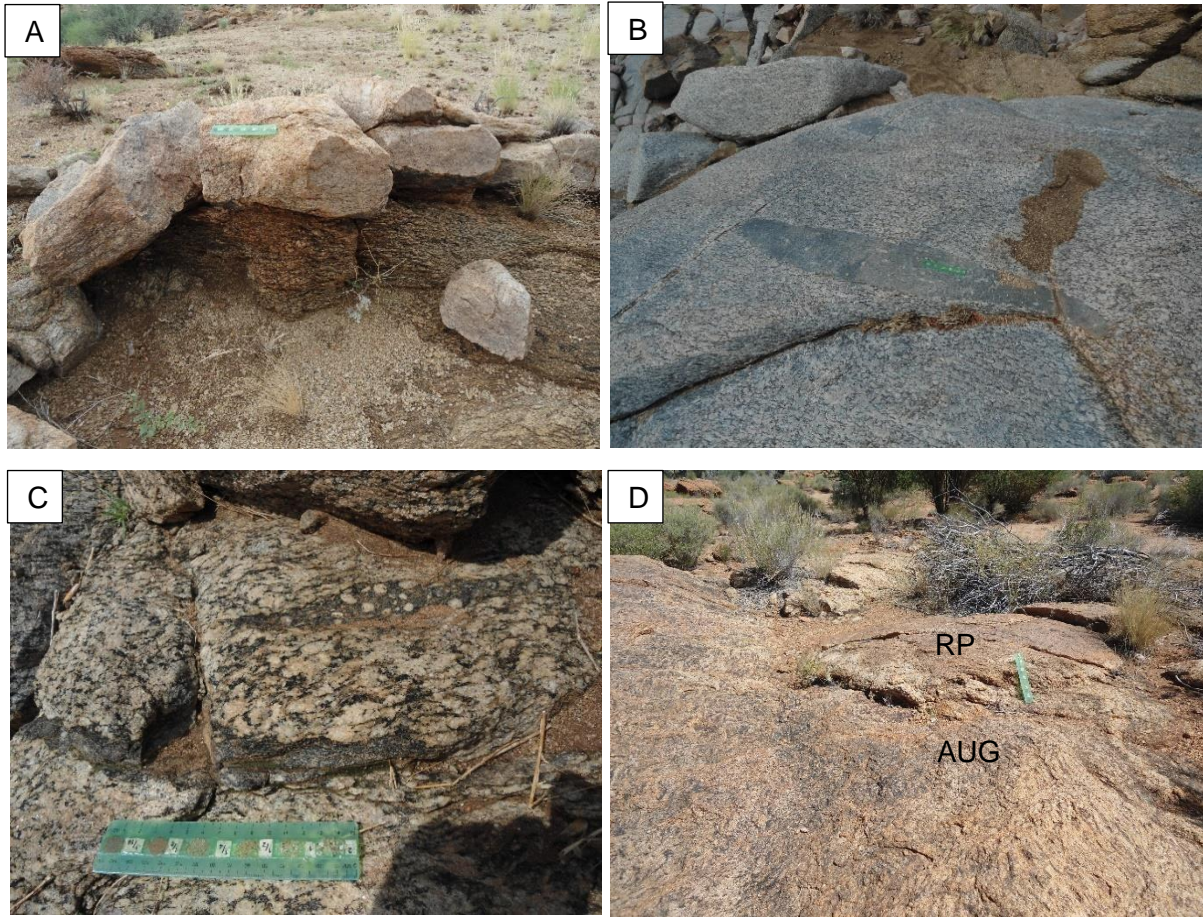


Figure 2-29: Rooipad gneiss. A: metre scale feldspathic gneiss xenolith in the Rooipad gneiss (flat-lying regional foliation). B/C: Incipient melting of Rooipad gneiss with quartz-feldspar porphyroblasts growing across biotite-amphibole gneiss xenolith. D: lit-par-lit intrusive relationship between the Augrabies gneiss (AUG) and Rooipad gneisses (RP); a tongue of Rooipad gneiss intruded into the Augrabies gneiss, indicating that the Rooipad gneiss is younger than Augrabies gneiss.

2.3.1.2.2 Harpersputs Gneiss

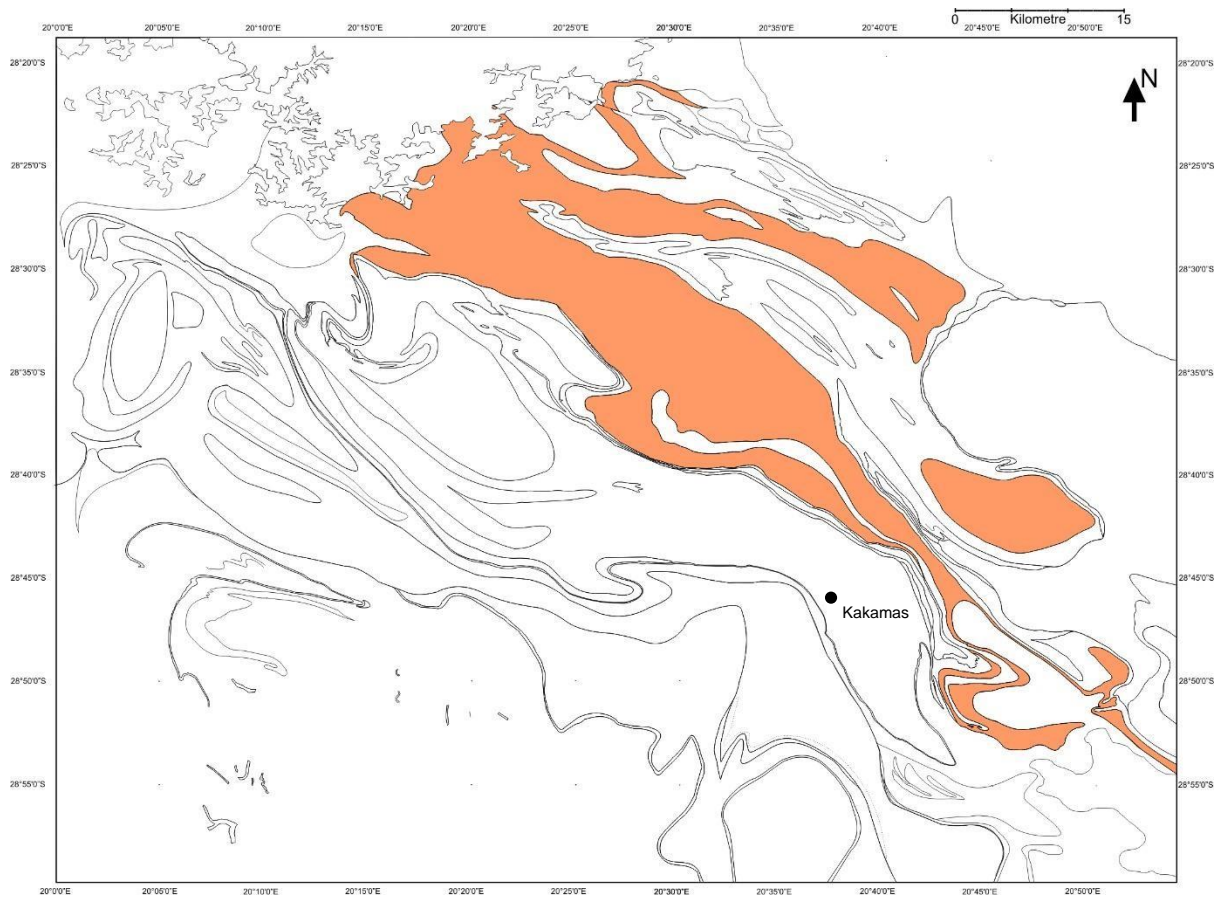


Figure 2-30: Stratigraphic distribution of the Harpersputs gneiss.

The Harpersputs Gneiss is the largest of the granitic bodies within the RK-MS and has a wide distribution (Figure 2-30). Harpersputs gneiss is a medium to coarse-grained biotite-feldspar-quartz gneiss with a well-developed foliation. It is overlain in the northern section by the Puntsit and Goede Hoop Formations, on the southern boundary the Harpersputs gneiss overlies the Vaaldrift sheath fold. Harpersputs gneiss closes off in the north-west and south-east in isoclinal fold closures within the Eendoorn gneiss. In the western portion Harpersputs gneiss wedges out along the underlying Waterval thrust.

Geringer (1973) and Von Backström (1964) interpreted Harpersputs gneiss to have a meta-sedimentary origin; Geringer (op.cit.) mentions that the rock contains porphyroblasts (K-feldspar augens) in certain localities. The Harpersputs gneiss is however classified as having an intrusive origin due to xenoliths and lit-par-lit contact relationships. Moen (2007) is also in agreement with Harpersputs gneiss having an intrusive origin.

On the farm Afdraai (20°27'3.78"E; 28°36'15.10"S) lenticular shaped xenoliths are found along the contact but it could not be established whether the xenoliths originated from the Omdraai

Formation (Figure 2-31A). The xenoliths are orientated parallel to the regional foliation, the foliation also cuts through the xenolith. Elsewhere fine-grained biotite-feldspar-quartz gneiss xenoliths of unknown origin are scattered through Harpersputs gneiss that range from centimetre to metre scale, all having tabular or lenticular shapes orientated parallel to the regional foliation (Figure 2-31B). The contact with the Puntsit Formation is sharp in the southeast due to the effects of the Neusberg Shear Zone, but elsewhere the contact is sharp-concordant and no relationship could be established (poor outcrop).

In the north-west where Harpersputs gneiss is in contact with Eendoorn gneiss, Moen (2007) claims that the Harpersputs gneiss is intruded by Eendoorn gneiss, but no evidence is found to substantiate this statement. Eendoorn gneiss is an early-tectonic granite (~1200 Ma) whereas Harpersputs gneiss is a syn-tectonic granite (~1100 Ma). The Harpersputs gneiss contains two foliations with the oldest of the two defining the intrafolial isoclinal folds and the younger a co-planar foliation formed by hinge transpositioning.

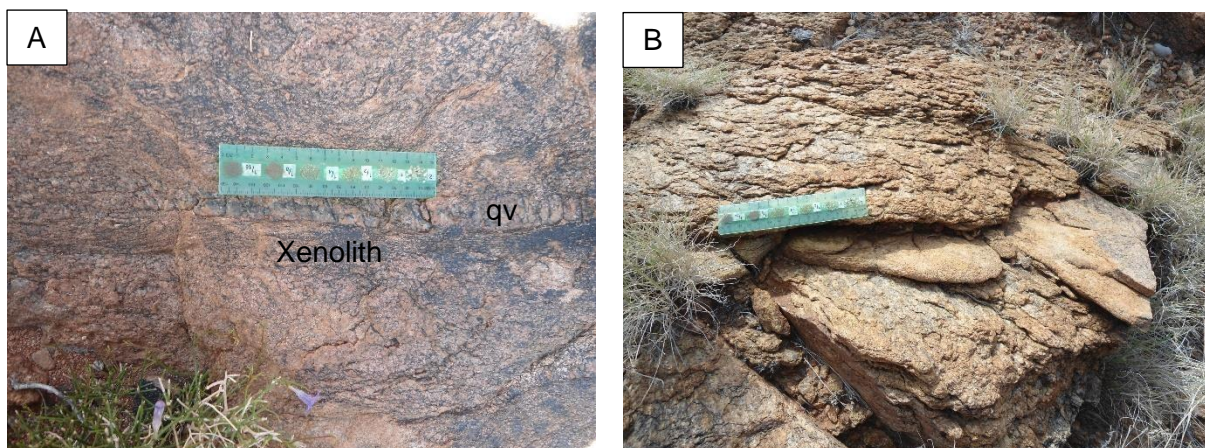


Figure 2-31: A: fine-grained quartz-feldspar-biotite gneiss xenolith within Harpersputs gneiss (below the quartz vein- qv), the xenolith is orientated at an angle to the regional foliation, which is transected by the Harpersputs gneiss foliation. B: lenticular shaped xenolith of fine grained quartz-feldspar-biotite gneiss within the foliation of Harpersputs gneiss. Both xenoliths (A and B) are overprinted by the regional foliation in the Harpersputs gneiss.

2.3.1.3 Brabees gneiss

Praekelt (1984) was the first and still the only author to date, who described the Brabees gneiss as an individual lithology and named it after the Brabees River on the farm Waterval. It occurs as a folded enclave in the Rooipad gneiss. The Brabees gneiss has the shape of large Ramsay Type 2 (mushroom structure) interference fold (Ramsay, 1967), with two fold closures towards the south and the northern closure being stretched out to a thin sliver (Figure 2-32).

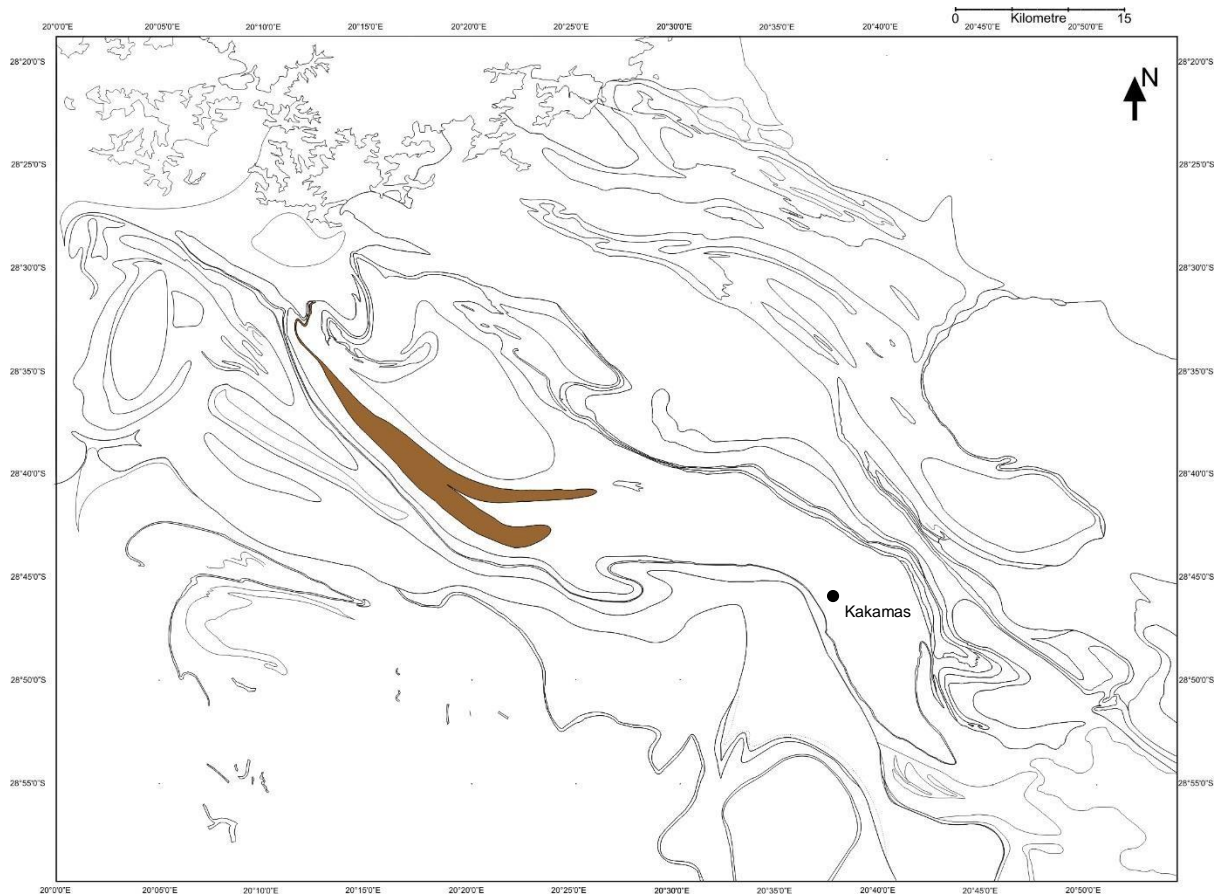


Figure 2-32: Stratigraphic distribution of the Brabees gneiss.

Brabees gneiss is coarse-grained, well foliated and contains sporadic porphyroblasts (mean size of 3mm). The foliation is defined by the alignment of hornblende nodules (Figure 2-33A) and individual growths of biotite and hornblende. It is the high concentration of hornblende and the small porphyroblasts that distinguishes the Brabees gneiss from Rooipad gneiss; Praekelt (op.cit.) states that the Brabees gneiss has very similar characteristics to the Rooipad gneiss, except for the concentrations of biotite and hornblende. Brabees gneiss consists of quartz, microcline, plagioclase, biotite and hornblende.

Xenoliths are scattered throughout Brabees gneiss they range from millimetre size to decametre size, the largest of the xenoliths was a lens shaped fine grained quartzite with dimensions of 100m x 1,5m (Figure 2-33B) . The smaller xenoliths of biotite-feldspar-quartz gneisses (some contain the porphyroblasts) are lens and lenticular shaped, they are orientated with long axes sub-parallel to the regional foliation; the foliation in the xenoliths is coplanar with the regional foliation in the gneiss. The xenoliths have the same composition as the Rooipad gneiss. The contact relationships between the Brabees gneiss and the Rooipad gneiss are sharp (Figure 2-33C) and no intrusive relationship was documented. However an

intrusive origin for the Brabees gneiss is deduced on the occurrence of xenoliths within the said gneiss.

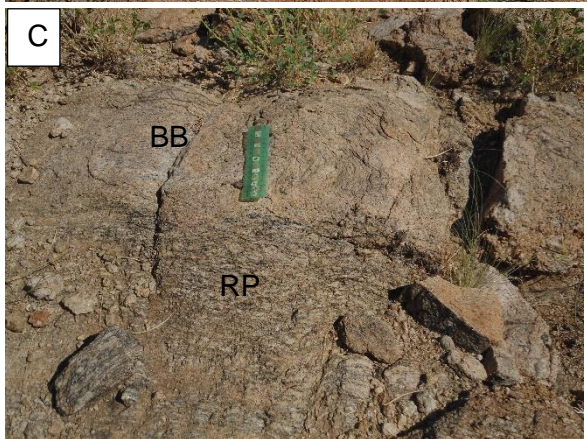


Figure 2-33: Brabees gneiss. A: hornblende nodules in the matrix; the nodules are equidimensional and orientated within the regional foliation. B: 100 x 1.5m feldspathic quartzite xenolith in situated within the regional foliation along strike of the Brabees gneiss; the foliation within the xenolith is co-planar with the regional foliation. C: sharp contact between Brabees gneiss (BB; upper) and Rooipad gneiss (RP; lower).

2.3.1.4 Seekoeisteeek gneiss

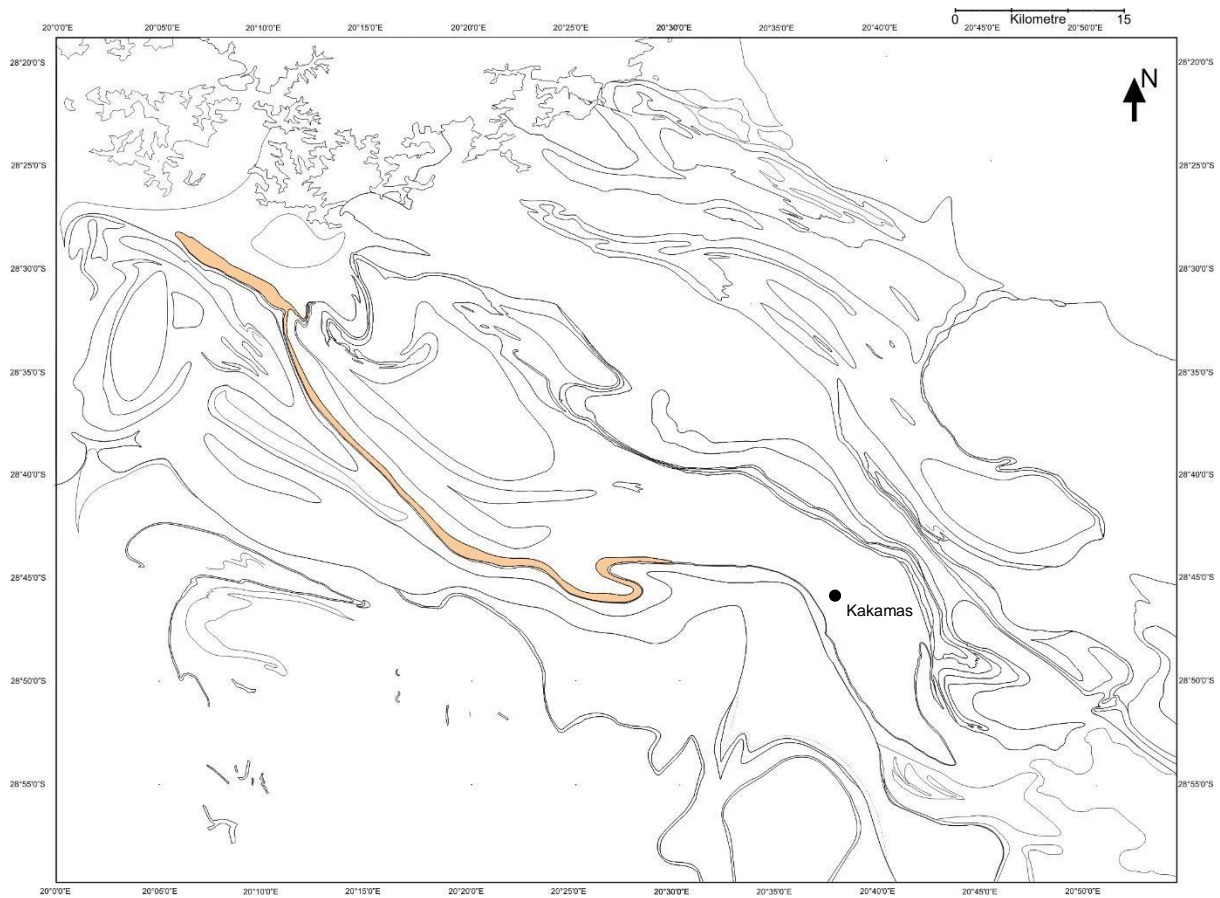


Figure 2-34: Stratigraphic distribution of the Seekoeisteeek gneiss.

The Seekoeisteeek gneiss is a plutonic rock situated in the hangingwall of a thrust and is interpreted to be part of the imbricate system associated with the Waterval thrust (Figure 2-34 and Figure 3-9 in Section 3.3.2). Seekoeisteeek gneiss was first described by Praekelt (1984), who is the first and only author to recognise it as a separate lithology, it was named after the farm Zeekoe Steek. Geringer (1973) mapped it as part of the Riemvasmaak Formation, Von Backström (1964) described it as part of the Pink Gneiss series. Moen (2007) did not differentiate between the Seekoeisteeek and Rooipad gneisses. In this study, the remapping of the area has vindicated Praekelt's (1984) mapping of the Seekoeisteeek and Brabees as separate gneissic sheets that deformed within the Rooipad gneiss.

The Seekoeisteeek gneiss is a well foliated fine to medium-grained gneiss consisting of quartz, feldspar, biotite and hornblende. Oval shaped porphyroblasts (10mm) occur sporadically throughout the gneiss, but less frequent compared to the other plutonites. A mineral banding of 2 – 100 mm in the Seekoeisteeek gneiss is defined by bands of biotite-hornblende within the matrix of hornblende-biotite-feldspar-quartz (Figure 2-35A). None of the other granitic rocks of the AF-N contains such a well-developed mineral banding. Small lenticular and lens shaped xenoliths of fine-grained biotite-feldspar-quartz gneiss and fine-grained feldspathic gneisses

are sporadically distributed through the Seekoeisteek gneiss; they are orientated with their long axes parallel to the regional fabric (Figure 2-35B). On average the xenoliths are less than 1m in length; a single large lens shaped feldspathic gneiss with dimensions of 6 x 1.5m was observed.

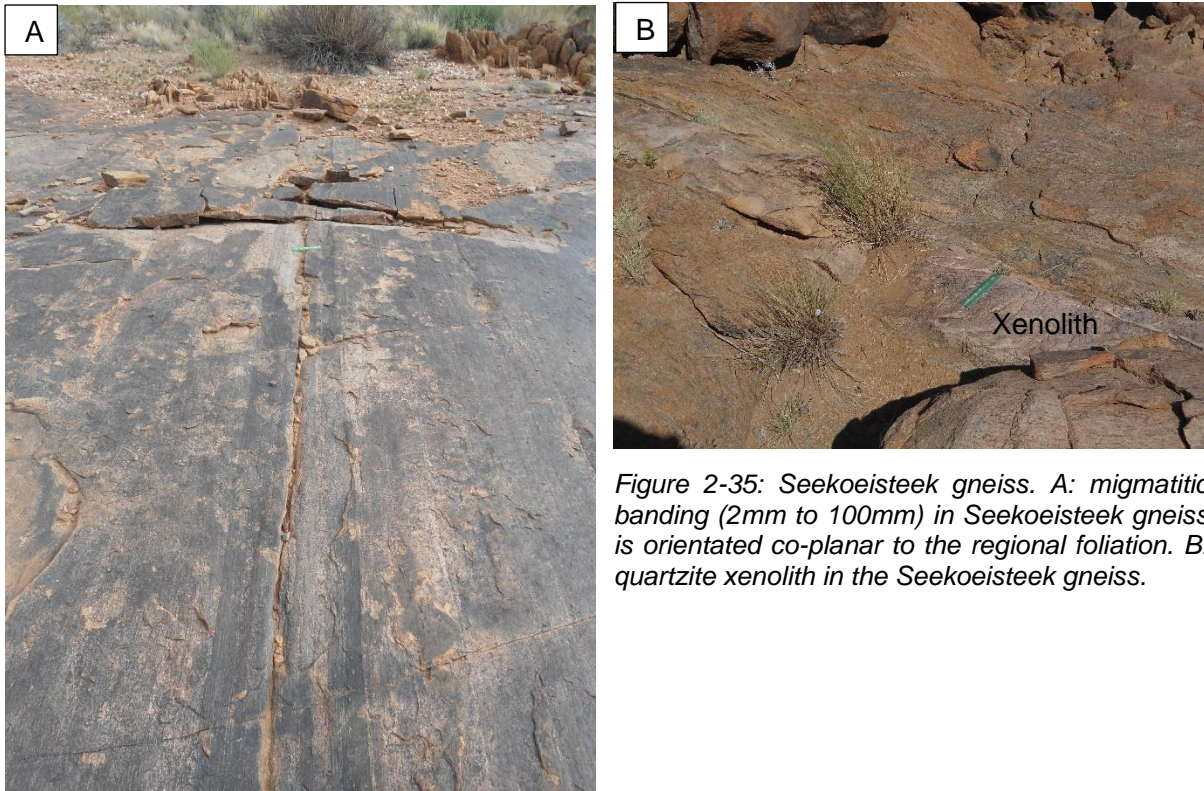


Figure 2-35: Seekoeisteek gneiss. A: migmatitic banding (2mm to 100mm) in Seekoeisteek gneiss is orientated co-planar to the regional foliation. B: quartzite xenolith in the Seekoeisteek gneiss.

2.3.1.5 Metagabbro and Anorthosite (Oranjekom Complex)

Enveloped within the northern parts of the Rooipad gneiss is the Oranjekom Complex (OKC), a large (8km x 600m) layered mafic body consisting of metagabbro and anorthosite. It was described by Moen (2007) as a basic intrusive consisting of metamorphosed gabbro, leucogabbro and anorthosite.

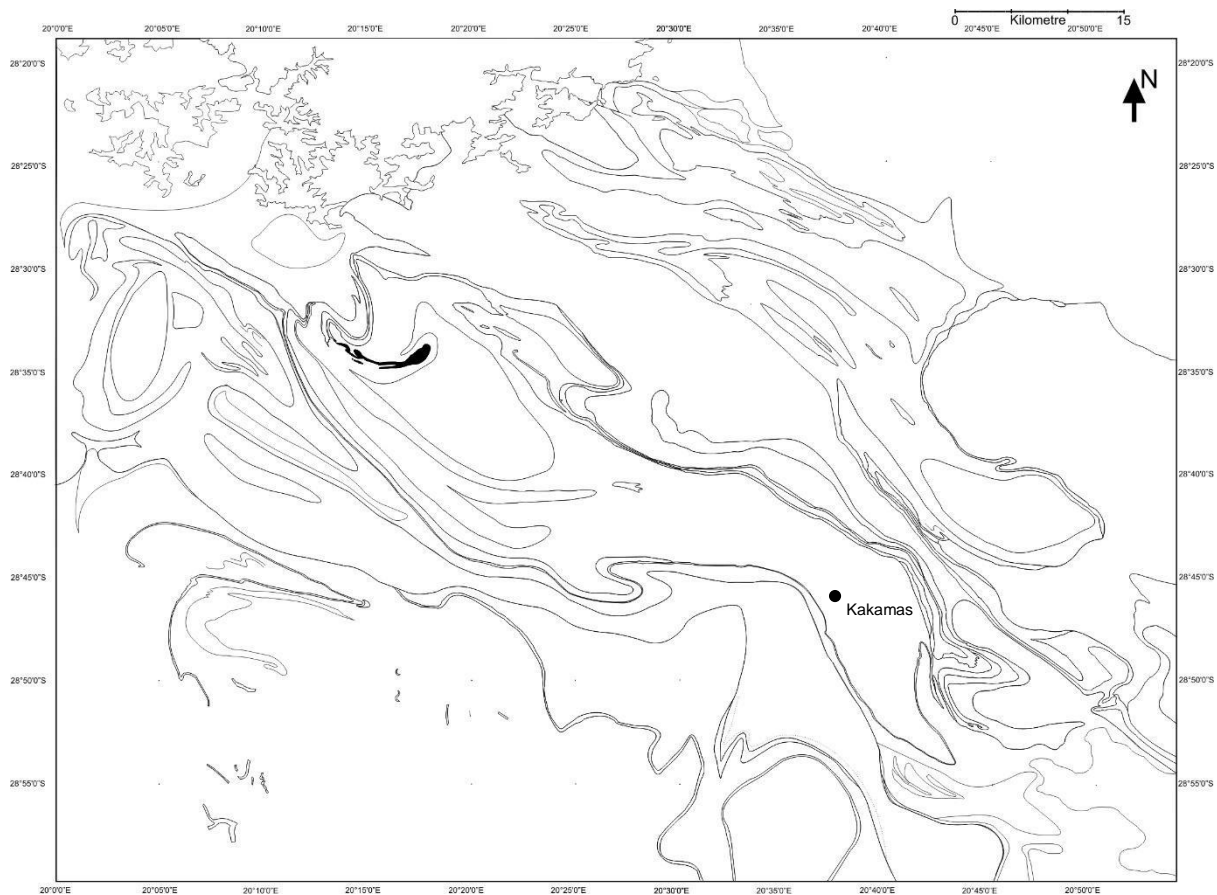


Figure 2-36: Stratigraphic distribution of the Oranjekom Complex.

Other authors described it as metagabbro and anorthosite (Praekelt, 1984), and as a layered metagabbro-anorthosite (Havenga, 1992; Kruger, et al., 2000). The rim consists of a well-foliated, fine grained metagabbro which alternates with anorthosites towards the centre, the core of the structure is a coarse grained metagabbro (Praekelt, 1984; Moen, 2007). Kruger, et al., (2000) mentions satellite plugs of the Oranjekom Complex east and west of the main body along strike of the regional fabric, but no other Oranjekom Complex bodies were found during the mapping. The Oranjekom Complex intrudes the Rooipad gneiss as a mafic sheet and is dated to have an emplacement age of 1095 ± 70 Ma (Kruger, et al., 2000); while Moen (2007) reports of an age of 1128 ± 45 Ma, which fits better with the tectonic framework of the area.

It is best seen from the Swartrante viewpoint in the Augrabies Falls National Park (Figure 2-36). The contact relationship between the Rooipad gneiss and Oranjekom Complex is sharp, the two lithologies have been deformed together. Havenga (1992) describes xenoliths (lenses) of Rooipad gneiss within the Oranjekom Complex ranging from 10cm to 4m which occur near the contact zones. Xenoliths of quartzite are sporadically found through the metagabbro and range from centimetre to metre scale (Figure 2-37B). The contacts between the xenolith and

host rocks forms an assimilation zone. The xenoliths are mostly lens shaped with intermediate axis orientated parallel to the regional foliation.

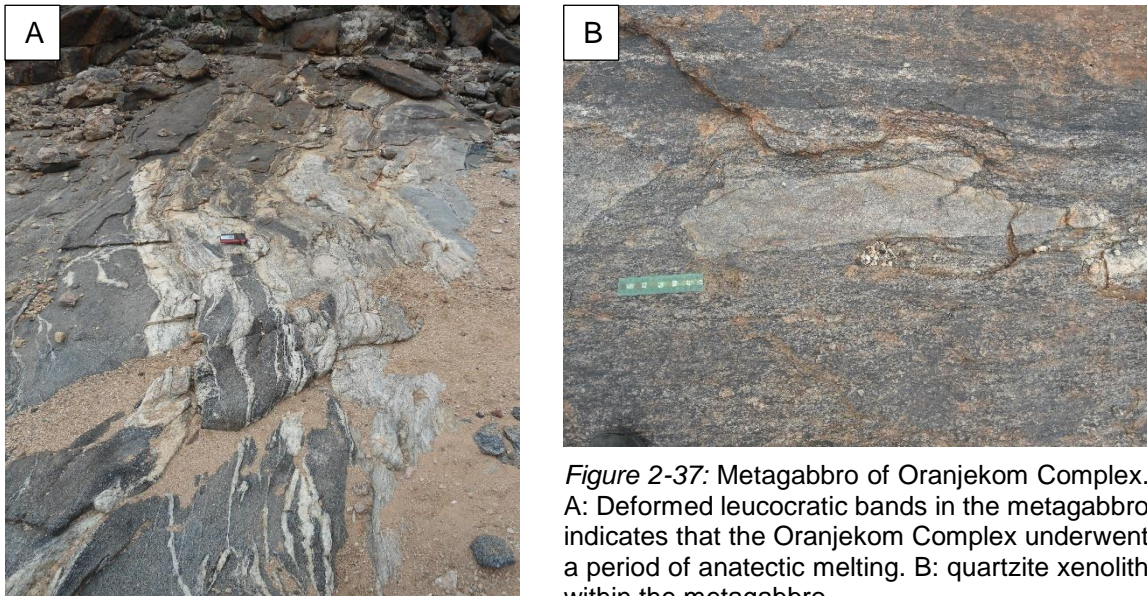


Figure 2-37: Metagabbro of Oranjekom Complex. A: Deformed leucocratic bands in the metagabbro indicates that the Oranjekom Complex underwent a period of anatectic melting. B: quartzite xenolith within the metagabbro.

2.3.1.6 Friersdale Charnockite

The youngest of the plutonic rocks is the Friersdale Charnockite, it was first referred to as the Charnockitic Adamelite-Porphry (Von Backström, 1964), and Van Bever Donker mapped it as the Warm Zand Charnockitic Adamelite. For the purpose of this study the nomenclature of Moen (2007) will be used which refers to it as the Friersdale Charnockite. Cornell, et al. (2012) states that the Friersdale Charnockite is an undeformed mafic-felsic hybrid rock which was emplaced after the juxtaposition of terranes; field relationships and the characteristics of the lithology are in agreement with this statement. The lithology is however recorded to be undeformed but regional mapping of the area shows that the bodies do contain a foliation, albeit a weak one defined by the alignment of mafic minerals (biotite and hornblende).

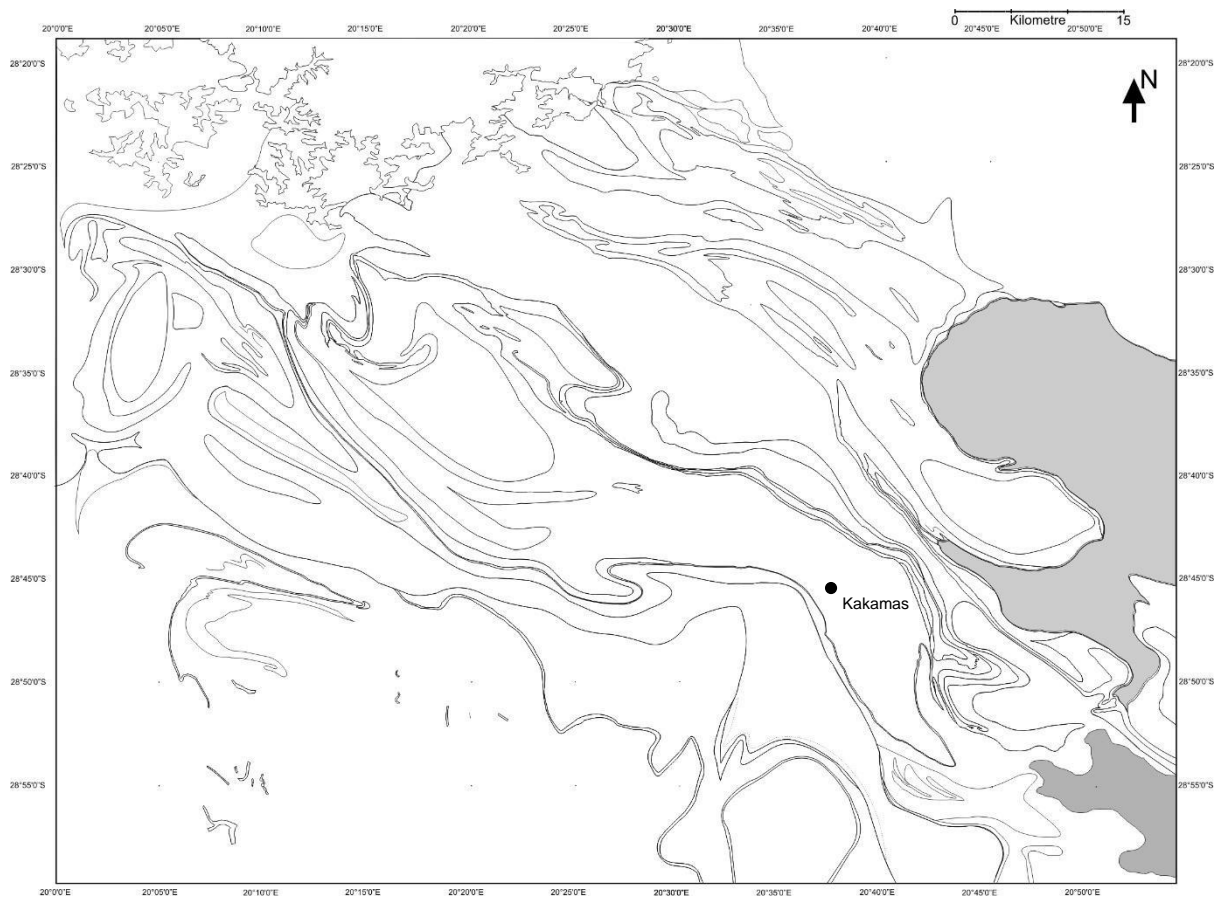


Figure 2-38: Stratigraphic distribution of the Friersdale Charnockite.

The distribution of the Friersdale Charnockite also indicates that it post-dates the formation of the RK-MS; the main body is situated in the hinge zone of a mega scale sheath fold (Figure 2-38). A second body of Friersdale Charnockite intrudes the Eendoorn gneiss and Blouputs Formation on Middel Post. The Friersdale Charnockite was interpreted as a phacolith (Von Backström, 1964) due to the magma intruding into the synclines and anticlines of the large sheath folds; thus the shape and distribution of the Friersdale Charnockite is controlled by fold structures. A phacolith was first described by Haker (1909) as a concordant intrusive body introduced concurrently with folding.

The contacts between the charnockite and the surrounding lithologies are variable and can be: concordant to sharply discordant, have chilled margins, transgressive or cross-cutting (Von Backström, 1964; Moen, 2007). According to Moen (2007) along the transgressive contacts, in the reaction aureoles new minerals have formed, Von Backström (1964) records no effects along the concordant boundaries.

Moen (2007) classified the Friersdale Charnockite as a monzogranite with average modal composition of quartz (28%), plagioclase (29%), K-feldspar (23%), biotite (7%), orthopyroxene (1%), clinopyroxene (3%) and hornblende (5%). Xenoliths of exotic mafic and leucocratic

lenses, blocks of feldspathic quartzite as well as calc-silicate rocks with varying shapes and sizes are commonly seen throughout the charnockite (Van Bever Donker, 1980). Blue quartz is a unique characteristic of the Friersdale Charnockite and is formed by ilmenite needles with equal Fe and Ti (Cornell, et al., 2012). Two samples of the Friersdale Charnockite gave weighted mean ^{207}Pb - ^{206}Pb ages for concordant magmatic zircon, with a magmatic crystallisation age for the Friersdale Charnockite at 1080 ± 13 Ma (Cornell, et al., op.cit).

2.3.2 Plutonic Rocks – Grünau Terrane

The rocks of the Grünau Terrane, excluding the RK-MS, consist of three major gneisses with magmatic origin, namely: Eendoorn, Witwater and Nelshoop gneiss. The Eendoorn gneiss is the oldest of the three and dates to a melting event in the Grünau Terrane that coincides with terrane accretion. The Nelshoop gneiss is interpreted as a sheet intrusive granite that intruded during the ~1100Ma event, during which all large sheet intrusive intruded the Grünau Terrane. The Witwater is a leucocratic granite that formed during a second melting event in the Grünau Terrane. The Witwater and Eendoorn are wrapped around the RK-MS, whereas the Nelshoop gneiss is contained within structures.

2.3.2.1 Eendoorn Gneiss

The Eendoorn gneiss is an early syn-tectonic megacrystic granite (Beukes, 1973; Geringer, 1973; Blignault, 1977; Du Plessis, 1979) and was first described by Beukes (op.cit) in the Warmbad area. Other authors referred to the Eendoorn gneiss by various names: Bakrivier and Kouroprivier granite (Geringer, 1973), Wolfkop Biotite Gneiss (Van Bever Donker, 1980), Eendoorn granite (Beukes, 1973; Du Plessis, 1979; Praekelt, 1984; Colliston, 1990), Megacrystic granite (Blignault, 1977; Nordin, 2009), Tsirob Gneiss (Jackson, 1976; Diener, et al., 2013), Porphyroblastic Grey Gneiss (Von Backström, 1964), and Moen (2007) refers to it as the Eendoorn Suite (sub-divided into: Donkieboud granite, Bak River granite, Twakputs gneiss and Bok-se-put gneiss). All of the above mentioned authors agree that the Eendoorn gneiss is a well foliated porphyroblastic granite. The Eendoorn gneiss has a wide distribution and is always associated with the north-west trending Grünau Terrane (Aus –Diener, et.al. (2013), Warmbad district- Beukes (1973), Augrabies – Praekelt (1984), Kakamas – Van Bever Donker (1980)). In the study area the Eendoorn gneiss surrounds the RK-MS; on the southern limb it forms the footwall sequence of the Waterval thrust. Along the northern boundary the Eendoorn gneiss overlies the Biesje Poort Sheath folds, and the hangingwall sequence of the overturned WVT (Figure 2-39; Appendix E). Eendoorn gneiss is classified as a biotite-feldspar-quartz-amphibole-garnet megacrystic gneiss; the K-feldspar megacrysts are oval shaped and

range from 10mm to 100mm in size (Figure 2-40A). They are orientated with their intermediate axis parallel to the strike of the foliation and the long axis oblique with the regional foliation. The feldspar megacrysts are primary structures of the Eendoorn gneiss considered to represent phenocrysts (Vernon, 1986). In high strain areas the ED contains a mylonitic fabric, draped around flattened and stretched megacrysts.

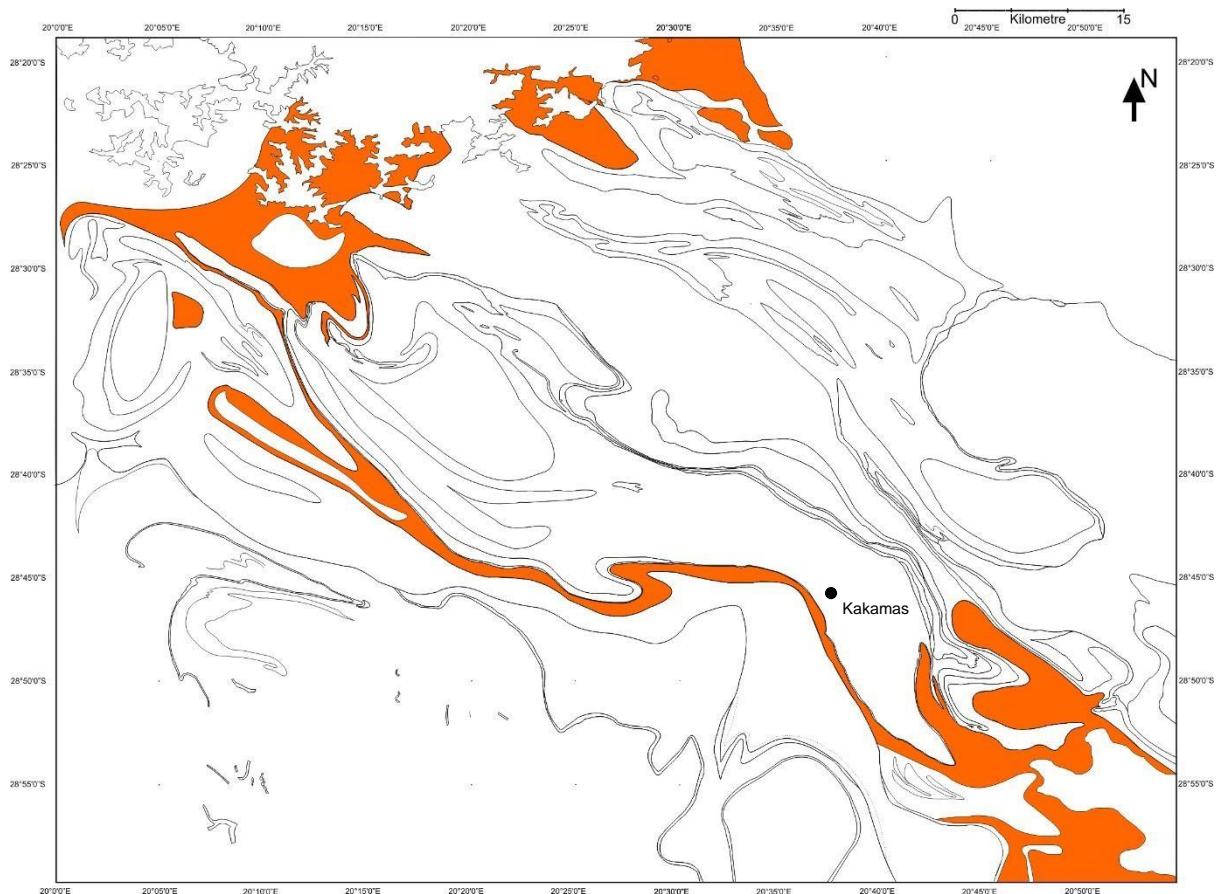


Figure 2-39: Stratigraphic distribution of the Eendoorn gneiss.

The Eendoorn gneiss is interpreted as a granite on the basis of its xenoliths and intrusive contact relationships (Figure 2-40F). The xenoliths have various sizes (centimetre to decametre scale) and composition. Flattened and stretched xenoliths of the Koekoepkop Formation and Blouputs Formation occur throughout the Eendoorn gneiss, with their long axes defining a stretch direction. The most frequent xenoliths are fine grained biotite-feldspar-quartz gneisses, amphibolites, biotite-amphibole gneiss and biotite schist (Figure 2-40E). Xenoliths of garnet bearing biotite gneiss, quartzites, amphibolites, biotite gneiss, aluminous gneiss, granulites and meta-sedimentary xenoliths are all described by above mentioned authors; Beukes (1973), Du Plessis (1979) and Geringer (1973) have interpreted the xenoliths as Blouputs Formation. The xenoliths of Koekoepkop Formation are only found in close proximity with the Koekoepkop Formation. An intrusive contact relationship (lit-par-lit) exist between

Eendoorn gneiss and the neighbouring lithologies (Geringer, 1973; Figure 2-40B). Eendoorn gneiss contains a well-developed regional fabric defined by the alignment of biotite and the intermediate axis of megacrysts. Regionally the Eendoorn gneiss contains centimetre to decametre scale leucocratic vein networks (Figure 2-40C and D) interpreted to represent anatectic melts, and was also observed by Praekelt (1984), Blignault (1977) and Du Plessis (1979). Where the melts form large bodies they resemble the Witwater gneiss. The presence of megacrysts and garnet is an important characteristic of the Eendoorn gneiss; two phases of garnet exists in the Eendoorn gneiss, one being syntectonic with second being post-tectonic.

The Eendoorn gneiss is one of the oldest granites of the area with an emplacement age of 1198 ± 7 Ma, this coincides with the first macroscopic scale anatectic melting (1204-1197Ma) observed in the Blouputs Formation (Nordin, 2009). This observation implies that the Blouputs Formation was the source of the Eendoorn gneiss. Diener (2013) suggests granulite facies metamorphism with peak metamorphic conditions at 825°C and 5.5kbar during this phase.

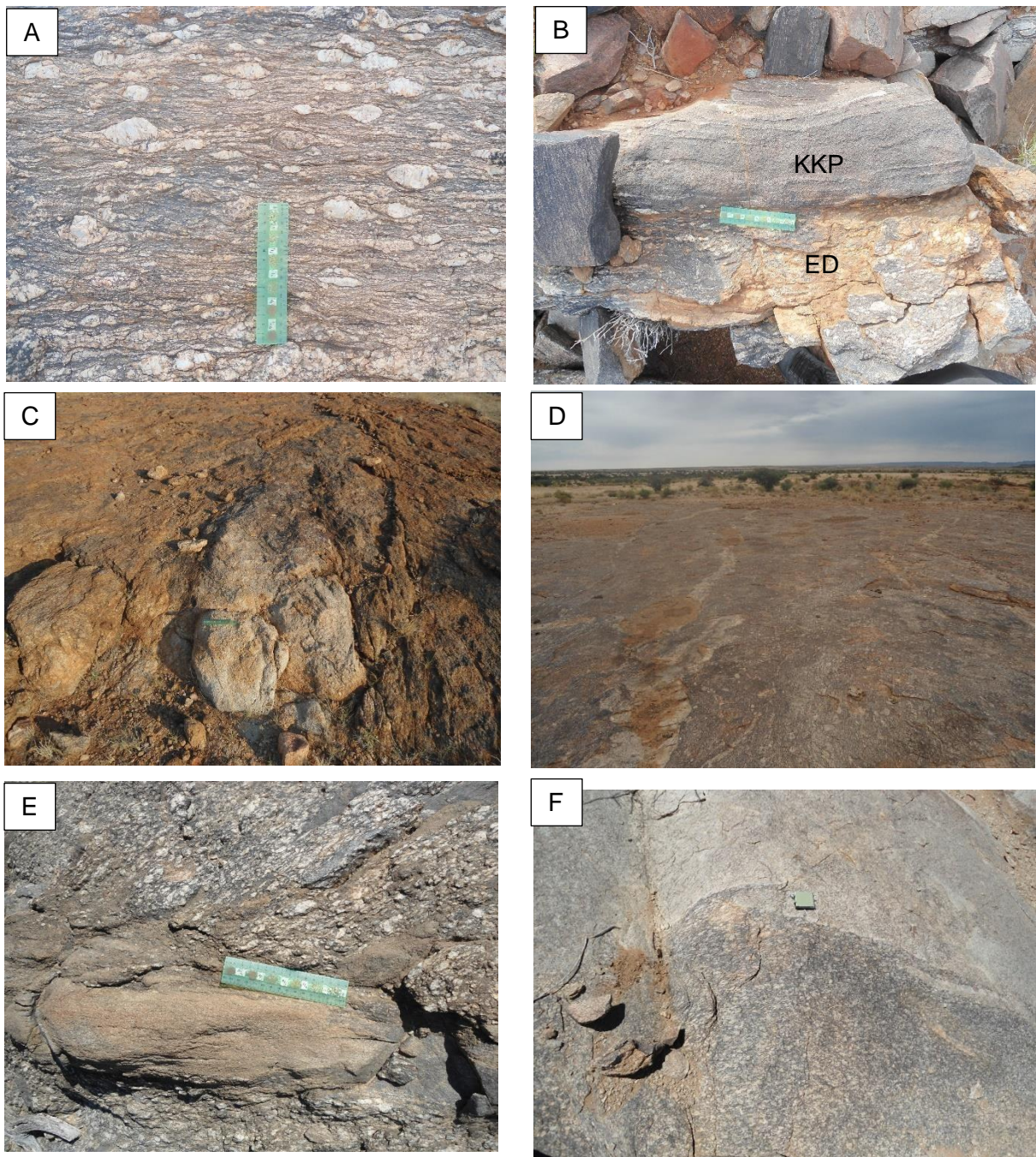


Figure 2-40: Features of the Eendoorn gneiss. A: General texture illustrated by the regional foliation on the yz plane (looking north –down dip), large (2 – 50mm) megacrysts situated with intermediate axis parallel to the strike of the foliation. The shape of the megacrysts indicates high strain and later shear (sigmoidal shape, dextral shear with top to the east). The foliation is defined by the alignment of biotite and megacrysts. B: The north dipping sharp contact between the Koekoepkop Formation (KKP) and Eendoorn gneiss (ED). The sharp contact is defined as the Waterval Thrust and represents a decollement. C/D: Sheets of Witwater gneiss intruding the Eendoorn gneiss during the second stage of kilometre scale anatexis of the Grünau Terrane (late sub-vertical north-west shear zone). E: Fine-grained quartz-feldspar-biotite gneiss xenolith with a pre-Eendoorn foliation, which is at an angle to the foliation in the Eendoorn gneiss. F: lit-par-lit intrusive relationship between Eendoorn gneiss and the Blouputs Formation (quartz-feldspar-biotite gneiss) with co-planar foliation relationships.

2.3.2.2 Witwater gneiss

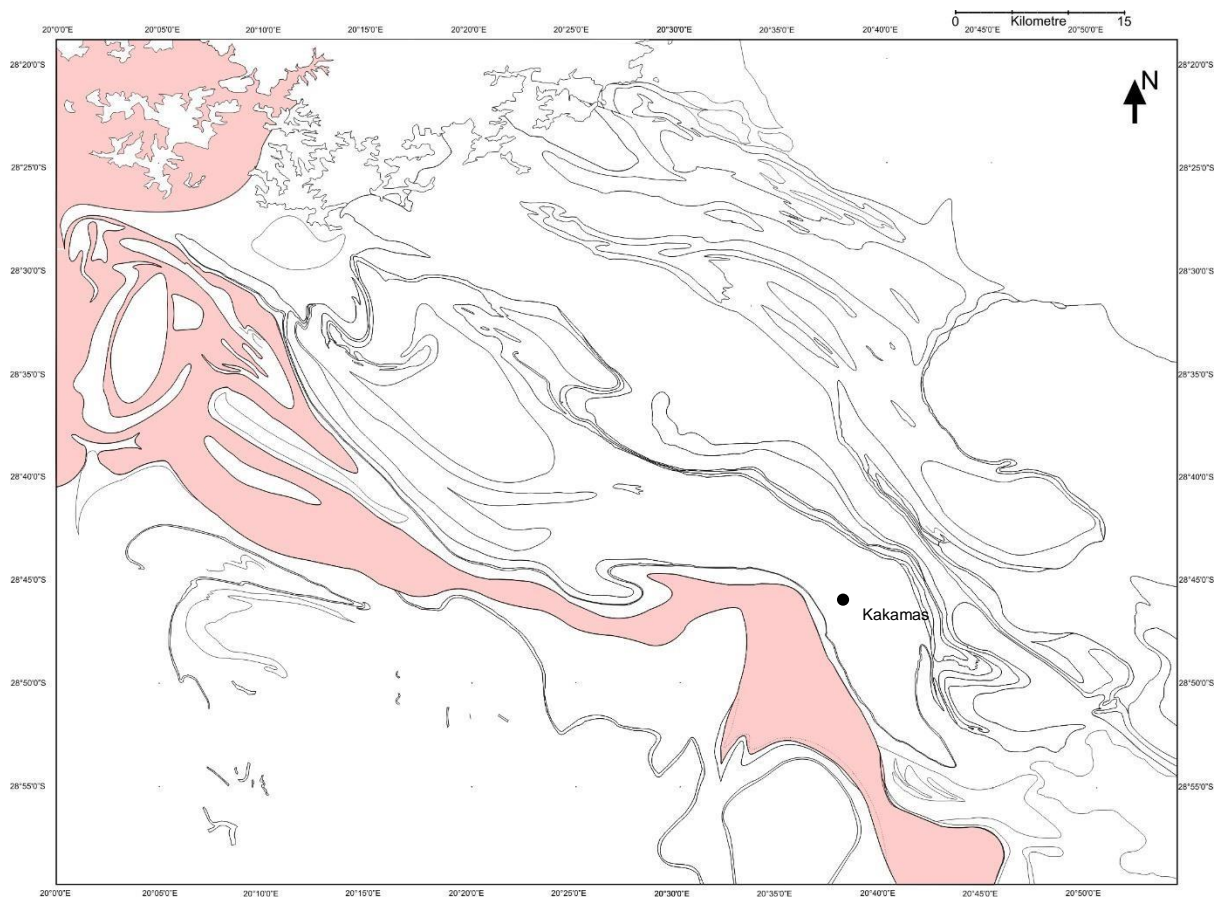


Figure 2-41: Stratigraphic distribution of the Witwater gneiss.

The Witwater gneiss is a coarse-grained leucocratic lithology classified as a sillimanite-garnet-quartz-feldspar pegmatitic gneiss which is closely associated with the Blouputs Formation and the Eendoorn gneiss (Figure 2-41; Appendix F). Large enclaves of Blouputs Formation (metre to decametre scale) and Eendoorn gneiss (enclaves in excess of 300m) have been mapped in throughout the Witwater gneiss. The Witwater gneiss can be megacrystic in some areas, and it is also the youngest of the lithologies associated with the Grünau Terrane, representing the second phase of anatexis in the Grünau Terrane. It has been mapped by various authors and interpreted as a pegmatitic granite. The term “Witwater” was first used by Du Plessis (1979), and adopted by Praekelt (1984). It was also mapped by various other authors: Von Backström (1964) mapped the Witwater Granite as a Grey Gneiss, Geringer (1979) refers to it as the Toeslaan Formation (interpreted to represent granulites having sedimentary origin) and Moen (2007) divided the Witwater gneiss into the Witwater gneiss and the Kenhardt Migmatite (Witwater gneiss grading into the Kenhardt Migmatite). Van Bever Donker (1980) did not differentiate between the Eendoorn gneiss and the Witwater gneiss. In the Aus area in southern Namibia the Witwater gneiss is referred to as the Kubub/Aus gneiss (Jackson, 1976; Diener, et al., 2013), having an emplacement age of 1123 ± 6 Ma (Diener, et al., 2013).

Beukes (1973) called it Warmbad Granite and explains that it is a late granite that cuts across and intrudes the Blouputs Formation, occurring as large dyke-like bodies; he also suggested that the Witwater gneiss is the product of anatectic melting of the supracrustals (in this area the Blouputs Formation is the equivalent). Field relationships and associations with the surrounding lithologies (Eendoorn gneiss and Blouputs Formation) agree with the argument of Beukes (op.cit) (as well as Du Plessis, 1979 and Praekelt, 1984), which suggests the Witwater gneiss is a late phase of melting of the Eendoorn gneiss, causing leucocratic fluids to spread throughout the lithologies (vein networks in Eendoorn gneiss and Blouputs Formation (Figure 2-42) and incorporating large xenoliths of both Eendoorn gneiss and Blouputs Formation. Beukes (op.cit.) suggested that the Witwater gneiss formed at a depth of 2-5kbar at 350-500°C in the Grünau Terrane.

The Witwater gneiss consists of quartz, microcline, and plagioclase with accessory garnet, biotite and sillimanite (Moen, 2007), sporadic megacryst averaging at 20mm (Figure 2-42A). Garnet is not always present in the granite but it is in some places the only ferromagnesian phase, suggesting the Witwater Granite may have crystallised from a “dry” magma at a temperature significantly higher than that required for the formation of “wetter” magmas (e.g. biotite-rich granites like the Eendoorn) (Du Plessis, 1979; Moen, 2007). Two sets of garnets occur in the Witwater gneiss: one being related to the regional fabric and the second is a post-tectonic growth. The Witwater gneiss is also observed in the Nelshoop sheath folds.

With the close association the Witwater gneiss has with the Blouputs Formation and Eendoorn gneiss (Figure 2-42B), a wide distribution can be expected, from Aus (Diener, et al., 2013) to Augrabies (Praekelt, 1984). In the study area it is situated between the Eendoorn gneiss and the Hartbees River Thrust (HBRT). A lit-par-lit contact relationship exists between the Witwater gneiss and all of the lithologies it is associated with. Du Plessis (1979) mentions that the Eendoorn and Witwater Granites are rarely concordant and the contacts are predominantly intrusive of nature.

The best exposures of the Witwater gneiss and its xenoliths/enclaves are seen on the farm Boesmansrivier (Regt Kyk 62) and the Augrabies Falls National Park. The xenoliths of sheath folds on Boesmansrivier (Regt Kyk 62) are on metre scale and consist of quartzites, biotite schist's, amphibolites and biotite-feldspar-quartz gneisses. The regional fabric of the Witwater gneiss and the fabric in the xenoliths are coplanar. The contact between Eendoorn gneiss and Witwater gneiss (Boesmansrivier farm; Regt Kyk 62) is characterized by a ~100m wide migmatite zone. The migmatitic phase is younger than Witwater gneiss as leucosomes cut both the Witwater gneiss and Eendoorn gneiss and is associated with a later shear zone that

strikes parallel to the contact. The regional fabric in the Witwater gneiss is defined by the planar arrangement of biotite laths and K-feldspar megacrysts (where present).

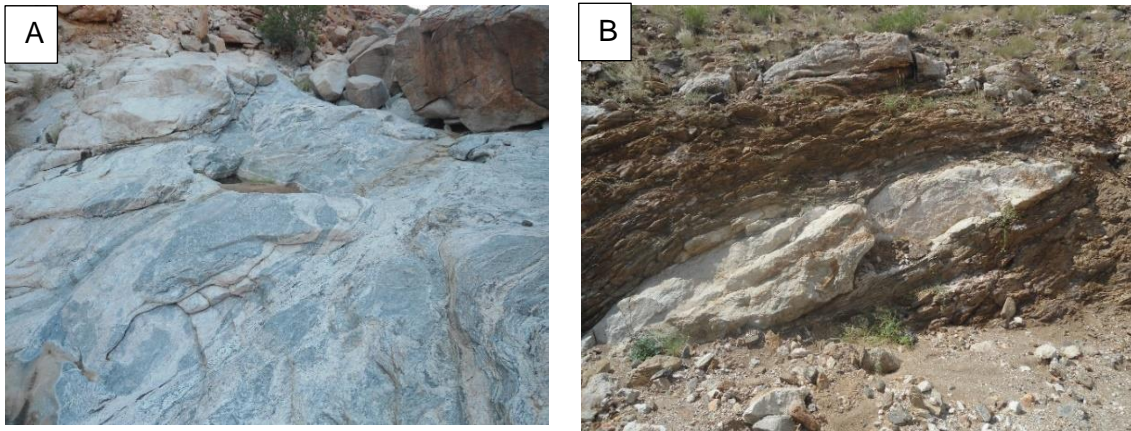


Figure 2-42: Witwater gneiss. A: large veins and melt sheets of Witwater gneiss intruding the Blouputs Formation; the dark patches represents paleosome of Blouputs Formation after the Grünau Terrane melted for the second time forming an anatectic melt (Witwater gneiss). B: A road cutting on the Blouputs Road shows a sheet of Witwater gneiss intruding the Blouputs Formation (biotite-amphibole-garnet gneiss) along the regional foliation with pinch-and-swell structure.

2.3.2.3 Nelshoop Gneiss

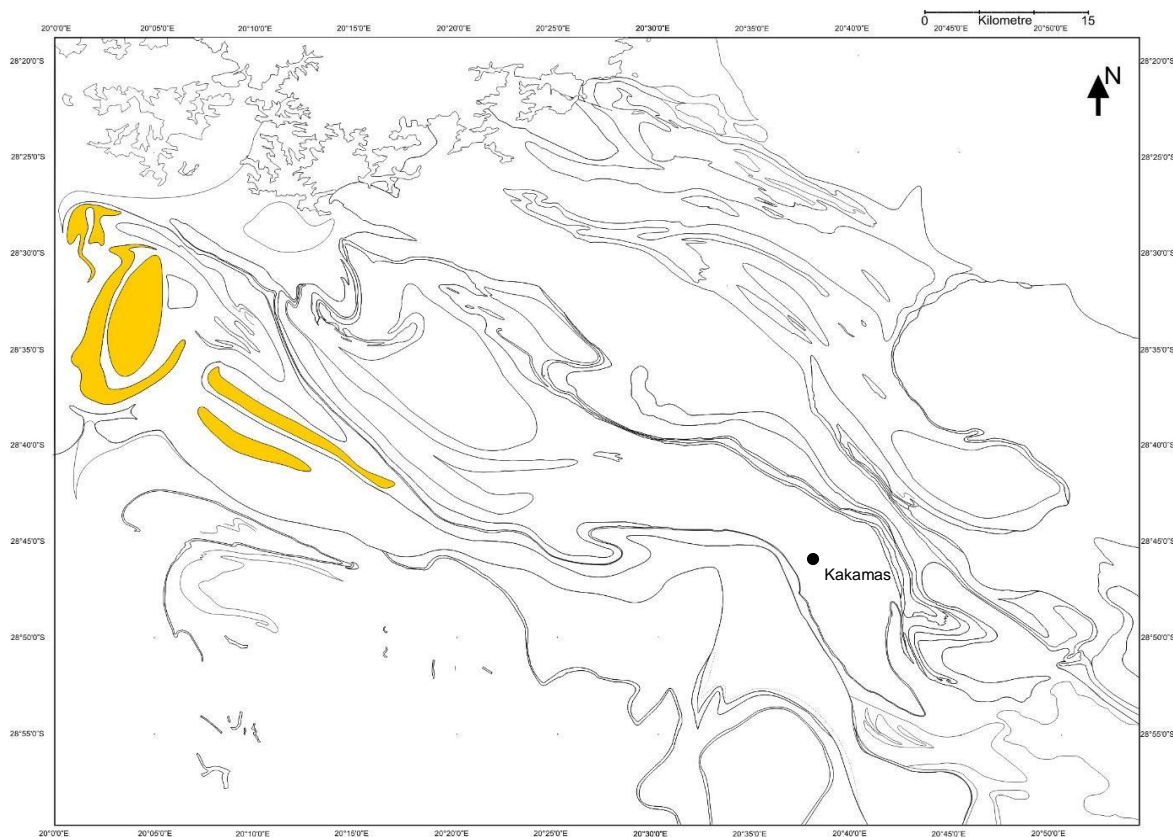


Figure 2-43: Stratigraphic distribution of the Nelshoop gneiss.

Large granitic bodies (kilometre scale) with elliptical shapes are situated within the Witwater and Eendoorn gneiss in the western part Grünau Terrane (Figure 2-43). The structures consist of the Nelshoop gneiss (in close proximity to the farm Nelshoop) comprised of homogeneous coarse-grained garnet-hornblende-biotite-feldspar-quartz gneiss with accessory magnetite. Praekelt (1984) did not differentiate between the Nelshoop – and Seekoeisteeke gneisses; Moen (2007) however, did not differentiate between any of the sheet granites in the GT.

Detailed structural and stratigraphic investigation during the current study concluded that there is indeed a compositional difference between the Nelshoop gneiss and Seekoeisteeke. The Nelshoop gneiss has a limited distribution between 3 oval shaped bodies, 1 lenticular body and 1 Ramsay Type 2 interference fold (mushroom structure). One of the flattened and stretched Nelshoop gneiss bodies is situated within the Eendoorn gneiss and the rest within the Witwater gneiss. The gneiss has a metamorphic fabric defined by the alignment of biotite. According to Praekelt (1984) a lit-par-lit contact relationship exists between the Nelshoop gneiss and Witwater gneiss. Lenticular to oval/lens shaped xenoliths (centimetre to metre scale) of fine grained quartz-feldspar gneiss are scattered through the Nelshoop gneiss (Figure 2-44). The xenoliths are orientated with long axis parallel to the regional linear fabric, both the gneiss and xenolith contain the same regional foliation. The origin of the xenoliths is not known. The lit-par-lit contact and xenoliths suggest a magmatic origin for the Nelshoop gneiss as a sheet intrusive.



Figure 2-44: Nelshoop Gneiss with a lenticular shaped feldspathic quartzite xenoliths situated sub-parallel to the regional foliation in the host gneiss.

2.3.3 Undifferentiated rocks of the Grünau Terrane

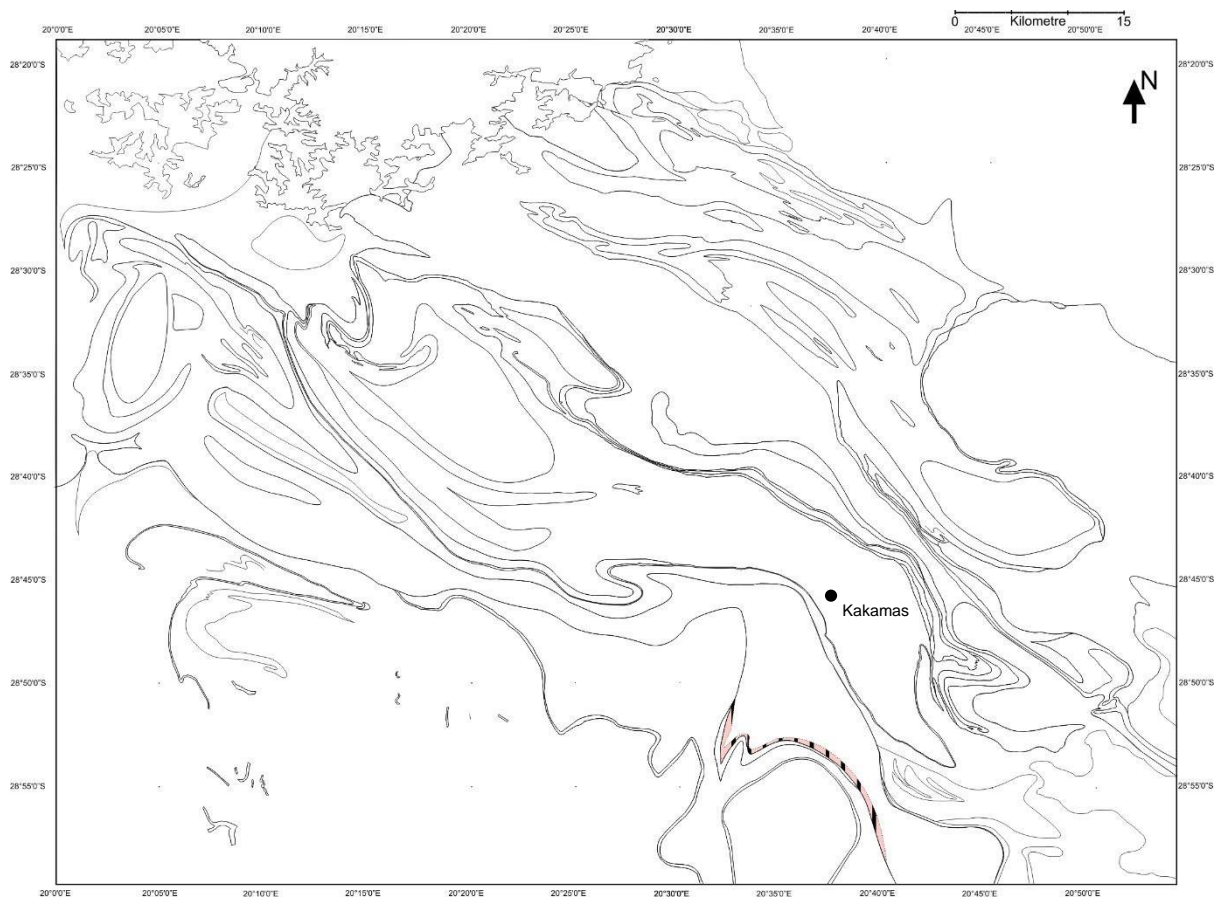


Figure 2-45: Stratigraphic distribution of the undifferentiated gneisses.

Two gneisses (biotite-feldspar-quartz augen gneiss (1) and plagioclase-biotite-feldspar-quartz (2)) are reported here for the first time and mapped in association with the Witwater gneiss as part of the Grünau Terrane. Outcrops can be observed on the farm Boesmansrivier (Regt Kyk 62; Figure 2-45). They form the hangingwall sequences to the HBRT and are overlain by the Witwater gneiss.

1. The augen gneiss is a well foliated coarse-grained gneiss consisting of K-feldspar augens (10 – 50mm) orientated within the foliation (Figure 2-46). There are small xenoliths of fine grained feldspathic gneisses which are also orientated sub-parallel to the regional fabric, which leads to the interpretation that the augen gneiss is an intrusive and the augen porphyroblast are phenocrysts.
2. The leucocratic gneiss overlies the augen gneiss; it has a pegmatitic texture due to the coarse grains and has a weakly developed fabric. A millimetre thick compositional banding was recognized in some of the outcrops, and the banding is defined by the alternation of quartz-feldspar and plagioclase bands.



Figure 2-46: Undifferentiated augen gneiss of the Grünau Terrane

2.3.4 Plutonic Rocks – Bladgrond Terrane

2.3.4.1 Putsies Migmatite Complex

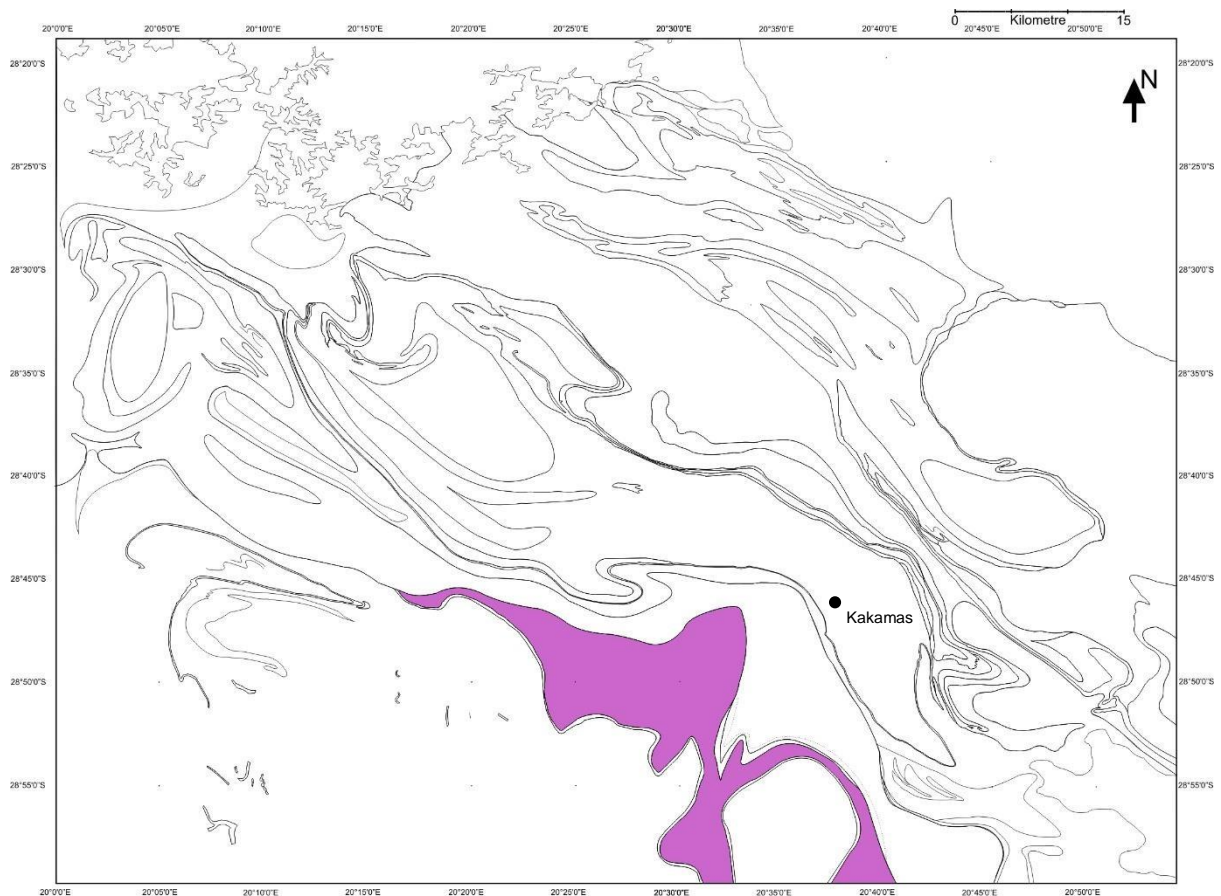


Figure 2-47: Stratigraphic distribution of the Putsies Migmatite Complex.

The Putsies Migmatite Complex is situated within the Bladgrond Terrane and forms the footwall sequence to the HBRT in the south-eastern portion of the mapped area (Figure 2-47). It is bounded in the south by another thrust, suggesting that the Putsies Migmatite complex can be interpreted as a thrust sheet along the HBRT as it cuts out (branch points) along the hangingwall thrust (HBRT).

The Putsies Migmatite complex was previously referred to as the Wolfkop Gneiss (Van Bever Donker, 1980), Putsies Gneiss (Moen, 2007), Putsies granitoid (Praekelt, 1984) and a Porphyroblastic Grey Gneiss (Von Backström, 1964). The Putsies Migmatite complex is a sack name for a series of plutonic rocks and migmatites that dominate the Putsies thrust sheet. Moen (2007) states that the Putsies Migmatite complex consist of migmatitic, granitoid gneisses but argues that the Putsies Migmatite complex has a sedimentary precursor due to the same stratigraphic position it maintains over a distance of 120 km. Praekelt (1984) regarded the Putsies Migmatite complex as a migmatized granite. Both authors agree that the Putsies Migmatite complex underwent a considerable amount of insitu melting. Moen (2007) observed intrusive contacts with the neighbouring rocks, and Praekelt (1984) mentions that inclusions (xenoliths) of quartzites and amphibolites are found in the gneiss; these observations argue for a magmatic origin.

Certain proportions of the Putsies Migmatite complex consist of large migmatite zones represented by dark amphibolitic units and neosome material with varying migmatite structures (Figure 2-48); a complex relationship between this migmatized leucogranitic rock and syn- to post-anatectic structures arise (Kalpakiotis, 2016). Melting is encompassed within neosome material on a large scale and appears to be widespread as nebulitic patterns (Kalpakiotis, 2016). Areas of the Putsies Migmatite Complex that do not display large scale migmatites consist of calc-silicates, amphibolites, biotite-hornblende gneiss and a fine-grained biotite-feldspar-quartz gneiss. The anatectic phase of the migmatite (neosomes - Putsies granite) can be described as a coarse-grained biotite-feldspar-quartz gneiss with a well-defined fabric and a distinctive mineral banding between felsic and mafic minerals. Calc-silicate bands of 300 mm to 1 m thick alternate with a fine-grained biotite-feldspar-quartz gneiss.

The southern contact of the Putsies Migmatite Complex is defined by a 20m thick calc-silicate ridge as part of the Driekop Group of the Bladgrond Terrane, which was previously referred to as amphibolites by Von Backström (1964) and Van Bever Donker (1980). The Putsies Migmatite complex has a crystallization age of 1188 ± 8 Ma (Pettersson, 2008), which is a questionable age due to the degree of migmatization in the thrust sheet.



Figure 2-48: Interbanded Metatexites and diatexites in the Putsies Migmatite Complex deformed by late north-west shears (D4).

2.3.4.2 Karama'am Augen Gneiss

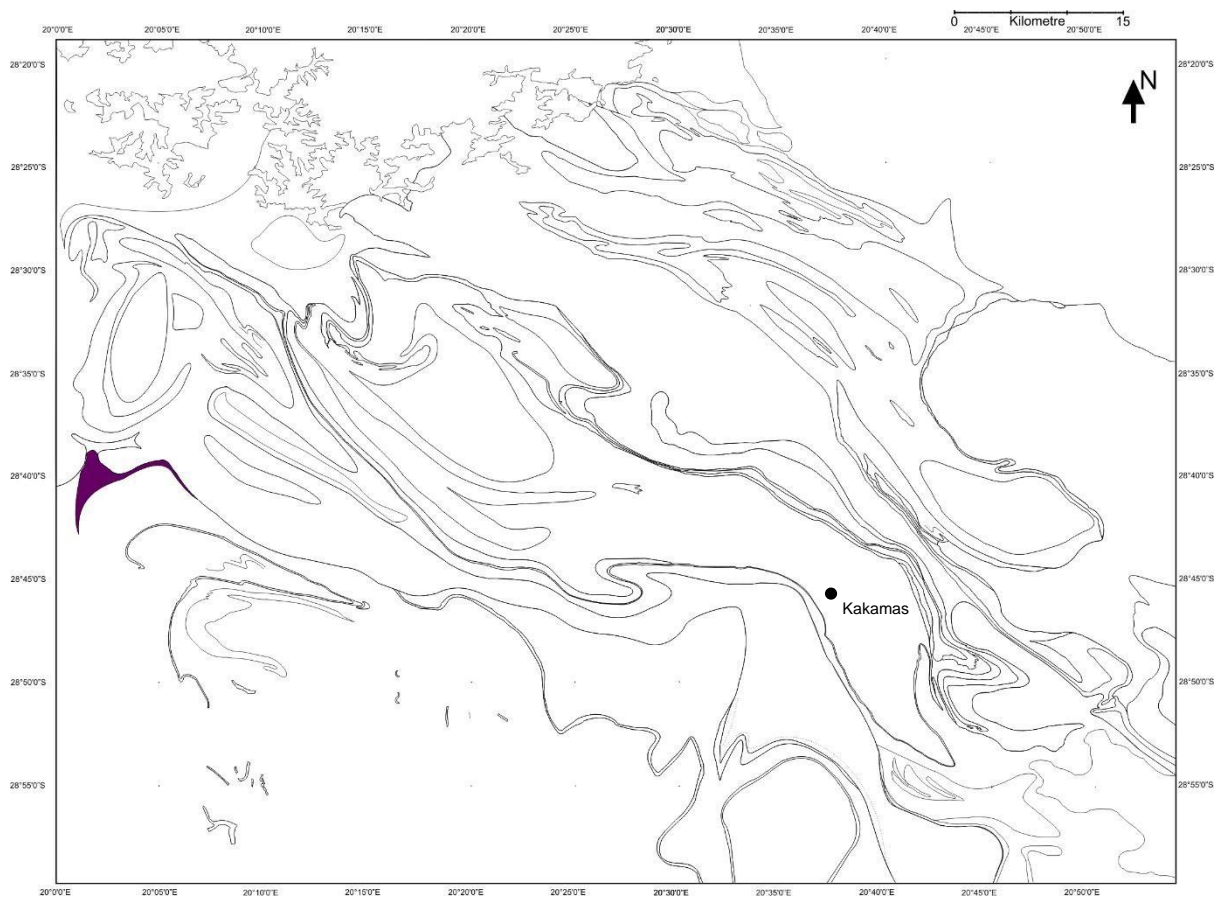


Figure 2-49: Stratigraphic distribution of the Karama'am Augen gneiss.

Situated along the HBRT as a footwall sequence is the Karama'am Augen Gneiss (Figure 2-49) defined as a fine to medium-grained biotite-feldspar-quartz augen gneiss (Colliston, et al.,

2015). The Karama'am Augen Gneiss forms part of the Droëboom Granitoid (Praekelt, 1984), it is the most abundant of the three end members (the other two being, leucogneiss and hornblende gneiss). Moen (2007) has placed the Karama'am Augen Gneiss as part of the Banksvlei Gneiss (Droëboom Granitoid) which is part of the plutonic rocks of the Bladgrond Terrane.

The augens are comprised of quartz and feldspar aggregates that are flattened; small xenoliths of felsic and mafic inclusions are in abundance (Praekelt, 1984). The Karama'am Augen Gneiss represents a competent body between incompetent country rocks (schist's and calc-silicates) and has a weakly developed fabric defined by quartz-feldspar augen and mafic bands (Colliston, et al., 2015). The mean crystallisation age of the Karama'am Augen Gneiss is 1108 ± 4 Ma. (Colliston, et al., 2015).

2.3.5 Undifferentiated rocks of the Bladgrond Terrane

Praekelt (1984) describes the areas south of the Putsies Migmatite Complex as a "sea" of various granites which intruded the Driekop Group, and named it the "Droëboom Granitoid". In the Regt Kyk area, south of the calc-silicate ridge (Driekop Group) as mentioned above is an amphibole-biotite-feldspar-quartz gneiss previously referred to as the De Baken Gneiss and Regt Kyk gneiss by Moen (2007), and the Boesmansrivier Leucogneiss and Regt Kyk amphibole-quartzite by Van Bever Donker (1980). The various gneisses described by the above mentioned authors relate to a compositional variation in the gneiss. No xenoliths or intrusive contact relationships could be identified, but Praekelt (1984) describes some small xenoliths in the various gneisses which is the only evidence that indicates whether the undifferentiated rocks of the Bladgrond Terrane having a magmatic origin.

3 Structural divisions description

Describing structural features of a large study areas can be a daunting task, with the main problem that key elements are lost in the bulk of the data. It however became apparent that the structural map can be subdivided into 5 domains related to major structures in the study area (Map 2). Each domain will be described according to the stratigraphy and structural features on various scales. The domain divisions are controlled by regional structures containing their own stratigraphy. The 5 domains are:

1. Bladgrond Terrane (BdT)
2. Grünau Terrane (GT)
3. Augrabies Sheath Fold (AF-N)
4. Vaaldrift Sheath Fold (VSF)
5. Puntst/Goede Hoop Domain (sub-divided into Neusberg and Cnydas sub-domains)

The comparison of structures between domains is not always possible over large areas as demonstrated by Robinson & Fyson (1976) for the southern Stoke Mountain area, Québec, where folds from one domain to another are not necessarily of same age based on the fold style and orientation. Within one domain smaller sub-domains can contain multiple fold phases which are younger or older than the same fold phases of the regional deformation. The different domains have their own structural framework specific to structures in the domain and do not necessarily correlate with the surrounding domains; a single overlapping structure can have different deformation events, depending on the domains framework. The contact and cross-cutting relationships between lithologies and structures provided key insights to the age relationships of the formation and deformation of a domain. The domains are separated by kilometre scale planar structures which will be classified and described in detail for each domain.

The convention to be used to describe the deformation episodes and planar/linear tectonites are as follows:

- Deformation episodes: D_n , D_{n+1} , D_{n+2} .
- Fold phases (structural event): $D_n F_n$, $D_{n+1} F_{n+1}$, $D_{n+1} F_{n+2}$ combined with the relevant deformation episode (D_n).
- Planar fabric: S_n , S_{n+1} , S_{n+2}
 - Three main S-fabrics were defined during this study, namely: S_0 , S_1 and S_2 .
 - S_0 : compositional banding.

- o S1: shear related fabric formed in supracrustals and intrusive rocks; it is co-planar to the xy plane of strain ellipsoid and observed in the earliest documented folds (D1(a) folds).
- o S2: regional foliation recognised as an axial planar foliation produced by folding the D1(b)F1 folds.
- o S0/S1 is folded by D1(b)F1 sheath folds and can only be distinguished from S2 in hinge zones.
- o Along limbs of structures S0/S1 is co-planar to S2
- Linear fabrics: L_n , L_{n+1} , L_{n+2}

The geometry of structures will be described and illustrated on equal-area stereographic projections (stereonet). All values of planar fabrics (S; black dots represent poles to S) are referred to as direction of dip and dip (000-00) and the linear-fabrics (L; red dots represent fold axis and green dots stretching lineations) as trend and plunge (000-00), unless stated otherwise. Stereonet software that is utilised in this study is a combination of Stereonet 9.6.1 (Allmendinger, et al., 2013; Cardozo & Allmendinger, 2013) and Orient 3.4.2: Spherical Projection and Orientation Data Analysis Software (Vollmer, 2015).

3.1 Domain 1: Bladgrond Terrane

The Bladgrond Terrane (BdT; Figure 3-1) is an amphibolite facies terrane, which consist of biotite-feldspar-quartz gneisses, banded calcsilicates with amphibolites, marbles, conglomerates and quartzites (Praekelt, 1984). It is intruded by migmatitic gneisses and various augen-, hornblende- and biotite granite-gneisses as well as minor granodioritic gneisses and metabasites (Colliston, et al., 2014). In the study area the BdT occurs in the south-eastern quadrant of the mapped area; it is typically covered by sand, grass and shrubs, but prominent mountains (e.g. Africa's Mountain), ridges and large slabs provide sufficient outcrop for structural studies (Figure 3-1). Van Bever Donker (1980) infers three phases of isoclinal recumbent folds with northerly plunging axes for the BdT, but notes that no fold closures were recognised. According to Praekelt (1984), four deformation periods can be recognised in the BdT with the folds and interference structures that differ from the Grünau Terrane.

3.1.1 Stratigraphy

The Bladgrond Terrane consist of meta-sediments from the Driekop Group which includes the Bysteeek, Witklip and Saamwerk Formations situated in a sea of granitic rocks (Praekelt, 1984). The Driekop Group metasediments are characterised by various composition quartzites, calcsilicates, amphibolites and feldspathic gneisses. In the 'fish' structure (Figure 3-1) where

the HBRT is folded, the Karama'am Augen Gneiss, a late tectonic sheet intrusive, intrudes into the meta-sediments (Colliston, et al., 2015). The Putsies Migmatite Complex forms a thrust sheet that cuts out Hartbees River Thrust (HBRT). McClay (1991a) defines a thrust sheet as a volume of rock bounded by thrust faults, while the cut off points can be defined as branch points, which are the intersection of a branch line and the erosional surface. In the large dome structure (Regt Kyk structure of Van Bever Donker (1980)) on the farm Boesmansrivier (Regt Kyk 62), a series of undifferentiated gneisses occur whose origin could not be determined ; they could represent the "sea of granitic rocks" described by Praekelt (1984).

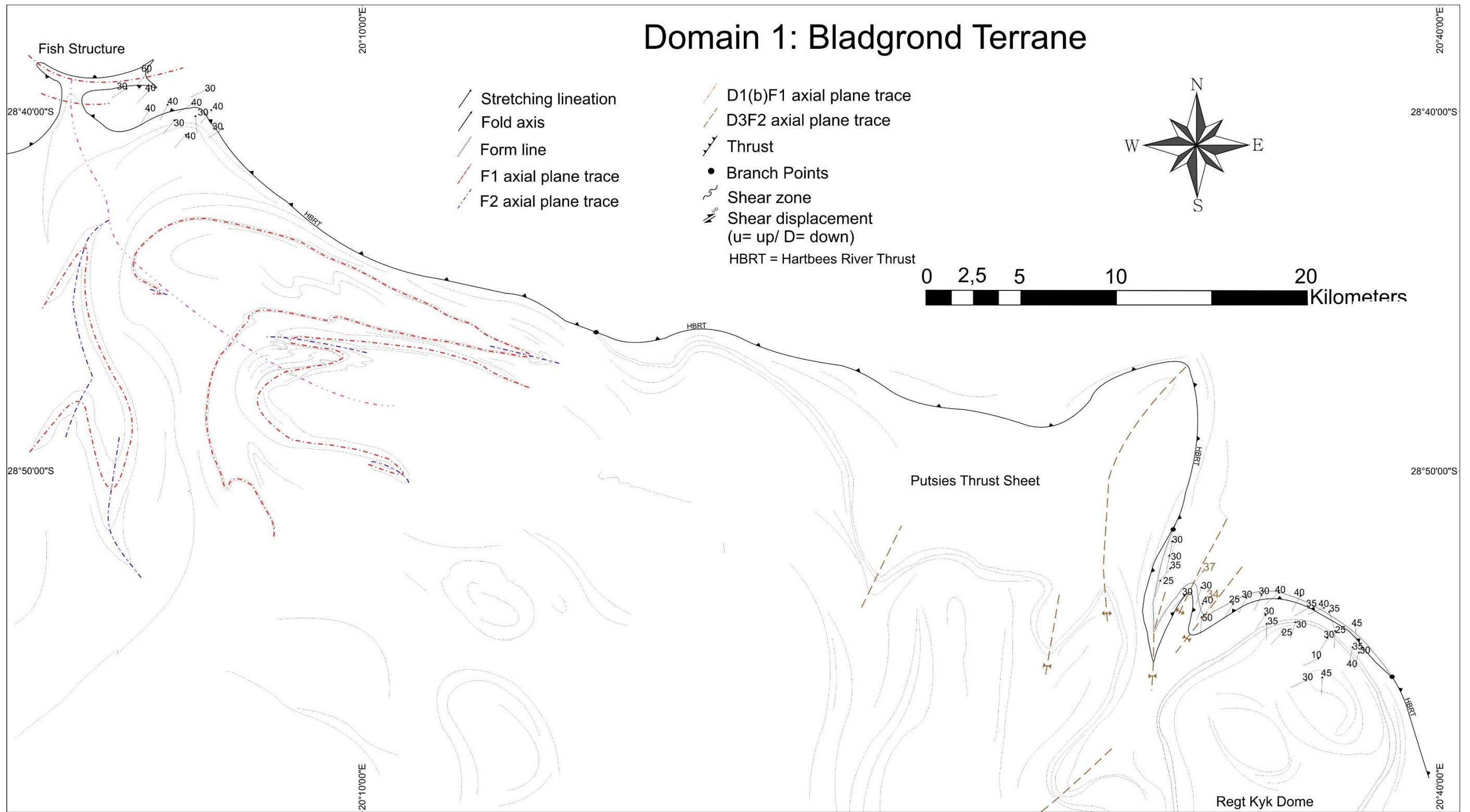


Figure 3-1: Structural map of domain1: Bladgrond Terrane.

3.1.2 Domain boundaries

A thrust system can be defined as an interconnected network of thrust faults that are kinematically and mechanically linked (McClay, 1991a). However thrust sheets such as the Putsies Migmatite Complex (as well as the Koekoepkop and Seekoeisteeek thrust sheets on the Waterval thrust (Domain 3; section 3.3.2 Domain boundaries)) are defined as thrust sheets. According to Boyer and Elliott (1982), thrust sheets are large volumes of rock with distinct stratigraphy which can be correlated over large distances and are bounded by a footwall thrust. Wedging of stratigraphy occurs along strike of the thrust sheet and is bounded above and below by opposite verging thrusts and can cause tectonic delamination at various stratigraphic levels (Price, 1986). When stratigraphy wedges out along a thrust, an intersection between the thrust planes is seen on the surface which can be termed a branch point; the intersection between two thrust sheets forms branch lines (McClay, 1991a). In areas where the thrusts in a system repeats the size and shape of the neighbouring thrust so that the thrust sheet overlaps, all dipping in the same direction, the system can then be defined as a imbricate thrust system, bounded by a footwall and hangingwall thrust (Boyer & Elliott, 1982). All of the above mentioned characteristics of a thrust system can be applied to the HBRT and Waterval thrust systems.

The Bladgrond Terrane underlies the Grünau Terrane (GT) and is separated by the HBRT which represents an inter-terrane thrust (terrane bounding thrust). The HBRT is interpreted to have formed at approximately 1200Ma when the terranes started to accrete (Colliston et al., 2015). The HBRT is a 200-500m wide, steep ($>60^\circ$), north dipping zone that has been refolded after the terranes accreted. The granulite GT is thrust over the BdT (granulite grade rocks thrust onto amphibolite grade rocks) in a south-south-westerly direction. During the late shearing event the HBRT became reactivated as a transpressional shear zone.

3.1.3 Regional Foliation

The regional foliation defined as the first structural imprint on the Bladgrond Terrane, is the most pervasive structural element present and is folded by the first phase of folding. Praekelt (1984) states that the foliation in the sediments is the same as the foliation in the gneisses which suggests that the gneisses are syn-tectonic. A second foliation is present as an axial-planar foliation and is defined by the transposed hinges of the first fold phase in the metasediments. The regional foliation is characterized by the alignment of biotite and amphibole needles.

3.1.4 Macroscopic structures

Praekelt (1984) suggests that at least 4 deformation phases can be recognised, the fold structures change drastically from the north-west to south east. In the north-west kilometre scale Ramsay Type 3 interference folds occur whereas the south-eastern part is dominated by Ramsay type 1 interference folds. The large domal shape of the HBRT and the undifferentiated rocks of BdT in the south-eastern part of domain 1 was interpreted by Van Bever Donker (1980) as the Regt Kyk interference structure, with an isoclinal recumbent fold as the first phase of folding. However the interference fold is inferred from a schematic section across the area. The BdT has three fold phases in the western part of the domain related to the development of the Ramsay Type 3 interference fold. The first 2 phases defines the Ramsay Type 3 interference fold and the third phase (F3) refolds the Ramsay Type 3 interference fold. The F3 trace strikes north-west and rotates northwards where it refolds the “fish” structure, which has an east-west trending axial trace.

3.2 Domain 2: Grünau Terrane

The granulite facies Grünau Terrane (GT; Figure 3-2) is characterized by distinctive high-grade supracrustals including cordierite-biotite-sillimanite garnet gneisses (Colliston & Schoch, 2006), calc-silicates, quartzites, amphibolites and schists; it is intruded by a megacrystic granite gneiss, and migmatites with quartz-feldspar-garnet leucosomes (Colliston, et al., 2014). The Grünau Terrane occurs over a vast area that stretches for more than a 1000 km across the Namaqua Province (including RSA and Namibia), with a general north-west south-east trend (Figure 3-2). In the study area the RK-MS is located within the GT, but in a more regional scale the GT is overthrust the Bladgrond Terrane and is overthrust by the Upington Terrane (Figure 1-1; Colliston et al., 2014). Both Van Bever Donker (1980) and Praekelt (1984) have noted at least three deformation periods for the Grünau Terrane and which included Ramsay Type 2 interference folds (Ramsay, 1967). Anatectic melting in the GT indicates that temperature and pressure conditions of 500-700° and 2-7Kbar was reached (Beukes, 1973; Du Plessis, 1979; Praekelt, 1984; Nordin, 2009; Diener, et al., 2013).

3.2.1 Stratigraphy

The most dominant lithology of the Grünau Terrane is the Witwater gneiss which is a product of anatectic melting of the pre-existing rocks in the GT, namely the Blouputs Formation and Eendoorn gneiss (Appendix D, Appendix E, and Appendix F). The Witwater gneiss intruded the Blouputs Formation as well as the Eendoorn gneiss; post-tectonic cross cutting veins and

dykes range from centimetre to metre scale. The Witwater gneiss is the youngest intrusive in the Grünau Terrane and forms significant lit-par-lit contact relationships with both the Blouputs Formation and Eendoorn gneiss; metre scale enclaves of both units are widely spread throughout the Witwater gneiss. The Eendoorn gneiss is a massive sheet intrusive of mafic megacrystic granite. It has a lit-par-lit intrusive relationship with the Blouputs Formation and it carries abundant xenoliths of the Blouputs Formation (various scales). The Blouputs Formation contains the oldest rocks (~1.8 Ga) within the GT domain; it represents a series of aluminous sediments and volcanics with various compositions. Anatectic melting occurred on a crustal scale throughout the distribution of the GT and resulted in the three units to have a close association with one another. The Nelshoop gneiss situated in the western part of the GT predates the second phase of anatectic melting (Witwater gneiss) and is contained in kilometre scale sheath folds. Praekelt (1984) reports of a lit-par-lit relationship between the Witwater gneiss and the Nelshoop gneiss. The amphibolite sequence on the HBRT is also intruded by sheets of Witwater gneiss.

3.2.2 Domain boundaries

In the study area the GT is bounded to the Bladgrond Terrane in the south by the inter-terrane Hartbees River Thrust as described above. Towards the north of domain 2 the Grünau Terrane forms a boundary with the RK-MS defined by the intra-terrane Waterval thrust (after Praekelt, 1984). This intra-terrane thrust wraps around the RK-MS and defines its boundaries (the Waterval thrust will be discussed in detail in section 3.3.2. Domain boundaries). In the western part of domain 2 the HBRT boundary is defined by an amphibolite sequence as the hangingwall unit of an imbricate system; the sequence pre-dates the thrust and forms branch points along strike of the thrust (Figure 3-2). The amphibolite sequence forms branch points along strike of the HBRT.

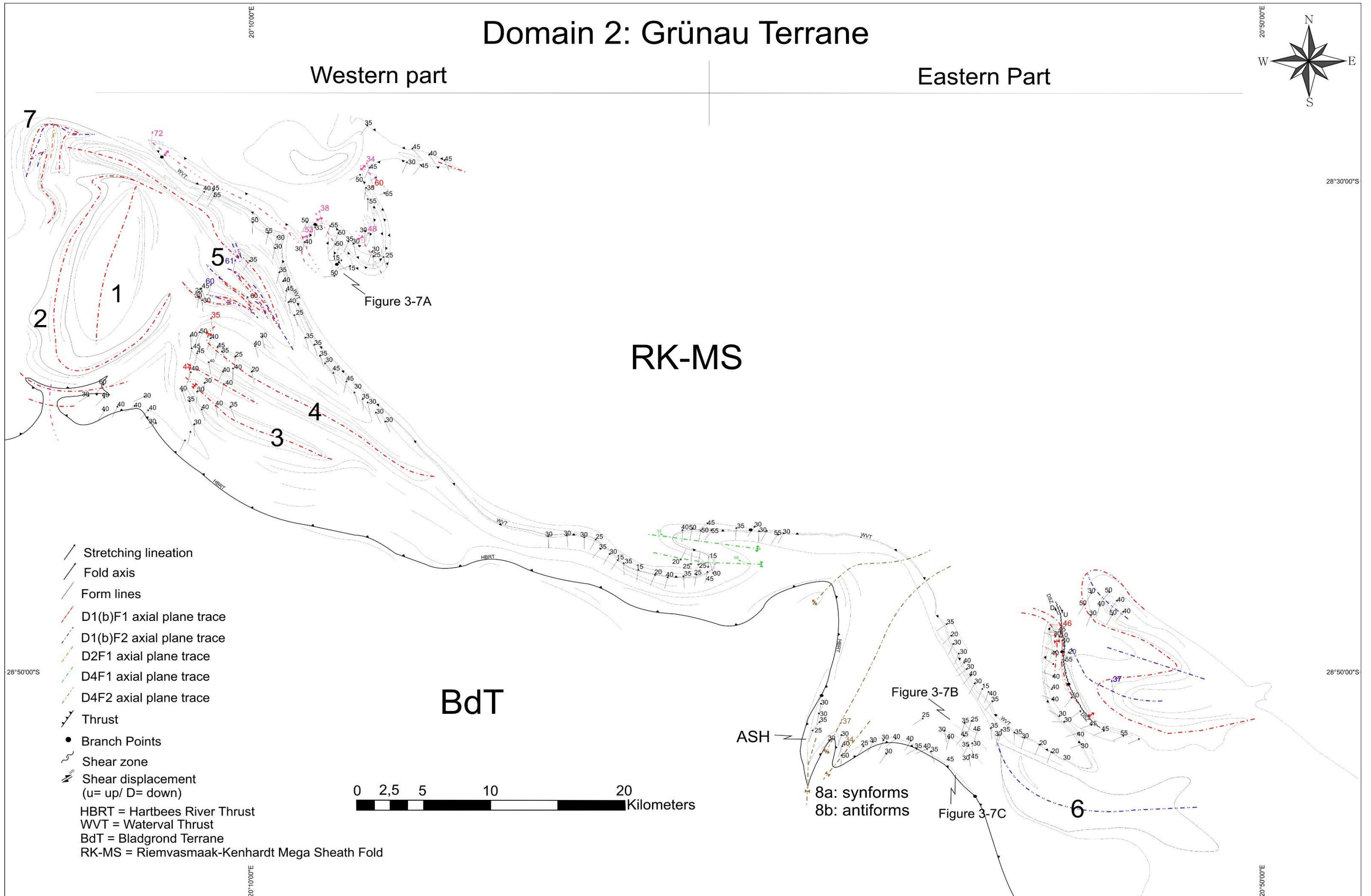


Figure 3-2: Structural map of domain 2: Grünau Terrane. Numbers, 1 to 7, represents D1(b)F1 macroscopic sheath folds in the Grünau Terrane; 1-4 and 7 consist of Nelshoop gneiss, whereas 5 and 6 contains Blouputs Formation. 8a and 8b represent the synforms and antiforms associated with the D4F2 folding.

3.2.3 Regional Foliation

The mean foliation orientation of domain 2 can be divided into a western and eastern part. In the western part the regional foliation strikes north-west, dipping towards the north-east (mean S: 03246) and in the eastern part (mean S: 04046), (Figure 3-3).

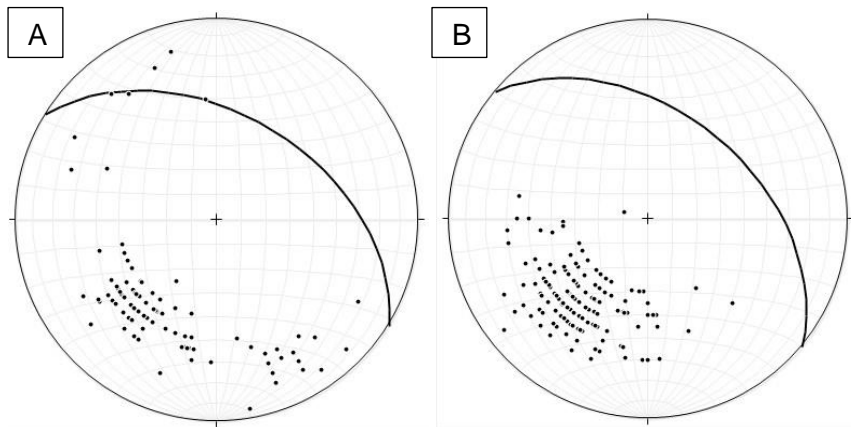


Figure 3-3: Stereonets representing the regional foliation (S2 in the western and eastern sub-domains (Figure 3-2). A: the regional foliation of the western Grünau Terrane (with late rotation to the north) with a mean foliation orientation of 03246 (n=104). B: eastern part of the Grünau Terrane with a mean foliation of 04046 (n=169). Dots represents the poles to foliation.

The foliation in the Eendoorn gneiss is co-planar to the leucosome banding (migmatitic bands) and is well defined by the alignment of the megacrysts (oval shaped with intermediate axes parallel to the strike of the foliation), hornblende and biotite. Blignault (1977) explains that the foliation in the Eendoorn gneiss is a primary flow foliation along which a tectonic foliation developed. The foliation in the Eendoorn gneiss wraps around the megacrysts and it is deduced that the megacrysts represent primary phenocrysts. The megacrystic growth is a pre-tectonic feature; the alignment of the megacrysts with the regional foliation is a result of general shear under ductile conditions. The foliation wraps around the megacrysts and does not pass through them. The Blouputs Formation contains a superimposed foliation that is co-planar to the foliation in the Eendoorn gneiss; the now-existing foliation is superimposed on a pre-existing foliation. In low strain areas a pre-existing foliation can still be recognised that pre-dates the Witwater gneiss leucosomes cross-cutting the meta-sediments of the Blouputs Formation.

The foliation in the meta-sediments is mostly defined by biotite and amphibole. In the Witwater gneiss the foliation is weakly defined, but is characterized by the alignment of K-feldspar, quartz and if present biotite laths. The foliation in Witwater gneiss is a late tectonic foliation which developed during the latter part of the main deformation episodes. Two ages of garnet

growth is present in all three of the stratigraphic units, one being syn-tectonic with the development of the regional foliation and a post-tectonic garnet that overgrows the foliation. The Blouputs Formation contains structures and a foliation that predates the intrusion of Witwater gneiss; both are folded together during a later stage. Nelshoop gneiss contains a foliation defined by the alignment of biotite which is co-planar to the regional foliation.

The regional foliation which is dominant throughout the stratigraphic units in the GT is defined as a S2 foliation. S1 is only observed in the Blouputs Formation and formed during the intrusion of the sheet granites under a sub-horizontal shear regime. S2 is superimposed over all of the pre-existing foliations (S0, compositional banding, and S1) and transposes the hinges of isoclinal folds, and is characterised by the foliation in the Witwater gneiss. S1, S0 and S2 are co-planar along the limbs of isoclinal folds; only in the hinges of the F1 and F2 isoclinal folds the S1/S0 (still co-planar) can be separated from the S2 foliation, given that the hinges are not totally transposed. During the D4 event all of the above mentioned foliations are folded.

3.2.4 Regional Lineation

In the western and eastern parts of the mapped GT the stretching lineations lie within the regional foliation planes (xy planes) and have a mean trend towards the north-north-east (western part), with the eastern part more towards the north-east. The average orientation for the western part is 00838 and for the eastern part 01637 (Figure 3-4). Various mineral aggregates defines the stretching lineation; in the Witwater gneiss sillimanite needles the most dominant and in the Eendoorn gneiss the long axes of megacrysts.

In the meta-sediments of the Blouputs Formation the stretching lineations are mostly defined by the alignment of amphibole needles and sillimanite needles. The stretching lineations are parallel to the regional tectonic transport direction deduced to be from north-north-east to south-south-west of the terranes, the same direction is reported by Colliston et al., 2014.

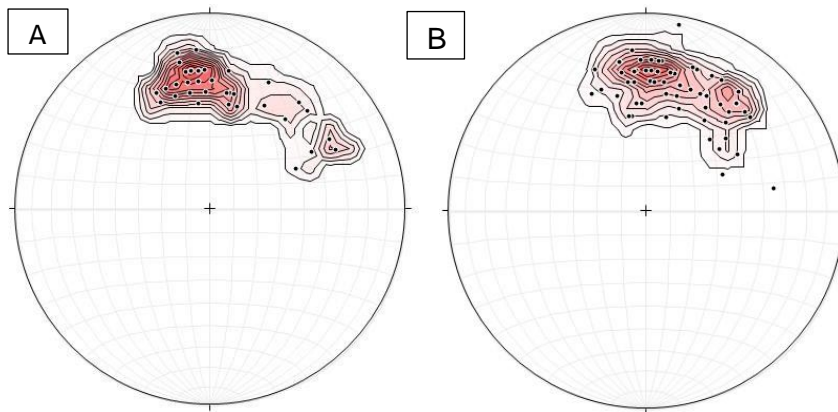


Figure 3-4: Stereonets of the regional stretching lineations (L1; mineral and augen) for the western and eastern sub-domains of Domain 2 (Figure 3-2). A: The lineations in the western part forms a girdle with point maximum of 00838 (n=38). B In the eastern part form a girdle with point maximum at 01637 (n=63). The girdle distribution of lineations is probably caused by the rotation of the strata by late north-west shear zones (D4). In compensation for late rotation, the lineations for both the western and eastern sub-domains indicate that the tectonic transport direction during ductile thrusting was towards the south-south-west.

3.2.5 Macroscopic Structures

Historically the fold structures in the Grünau Terrane have been documented as Interference folds. This study reinterpreted the interference structures and deduced that the GT is dominated by sheath folds. The GT has a different fold style than the BdT; sheath folds are refolded into Ramsay type 2 and 3 interference folds shapes. The best known example is the RK-MS which is a mega sheath fold (Colliston, et.al. 2015); the study area only includes the north-western portion of the RK-MS, but smaller sheath folds are present throughout the GT and can be seen in the western and eastern parts of the domain (Figure 3-2). The only continuous outcrop of Blouputs Formation in the western part of the GT is a refolded mushroom structure (“squid shape”; Figure 3-2, #5) that underwent 43% shortening. This structure is dominated by co-planar F2 fold axial traces striking north-west. The D1(b)F1 axial trace has a regional orientation sub-parallel to the trend of the localised D1(b)F2 trace but is refolded multiple times by the D1(b)F2 isoclinal folds. The Blouputs Formation in the Middlepost structure (Figure 3-2, #6) in the south-east is also a sheath fold, deformed by a series of shear zones developed along the limbs of the folds.

A kilometre scale Ramsay Type 2 (mushroom structure, Ramsay (1967)) occurs on the western border of the mapped GT (Figure 3-2, #7). The sheath fold with north-east plunging fold hinges presents the shape of a mushroom structure, however there is no field related evidence to support previous research that this structure formed by the process of interference folding. The structure consist of Nelshoop and Witwater gneiss. According to Ramsay (1967)

the first order fold hinges should be bowed upward and downward by the flow of the second order folds, meaning that the hinges should plunge in different directions. The angle between them will be determined by the interlimb angle of the second order folds. The second order fold hinge should be orientated parallel to the direction in which the crest is pointed. However the Nelshoop gneiss mushroom structure has fold hinges plunging in the same north-westerly direction, which indicates that the structure is elongated (sheath like) in the direction of stretching (lineations direction). Although the structure is interpreted as a sheath fold it consist of at least three fold phases. D1(b)F1 being the initial isoclinal recumbent fold, the second order fold is localised (D1(b)F2) refolded F1, but does not represent the upright fold from Ramsay's (1976) models. The D2F1 axial trace is interpreted as the upright phase. The mushroom structure formed as part of progressive folding and resulted in a three-fold phase sheath fold. When the 3rd fold phase (D2F1) is removed from the structure an omega shape sheath fold remains ("omega shape" refers to the double verging geometries of sheath folds modelled by Alsop and Holdsworth, 1999, 2004b).

In the western part the most noticeable series of structures is the elliptical shaped Nelshoop gneiss which is confined to a number of sheath folds, with various orientations (Figure 3-2, #1-4). Towards the west is the largest of the sheath folds (1) with a D1(b)F1 fold axial trace (y-axis of a sheath fold) trending north-south and the z-axis (short axis) striking east-west, the x-axis (long axis) is plunging parallel to the lineations. The structure is surrounded by a Ramsay Type 2 interference fold (2), with a D1(b)F1 trace wrapping around sheath fold 1. The two north-west south-east striking sheath folds (3 and 4) are flattened and stretched. Sheath folds 3, 4 and 5 are the three structures that are the closest to the original orientation (D1(b)F1 axial traces trending north-west south-east), 5 is however refolded. Sheath folds 1, 2 and 7 are distorted due to the rotation of the D1(b)F1 axial trace towards the north. These rotations of axial traces are as a result of a dextral shear. The S1 foliation is folded by these structures, but the regional S2 fabric transposes the hinge zones. Fold closures are recognized by a change in stratigraphy along the axial trace of the folds and a symmetry normal to the strike of the axial trace. All six of the structures resemble sheath folds that are refolded into the shape of interference folds by progressive deformation.

Exposed hinge zones of the tight isoclinal sheath folds (Nelshoop sheath folds 3 and 4 and Blouputs sheath fold) were measured and a fold axis for the structures were calculated using stereographic projections (Figure 3-5; 00544 for sheath fold 3 and 35535 for sheath fold 4). Sheath fold 3 has a synformal D1(b)F1 axial trace whereas sheath fold sheath fold 4 has an antiformal trace which is associated with Ramsay Type 1 ("dome and basin") interference folds. However during this study the structures are classified as sheath folds. The sheath fold

enveloped in the Eendoorn gneiss (3) has a fold axis orientation of 00544 and sheath fold 4 has a fold axis orientation of 35535. Both fold axes plot within the cluster of stretching lineations, i.e. they are collinear, indicating that the lineations and folds are the same age. The large refolded Blouputs Formation sheath fold (Figure 3-2, #5), situated in the Witwater gneiss north of the Nelshoop sheath folds have fold axes with orientations of 01460 and 01061.

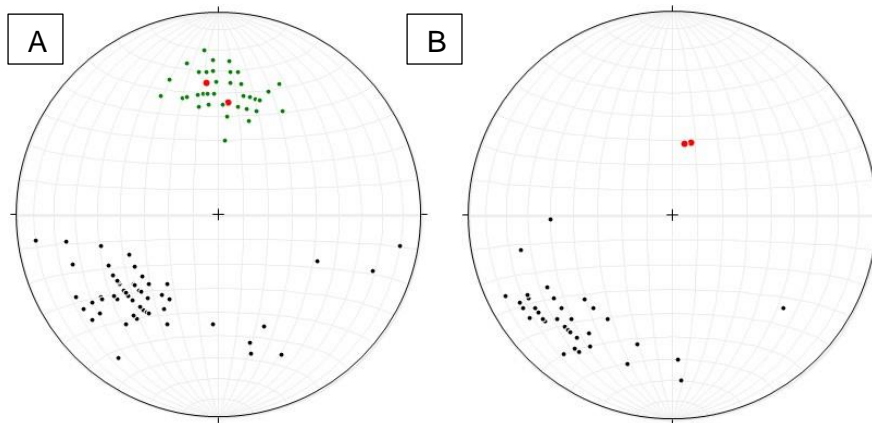


Figure 3-5: Stereonets of the macroscopic sheath folds (D1(b)F1) for the western sub-domain of Domain 2 (Figure 3-2). A. Nelshoop sheath fold; the hinge line plunges 00544 for sheath fold 3 and 35535 for sheath fold 4. Note that the fold hinges plots within the cluster of mineral stretching lineations. B. Two well exposed closures of the Blouputs Formation sheath fold (sheath fold 5) in the west have fold hinge orientation of 01460 and 01061. The steep plunges of the closures indicates that the sheath folds were deformed by the later transpressional shear system (D4) which rotated the hinges towards the vertical. The fold axes of the sheath folds are co-linear with the stretching lineations and indicate a tectonic transport direction to the south-south-west (compensating for D4 shear rotation).

In the eastern part of domain 2, the HBRT is folded by a series of anticlines and synclines (D4F2) with axial traces that strike north-south (Figure 3-2, 8a and 8b). These folds, fold the Putsies and Amphibolite sequence thrust sheets of the HBRT. The syncline has a fold axis of 02634 and the anticline's fold axis is 02737, both plotting within the mineral stretching lineation cluster (Figure 3-6). The folds represent an east-west compressional phase across the terranes.

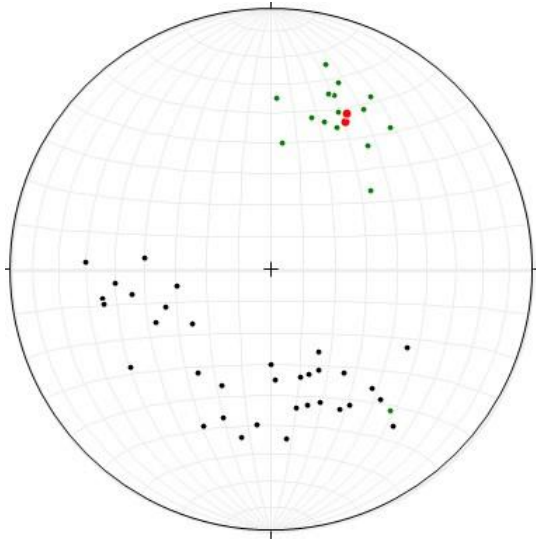


Figure 3-6: Stereonets of the D4F2 folds for the western sub-domain of Domain 2 (Figure 3-2). The synclinal and anticlinal fold axes (respectively 02634 and 02737) are co-linear with the mineral stretching lineations (n=16; poles, poles to S2, n=35).

3.2.6 Mesoscopic Structures

After the accretion (ductile thrusting) of the terranes, progressive deformation continued and produced structures on various scales, including centimetre to decametre folds, shear zones, s-c fabrics and sheath folds. It became apparent that along strike of any stratigraphic unit mesoscopic folds display different fold styles, symmetries and vergence; i.e. model 1 and model 2 folds. Model 1 and 2 folds form simultaneously during progressive shear deformation (see section 3.3.5 Macroscopic Structures). Under ductile conditions folds such as these are the result of flow perturbation processes where folds of different style develop simultaneously in different parts of a flow cell (see section 3.3.5 Macroscopic Structures; Alsop & Holdsworth, 2002; 2007).

The millimetre to centimetre (metres scale fold were rarely observed) S and Z-folds occur in the same stratigraphic level along strike and have fold axes orientation sub-parallel to the regional stretched mineral lineations and the axial planes are co-planar to the regional foliation. S and Z fold occurring in the same structural level defines or relates to decametre scale “omega” shaped sheath folds. At least two sets of S/Z folds have been documented. The earliest folds are the intrafolial folds, these folds occur on millimetre scale and are flattened within the foliation, they are mostly observed in the Eendoorn gneiss (Figure 3-7A). The second set of S/Z folds related to the formation of the F1 fold closures and is defined by the folded S1(a/b) foliation. These folds occur on centimetre to metre scale. The S2 foliation is present in both sets of folds as an axial planar foliation co-planar to the axial planes of the

folds. This supports the S2 being the main regional foliation observed in Domain 2; S1(a/b) can only be separated from S2 in the hinges of folds that are not totally transposed.

Centimetre scale sheath folds were observed predominantly in the compositional banding of the Blouputs Formation. The long axes (x-axis) of the sheath folds are co-linear to the stretched mineral lineation, which indicates that the mesoscopic structures developed at the same time as the mega sheath folds. On the farm Boesmansrivier (Regt Kyk 62) the Blouputs Formation is dispersed throughout the Witwater gneiss as large enclaves defining sheath folds; the rafts range from metre to tens of metre in size (Figure 3-7B). The sheath fold in Figure 3-7B is orientated with the y-axis sub-parallel to the strike of the S2 foliation and the axial plane (yx plane) is co-planar to S2; this foliation also transposed their hinges.

Deca- to centimetre scale shear zones occur in the volcanic sequence on the HBRT; they are the result of transpressional shear during the reactivation of the HBRT as a sub-vertical shear zone. The shear zones and s-c fabrics are used as kinematic indicators of the shear event (Figure 3-7C). The microstructures on the HBRT indicated that the shear zone has an oblique sense of movement; the northern block (GT) moves up with a right-lateral shear component (towards 215°).

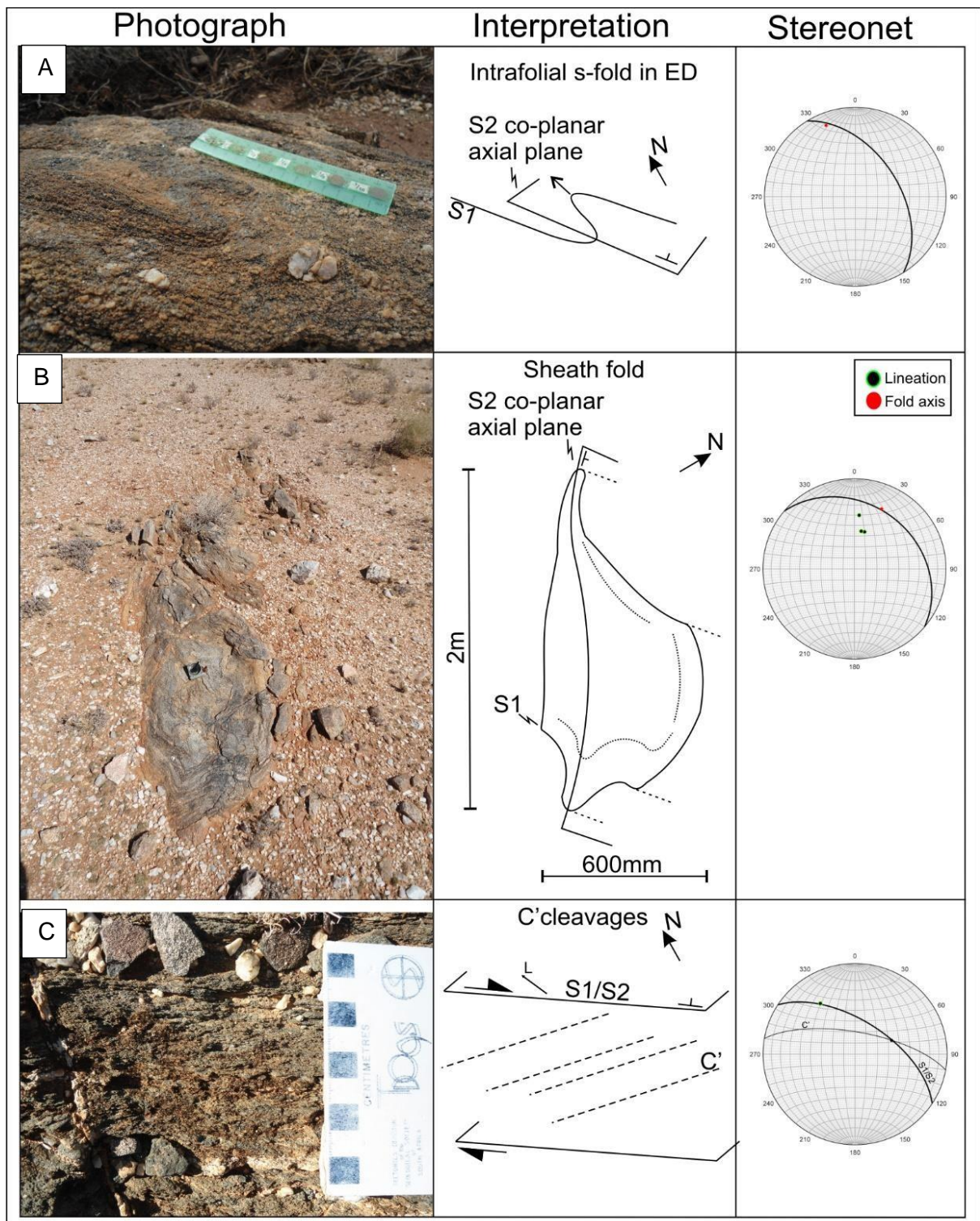


Figure 3-7: Mesoscopic structures of the western (A) and eastern sub-domains (B, C) in domain 2 (Figure 3-2). A. A D1(a) intrafolial S-fold in the Eendoorn gneiss with fold axis plunging towards the north-north-west (33634). B. A metre scale sheath fold in the Witwater gneiss on the farm Boesmansrivier. It contains transposed hinges and an axial planar S2 cleavage co-planar to the regional foliation. C. S-c cleavages associated with the dextral sense of D4 shear along the reactivated HRBT; the intersection of C' and S2/S1 indicates that there is an oblique sense of shear with north up.

3.2.7 Discussion and summary of domain 2: Grünau Terrane

- The granulite GT terrane is dominated by supracrustals (Blouputs Formation: ~1.8Ga) and is intruded by three ages of granites, two of the granites are the result of kilometre scale anatexis melting (migmatization of the supracrustals; Table 3-1).
- The oldest of the granites the Eendoorn gneiss intruded the Blouputs Formation during terrane accretion at (D1(a); 1200Ma) and represents the first phase of melting of the Blouputs Formation (Appendix D).
- This was followed by the Nelshoop Gneiss, emplaced as a sheet granite during the second phase of the accretionary process (D1(b), 1168-155Ma).
- The sheath folds in the GT developed during progressive folding of pre-existing isoclinal folds which developed during the accretion of terranes (D1(b)F1 to D2F1).
- Crustal scale anatexis melting throughout the GT formed large amounts of melt which accumulated as the Witwater gneiss during the second melt event (Appendix F).
- The melt intruded the pre-existing structures and lithologies in a “finger like fashion” as sills and vein networks; where the networks connected melt pockets developed.
- The reactivation of the HBRT as a transpressional shear occurred after the intrusion of the Witwater gneiss and well-developed sheath folds.

Table 3-1: Structural framework for Domain 2: Grünau Terrane.

Deformation event	D1a	D1b			D2	D3	D4		
Structural event	Model 1 and 2 folds	Intra-terrane	F1	F2	F1	Charnockite	F1	F2	NW shear zones
Domain 2: Grünau Terrane	x	x	x	x	x	x	x	x	x

3.2.7.1 Characteristics of sheath folds

The structures in the domain are interpreted as sheath folds which formed during progressive shear deformation rather than interference folds formed by two separate folding events. The geometry of the structures indicates that the fold hinges of all the sheath fold closure have a co-linear orientation to the stretching direction as defined by stretching lineations. D1(b)F1 and D1(b)F2 axial traces are sub-parallel and the hinges co-linear, in interference folds (Type 2, mushroom structures) the fold axes of the two fold phases should be perpendicular

(Ramsay, 1976). The second phase of folding for a Ramsay Type 2 mushroom structure should be upright to semi-upright but during extensive mapping no evidence of an upright fold on this scale or of this age could be established. The sheath folds are formed and deformed during progressive shear; the axial planes of the sheath folds are co-planar to the xy plane (flattening regime) of the strain ellipsoid of the area and the x-axes are co-linear to the stretching lineations. Sheath folds initiate with fold axes at an angle to the regional stretching direction and rotate towards the stretching direction, either by clockwise or anticlockwise rotation, during progressive shear (Alsop & Holdsworth, 1999). The D1(b)F1, D1(b)F2 and D2F1 fold axes have the same orientation as the result of progressive shear. With a change in the shear plane orientation and direction the strain ellipsoid over the area changes; this results in pre-existing sheath folds are now orientated within the shortening sector of the strain ellipsoid and refolding takes place (Coward & Potts, 1983).

3.3 Domain 3: Augrabies Sheath Fold

The Augrabies Sheath fold (A-FN; Colliston, et al., 2015; Mathee, et al., 2016; Figure 3-8) is a mega sheath fold situated in the RK-MS as part of a sheath fold complex. Stratigraphically the A-FN underlies all the other sheath fold complexes. It has outcrop dimensions of 60 km x 20 km and was previously referred to as the Augrabies Terrane or Augrabies Klippe (Colliston & Schoch, 2000), Upington thrust sheet (Praekelt, 1984) and the Augrabies Fragment (Praekelt, et al., 1986). The A-FN is bound by the underlying Waterval thrust (WVT) and overlying Kliprug thrust (KRT) that also separates it from the overlying Vaaldrift Sheath Fold (Figure 3-8); both thrusts are intra-terrane thrusts. Praekelt (op.cit) recorded at least four major deformation events across the north-western part of the AF-N. In the south-eastern part of the AF-N, Van Bever Donker (1980) suggested that only two of the last deformational events can be seen.

3.3.1 Stratigraphy

All the stratigraphic units of the A-FN (Brabees, Seekoeisteeek, Rooipad, and Augrabies gneiss, Koekoepkop Formation and the Oranjekom Complex) are contained within it and do not occur outside the boundaries of the structure; together with the traces defining the elliptical shape of a sheath fold. The Koekoepkop Formation forms the southernmost boundary of the structure and represents a thrust sheet; it is overlain by the Seekoeisteeek and Rooipad gneiss and underlain by the Eendoorn gneiss. The Seekoeisteeek thrust sheet consists of Seekoeisteeek gneiss and is overlain by the Rooipad gneiss. Both the above mentioned thrust sheets are bounded by a footwall thrust and a roof thrust and form part of the Waterval thrust imbricate system. In the core of the structure is the Augrabies gneiss with an emplacement age of 1168 ± 6 Ma (Colliston, et al., 2015). Encompassing the Augrabies gneiss is the Rooipad

gneiss which is the largest and most wide spread sheet intrusive with an emplacement age of ~1155Ma (Pettersson, 2008). Detailed stratigraphic investigation indicated that the Rooipad gneiss and Augrabies gneiss have a lit-par-lit contact relationship with Rooipad gneiss intruding into the Augrabies gneiss, confirming the published ages of the granites.

The Brabees gneiss is a 30km long recumbent isoclinal fold within the Rooipad gneiss. No isotope analysis has been done on the Brabees gneiss and no intrusive contact relationship between the two granites could be recognised, for most areas the contact is sharp, suggesting that an isotopic study is necessary to determine the age relationship between the two granite gneisses. Mafic bodies are scattered throughout the domain, with metagabbro of the Oranjekom Complex being the most noticeable one, it intruded the Rooipad gneiss and defines a large sheath fold. A Sm-Nd and Rb-Sr age of ~1100Ma has been determined for the Oranjekom Complex; this late folding event falls within the major sheath folding episode (Table 4-3).

3.3.2 Domain boundaries

Both the northern and southern boundaries of the A-FN are demarcated by intra-terrane thrust (Kliprug and Waterval thrust, respectively), the southern one being the Waterval Thrust (WVT), first recognised as a thrust fault by Praekelt (1984). Previously the highly deformed zone was mapped as the Kakamas shear zone (Van Bever Donker, 1980; Stowe, 1983). The northern boundary represents the intra-terrane thrust between the A-FN and the Vaaldrift Sheath Fold, the Vaaldrift sheath fold being the hangingwall sequence and the A-FN the footwall sequence. Both the intra-terrane thrusts dip towards the north-east and according to Praekelt (op.cit) the dip can range from 40°-85°; this has been proven to be the case as seen from the regional map (map 1). The areas affected by later superimposed shearing display a rotation of the thrust plane towards the vertical. The Waterval thrust also represents the main boundary of the RK-MS and the sole thrust of all intra-terrane thrusts; indicating that the northern Kliprug thrust (KRT) cuts out against the WVT in the western part of domain 3 sub-area "b".

Domain 3: Augrabies Sheath Fold

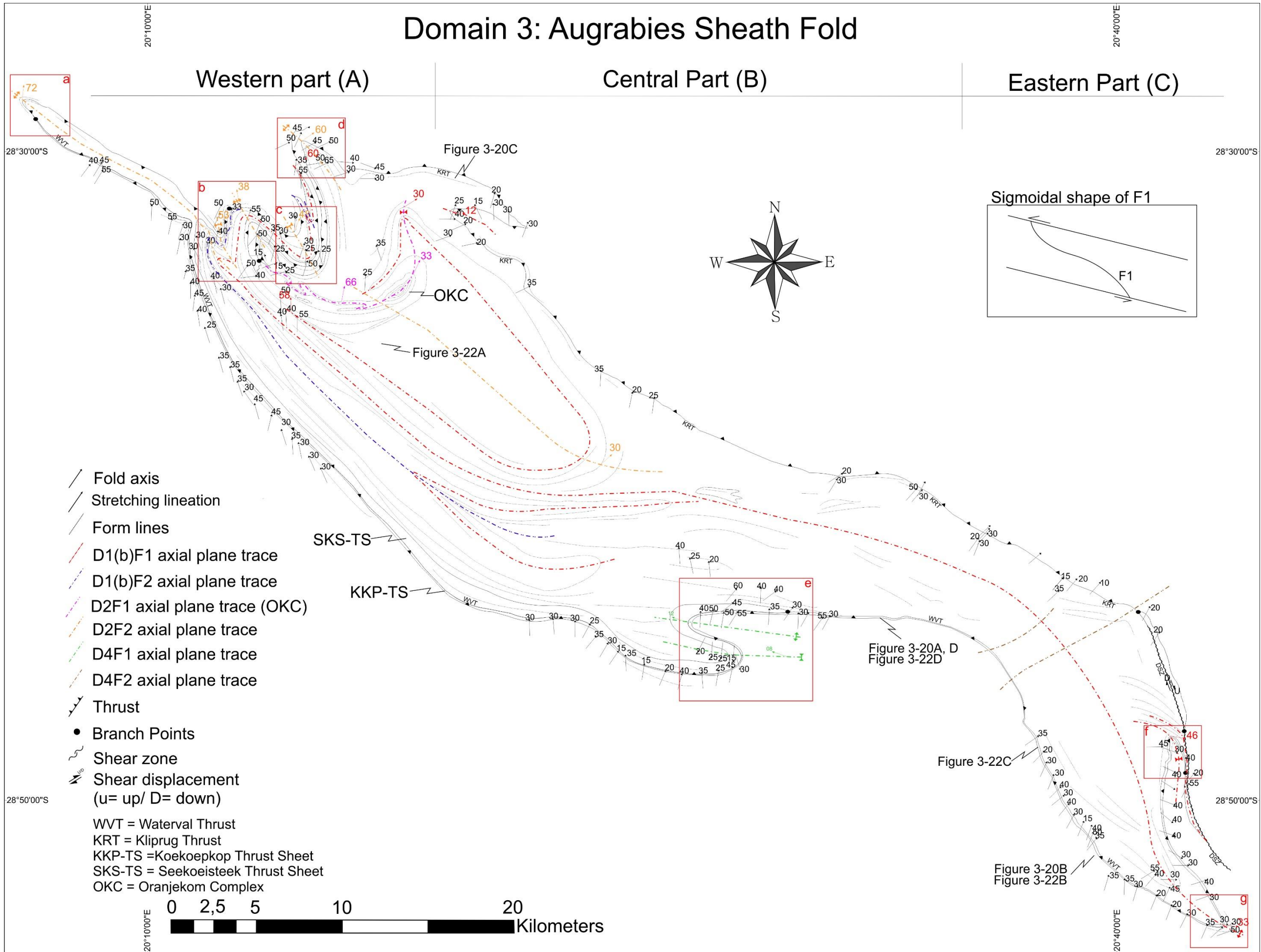


Figure 3-8: map of domain 3 (Augrabies Sheath Fold). Domain 3 is sub-divided into three sub-domains (A-C). The red squares (a-g) are sub-areas of associated folds and are referred to in the text. The inset are a schematic representation of the rotation of the D1(b)F1 axial trace (sigmoidal shape) of the AF-N which suggests kilometre scale sinistral shear during D4.

The intra-terrane thrust is recognised by a series of branch points associated with imbricates along strike of a thrust plane and is expressed as lithological cut-offs (Figure 3-9). The WVT being the main intra-terrane thrust, contains an imbricate system of separate thrust sheets, namely: Seekoeisteek and Koekoepkop thrust sheets (Figure 3-8, Figure 3-9). The thrust sheets are bounded by footwall and hangingwall thrusts. The contacts between the thrust sheets are sharp and can be defined as branch lines of a thrust system after McClay (1991a). The above mentioned thrust sheets have been mapped out for over 100km along strike and rapidly decrease in thickness towards their branch points (wedges). The Seekoeisteek thrust sheet overlies the Koekoepkop thrust sheet and wedges out against it in the central part of the domain (Figure 3-8). In the north-west the Koekoepkop thrust sheet wedges out against the footwall thrust (Eendoorn gneiss) after which the Seekoeisteek thrust sheet continues, until it wedges out against the Eendoorn gneiss (sub-area "b"). In the southern part, the Koekoepkop thrust sheet wedges out against Rooipad gneiss (sub-area "f"). The Koekoepkop Formation has four major units with a wide variety of lithologies; along strike the content of the stratigraphic sections changes significantly as a result of the thrust system. Tectonic wedging occurs on various scales (decametre to kilometre scale wedging); the main units of the Koekoepkop Formation wedge out along strike (kilometre scale), but internally lithologies wedge out within a couple of metres (decametre scale). The thrusts are folded during the D1(b)F1 phase of deformation (Table 4-3).

Moen (2007) questions the observations and interpretations of Praekelt (1984) concerning the existence of a thrust plane between the Eendoorn gneiss and the Rooipad gneiss (Waternal thrust system – this study). The above mentioned characteristics contradict the conclusions of Moen (2007), and prove and support the observations and interpretations by Praekelt (1984). The same structural characteristics are observed along the Kliprug thrust with the exception that the thrust cuts out along the sole Waternal thrust.

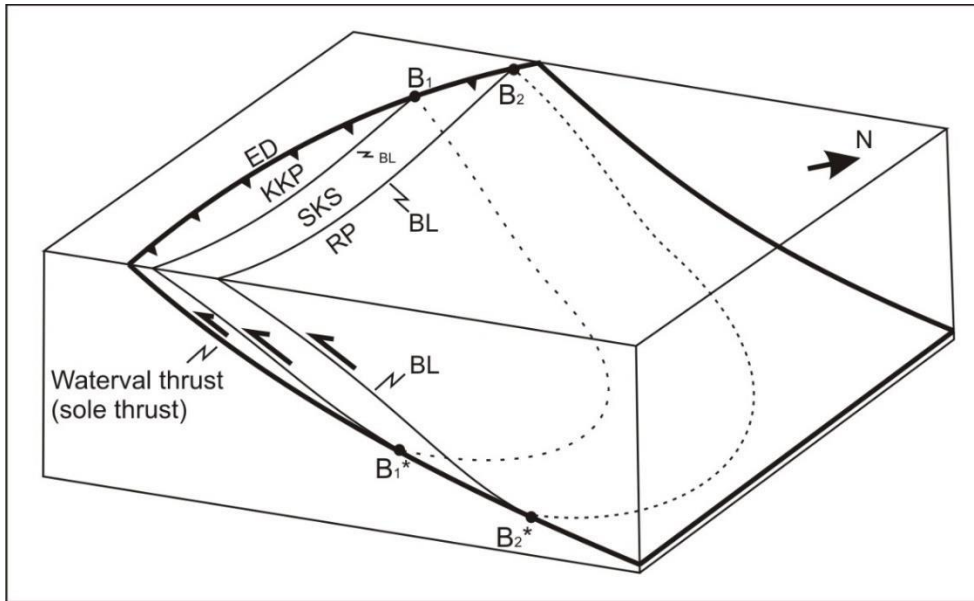


Figure 3-9: Thrust model adapted after McClay, 1991a for the Waterval thrust system (Figure 3-8). Koekoepkop thrust sheet (KKP) and the Seekoeisteeke thrust sheet (SKS) are two imbricates overlying the footwall Eendoorn gneiss (ED), along the Waterval thrust (sole thrust). The two thrust sheets wedge out along strike (B1 and B2) and in depth (B1* and B2*) at branch points (B) against the sole thrust. The internal thrust separating the thrust sheets is represented by branch lines (BL). The Waterval imbricates are overlain by the Roopad thrust which forms a roof thrust sheet and is defined by Roopad gneiss (RP).

3.3.3 Regional foliation

The regional foliation in the domain is S2 with S1 only recognized in the hinges of the D1(b)F1 isoclinal folds and sheath folds. The syn-tectonic granite gneisses, e.g. Roopad gneiss, contain a foliation pre-dating the S2 foliation and is defined as the S1 foliation formed with the intrusion of the plutonites. Praekelt (1984) suggested that the main foliation in the lithologies are the result of the initial deformation phase. S1 is folded by the D1(b)F1 and D1(b)F2 folds while the S2 is an axial planar foliation transposing the hinges of the D1(b)F1 folds. The S1 is coplanar to the regional S2 fabric except in hinge zones of the D1(b)F1 isoclinal closures. The foliation in the granitic rocks is defined by the alignment of K-feldspar augens, feldspar and quartz aggregates, biotite and hornblende. The foliation in the Koekoepkop Formation supracrustals is defined by parallel alignment of mafic minerals such as hornblende and biotite. Due to the large open fold (D4F2) in stretching across the central (sub-domain B) and eastern (sub-domain C) parts of the domain the orientation of the regional foliation rotates towards the east in the eastern part (C). In the western part (sub-domain A) the foliations are steeper as a result of sub-vertical shears superimposed over the domain, but the foliation remains dipping towards the north-east (mean foliation: 05466) (Figure 3-10A). Towards the centre of the structure the foliation has an average dip of 33° towards the north and north-north-east (01533) (Figure 3-10B). East of the large open fold (D4F2) the foliation dips steeper

towards the east (06644) (Figure 3-10C). From the stereographic projections in Figure 3-10, it can be noted that the regional foliation of the AF-N is rotated towards the north-east to east-north-east, both east and west of the central part; the rotation displays the pattern of a sigmoidal shaped structure, which is also defined by the shape of the D1(b)F1 axial trace of the AF-N (Figure 3-8).

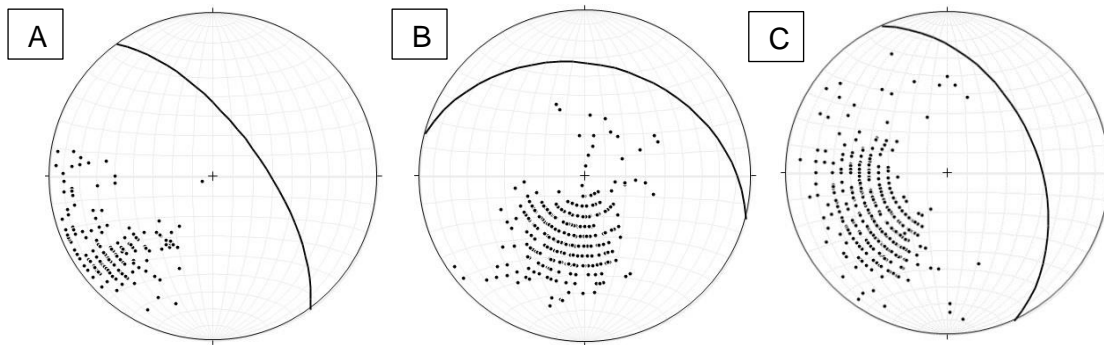


Figure 3-10: Stereonets showing the sigmoidal rotated distribution of the regional (S2) foliation in Domain 3 (Figure 3-8). A. Western part with a mean S of 05466 (n=196). B. Central part with a mean S of 01533 (n=419), and C: eastern part with a mean S of 06644 (n=473).

During the D1(b) (Table 4-3) phase the penetrative foliation developed in the supracrustals sequence and the sheet intrusives, except in the Oranjekom Complex (it was not present at the time), representing the S1 foliation. During the development of the sheath folds (D1(b) to D2) the S1 foliations are deformed and folded by large isoclinal, plunging inclined folds. With the continuation of progressive shear deformation the sheath folds are refolded and closures are partially to totally transposed by the younger S2 foliation.

3.3.4 Regional lineations

Praekelt (1984) notes that a pervasive lineation occurs throughout the entire domain. The regional lineation of the AF-N is defined by long axes of augen in the granitic rocks, amphibole needles, and stretched-out quartz and feldspar aggregates; the minerals define stretching lineations and are geometrically co-linear. The lineation shows rotation to the north-north-west, north-north-east and east-south-east in the A, B and C sub-domains, respectively (Figure 3-8). The lineations are not folded by the large D1(b)F1 isoclinal folds, sheath folds (D1(b)F1, D1(b)F2) and neither is the D2F2 folds folding the lineations (Figure 3-11A) so that the regional lineation and fold axes of different folds are co-linear; the lineations are only deformed by D4F1 and D4F2. The western part represents the highly folded area in the Augrabies Falls National Park. The mean orientation of lineations in this part trends towards the north with a plunge of 37° (mean lineation orientation: 35037). Along the Waterval thrust in the western part, the lineations trend towards the north-west but along strike (northwards)

the orientation of the lineations rotates through north towards the north-north-east accompanied by an increase in plunge. This rotation is the result of the north-west trending shears superimposed on the pre-existing L and S fabrics. The age of the shears is probably associated with large scale sigmoidal rotation of the domain (360°-60°) from north-west to south east.

The sub-domain “B” (central part Figure 3-8) of the regional lineations has a wide spread of orientations (Figure 3-11B), this is the result of a younger large S-fold (D4F1) along the southern boundary of the AF-N. The mean trend of lineations is towards the north (01232) and is mostly defined by stretched feldspar minerals on the foliation planes of the Koekoepkop Formation and stretched augens in the Rooipad gneiss (Figure 3-11B). In the eastern part of the AF-N the mean trend of the lineations is towards the north-east (06042) as a result of rotation along the eastern limb of the large open fold (D4F2; Figure 3-11C). If the eastern limb of the D4F2 fold is unfolded the lineations will trend towards the north. The wide distribution of the lineations of the eastern area is the result of late shearing along the eastern limb of the macro-sheath fold (AF-N); the shear zone is known as the Duiwelsnek shear zone (DSZ) after Van Bever Donker (1980).

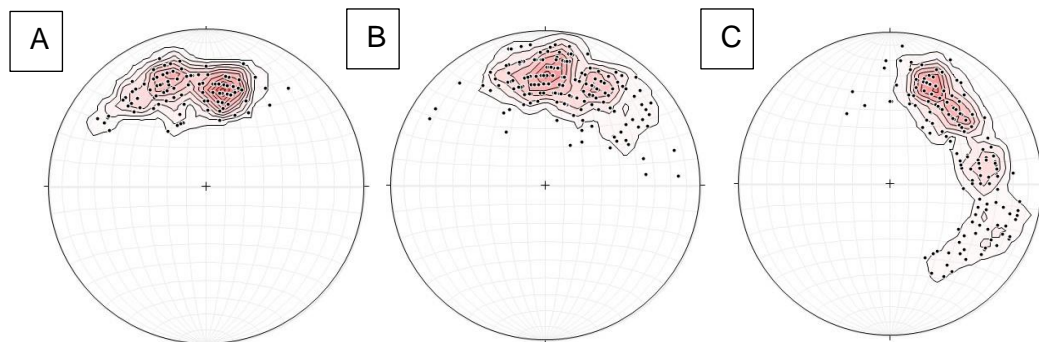


Figure 3-11: Stereonets showing the distribution of the regional stretching (L1) lineation in Domain 3 (Figure 3-8). A. the western part has a mean mineral stretching lineation of 35037 (n=117). B. The central part is defined by a mean lineation of 01232 (n=180). C. In the eastern part of the domain the mean lineation has an orientation of 06042 (n=189). The girdle at C, is caused by rotation due to dextral shear of the Duiwelsnek shear zone (D4).

3.3.5 Macroscopic Structures

The macroscopic structural development of Domain 3 is described from north-west to southeast, beginning with sub-domain A. Domain 3 (Figure 3-8) represents one large sheath fold (AF-N) developed after the onset of terrane accretion with the Augrabies gneiss as the central core (sub-domain A) The sheath fold is refolded towards the end of the sheath fold formation phase. The most noticeable folds are the D2F2 Z-folds in the western part of the

domain where all of the stratigraphy have been folded and the refolding of pre-existing isoclinal fold closures (sub areas a, b, c, and d in Figure 3-8). The folds represent a series of tight synforms (subareas b, c) and antiforms (sub-areas a, b and d) folds with D2F2 axial traces trending north-north-west to south-south-east. The antiforms have fold axes orientation of 05660 and 35138 and the synforms 02753, 02548 (Figure 3-12). Praekelt (1984) explains that the Waterval thrust is folded by these folds and the isoclinal fold in the west, making the thrusting event older than the folds. The folds are interpreted as D2F2 folds because the Brabees structure has a north trending D1(b)F2 trace refolded by these folds (Figure 3-8), meaning that they should post-date the D1(b)F2 folds. However the D2F2 folds also fold the main D1(b)F1 axial trace of the AF-N and the D1(b)F1 trace of the Vaaldrift sheath fold. The fold phases are associated with the D1(b) – D2 episodes (Table 4-3).

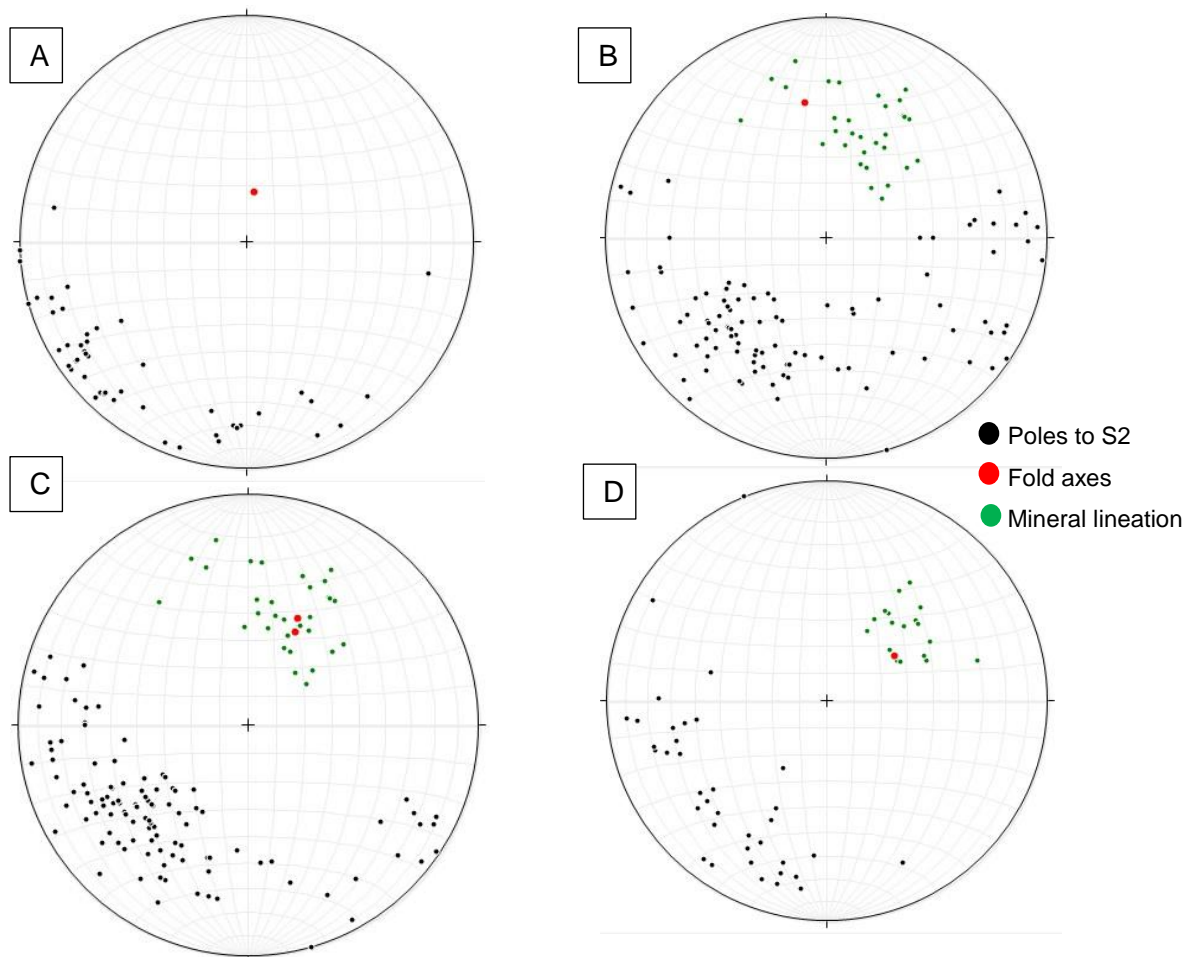


Figure 3-12: Stereonet presenting the fold axes for the D2F2 folds in sub-areas a-d, that form part of the tight Z-fold of sub-domain A (Figure 3-8). The mean lineations for the area is 01956. A: stereonet of the D4F2 isoclinal closure of sub-area a, the fold axes have an orientation of 00972. B: represents the geometrical data for the antiform in sub-area b with a fold axis orientation of 35138. C. Stereonets representing the orientation of the two synforms in sub-area b (02753) and sub area c (02548), respectively. D. Stereonet indicating the geometrical orientation of the antiformal fold hinge in sub-area d with fold axis orientation of 05660.

The western hinge of the Vaaldrift sheath fold and its associated parasitic fold, the western closure of the Oranjekom Complex and isoclinal Eendoorn gneiss closure have been totally transposed with the development of the S2 foliation. The scale and recognition of transpositioning can be observed in sub-area b. The original, now transposed, hinge consist of an inner band of Eendoorn gneiss and an outer band of Rooipad gneiss. The hinge with the various bands (S1/S0) is displaced by a series of shear zones that are developed parallel to the macroscopic axial plane. The displacement along the shear planes placed the two gneissic bands geometrically side by side as illustrated in Figure 3-13. The axial planar foliation represents the regional S2, where it is co-planar with S0/S1. The distance between the shear zones vary from centimetre to decametre. The actual closure is not recognisable and can only be interpreted by the change of lithologies (from Eendoorn gneiss to Rooipad gneiss) along the axial trace of the fold. This same structural process happened to the Vaaldrift sheath fold closure and western closure of the Oranjekom Complex.

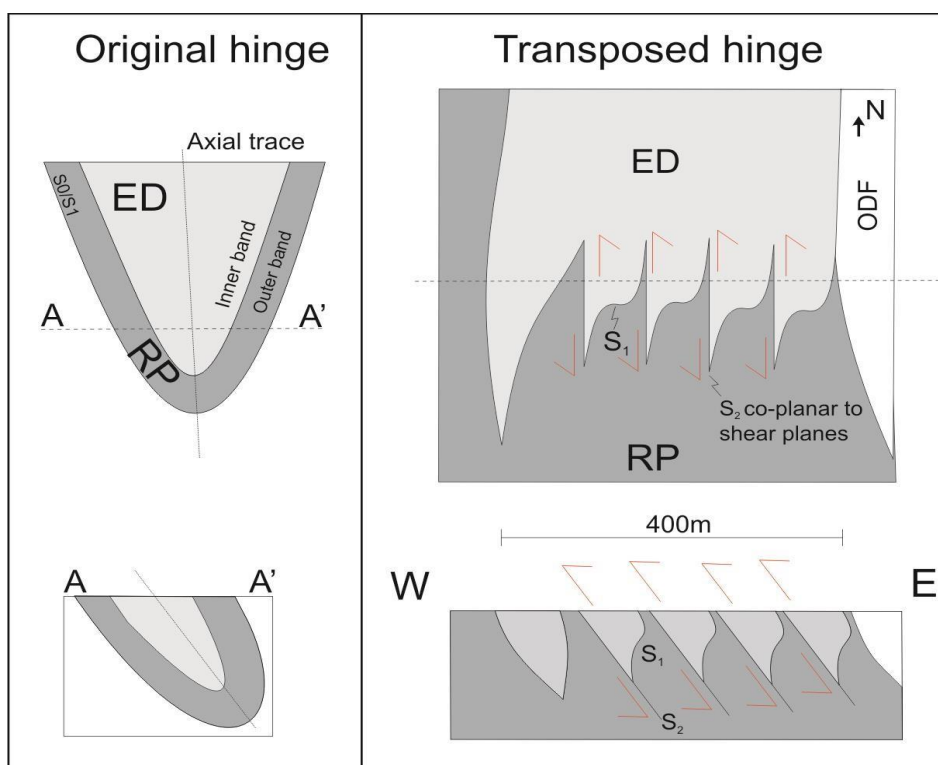


Figure 3-13: Transposition process of the isoclinal Eendoorn gneiss hinge in sub-area b (Figure 3-8). The original hinge contains a folded S0/S1 foliation with an inner Eendoorn gneiss (ED; core) and an outer Rooipad gneiss (RP). The closure is then transposed by shear zones developing sub-parallel to the axial trace of the original fold. The shears zones displace the lithologies (S0) and rotate the S1 foliation which causes the transposition and develops a new foliation (axial planar S2 foliation) which is co-planar to S0/S1 along the limbs of the macroscopic isoclinal fold. The displacement causes ED and RP to be placed side by side – creating an apparent lit-par-lit contact relationship.

The Oranjekom Complex and the north-western part of the Augrabies gneiss (sub-domain A) can be used to demonstrate the process of progressive folding (Figure 3-14). The Oranjekom Complex that intrudes the Rooipad gneiss was mapped by various other researchers (Geringer, et al., 1990; Havenga, 1992) and classified as different structures, e.g. Moen (2007) suggested that the Oranjekom Complex is folded into a curving, synclinal shape by progressive differential simple shear; however in this study the Oranjekom Complex is for the first time recognised as a sheath fold. It has a well-developed eastern closure, with the western closure totally transposed by the above mentioned transpositioning shear process (Figure 3-13). The overall shape of the metagabbro body and the elliptical rings in the eastern portion are typical of sheath folds and can be compared to the modelled forms of Alsop and Holdsworth (2004b). The average fold axis orientation for the Oranjekom Complex is 00866 (Figure 3-14). During the sheath fold development the Rooipad gneiss was folded with the Oranjekom Complex. On the southern limb, the three smaller outcrops of metagabbro occur in line with the southern closure and define boudins of the closure.

The youngest age of sheath fold development is illustrated by the D2F1 axial trace of the Oranjekom Complex sheath fold which folds the D1(b)F1 axial trace of the older Augrabies gneiss which is situated in the core of the AF-N. The D1(b)F1 formed during the D1(b) event when sheath folds initiated in the Grünau Terrane (Table 4-3), but the sheath folds continued to develop due to progressive shear deformation causing multiple F1 sheath folds to develop. The Oranjekom Complex intruded the now existing fabric of the Rooipad gneiss towards the latter part of D2 and simultaneously developed a sheath fold which deformed the Augrabies sheath fold. This progressive shear deformation results in multiple phases of sheath folds (F1 axial traces).

The Oranjekom Complex underwent anatexis with leucocratic melt bands striking parallel to the foliation in the metagabbro (Figure 2-37A). The leucosomes are orientated sub-parallel to the compositional banding and regional foliation which suggest that the melting was after the main fabric forming event; the foliation served as pathways for melt veins (Figure 2-37A). The same melting phase is recorded in the Rooipad gneiss. The south-eastern portion of the Oranjekom Complex is a series of elliptically shaped marker units towards the centre of the structure; the central part of the Oranjekom Complex consists of "finger-like" folds and omega shaped folds associated with the sheath fold closure in the west of the Oranjekom Complex.

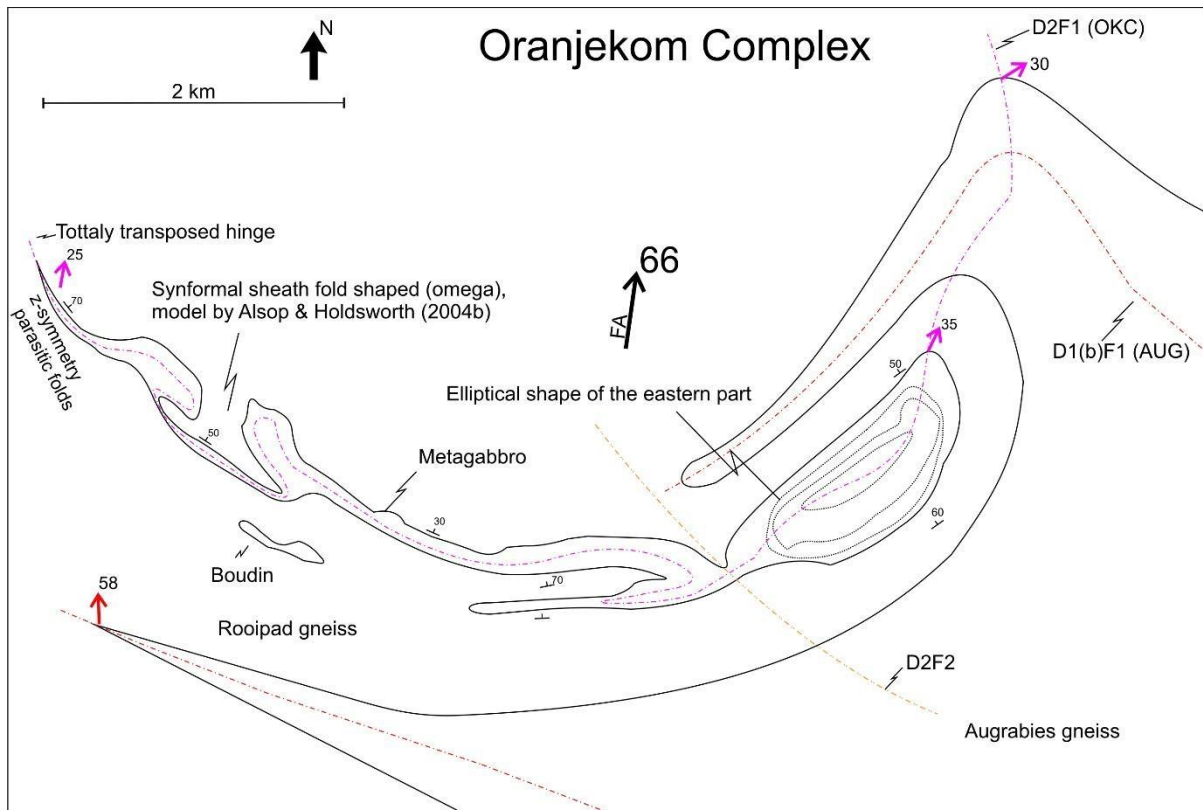


Figure 3-14: Structural map of the Oranjekom Complex sheath fold (OKC). The OKC is defined shape-wise by its closed elliptical lithological traces in the east and “omega” shaped folds in the west; the end isoclinal closure in the west is completely transposed. Geometrically the fold axes are sub-parallel with a mean trend and plunge of 08866. The D1(b)F1 axial trace of the Augrabies gneiss (core of the AF-N) is folded by the D2F1 fold of the Oranjekom Complex. This indicates that within one domain or structure multiple fold phases (ages) can exist and even refold each other. This is the type of effect associated with progressive deformation.

The Augrabies gneiss in the core of the AF-N forms a large sheath fold with fold closures towards the east and west. The large open fold closure in the east is incised by the Orange River and overlain by quaternary cover on which vineyards are distributed, but the western closures are well exposed. The south-western closure is an isoclinal closure which is attenuated along strike and is totally transposed; the hinge width varies from 500m to less than 2m in thickness where highly attenuated. The north-western isoclinal closure with an axial planar foliation is refolded by the Oranjekom Complex sheath fold. The overall shape of the Augrabies gneiss is similar to one half of a modelled sheath fold (Alsop & Holdsworth, 2004b). The structure has a refolded D1(b)F1 axial trace; folded by the D2F1 of the Oranjekom Complex (as explained above) and then the D1(b)F2 axial trace trending north-west to southeast.

On the southern limb of the AF-N a flat lying D4F1 S-fold (sub-area E), folds the WVT and surrounding lithologies (Rooipad gneiss, Seekoeisteeek gneiss, Koekoepkop Formation, Eendoorn gneiss and Witwater gneiss). The fold is interpreted to be younger than the sheath

fold event due to the folding of all the pre-existing meso- to microscopic structures, the lineations and foliation. The S2 foliation is folded around the closures and no transposed fabric is recognised. The fold axes of the synform and antiform plunge towards the west (28911) and this does not relate to the other fold axes of domain 3 that plunge north to north-east (Figure 3-15). The southern synformal closure consists of five smaller individual hinges that represent M and W symmetry folds. The D4F1 fold axial traces are limited to the S-fold and trend east-west. The folds relate to the younger sinistral shear period that occurred across the domain (D4 event discussed in the following section 3.3.6).

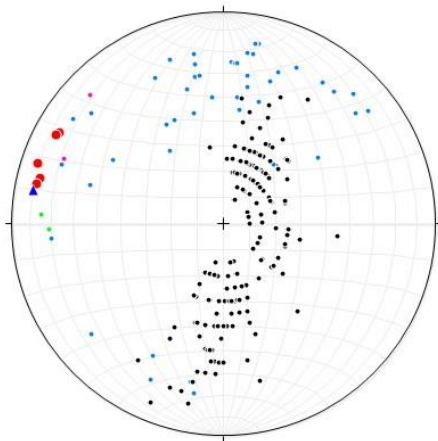


Figure 3-15: Stereographic projection of large S-fold (D4F1) on the southern limb of the Augrabies sheath fold (Figure 3-8). Fold axes symbols for the D4F1 folds are: synform (blue triangle), antiform (red dots), parasitic z (green), parasitic s (pink); L1 regional lineations (blue), poles to the regional S2 fabric (black).

The Brabees gneiss is a large granitic body enveloped within the Rooipad gneiss but has been folded into a large Ramsay Type 2 interference fold (mushroom structure, Figure 3-8). There are two closures towards the south-east and one larger stretched out closure towards the north. The mushroom structure of Brabees gneiss is also deformed into a sheath fold due to progressive folding after its intrusion into the Rooipad Gneiss (refer to explanation on the Nelshoop gneiss mushroom of Domain 2; section 3.2.5). The D1(b)F1 trace is refolded by the north-west striking D1(b)F2 axial trace. The north-western isoclinal closure and D1(b)F2 axial trace underwent extension and is thinned towards the north where it is folded by the D2F2 Z-folds in sub-area b. The closure is totally transposed by an axial planar S2 fabric. Towards the southern part of the structure the D1(b)F1 axial trace is nearly sub-parallel to the second order axial trace due to the flattening and stretching of the sheath fold.

The northern fold closure of the AF-N (sub-area d) has a fold axis orientation of 05660 and lies within the cluster of mineral lineations. There is a slight (clockwise) rotation between the

mean transport direction and the fold hinge. In the south-east on the farm Swartpad the AF-N has three major isoclinal plunging inclined fold closures. Connecting the northern D1(b)F1 axial trace and the southern D1(b)F1 axial traces gives rise to a sigmoidal shape for the trace of the AF-N (Figure 3-8 inset). It indicates crustal scale sinistral shear. The axial traces of the three southern closures trend north-west and developed a concave shape due to the dextral shear effects of the Duiwelsnek shear zone (sub-area C). The southern Swartpad isoclinal fold closure (sub-area g) has an orientation of 09533, and the northern Duiwelsnek isoclinal fold closure (sub-area f) has an orientation of 09946 (Figure 3-16A, B). The easterly plunge of the fold axis and the lineations are a result of the later open fold (D4F2), which rotated the eastern part of the structure towards the south, refer to the regional foliations of the eastern part (Figure 3-10C). If the rotation of the eastern part is eliminated or unfolded the fold hinges will plunge towards the north-east, which is sub-parallel to the rest of the AF-N fold closures.

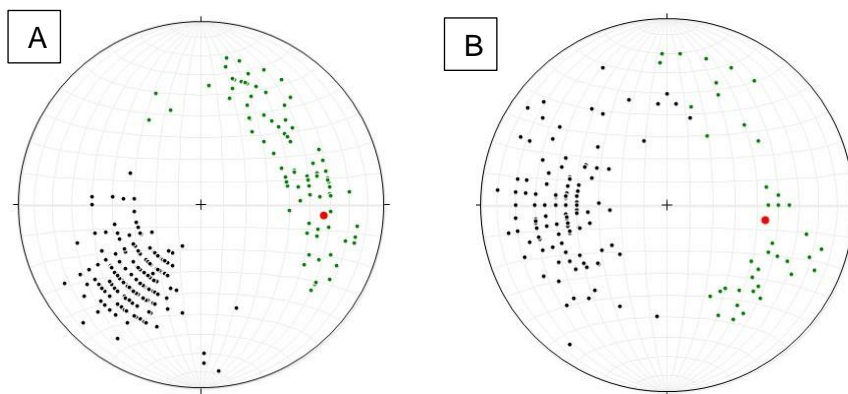


Figure 3-16: Stereonets presenting the structural features and geometries of the Swartpad and Duiwelsnek closures (sub areas “g” and “f”, respectively; Figure 3-8). The orientation of fold axes for the Swartpad (A) and Duiwelsnek (B) closures are 09533 and 09946, respectively. The easterly plunges of the hinge zones are the result of the D4F2 open fold that is produced by the regional shear events.

3.3.6 Mesoscopic Structures

Mesoscopic structures in the AF-N domain includes folds, shear zones, s-c fabrics and grain tail complexes. Primary structures (e.g. grading in the Koekoekop Formation; section 2.2.1.1) are in some localities still preserved in the supracrustals and give an indication of the facing and younging directions. The structures used as kinematic indicators display three periods of shear movement in Domain 3; the early intra-terrane thrust movement (D1(b); Table 4-3) coincides with the intrusion of the sheet granites and two younger periods of lateral movement which occur along the reactivated intra-terrane thrust boundaries, internal layering and foliations (Map 2; section 3.1.2).

Two dominant sets of D1(a)F1 folds are recognized in the AF-N and will be referred to as model 1 and model 2 folds, which is an indication of the fold style process of formation - not the age relationships (Figure 3-17; Figure 3-18). Characteristics of the two fold types:

- Model 1 (D1(a)F1; Figure 3-17; Figure 3-19; Figure 3-20A, B):
 - o Intrafolial and bounded within layers on centimetre to metre scale.
 - o Folds S0 and gives rise to a prominent regional S1 fabric which is co-planar with S0.
 - o “S” and ‘Z” symmetries seen in yz plane.
 - o Fold axes and regional lineation (L1) are co-linear.
 - o Axial planes are co-planar to S0/S1.
 - o Fold hinge transposed, forming a penetrative axial planar cleavage (S2).
 - o Fold boundaries are shear planes defined by incompetent layers.
 - o Relates to D1(a).

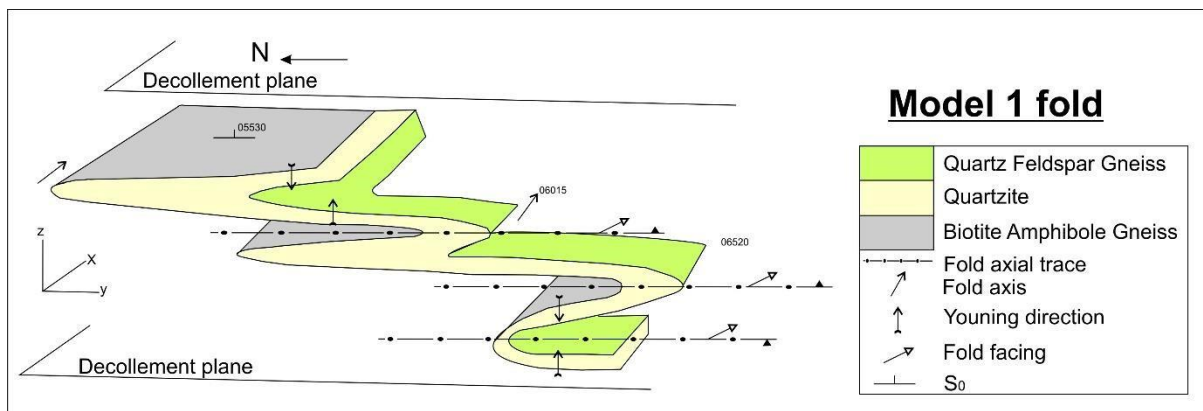


Figure 3-17: Schematic illustration of the model 1 folds (D1(a)F1) formed by layer-normal shear during the flow perturbation process. The fold axes are co-linear with the stretching lineation or tectonic transport direction ($<45^\circ$ to the flow direction). In this case the transport direction is out of the page (parallel to the co-linear linear fabrics).

- Model 2 (D1(a)F1'; Figure 3-18; Figure 3-19; Figure 3-20A, C):
 - o Occurs interbanded within layering and is also intrafolial on centimetre to meter scale.
 - o “S” and ‘Z” symmetries, with “S” dominant in the xz plane.
 - o Fold axes forms an acute angle with the regional lineation (L1).
 - o Axial plane is co-planar with S0/S1.
 - o Fold hinges are transposed, producing a penetrative fabric which is co-planar with Model 1 axial plane, regional foliation and layering (S0).

- o Contained between shear planes defined by incompetent layers
- o Relates to D1(a).

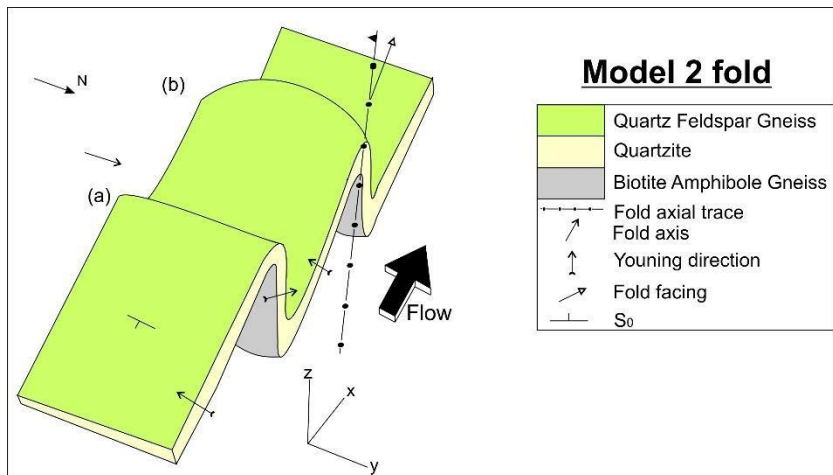


Figure 3-18: Schematic illustration of the model 2 folds (D1(a)F1') formed by layer-parallel shear during flow perturbation. Fold axes are at a high angle ($>45^\circ$) to the flow direction/transport direction/ mineral stretching lineations.

Comparison of Model 1 and Model 2 folds:

- Profile of Model 1 (D1(a)F1) develop on yz plane of shear zone.
- Profile of Model 2 (D1(a)F1') develop on xz plane of shear zone.
- The angle between Model 1 and 2 axes vary between 45° and 90° .
- Model 2 originates with fold axes perpendicular to the stretching direction, but during progressive shearing the fold axes rotate towards the stretching direction (X-axis) to become almost co-planar with Model 1 fold axes (formation of a mesoscopic sheath folds).
- Model 1 and 2 have co-planar relationships with regional foliation and bedding. Linear features differ, with Model 2 fold axes forming acute angles with both mineral lineation and fold axes of Model 1.
- Mineral lineation occurring in the foliation planes is associated with both Model 1 and 2 indicates coeval development.
- No interference structures are observed.

Based upon the above, both Model 1 and 2 folds formed simultaneously as part of a regional shear regime during D1(a) event. The model for their development is illustrated in Figure 3-19, by the process of flow perturbation during progressive ductile shear (Alsop & Holdsworth, 2007). Model 1 folds formed by layer-normal shear along boundaries of flow cells (lateral ramps) while the model 2 fold formed by layer-parallel shear along the frontal ramps (Coward & Potts, 1983). The folds developing along the lateral ramps (model 1) will have fold axes sub-parallel ($<45^\circ$) to the tectonic transport direction (thrusting direction = stretched mineral

lineations), while in the frontal ramp folds (model 2 folds) will have fold axes normal ($>45^\circ$) to the transport direction (Alsop & Holdsworth, op.cit).

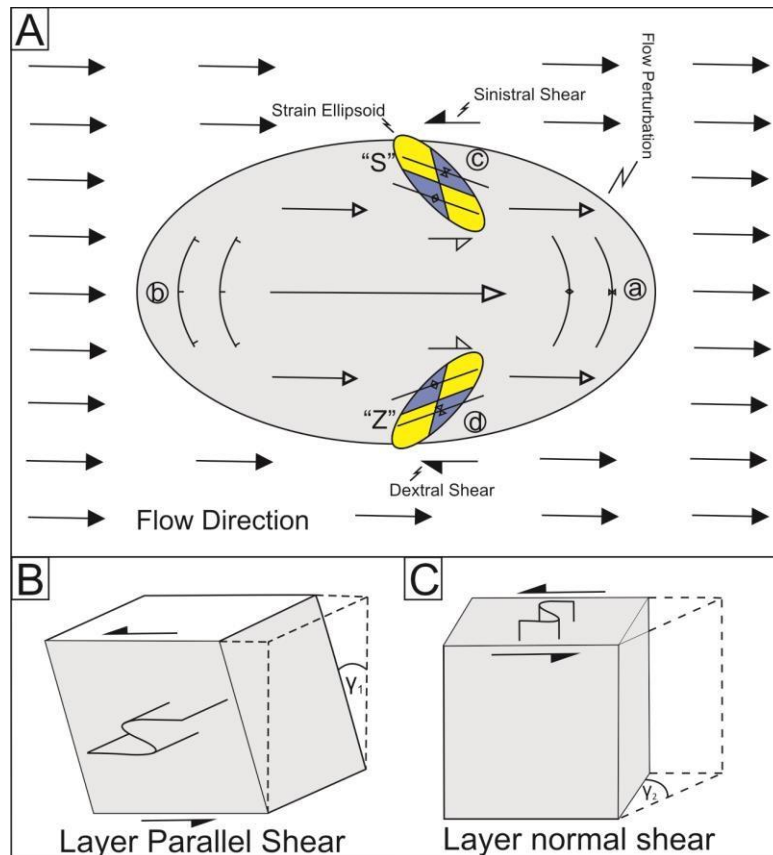


Figure 3-19: General shear models of flow cells and related layer-parallel and layer-normal shear processes (modified from Alsop and Holdsworth, 1993, 2007). A: Schematic plan view of a flow cell in non-coaxial flow. The grey ellipse represents the flow cell, and the length of the open arrows within in the flow cell indicates the relative flow velocities. In areas “c” and “d” differential sinistral and dextral shear, respectively, are caused by the retardation in flow (indicated by half, open arrows). Strain ellipsoids are represented by the blue (shortening sector) and yellow (stretching sector) ellipsoids. Areas “c” and “d” fall within the shortening sectors (blue) of the strain ellipsoid and results in S- (“c”) and Z- fold (“d”) symmetries – the model 1 folds of this study. Z-folds will have a fold axis sub-parallel or clockwise sense of obliquity to the flow direction; S-fold fold axes will be sub-parallel or they will have an anticlockwise sense of obliquity to the flow direction. At area “a” layer-parallel shear will form folds at high angle to the flow direction (model 2 folds), verging in the direction of flow. Area “b” represents an area of elongation and stretching. B: Shear strains associated with layer-parallel shearing develop at the frontal tips (“a” in A) to thrusts and shear zones, resulting in folding at a high angle to transport, i.e. Model 2 folds. The layering (S₀) and S₁ foliation lie approximately parallel to the base of the cube. C: Differential shear strains associated with layer-normal shearing develop at lateral ramps to thrusts and shears, resulting in asymmetric buckle folds with axes oblique or even sub-parallel to the direction of flow, i.e. Model 1 folds.

Model 1 and model 2 folds occur on centimetre to metre scale and may be observed in a single outcrop (Figure 3-22A). The model 1 folds have s- and z- symmetries along strike and do not relate to D5 north-west shearing (Table 4-3) but rather to the D1(b) thrusting event (thrusting direction is sub-parallel to mineral lineation and fold axes of Model 1 folds). The geometric features (L and S fabrics) indicate a south-westerly tectonic transport direction, implying overthrusting of the AF-N onto the Grünau Terrane along the Waterval thrust.

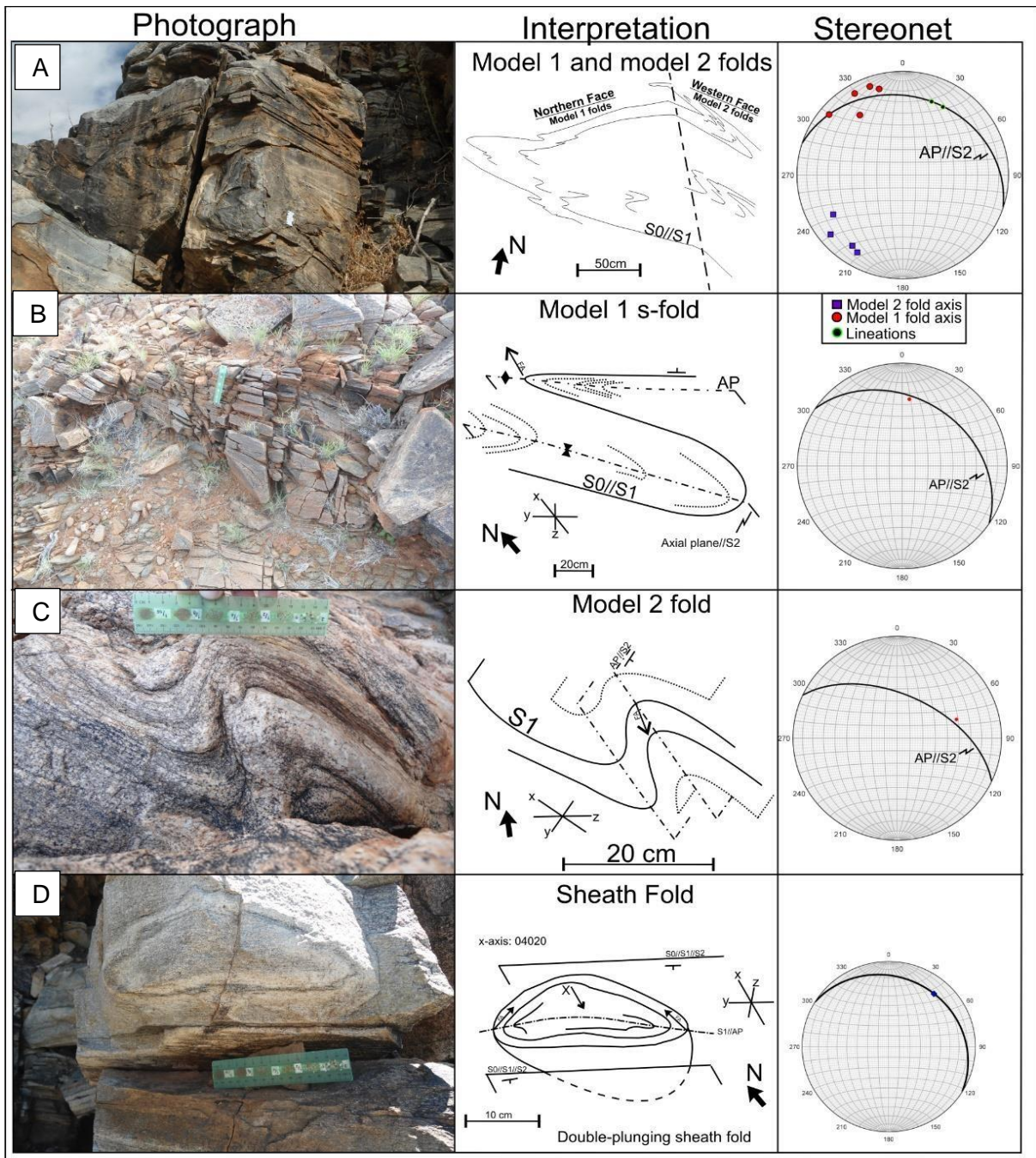


Figure 3-20: Mesoscopic structures of Domain 3 relating to the D1(a/b) deformation events. A: A single outcrop containing both model 1 and model 2 folds; the folds formed simultaneously. B. Model 1 S-fold in the Koekoepkop Formation with S2 as an axial planar cleavage. C. Centimetre scale model 2 S-fold also having transposed hinges and an S2 axial planar cleavage. D. Sheath fold in the Koekoepkop Formation, the long axis plunges towards the north-east which is sub-parallel to the regional stretching lineation. The axial plane of the sheath fold is co-planar to the regional S2 foliation (xy-plane of the strain ellipsoid).

A series of late crosscutting shear zones are found only in the Augrabies gneiss (D4; metre scale), namely: north-south (350-170/ 005-185) and north-westerly (130-310) trending shear zones (Figure 3-21, Figure 3-22A). The north-south shears are the older set of shears, the southeast north-west trending shears cut across them. The north-south shear zones have a

sinistral sense of shear combined with a sub-vertical component (western block moves up with respect to the eastern block; Figure 3-22). The north-south shear zones anastomose on a regional scale and rotate the foliation of the gneiss. The width of the north-south shear zones can range up to 5m.

The north-westerly trending shear zones have two sets of movement with the dominant one being an oblique sense of shear, left lateral movement with the northern block moving down relative to the southern block and the less dominant being the dextral shear zones. They have a smaller width than the north-south shear zones and occur more frequently throughout the gneiss. They have the same orientation as the D5 kilometre scale shear zones and relate to the D4 event. In some localities it was found that the north-westerly trending shear zones cross cut the Augrabies and Roopad gneiss contact. The shears in these localities are on centimetre scale with an average of 6 shear bands per square metre. The wavy fabric in the Augrabies gneiss is a result of the second set of shears. The schlieren structures (Figure 2-27A, D) in the Augrabies gneiss pre-date the shearing events.

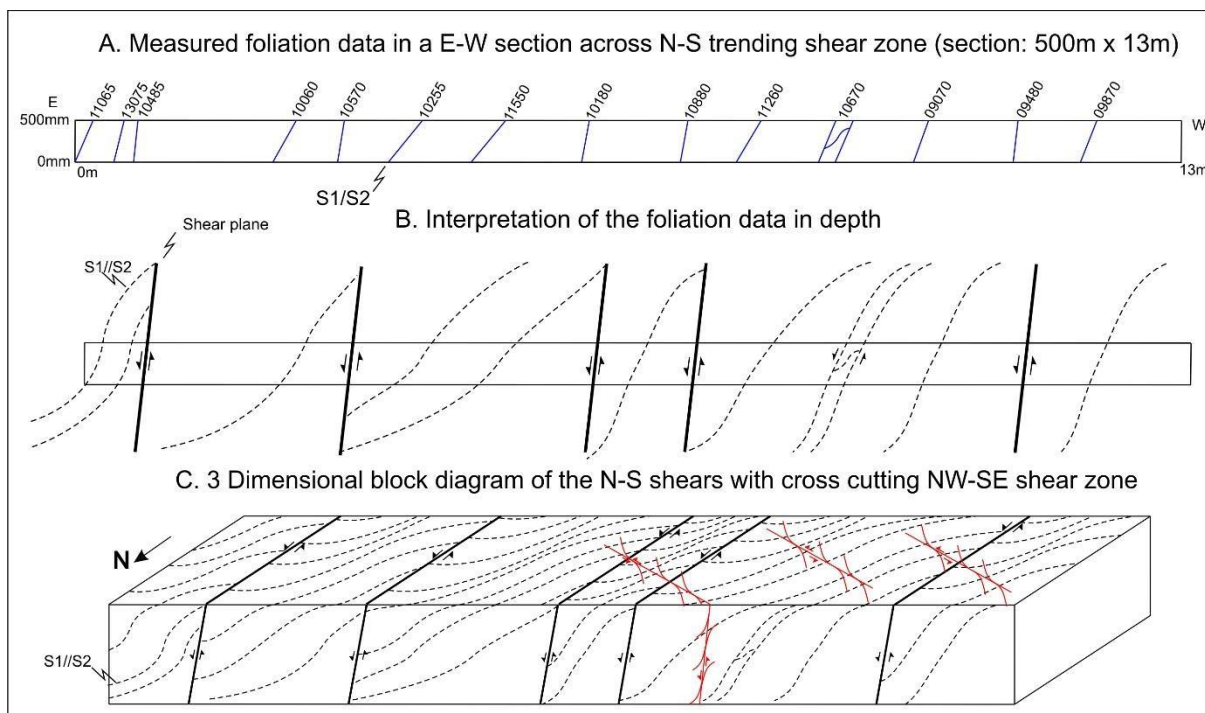


Figure 3-21: Structural interpretation of D4 shears in the Augrabies gneiss. A shows a 500mm high cross section measured in the Augrabies gneiss, the planes above the section are measured in dip direction and dip. B. The increase in dips of foliation are interpreted to represent sheared fabric between the shear planes. The foliation (S1/S2) with the shallower dips presents the foliation outside of the shear zones, they rotate to the vertical in close proximity of the shear planes. C. The three dimensional block diagram displays the relationship of the north-south shear zones with the north-west south-east shear zones, the latter being the youngest.

Another type of mesoscopic structure developed are shear cleavages (s-c fabrics) and are especially apparent with reactivated D1 thrusts and associated thrust sheets (Figure 3-22B); they serve as kinematic indicators for the ductile shear directions in the AF-N. The younger (D5) lateral shear along the southern boundary of the AF-N (Waternal thrust) displays an oblique movement with coeval lateral and vertical components; the lateral component is sinistral with west-up. The sinistral shear (Figure 3-22B) in the Basal Unit of the Koekoepkop thrust sheet is supported and confirmed by grain tail complexes (Figure 3-22C) in the underlying Eendoorn gneiss. A second lateral shear event is recorded by s-c fabrics and grain tails indicating the right lateral shear (Figure 3-22D), however they are not abundant.

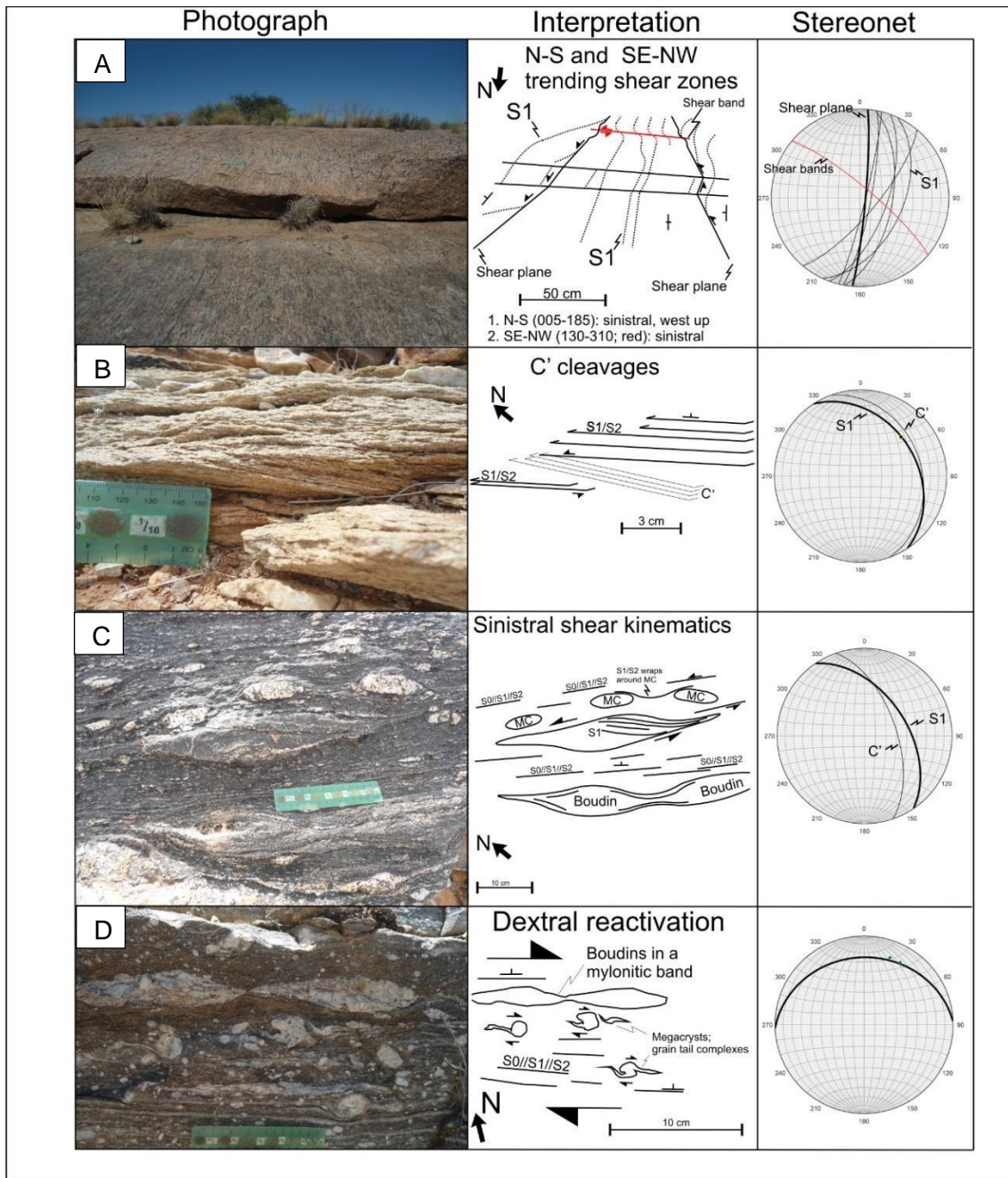


Figure 3-22: Mesoscopic structures associated with the D4 late shearing. A. Cross cutting metre scale shear zones in the Augrabies gneiss. Two sets of shears, older (larger) north trending shear zone is cut by a younger (smaller, red) south-east trending shear zone. B and C are associated with the sinistral shearing along the Waterval thrust after when the thrust was reactivated as a shear zone during D4. B. S-c' cleavages indicates sinistral shearing. C. Mylonitic bands in the Eendorn gneiss contains boudin structures due to the shearing. Present in the mylonitic band is the primary S1 fabric which is rotated anticlockwise, indicating sinistral shearing. Elsewhere S1 and S2 is co-planar in the gneiss. The shearing has also rotated the megacrysts. D is an xz plane of the later dextral shearing along the Waterval thrust; it contains boudins and grain tail complexes indicating dextral shear.

3.3.7 Summary of Domain 3: Augrabies Sheath Fold

- Intra-terrane thrusting (Waterval and Kliprug thrust initiated at D1(b) (Table 3-2).

- The granite gneisses of the Augrabies sheath fold intruded the supracrustals during the D1(b) event along the intra-terrane thrust; the sheath fold is bounded by roof and sole thrusts (Kliprug and Waterval thrusts).
- The S1 shear fabric formed during the intrusion of the granites in a sub-horizontal shear regime.
- After the intrusion of all the granites, both the supracrustals and plutonic rocks and the intra-terrane thrusts are deformed by progressive folding forming macroscopic sheath folds. This resulted in folding of the S1 fabric and structures relating to the thrusting event (e.g. model 1 and model 2 folds = D1(a)F1 and F2' folds).
- D1(b)F1 axial traces of the sheath folds have a north-easterly trend.
- D1(b)F1 sheath folds are the first of the macroscopic fold structures to develop.
- The hinges of the sheath fold are transposed and a S2 fabric developed as an axial planar cleavage. Along the limbs of the structures the S2 is co-planar to the S0/S1 foliations.
- S0/S1 is only recognised in the hinges of semi-transposed fold closures, implying that the S2 is the regional foliation.
- The sheath folds (D1(b)F1/F2 and D2F1) and associated S0/S1/S2 foliation have been folded by D2F2 folds during the latter part of D2.
- Sheath folding continued from D1(b) to the end of D2 when the Oranjekom Complex intruded as part of progressive shear deformation. This resulted in two phases of F1 folds; the D2F1 axial trace of the Oranjekom sheath folds the D1(b)F1 axial trace of the Augrabies gneiss.
- The intra-terrane thrust and associated thrust sheets are reactivated as north-west trending sub-vertical shear zones during D4.
- D3 (Friersdale Charnockite) is not present in Domain 3.

Table 3-2: Structural framework for Domain 3: Augrabies sheath fold.

Deformation event	D1a	D1b			D2		D4		
Structural event	Model 1 and 2 folds	Intra-terrane	F1	F2	OKC-F1	F2	F1	F2	NW shear zones
Domain 3: Augrabies sheath fold	x	x	x	x	x	x	x	x	x

3.4 Domain 4: Vaaldrift Sheath Fold

Structurally overlying the AF-N is the Vaaldrift sheath fold (VSF) separated by a decollement interpreted as the Kliprug intra-terrane thrust (KRT; Figure 3-23). The VSF can be sub-divided into four sub-domains (Figure 3-23). The western sub-domain consists of multi-refolds of the north-western fold closure. The long limb of the sheath fold defines the central sub-domain; the limb trends west and then north-west as it is folded by the large open fold (D4F2)

The eastern sub-domain consist of the south-eastern tail-end where it is refolded into a Ramsay Type 3 interference folds. The northern sub-domain is a smaller sheath fold (N-VSF) that strikes parallel to the VSF and contains its own stratigraphic packages. Van Bever Donker (1980) describes at least three major deformational events for the eastern part (3) of the VSF, which would correlate with D1(b) and D2 of this study.

3.4.1 Stratigraphy

The VSF consist of the Omdraai Formation which is a metamorphosed volcano-sedimentary sequence with thick units of felsic rocks (Praekelt, 1984). The core of the sheath fold is defined by sequences 3 and 4, with 4 in the centre (“eye”). Sequences 1 and 2 only occur on the northern limb of the sheath (footwall to the Harpersputs thrust, HPT), where they form branch points at either end over a distance of approximately 60km. Sequence 5 occurs only along the southern limb of the eastern sub-domain, forming branch points along the Kliprug thrust with the Rooipad gneiss as footwall. Sequence 6 is contained within the N-VSF.

The contacts between the 6 sequences of the Omdraai Formation are sharp and planar, locally the internal contacts between units of individual sequences are gradational. The amphibolite sequence within the third sequence in the western sub-domain pinches out along strike. Along both the Kliprug and Harpersputs thrust lenses of the Omdraai Formation (centimetre to metre scale) occur in the overlying Harpersputs gneiss and underlying Rooipad gneiss. These lenses are interpreted as imbricates of the thrust and do not reflect a lit-par-lit contact relationship. Based upon the contact relationships of the 6 sequences in the VSF the Omdraai Formation is interpreted as structural unit, i.e. a stacking of thrust sheets with the primary stratigraphic order of the sequences equivocal.

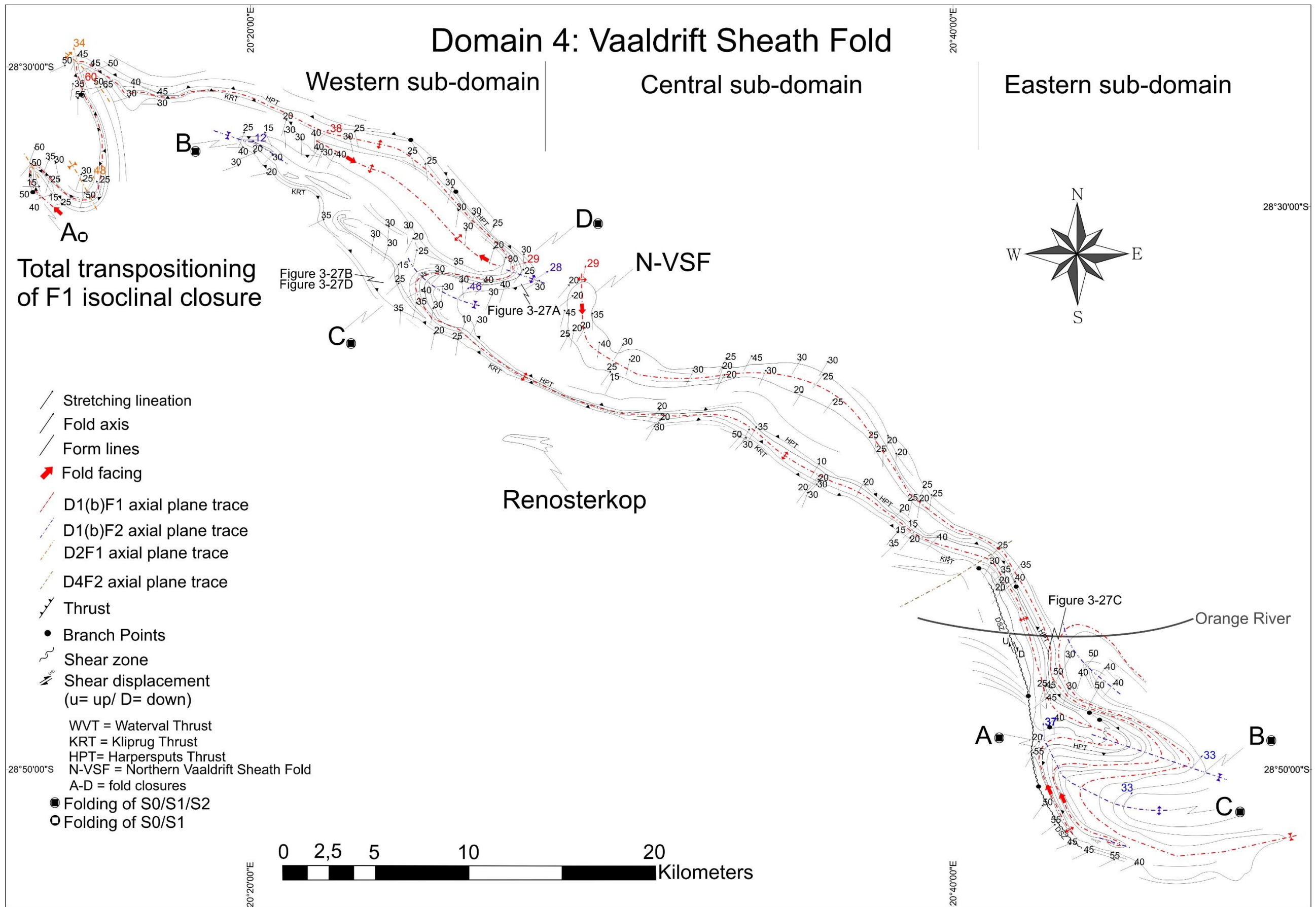


Figure 3-23: Structural map of domain 4: Vaaldrift Sheath Fold. Domain 4 is sub-divided into a western, central and eastern sub-domains. The western sub-domain contains fold hinges A to D associated with the D1(b)F1 and D1(b)F2 sheath folding events. The area between B, C and D is classified as a culmination zone whereas the central and eastern sub-domains are depression zones. The N-VSF is the northern Vaaldrift sheath fold and contains the sixth sequence of the Omdraai Formation. The S-fabrics in the N-VSF is co-planar to the regional VSF S-fabric and the L-fabrics are co-linear.

3.4.2 Domain boundaries

The VSF is boarded by two major decollements, namely the Kliprug (KRT) and Harpersputs (HPT) thrust. The southern limb of the sheath fold is defined by Kliprug thrust and the northern limb by the Harpersputs thrust. A characteristic of the Kliprug thrust is the branch points that formed along the contact of the number three sequence which can be observed on a metre scale. This character can be noted on a kilometre scale along the northern Harpersputs thrust where the first and second sequences forms branch points in the western and eastern subdomains.

In the southern part of the eastern sub-domain the KRT have been reactivated as a kilometre scale sub-vertical shear zone and mapped as the Duiwelsnek shear zone (DSZ; Van Bever Donker, 1980). The DSZ has a dextral sense of shear and according to Van Bever Donker (op.cit) a considerable amount of vertical displacement, with east up. Towards the eastern part of the domain the smaller macroscopic sheath fold (N-VSF) is in contact with the main VSF due to the effects D4 shearing; the underlying Harpersputs gneiss is thinned out as a result.

3.4.3 Regional foliation

The regional S2 foliation in the lithologies of the Omdraai formation is typically defined by the planar alignment of biotite, amphibole and feldspar. In the western sub-domain, the foliation has a general dip of 30° towards the north-east (04530) and is folded, together with the coplanar S0 and S1, around the large fold hinges in the sheath fold (Figure 3-23, closures B, C and D). The distribution of S2 poles in the various folds of the western sub-domain is shown in Figure 3-24A.

In the central sub-domain along the long limb of the VSF there is a 5° rotation of the foliation towards the north-north-east with the dips remaining the same (04029; Figure 3-24B). In the eastern sub-domain of the VSF the foliation has been rotated towards the east due to the large open fold (D4F2) and the dips are steeper due to effects of the DSZ; the mean orientation of the regional foliation in this part of the VSF is 08242 (Figure 3-24C). The foliation of the N-

VSF is co-planar to the foliation of the main VSF. The mean dip of the foliation in the N-VSF is 31° towards 46° (north-east dipping; Figure 3-24D).

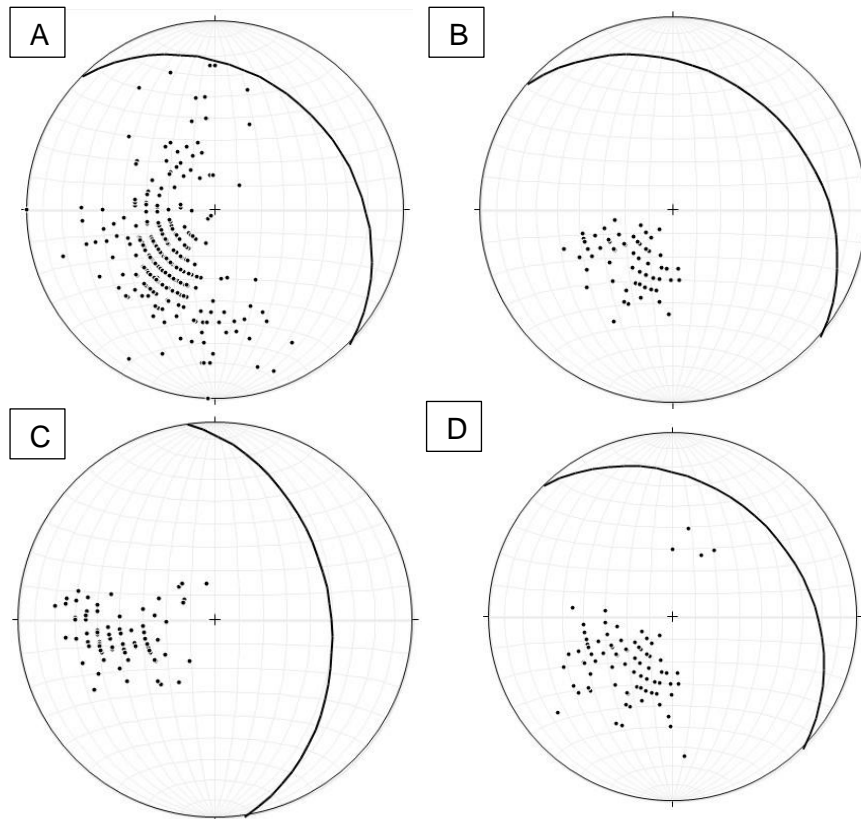


Figure 3-24: Stereonets of the regional foliation (S2) in the three sub-domains and Northern-Vaaldrift sheath fold (N-VSF) of Domain 4 (Figure 3-23). The poles to the S2 foliation show a distribution around the great circle for the western and eastern sub-domains; the central approximates a point maximum: the variable distribution of poles is due to late D4 regional shearing effects on mesoscopic folds and limbs. A. Western sub-domain with a mean S of 04530 (n=343). B. The long limb of the VSF (central sub-domain) has an average S2 foliation of 04029 (n=67). C. The eastern sub-domain has a mean S2 foliation of 08242 (n=82), the rotation being the result of the D4F2 open fold. D. For the N-VSF the S2 foliation is generally co-planar to the S2 foliations in the underlying VSF, 04631 (n=102).

3.4.4 Regional lineation

The regional lineation in the VSF is generally dominated by stretching lineations defined by co-linear quartz and feldspar aggregates (all sequences), and by sillimanite and amphibole needles in sequences 1 and 6. The western sub-domain has a mean value of 02935 (Figure 3-25A) which is sub-parallel to the regional stretching direction (x-axis of strain ellipsoid; 02836) indicating that the lineations are forming under simple shear processes.

In the central sub-domain of the VSF the lineations have a shallower plunge and rotate from a north-north-easterly trend (in the western sub-domain) towards a north-easterly trend

(03927; Figure 3-25B), which is a 10° rotation. In the eastern sub-domain of the VSF the mean trend of the regional lineation is towards 39 with a plunge of 31 (Figure 3-25C), which is co-linear with the lineation of the central sub-domain. The lineations in the smaller macroscopic N-VSF are co-linear with the lineations of the main VSF with a mean orientation of 03128 (Figure 3-25D), again the lineations of the northern sheath fold are co-linear to the stretching direction with 3° of obliquity.

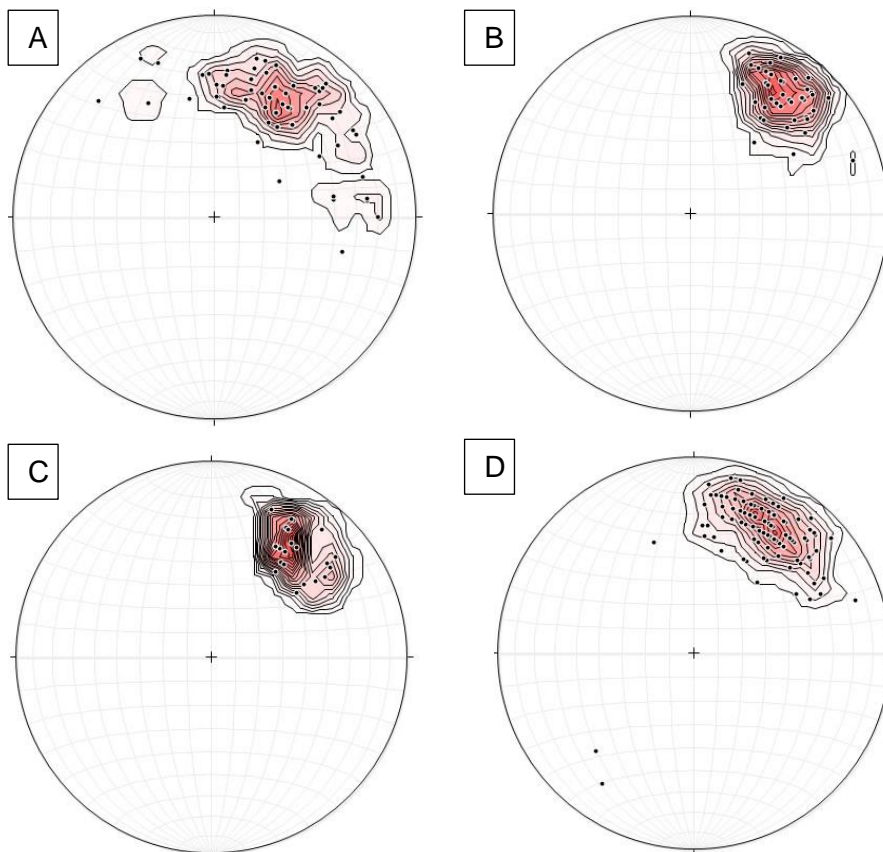


Figure 3-25: Stereonets showing the distribution of the regional stretching lineation (L1) in the VSF. A. Western VSF with a mean orientation of 02935 (n=68). B. Central VSF with a mean orientation of 03927 (n= 47), C. Eastern VSF with a mean lineation orientation of 03931 (n=23). D. N-VSF with a mean lineation orientation of 03128 (n=92), which is co-linear to the regional lineation in the underlying VSF.

3.4.5 Macroscopic Structures

The shape of the VSF in the western sub-domain of the structure is similar the schematic modelled omega shape of a sheath fold by Alsop and Holdsworth (2004b, Figure 4-2), but with only one well developed side of the omega and will be referred to as a semi-omega (Ω) shaped sheath fold from here onwards. The mechanism of formation is described and discussed in section 3.4.7. The structural history of the Vaaldrift sheath fold indicates that it consist of two phases of sheath folding namely: the first phase of folding deforms the S0/S1 and produces

the S2 axial planar foliation (becomes the regional foliation) in the south-eastern and north-western closures - D1(b)F1, the main regional F1 axial trace of the VSF. The second phase of sheath folding is the result of localised shortening around the “eye” structure of the VSF deforming the original sheath fold and develops the semi-omega shape – localised D1(b)F2. The semi-omega structure is characterised by a kilometre scale D1(b)F2 “Z” fold with a south-easterly vergence and facing. The western sub-domain is interpreted as a culmination zone with the fourth sequence of the Omdraai Formation as the core and the thickened stratigraphy. The central and eastern sub-domains are interpreted as the depression zones of the shear regime. Culmination and depression zones are defined as areas with an increase in flow velocity (culmination) and areas with slugging flow velocity (depression) by Alsop and Holdsworth (1999, 2007).

In the western sub-domain the north-eastern hinge zone (Figure 3-23, fold hinge A) is an isoclinal fold closure that have been boudinaged and refolded by the tight Z-folds in the Augrabies Falls National Park (section: 3.3.5 “Macroscopic Structures of Domain 3”) and the same model for transposition in the Eendoorn closure (section: 3.3.5, Figure 3-13) can be applied to this isoclinal closure of the VSF with the Rooipad gneiss. The western limb of the isoclinal closure forms a branch point along the Waterval thrust. The north-western hinge (Figure 3-23, fold hinge B) is a synformal closure with fold axis orientation of 09912 (Figure 3-26).

In the western sub-domain of Domain 4, the F1 trace of the VSF is folded by D1(b)F2 and D2F1 (Figure 3-23). The large D1(b)F2 isoclinal Z-fold of the omega shape structure on the boundary between the western and central sub-domains has a synformal (C) and an antiformal (D) hinge zone. The antiformal fold axis plunges 28° towards 058° while the synformal fold axis plunges 43° towards 46° (Figure 3-26). Both the synformal and antiformal hinges of the Z-fold have a clockwise sense of rotation with respect to the stretching direction. The angle between the synformal- and antiformal hinge and the stretching direction is 16° and 34° respectively.

The central sub-domain of the VSF is defined by the long limb of the structure and connects the western and eastern sub-domain and is also folded by the large open fold (D4F2) that folded the AF-N (section 3.3.5), the hinge having an orientation of 02829 (Figure 3-26). The long limb of the structure is thinned out along strike from 250m to less than 100m due to stretching, however the stratigraphic polarity remains constant northwards along strike of the D1(b)F1 axial trace.

The eastern sub-domain of the VSF has not been mapped in its entirety during this study; access was denied to the 3000ha which contains mostly areas B and C (Figure 3-23). The information presented here is based upon mapping of boundaries and re-interpretation of Van Bever Donker (1980) published results. This sub-domain is characterised by a large Ramsay Type 3 interference fold that developed after the wedging of the lithologies. There are two co-planar D1(b)F1 fold axial traces associated with both the south-eastern closures of the VSF and NVSF which are refolded by D1(b)F2. Van Bever Donker (1980) divided the area into 3 subareas (A, B and C). He classified the synformal fold at B as class 1C fold (Ramsay, 1967) with the fold axis plunging 33° towards 40°. The hinge at C is an antiformal structure with a hinge plunging 37° towards 354° which classifies the fold as a plunging inclined fold (Van Bever Donker, op.cit). The fold axes of areas B and C suggest that the hinge zones are co-linear with the rest of the fold closures in the VSF and reflect one progressive folding event. The folds defined by Van Bever Donker (1980) are considered to be F2's of the D1(b) event.

Stratigraphic sequence 5 can be defined as a thrust sheet situated on the southern intra-terrane thrust of the VSF; it has branch-points towards the north and south on the footwall thrust (Rooipad gneiss). The only sequence that forms a fold closure in the eastern part is stratigraphic sequence 2. The rest of the stratigraphy exhibits branch points along strike. The N-VSF strikes parallel to the main VSF as indicated by the co-planar D1(b)F1 axial traces and the regional foliation (Figure 3-24). The structure consist of two closures, one in the north-west and another in the south-east, linked by an F1 axial trace. In the north-west the structure closes off and folds the S1 foliations with no apparent transposition occurring in the hinge. The north-western fold axis has an orientation of 01129 (Figure 3-26), with a slight rotation of the hinge zone towards the north. The south-eastern closure of the N-VSF is refolded into a Ramsay Type 3 interference fold.

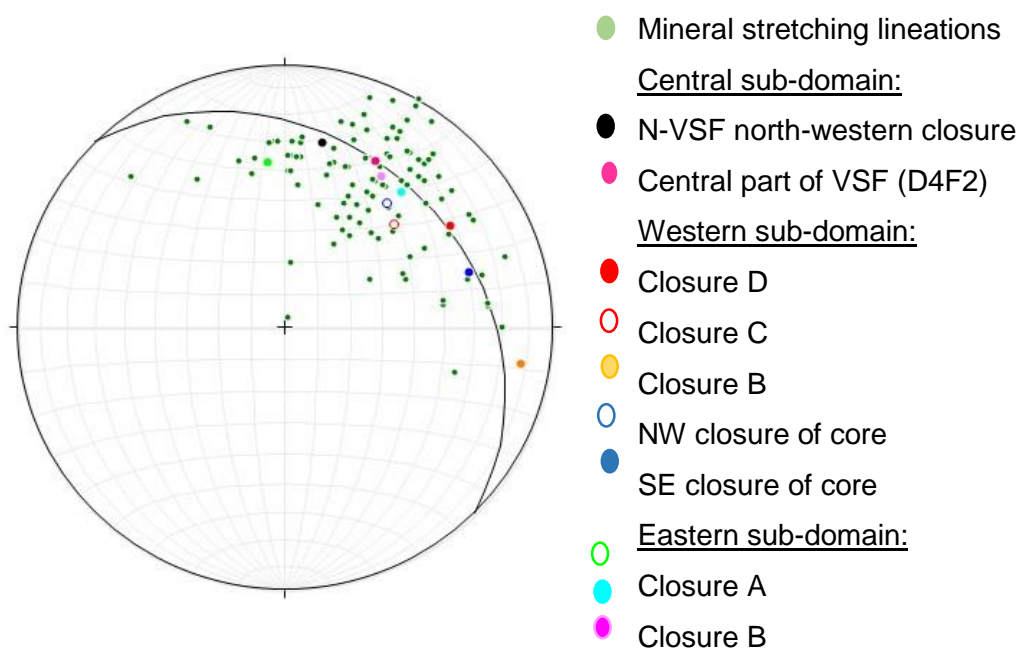


Figure 3-26: Combined linear elements (fold axes and stretching lineations) of the Vaaldrift sheath fold (Figure 3-23). Western sub-domain fold axes for closures: D = 05828, C = 04346, B = 09912, north-western core hinge = 03938, south-eastern = 07329. Central sub-domain fold axes: north-western hinge of N-VSF = 01129, D4F2 hinge = 02829. Eastern sub-domain fold axes: A = 03543, B = 04433 and C = 03233 (B and C after Van Bever Donker, 1980).

3.4.6 Mesoscopic Structures

3.4.6.1 Western sub-domain

The isoclinal hinges (A to D, Figure 3-23) reflecting folds of the D1(b)F1 and D1(b)F2 events, fold the model 1 and 2 recumbent isoclinal folds of the D1(a) event and do not represent parasitic structures related to the D1(b) folds. The model 1 folds are observed in profile along the yz plane of the regional strain ellipsoid, where the xy plane represents the compositional banding and the regional co-planar foliation. Model 2 folds are seen in a profile plane perpendicular to the banding and foliation (xy plane), i.e. the xz plane of the regional strain ellipsoid. Model 1 folds have both “S and Z” symmetries within singular competent bands defining omega structures (cf. see section 3.3.6: Mesoscopic structures of Domain 3 for the characteristics). The reversal in facing across the “S and Z” folds are an indication that a culmination zone (increase in flow velocity) of a flow cell has been crossed (Alsop & Holdsworth, 2002) during flow perturbation processes.

The variation in scale of model 1 and 2 fold (D1(a)) development in any stratigraphic sequence of the Omdraai Formation is a function of rheology and strain (Figure 3-27A). The thinner competent bands contain the centimetre scale development of the D1(a) folds and the thicker bands (metre thick and greater; Figure 3-27D) the larger D1(a) folds. Detachments seen as

high strain zones are recognised by pervasive co-planar foliation development and are located in incompetent bands (e.g. schist) which bound the competent layers. D1(a) folds fold the S₀ and develop a penetrative axial planar foliation (S₁) which is folded by D1(b)F₂ (B, C, and D, Figure 3-23).

Centimetre scale D1(a) sheath folds in the compositional banding of the meta-sediments occur throughout the western part of the VSF. The long axes trend north-east and are co-linear to the mineral stretching lineation (Figure 3-27). Shear bands deform the D1(a) folds on a centimetre scale; the axial traces of the folds become sigmoidally sheared together with the S₁ foliation (Figure 3-27) in a sinistral fashion (lateral movement on yz plane).

3.4.6.2 Central sub-domain (long limb)

The D1(a) mesoscopic folds (model 1 folds) along the long limb display similarly to the western sub-domain a reversal in symmetry and facing direction along strike of the same stratigraphic unit, which indicates that zones of increased flow (culmination) and slagging (depression) flow exist within the long limb, as deduced from the models by Alsop and Holdsworth (2007, 2004a, 2002) during the process of flow perturbation. The D1(a) folds with “Z and S” symmetries also have a sense of obliquity with respect to the transport direction (mean stretching lineation). The Z-folds having a clockwise sense of obliquity and the S-folds an anticlockwise obliquity. The mechanism of obliquity will be discussed in section 3.4.7.

3.4.6.3 Eastern sub-domain

All of the early structures discussed in the previous sub-domains also occur in the eastern sub-domain (i.e. S₁, S₂, D1(a) folds, L1 stretching lineations). The sub-domain is dominated by the Duiwelsnek shear zone (DSZ): it has a strike length of ~15km, trending north-west and dip sub-vertically eastwards. In the area of best exposure (south of the Orange River) the DSZ, has a width of ~2.5km, and shears all six of the main Omdraai Formation sequences, rotating the co-planar banding (S₀/S₁) and regional foliation (S₂) to the sub-vertical (Figure 3-27B). An oblique sense of shear is deduced with the lateral movement being sinistral (anticlockwise rotation of banding and regional foliation (S₀/S₁/S₂ at A, Figure 3-23) and east up.

A metre scale sheath fold occurs in a quartzite of #2, it is characterised by the folding of S₁ and a compositional banding. The x-axis have an orientation of 03538 with the two fold closures having hinge orientations of 05447, 02126. The x-axis is co-linear to the mean stretched mineral lineation trend and plunge of the area. The intermediate axis (y-axis) strikes north-south which is co-planar to the regional foliation).

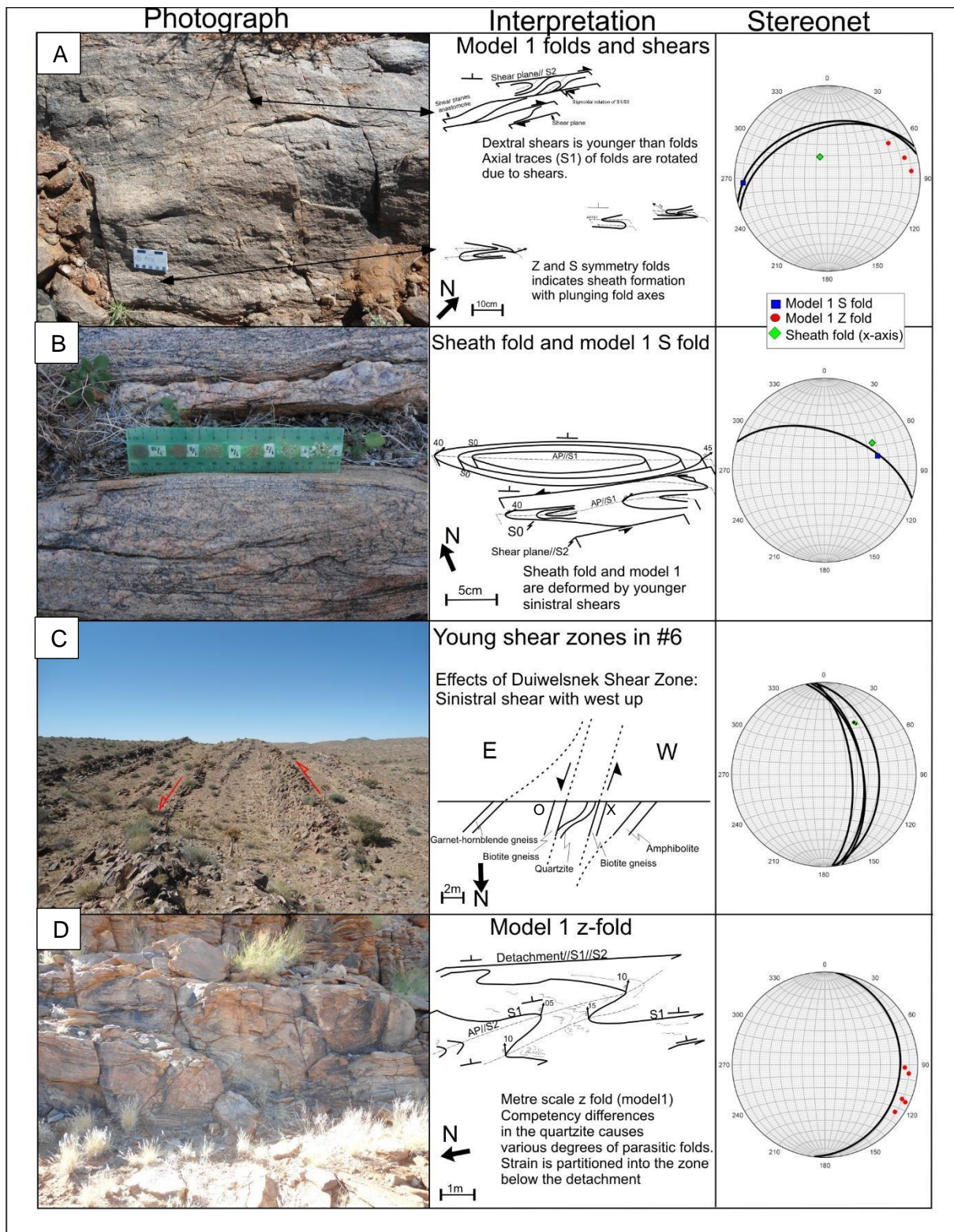


Figure 3-27: Mesoscopic structures associated with Domain 4, Vaaldrift sheath fold (VSF; Figure 3-23). A. centimetre scale model 1 S and Z folds (D1(a)F1) in the quartzites of the Omdraai Formation. The S1 axial traces of model 1 folds are rotated by a centimetre scale dextral shear zone (D1b) giving rise to a S2 foliation (regional). B. D1(a)F1 sheath fold and model 1 folds in the Omdraai Formation with transposed hinges and axial planar foliation (S1). The x-axis of the sheath fold and the fold axes of the model 1 folds are co-linear. The D1b shear also rotated the axial traces (S1) of the D1(a)F1 model 1 fold. C. Kilometre scale subsidiary shear zone associated with the larger Duiwelsnek shear zone (D4); the interpretation of the sigmoidal rotation of lithologies indicate west up. With sinistral shear. D. A series of metre scale model 1 Z folds with centimetre scale parasitic folds. The hinges of the folds are transposed forming the S1 axial planar cleavage.

3.4.7 Summary and discussion of Domain 3: Vaaldrift Sheath Fold

- S-fabrics present in the VSF are defined as S0/S1 and S2 with S2 being the regional foliation. S1 is a shear fabric formed during D1(a), giving rise to model 1 and 2 folds.
- The VSF is bounded along the northern limb by the Harpersputs thrust and along the southern limb by the Kliprug thrust.
- The VSF has the geometrical features and shape (i.e. semi-omega shape, “eye” structure, culmination and depression zones and co-linear L-fabrics) of modelled sheath folds (Figure 3-28).
- Co-planar S-fabrics (S0, S1 and S2) and co-linear L-fabrics (fold axes of D1(a), D1(b) and D2 folds as well as stretching lineations) dominate the Vaaldrift sheath fold.
- Two phases of sheath folding; phase one represents the regional macroscopic formation of the D1(b)F1 sheath folds and the second phase represents localised refolding of D1(b)F1 into a semi-omega sheath fold (D1(b)F2; Table 3-3, Figure 3-29).
- The VSF has a reversal in fold facing along the F1 axial traces through both lateral hinges and eye structure which can be interpreted as a double-plunging structure (Passchier, et al., 2011).
- The lateral isoclinal fold closures (D1(b)F1) of the VSF are transposed and contain a penetrative axial planar foliation –S2 (regional foliation).
- The localised D1(b)F2 folds the co-planar S0/S1/S2.
- Mesoscopic model 1 and 2 folds (D1(a)) are folded by the VSF event (D1(b)F1 and D1(b)F2).
- The anticlockwise and clockwise sense of obliquity of the mesoscopic model 1 “S and Z” folds respectively, suggests that the D1(a) folds developed during flow perturbation in a contractional system– ductile thrusting (Alsop & Holdsworth, 2007, Figure 12).
- The angle between regional stretching direction and the model 1 fold axes is smaller than 45° meaning that these folds formed due to layer-normal differential shear and the angle between the model 2 folds and the transport direction is larger than 45°, meaning that they formed by a process of layer-parallel differential shear (refer to section 3.3.6).
- With progressive shear the model 2 fold axes can rotate towards the stretching direction.
- The mean stretching lineation across the four sub-domains is 03530. The regional stretching lineation is not folded by either the mesoscopic or macroscopic folds and represents the long axis of the regional strain ellipsoid – “X” direction which is sup-parallel to the deduced south-western tectonic transport direction (215°).

- The Vaaldrift sheath fold (D1(b)F1) in the eastern sub-domain is deformed by later shearing, the D4 event; the zone of shear deformation (Duiwelsnek shear zone) is situated between the reactivated footwall and roof thrust (Kliprug and Harpersputs thrust, respectively).
- The apparent boudinage effects (thickening and thinning) of the VSF is caused by culmination and depression zones (culmination = thickening and depression = thinning) developed during layer-parallel and layer-normal shear processes which produced the macroscopic sheath folds.
- The lateral fold closures of the VSF are refolded by later folding: the refolding of the south-eastern (eastern sub-domain) and north-western (western sub-domain) closures forms Ramsay Type 3 interference structures (D2F1).
- D3 (Friersdale Charnockite) is not present in Domain 4.

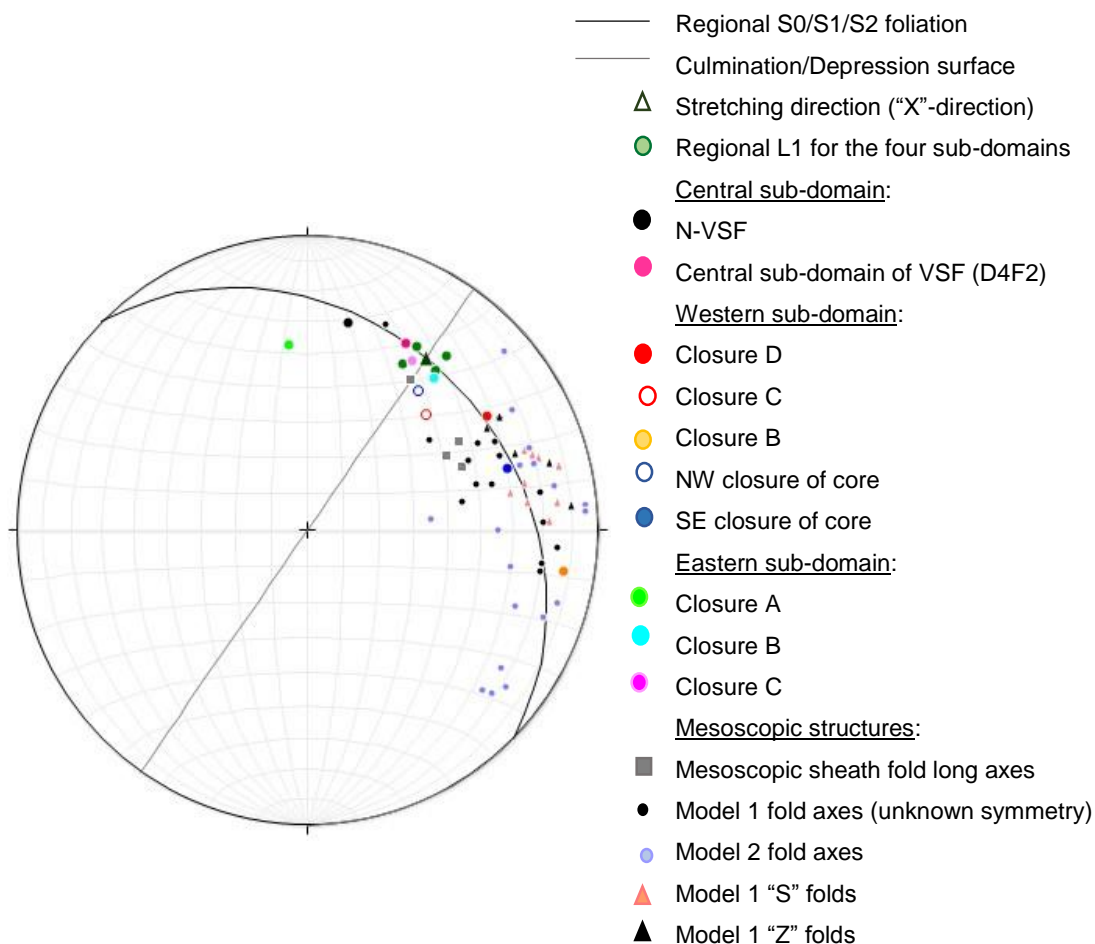


Figure 3-28: Synthesis stereographic projection of planar and linear fabrics of Domain 4 (Vaaldrift sheath fold; VSF Figure 3-23). The LS fabrics are deformed by the late D4 regional shear event and are not restored on this data projection. Note the large angle between D1(a)F1 and D1(a)F1' folds (model 1 and model 2, respectively) is still retained (c.f. section 3.3.6).

Table 3-3: Structural framework for Domain 4: Vaaldrift sheath fold.

Deformation event	D1a	D1b			D2	D4		
Structural event	Model 1 and 2 folds	Intra-terrane	F1	F2	F1	F1	F2	NW shear zones
Domain 4: Vaaldrift sheath fold	x	x	x	x	x		x	x

3.4.7.1 Model and mechanism for the formation of the Vaaldrift sheath fold:

The Omdraai Formation represented a single flow cell with the two intra-terrane thrusts serving as major detachments during D1(b) - the formation of the VSF (Figure 3-30A). The main processes that formed the VSF are layer-parallel and layer-normal differential shear during progressive flow perturbation (Figure 3-30B). The macroscopic D1(b)F1 sheath fold formed by layer-parallel dominated shear. It is interpreted that the semi-omega shaped western subdomain with opposing facing and symmetry folds formed by localised second phase layer normal differential shear (Figure 3-30C). The semi-omega shaped western sub-domain is characterised by a central core or “eye” structure consisting of the fourth stratigraphic sequence; the elliptical shape of the core is indicative of layer-parallel shear (Figure 3-30C). The eye structure localises the layer-parallel process giving rise to the D1(b)F2 folds. The D1(b)F2 “Z” shaped macroscopic fold hinge defining the semi-omega shape, has a hinge orientation less than 45° to the south-westerly transport direction which is an indication of layer-normal differential shear (Alsop & Holdsworth, 2007). The long limb in the central subdomain is not affected by the localised layer-normal shearing phase where layer-parallel differential shear is the prominent process according to the classification of Alsop & Holdsworth (2007).

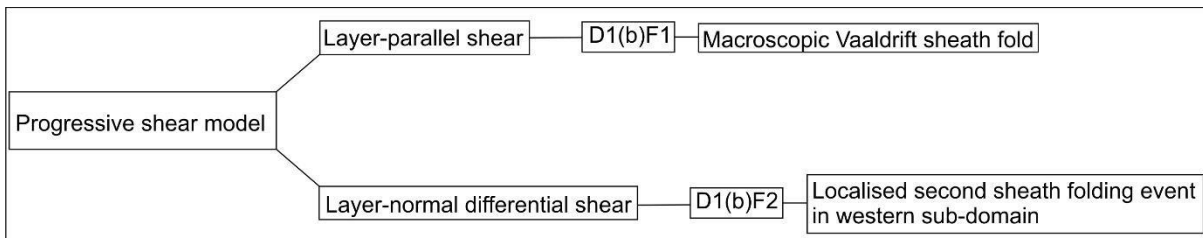


Figure 3-29: Flow diagram illustrating the processes associated with the production of macroscopic D1(b)F1 and F2 folds during regional progressive general shear.

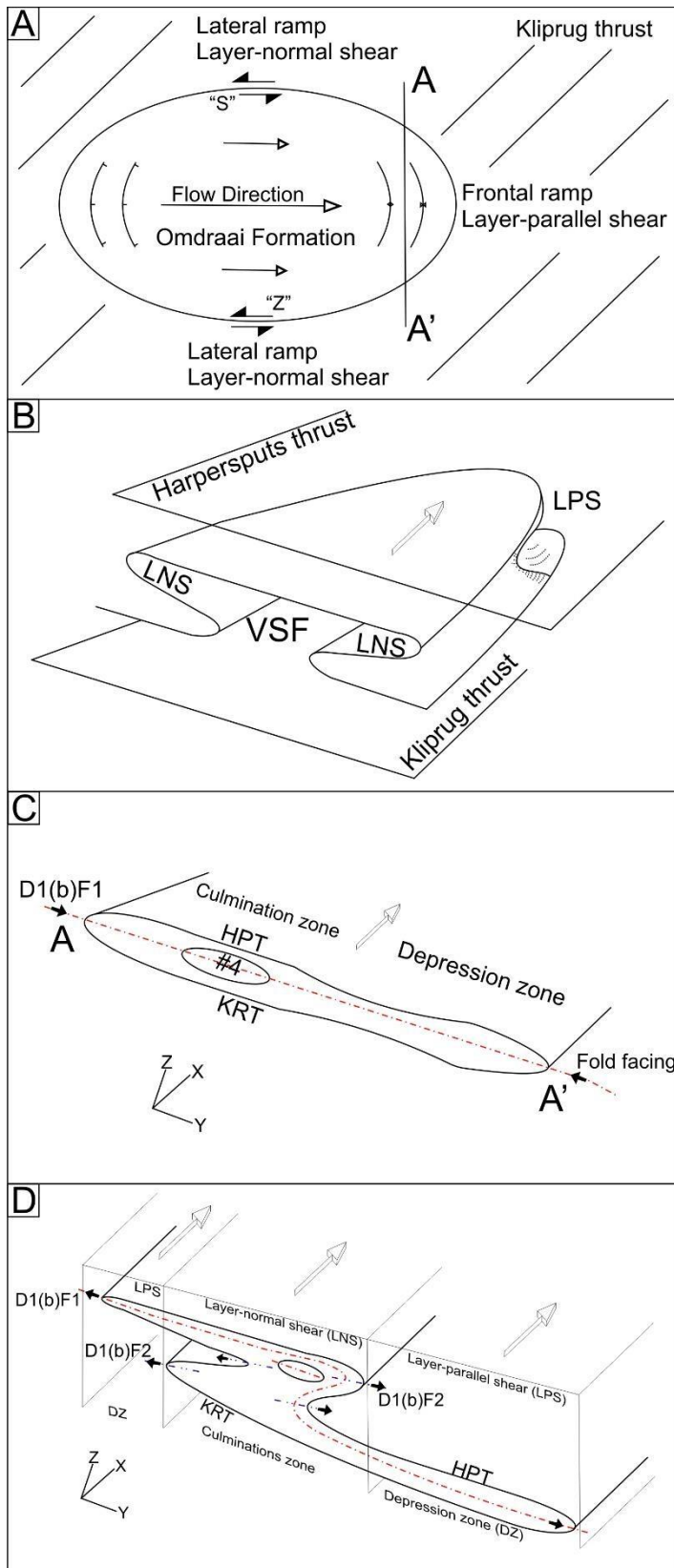


Figure 3-30: Model and mechanism for the formation of the Vaaldrift Sheath Fold. A: Flow cell model for the Omdraai Formation overlying the Kliprug thrust which serves as a detachment. Flow direction is from left to right (tectonic transport direction, open arrows in B, C and D). The section A-A' is illustrated in figure C. B: The main processes involved in the formation of the Vaaldrift Sheath fold are layer-normal shear (LNS) and layer-parallel shear (LPS); a combination of the two shear processes results in double-verging fold. C. The section A-A' represents the yz plane of the first phase of D1(b)F1 regional sheath folds, formed by the process of layer-parallel shear. The core (containing the # four stratigraphic sequence) developed as part of a culmination zone. The VSF at this phase already shows a reversal in fold facing. D. 3D schematic yz profile of the current VSF. Localised layer-normal differential shear (LNS) causes the D1(b)F1 axial trace to be folded by the D1(b)F2 folds resulting in a semi-omega shape structure. The "Z" folds defining the semi-omega have a reversal in fold facing; the semi-omega structure is situated in a culmination zone of the shear regime

3.5 Domain 5: Puntsit/ Goede Hoop Domain with special reference to Harpersputs gneiss

Domain 5 forms a macroscopic sheath fold complex in the RK-MS (Figure 3-31). The supracrustals defining the structures are the Puntsit and Goede Hoop Formations together with the intrusive Harpersputs gneiss. The Harpersputs gneiss is contained within the sheath fold complex. The domain is divided into two sub-domains namely: Neusberg and Cnydas sub-domains and will be discussed separately in each section. The Neusberg sub-domain is situated in the south-eastern part of Domain 5 and includes the Warm Sand area and the structures south of the Orange River. Cnydas sub-domain can be divided into the Rondekop structures and the Biesje Poort structures. Domain 5 is bounded by two decollement boundaries, namely: the Waterval thrust in the north and Neusberg Shear Zone in the south.

3.5.1 Domain boundaries

This domain is bordered in the north by the Waterval thrust that wraps around the RK-MS (Map 1 and Map 2) and represents the northern extent of the intra-terrane thrust reactivated by younger shear events. The WVT is folded with the development of the D1(b) macroscopic sheath folds. The north-east dipping WVT in this area is also sheared by the younger Cnydas shear zone (D4).

The southern boundary of the Domain 5 sheath fold complex is defined by the north-east dipping Neusberg Shear Zone (D4) which is located on the contact between the Harpersputs gneiss and the Puntsit Formation and can be traced out along the southern limb of the Neusberg and Rondekop sheath folds for about 30km, where it continues under sand cover.

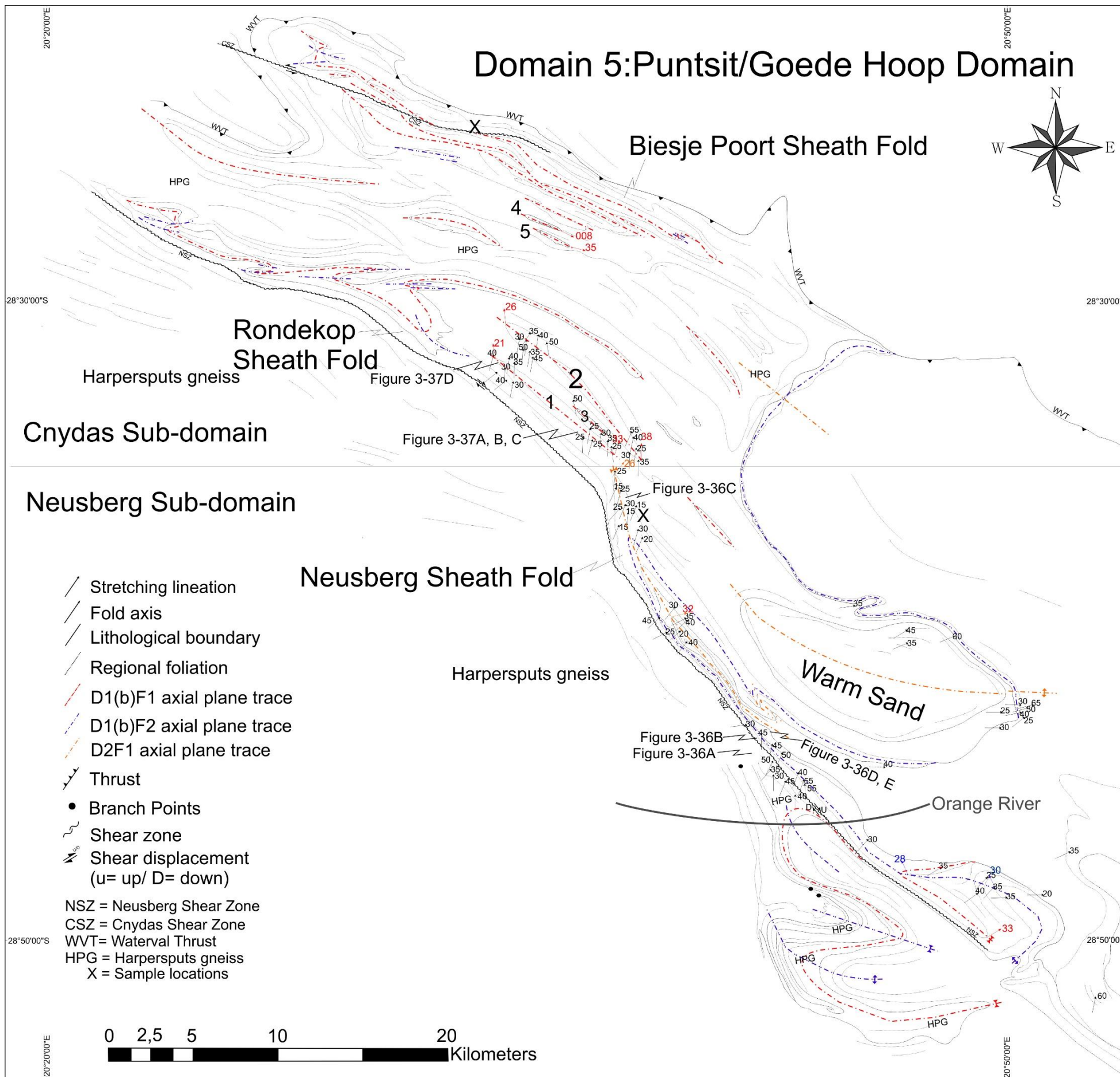


Figure 3-31: Structural map of domain 5 (Puntsit/Goede Hoop Stratigraphic Domain). Domain 5 is sub-divided into a northern Cnydas sub-domain and a southern Neusberg sub-domain. The Cnydas sub-domain contains a series of sheath fold complexes (1-5, Biesje Poort and Rondekop sheath folds). The Neusberg sub-domain contains the Neusberg sheath fold and the Warm Sand structure.

3.5.2 Stratigraphy

The Puntsit Formation represents a large volcanic sequence which Moen (2007) suggested underlies the quartzites of the Goede Hoop Formation (cf. section 2.2.1.3.) The Goede Hoop Formation is also in contact with the Friersdale Charnockite and occurs in the cores of various D1bF1 sheath folds. In the Cnydas area the core of the Biesje Poort sheath fold consists of the Goede Hoop Formation which is elliptically enveloped by the Puntsit. The Puntsit and Goede Hoop Formations are more widely distributed than the confines of the mapped area.

The Harpersputs gneiss has a distribution south of the Rondekop-Neusberg sheath folds; the contact is interpreted as structural. It also occurs between the two sheath fold complexes of

Domain 5 and contains large sheath fold “rafts” on kilometre scale. In the north-west the Harpersputs gneiss cuts out along the WVT and in the south-east the Harpersputs gneiss forms part of a Ramsay Type 3 interference fold.

3.5.3 Regional foliation

In the Neusberg sub-domain (Figure 3-31) the foliation is predominantly defined by the alignment of muscovite and biotite (biotite is not always present). The regional foliation dips towards the north-east with an average orientation of 04336 (Figure 3-32). The northern isoclinal closure of the Neusberg sheath fold is totally transposed by a younger set of axial planar foliations (S2). S1 is only recognised in the fold closure; along the limbs the S1 and S2 fabrics are co-planar, with S2 being the dominant foliation. A millimetre scale penetrative cleavage (S3) occurs throughout the quartzite, defining the northern-limb of the Neusberg sheath fold, with an average orientation of 02626 (Figure 3-32). This cleavage transects the banding and the co-planar S1/S2 foliation and makes an angle of 14° with the regional S2 foliation. It is interpreted to relate to the D4 Neusberg shear event and the intersection lineation of (34220) indicates oblique shear along the northern limb of the sheath fold. The flattened quartz pebbles are also rotated and lie within the penetrative cleavage.

In the Puntsit Formation the foliation is defined by the alignment of biotite, muscovite, hornblende, and feldspar. The regional foliation in both the sub-domains for the Puntsit and Goede Hoop Formations is the S2 foliation which is co-planar with the banding containing S1. Along the boundaries of domain 5 there is a steepening of foliation towards the D4 Neusberg shear zone where the foliation is becoming sub-vertical, which is an anti-clockwise rotation in the east and a clockwise rotation in the west, indicating east-up.

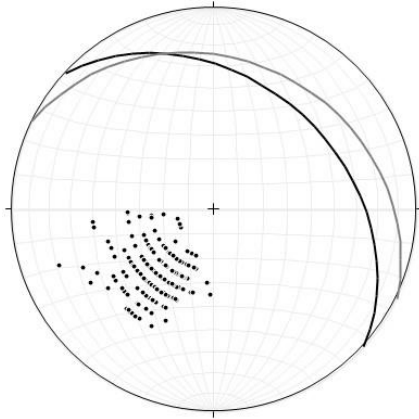


Figure 3-32: Stereonet illustrating the orientation of the regional foliation (S2) in the Neusberg sub-domain. The regional foliation is defined by co-planar S1 and S2 (dark greater circle). The mean orientation of the S2 foliation is 04336 (n=240). The penetrative cleavage (S3) that is superimposed across the north-western isoclinal closure of the Neusberg sheath fold has an average orientation of 026026 (grey greater circle) and is associated with the regional D4 shear event. The intersection of 34220 between the regional S2 foliation and the penetrative cleavage indicates oblique shear movement and has a sense of shear similar to the Neusberg shear zone (section 3.5.5.1).

Intrafolial folds in the Harpersputs gneiss suggest that there is more than one fabric forming event after emplacement as a sheet granite and that this gneiss is one of the oldest intrusives in the area. The intrafolial folds are flattened and contained within the S2 foliation. The folds are defined by feldspar-biotite aggregates representing the S1 foliation; they form as isoclinal folds (with variable symmetries) on millimetre scale (Figure 3-36A). The hinges of the intrafolial folds are transposed by the regional S2 foliation. The quartz-feldspathic gneiss xenoliths in the Harpersputs gneiss are co-planar with the regional S2 foliation.

3.5.4 Regional lineation

The regional lineation is weakly defined in the lithologies of domain 5, which would suggest that the domain is dominated by oblate strain (occurring in specific areas), this is confirmed with the fabric diagram of Van Bever Donker (1980, his Figure 3-27) as well as the strain analysis during this study (refer to section 3.5.7 for strain analysis). In the Goede Hoop Formation mica-fish is the dominant mineral that indicates the stretching direction. Where present the quartz-pebbles have been flattened and stretched with long axis co-linear to the stretching direction. In the Puntsit Formation mineral stretching lineations are defined by amphibole and sillimanite needles and long axes of quartz and feldspar aggregates. In the Neusberg sub-domain the general orientation of the lineations are plunging 31° towards 010 (Figure 3-33). The stretching lineations indicate a tectonic transport direction towards the

south for the Neusberg sub-domain. No lineations have been documented in the Cnydas subdomain.

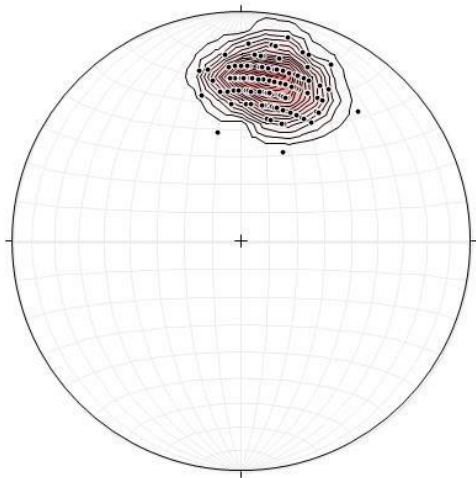


Figure 3-33: Stereonet illustrating the regional stretching lineation (L1) orientation for Neusberg sub-domain; 01031 (n=122). The lineations are defined by mica-fish and long axes of quartz pebbles in the Goede Hoop Formation and by amphibole, sillimanite and quartz-feldspar aggregates in the Puntsit Formation.

3.5.5 Macroscopic Structures

3.5.5.1 Neusberg sub-domain

The Neusberg shear zone (NSZ) can be traced out further northwards using the rotation of the F2 fold traces in the Rondekop sheath fold. The NSZ represents the reactivation of a pre-existing intra-terrane thrust separating the Puntsit and Goede Hoop Formations from the Harpersputs gneiss and associated supracrustals which form part of the southern complex of sheath folds. None of the stratigraphy within domain 5 exist south of the NSZ. The shear has affected an area of approximately 1km wide and Van Bever Donker (1980) mentions that the structures on both sides of the shear zone indicate severe flattening, he however suggested that no lateral (sinistral or dextral) movement took place, only over-thrusting towards the west. In this study the F2 fold axial traces of the Rondekop sheath fold along the shear zone indicates that an oblique sense of shear existed (Figure 3-31); cleavage intersections and fold axes orientations suggest that the east moved up with respect to the west together with a dextral sense of lateral shear. The over-thrusting towards the west as suggested by Van Bever Donker (op.cit) could relate to the earlier thrusting event. The rotation of the F2 axial traces indicates that the reactivation of the decollemént as a shear zone post-dates the folding of the sheath folds.

This sub-domain is dominated by the refolded Neusberg sheath fold (NSF); the NSF is deformed by kilometre scale isoclinal and open folds. The Neusberg sheath fold contains at least three major fold phases (D1(b)F1, D1(b)F2 and D2F1). The localised D1(b)F1 axial trace is situated in the south-east and characterises the earliest isoclinal fold event which is folded by the extensive D1(b)F2. The most noticeable structure of the sub-domain is the D2F1 isoclinal, north-western hinge of the Neusberg sheath fold (Figure 3-31, sub-area “a”). The D1(b)F2 trace is refolded by the D2F1 folds. The inclined plunging, D2F1 isoclinal fold closure consists of a series of internal closures of alternating lithologies along strike of the axial trace towards the south-east. All of these closures being transposed by the S3 axial planar foliation. The orientation of the isoclinal closures (on the inside) are 07732, 07844 and for the outermost closure 03826, (Figure 3-34). The clockwise rotation of the closure towards the north can be explained by the dextral sense of lateral shear of the NSZ. The isoclinal folds have an axial trace (D2F1) trending in a northwest direction, sub-parallel to the regional foliation (dipping towards the north-east). The fold is classified as a Class 2 (Ramsay, 1967) structure according to Van Bever Donker (1980). D2F1 folds of the Neusberg sheath fold contain the Warm Sand structure.

The northern limb of the sheath fold (containing the D1(b)F2 axial trace) is thinned and boudined along strike around the Warm Sand structure and is folded by the D2F1 fold phase. The NSF limb forms large inclined open folds with an S-symmetry and when it joins up with the Neusberg mountain range a series of tight to isoclinal S-folds developed in sympathy to the D2F1 hinges.

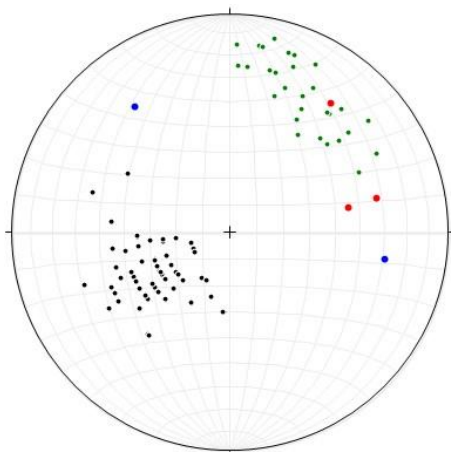


Figure 3-34: Stereonet presenting the stretching lineation and D2F1 fold axes of the north-western isoclinal closures of Neusberg sheath fold (03826). The two inner closures have hinges that plunge (32° and 44°, respectively) towards 077. The blue dots represent the northern (32329) and southern (10029) fold hinges of the Warm Sand dome structure (D2F1; data from Van Bever Donker, 1980).

The south-eastern sub-area of the sub-domain consist of a D1(b)F1 fold refolded by a D1(b)F2 fold resulting in a Ramsay Type 2 interference fold. The synformal D1(b)F1 fold has an orientation of 05933 with the antiformal D1(b)F2 fold having an orientation of 33628, 33530 according to Van Bever Donker (1980), the D1(b)F1 fold axis orientation is co-linear to the stretching direction of the area. The D1(b)F1, D1(b)F2 and the D2F1 axial traces, layering and S0/S1/S2 foliation are co-planar and trend north-west along both limbs of the Neusberg sheath fold.

The Warm Sand area is interpreted as a dome structure (Ramsay Type 1 interference fold) by Van Bever Donker (1980). The D2F1 axial trace of the dome coincides with the third order axial trace (D2F1) of the Neusberg sheath fold; it is interpreted that the D2F1 folding of the Neusberg sheath fold and the Warm Sand structure formed simultaneously. The synformal northern closure of the elliptical shaped structure have a hinge orientation of 32329 (Van Bever Donker, 1980; Figure 3-34). The axial trace trends west-north-west and has a concave shape. The antiformal southern closure has a fold axis that plunges 29° towards 100°. Along the axial trace of the elliptical structure the antiform is connected to the synform making it a double plunging structure and therefore it can be interpreted as a sheath fold where the hinges are at an acute angle to the regional stretching direction (01031; Figure 3-33).

3.5.5.2 Cnydas sub-domain

The Cnydas sub-domain is characterised by D1(b)F1 macroscopic sheath folds: Rondekop (central sub-area) and Biesje Poort (northern sub-area) sheath folds, respectively (Figure 3-31). The northern part with the prominent Biesje Poort sheath fold contains smaller kilometre scale sheath folds and the late Cnydas shear zone (D4; Table 3-4). The Biesje Poort sheath fold is a well-developed omega shaped sheath fold. The north-west striking, sub-vertical Cnydas Shear Zone (CNZ) has affected a ~1,7km wide area across the northern limb of the Biesje Poort sheath fold. Geringer (1973) states that the sinistral sense of lateral displacement along the shear zone is 500m with no vertical displacement and that the shear zone can be traced out along strike for 12km. The CNZ strikes parallel to the northern limb and cuts across the north-western closure. The shear zone rotated the S1/S2 fabric and stratigraphic packages in parts of the structure, indicating east-up. As there is also a small component of lateral displacement, the direction of movement is oblique in the shear plane.

The core of the Biesje Poort sheath fold is defined by an omega shape (Alsop & Holdsworth, 2007) consisting of Puntsit Formation. The sheath folds in the Cnydas sub-domain have intermediate axis that strikes west-north-west (co-planar to the regional foliation) and long axis that plunges towards the north. The D1(b)F1 axial trace of the Biesje Poort sheath fold strike

sub-parallel to the regional foliation. In the Biesje Poort sheath fold the smaller sheath folds (Figure 3-31; sheath folds 4 and 5) towards the south have fold axes orientations of 11708 and 10535. The plunges are towards the east-south-east, which suggest that the initial orientation of the sheath folds has undergone rotation-probably due to the effects of the Cnydas shear zone.

The central area is characterised by three small symmetrical sheath folds (sheath fold 1, 2 and 3) and the refolded Rondekop sheath fold (Figure 3-31). All of the sheath folds have F1 axial traces trending north-west to south-east, however the large sheath fold is refolded by east-west trending F2 folds. All of the sheath folds consist of Goede Hoop Formation situated within the Puntsit Formation. The orientation of the transposed hinges for sheath fold 1 are shown in Figure 3-35; hinges for sheath fold 1 are 35021, 01933 and sheath fold 2 are 00238 and 35426. All the hinges are co-linear with the regional stretching lineation and are not folded by them.

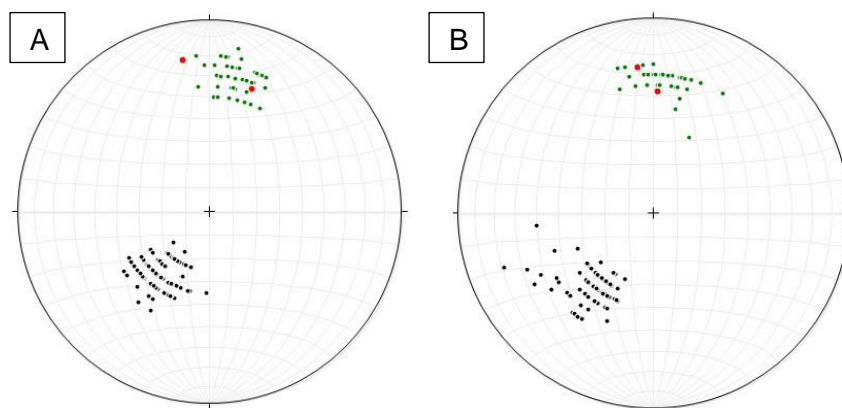


Figure 3-35: Cnydas sub-domain (Figure 3-31). A. Sheath fold 1's north-western and south-eastern D1(b)F1 closures fold axes orientations are 35021 and 01933, respectively. B. The geometries of sheath fold 2: north-western and south-eastern closures has fold axes orientations of 00238 and 35426, respectively. The D1(b)F1 fold axes orientation of both sheath fold 1 and 2 are co-linear with the lineations.

3.5.6 Mesoscopic Structures

3.5.6.1 Neusberg sub-domain

In the Neusberg sub-domain mesoscopic structures include folds that relate to different ages of events, shear zones, boudinaged lithologies and s-c fabrics. The Harpersputs gneiss contains mesoscopic D1(a)F2 Z-folds which folds S1 and contains S2 in the hinges (Figure 3-36A). The Z-fold has a fold axis orientation of 01025 and the axial plane is co-planar to the regional foliation (04645). Surrounding the Z-fold the foliation is defined by a co-planar S1 and regional S2. The Neusberg shear zone is dominated by flattened, stretched out, D1(a) Z-folds. The model 1 (D1(a)) folds pre-date the D4 shear event, their hinges are transposed, long limbs

are stretched and their short limbs are thickened which is a characteristic of the model 1 folds in the domain (Figure 3-36B). The axial planes of the model 1 folds are co-planar to the regional S2 foliation. These folds are defined by folded compositional banding (S0) with S1 as an axial planar foliation.

The transpositioning in the hinges of the D1(a) folds is caused by shear zones on centimetre scale and results in a rotation of the S0 banding into separate lenses within the hinge zone. This is the same process described for the macroscopic scale Eendoorn closure in the Augrabies Falls National Park (Figure 3-13) but on a mesoscopic scale.

Cleavages in the lithologies (Figure 3-36C) indicate dextral shearing; however the north-north-east plunging intersection lineation formed between the C' and S1/S2 suggests an oblique sense of shear with both a horizontal and vertical component (east up). The cleavages relate to the Neusberg shear zone (NSZ) with the internal fabric defined by S1/S2. In the Puntsit and Goede Hoop Formations, mesoscopic scale boudins (Figure 3-36D) relating to the Neusberg shearing event (D4) have fold axes plunging obliquely in the xy plane of the S2 fabric, which indicates that the NSZ has an oblique sense of shear.

On the xz-plane of the lithologies with respect to the shear event, the x-z ratios are determined for the quartz pebbles by measuring the lengths of each axis. Average xz ratio for 142 quartz pebbles is 5. Using the equation: $\frac{x-axis}{y-axis} = \gamma^2$; a gamma value ($\gamma = 2.24$) can be calculated. The Neusberg Shear zone effected a zone with a width of approximately 1070m. The lateral displacement along the NSZ can then be calculated at 2.4 km ($d = \gamma \times \text{width of shear zone}$).

Using cross bedding in the quartzites of the Goede Hoop Formation the facing of the Neusberg sheath fold can be determined (Figure 3-36E). The cross bedding indicates that the south-western limb is overturned and younging is towards the east. Using "Shackleton's rule on facing" (Shackleton, 1958) the facing for the Neusberg Sheath fold can be determined.

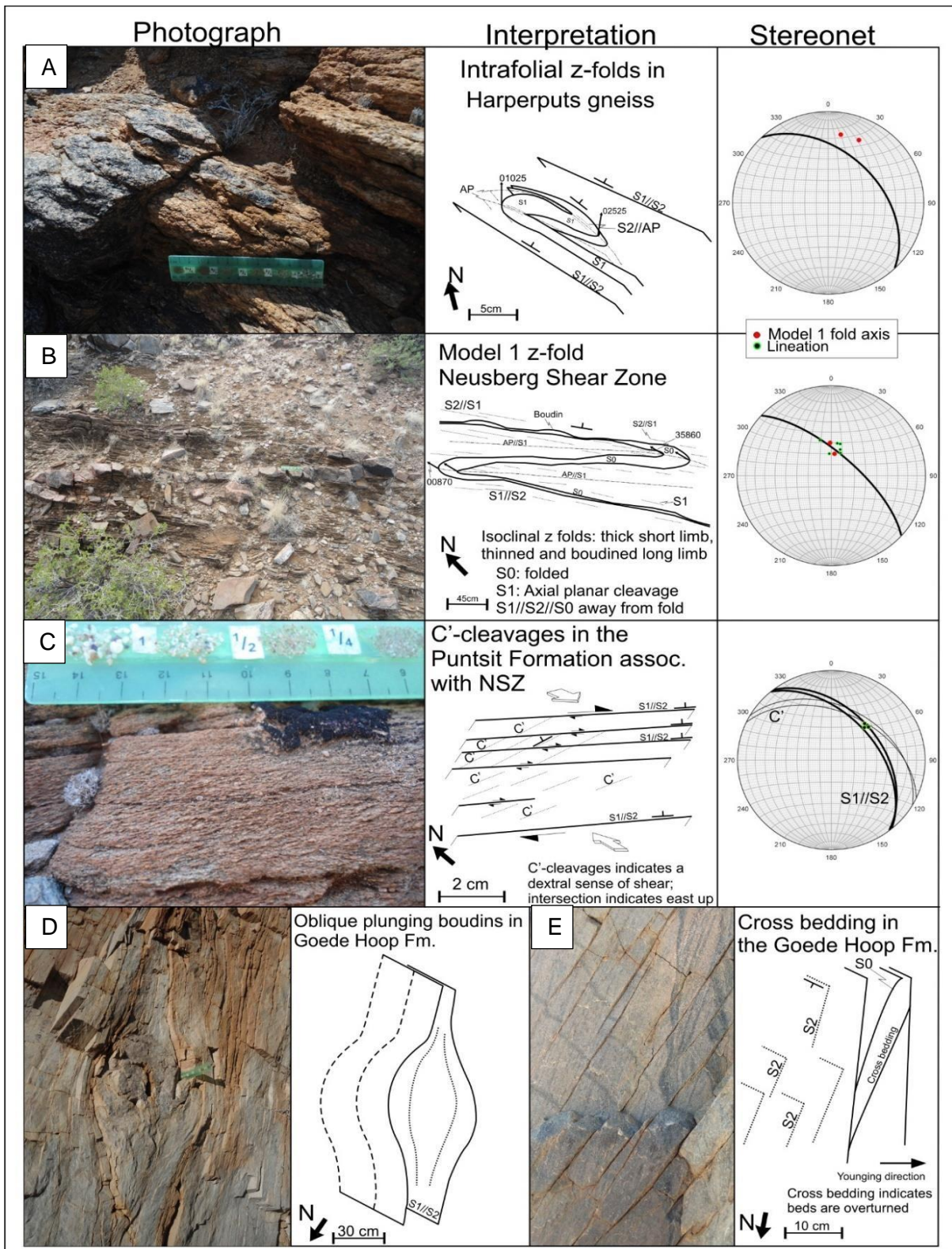


Figure 3-36: Mesoscopic structures of the Neusberg sub-domain (Figure 3-31). A. D1(a)F2 intrafolial Z-fold in the Harperputs gneiss; the fold is defined by folded S1 with S0 as an axial planar cleavage. S1 and S2 are co-planar elsewhere and fold axes co-linear. B. Metre scale model 1 Z-fold (D1(a)F1) which is flattened, steepened and boudined due to the D4 Neusberg shear zone; both S0, S1 and S2 are co-planar, whereas the fold axes and stretching lineations are co-linear. C. S-c cleavages associated with the Neusberg shear zone, indicating an oblique sense of direction with dextral sense of shear and east-up. D. Boudins in the Goede Hoop Formation with long axis plunging in the xy plane indicates an oblique sense of shear for the Neusberg shear zone. E. Cross bedding defined by S0 in the quartzites has a younging direction towards the west which indicates that the quartzites on the eastern limb of the Neusberg sheath fold are overturned.

3.5.6.2 Cnydas sub-domain

In the Cnydas sub-domain centimetre to metre scale D1(a) model 1 folds are characterised by the folding of S0 and S1 with S2 as an axial planar foliation. These folds have fold axes co-linear to the regional lineation and the fold axes of macroscopic sheath folds; the axial planes are co-planar to the regional S2 foliation. Along the limbs of mesoscopic and macroscopic (D1(b)) folds S1 and S2 are indistinguishable and can only be separated in the hinge zones. The mesoscopic scale folds can be classified as plunging inclined folds (Fleuty, 1964).

The three symmetrical sheath folds in the central area of the Cnydas sub-domain (Figure 3-31) contain mesoscopic layer-parallel shear zones with folds which are controlled by the rheology of the rock. The quartzites of the Goede Hoop Formation have a high anisotropy (mechanical and compositional) due to the well-developed compositional banding and scattered quartz pebbles. The rheological contrast caused by the variation in composition on a millimetre scale causes a variation in competency, which leads to the partitioning of strain into low strain and high strain areas during deformation (Lister & Williams, 1983). Within the southern limb of sheath fold 1 (Figure 3-31) the process of strain partitioning can be seen on centimetre to metre scale by shear zone development and can be divided into high and low strain zones (Figure 3-37A and B). High strain zones are characterised by co-planar foliation (S1 and S2) and development of a mylonitic texture; whereas the low strain areas are characterised by the folding of S0 and S1 and S2 as an axial planar foliation. Within the low strain areas various style and symmetries of folds occur (Figure 3-37A). The zones are dominated by z-symmetry folds with lesser S-folds. Pre-existing folds are refolded into Ramsay Type 3 interference folds (Figure 3-37B; Ramsay, 1967) with the fold axes of both fold phases co-linear. The sheath folds forming in the low strain zones are orientated with intermediate axis (y-axis) co-planar to the boundaries of the zones and the x-axis sub-parallel to the stretching direction for that zone (Figure 3-37C).

The Puntsit formation surrounding the sheath folds contains centimetre scale intrafolial S-folds that relate to early deformation events (Figure 3-37D). The fold axes having a mean orientation of 01140, the folds are isoclinal with axial planes co-planar to the S2 foliation (04555).

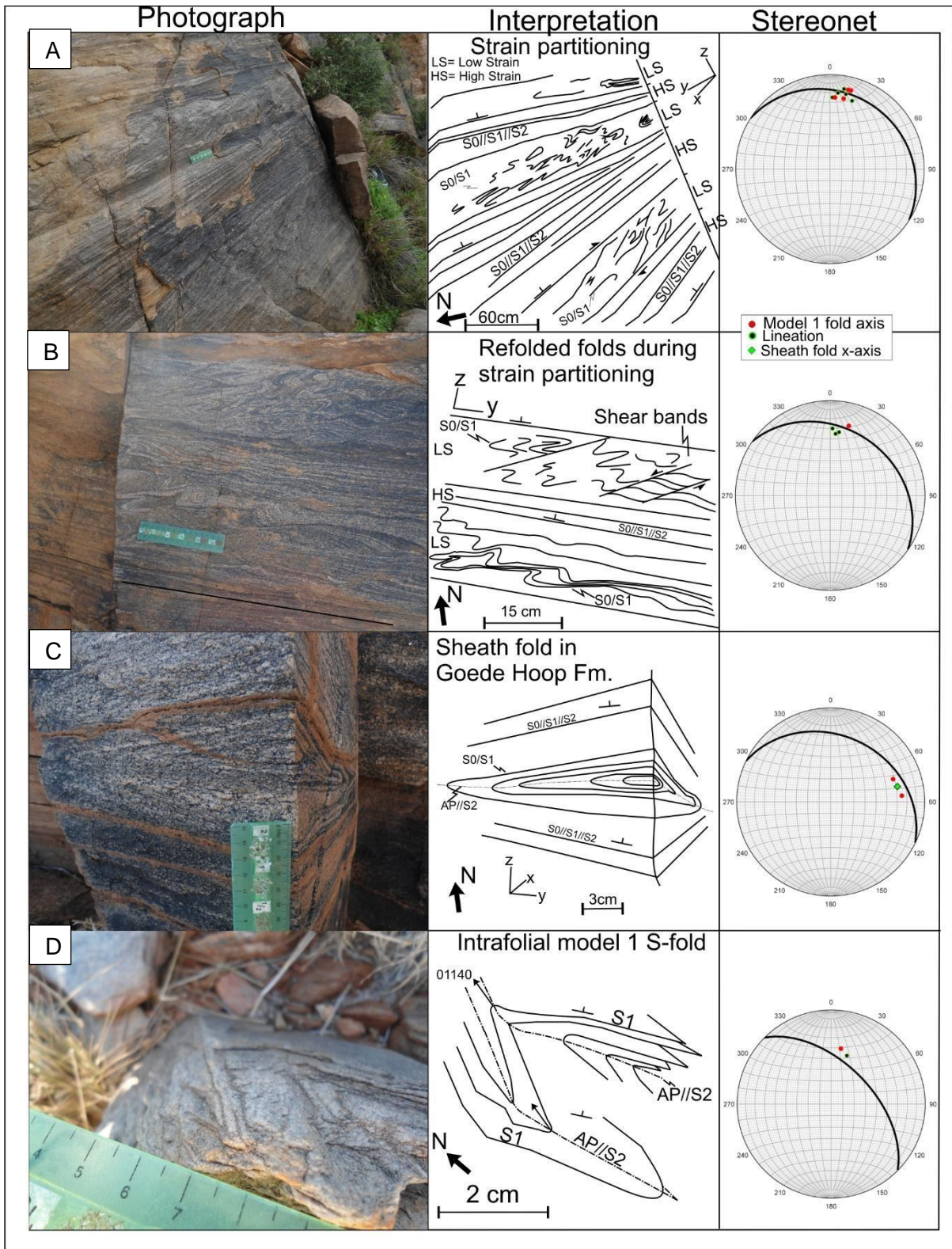


Figure 3-37: Mesoscopic structures in the Cnydas sub-domain (Figure 3-31). A. yz-plane indicating strain partitioning on a metre scale in the Goede Hoop Formation. The highly folded and contorted zones are associated with low strain zones, containing D1(a)F1 folds and S1 axial planar cleavage, separated by zones of high strain where the S-fabrics (S0, S1 and S2) are all co-planar and L-fabrics (L1, -stretching lineations and D1(a)F1 fold axes) co-linear. B. More detail on strain partitioning in A, showing Ramsay Type 3 interference folds. C. Centimetre scale sheath folds are also associated with the low strain zones. D. Intrafolial D1(a) model 1 S-fold in the Puntsit Formation with S1 as axial planar cleavage.

3.5.7 Strain analysis of the Puntsit/Goede Hoop Domain

Several methods exist for the determination of the finite strain ellipsoid from the shape of deformed pebbles, inclusions and xenoliths. The method used in the domain 5 includes the plotting of Hsu diagrams from the deformed pebbles from the two sub-domains. Deformed pebbles have been widely used in the past as strain markers (e.g. Hossack, 1968; Lisle, 1979). A Hsu diagram (initially suggested by Hsu (1966) and first employed by Hossack in 1968) is a sixty-degree circular wedge, where octahedral shear strain increase radially away from the origin, and the individual radii are values of constant Lode's ratio (Mookerjee & Peek, 2014). The R_{xy} and R_{yz} ratios of quartz-pebbles in the Neusberg sub-domain and gneissic-pebbles in the Cnydas sub-domain were used to construct Hsu diagrams (Figure 3-38). In both the areas the shape of the pebbles indicated that the sub-domains are dominated by flattening (oblate) strain. The high flattening strain resulted in the well-developed foliation (S-tectonites) in domain 5. Van Bever Donker (1980) also reported a dominant oblate strain across the Neusberg sub-domain.

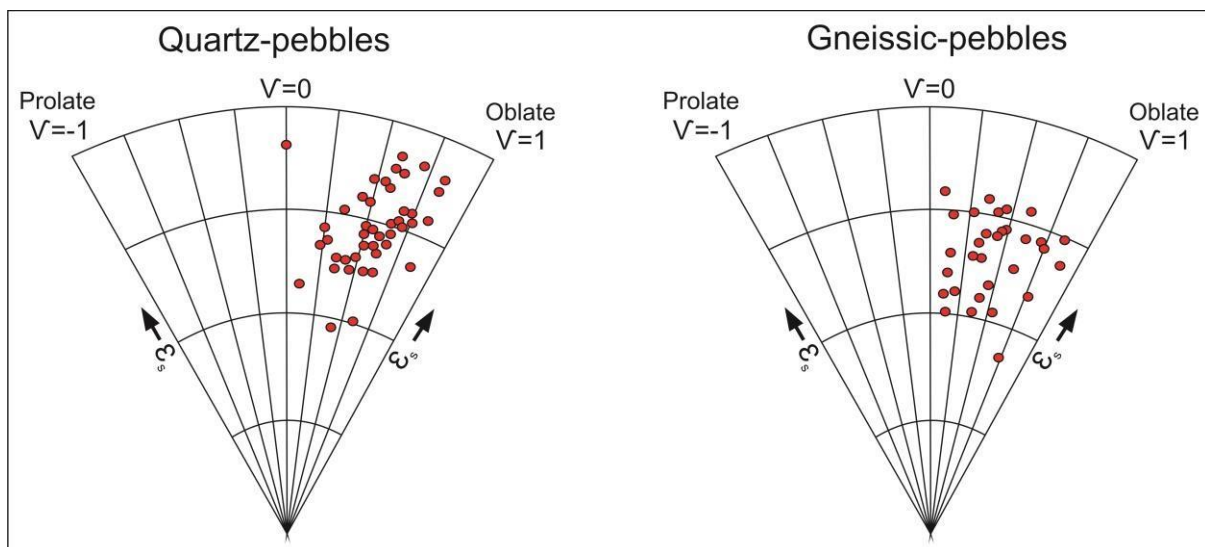


Figure 3-38: Hsu diagrams for the Neusberg sub-domain (quartz-pebbles) and the Cnydas sub-domain (gneissic-pebbles). Both areas plotted in the oblate strain sector of the Hsu plot indicating that domain 5 is dominated by flattening strain. Sample locations indicated on Figure 3-31.

3.5.8 Summary of domain 5: Puntsit/Goede Hoop Domain with special reference to Harpersputs gneiss

- The supracrustals of the Puntsit Formation and the Goede Hoop Formation were deformed during the D1(a) event when the terranes started to assemble.
- Domain 4 and 5 are separated by the Harpersputs gneiss, which intruded as a sheet intrusive during D1(b) event.

- The northern Waterval thrust and the southern Neusberg thrust represent two intra-terrane thrusts relating to the D1(b) event and serve as the respective boundaries for Domain 5.
- The Puntsit and Goede Hoop Formations are mapped as macroscopic sheath folds with D1(b)F1 axial traces trending north-west which is co-planar to the regional S2 foliation.
- The L-fabrics (fold axes of mesoscopic and macroscopic folds and stretching lineations) are co-linear across Domain 5.
- The D1(b)F1 macroscopic sheath folds are refolded by D1(b)F2 folds during the latter parts of the D1(b) event.
- A localised third fold phase is recognised in the Neusberg sheath fold (D2F1) only, with fold axis orientations co-linear to the stretching lineations.
- The Friersdale Charnockite intruded at $1080 \pm 13\text{Ma}$ (Cornell, et al., 2012) into pre-existing open D2F1 hinges; it is deduced that the intrusion of the charnockite has caused the D2F1 hinge (north-western closure of the Neusberg sheath fold) to become appressed and to form an isoclinal closure.
- During D4 the Neusberg thrust on the south-western limb has been reactivated as the sub-vertical dextral Neusberg shear zone. The macroscopic shear effects can be observed in the clockwise rotation of the D1(b)F2 axial traces of the Rondekop sheath fold.

Table 3-4: Structural framework for Domain 5.

Deformation event	D1a	D1b			D2	D3	D4	
Structural event	Model 1 and 2 folds	Inter-terrane / Intra-terrane	F1	F2	F1	Charnockite	F2	NW shear zones
Domain 5: Puntsit/Goede Hoop domain	x	x	x	x	x	x	x	x

4 Discussion

In this chapter the different domains will be compared (Table 4-1) to each other with respect to the various fold styles, fold phases and related structures. The theoretical models of sheath folds and how they relate to the structures of the study area will follow the comparative study, with the classification of the Vaaldrift sheath fold as an example. To the latter part of the chapter a tectonic frame work for the study area is proposed, based on age relationships between the stratigraphy, thrust faults and mega sheath folds and available geochronology on gneisses.

4.1 Comparison of domains

The comparison of the Bladgrond Terrane (BdT, Domain 1) and the Grünau Terrane (GT, Domain 2-5) is a difficult task as the two terranes are distinguished by their different stratigraphies, structures, ages and different metamorphic grades; the only common stratigraphy being the Karama'am Augen gneiss which cuts across the Hartbees River Thrust that separates the terranes. The one structural feature that occurs across the two terranes is that both terranes have a similar pervasively developed dominant foliation (S₂) in both the supracrustals and plutonic rocks relating to the deformation events after the terranes accreted. The BdT is dominated by mega scale Ramsay Type 2 and 3 interference folds striking east-west. The stratigraphy consist primarily of supracrustals intruded by younger plutonic rocks.

The Grünau Terrane is a north-west south-east striking Terrane dominated by plutonic rocks which intruded supracrustals along decolleménts and is compartmentalised in kilometre scale sheath folds (Domains 2, 3 and 5). The GT developed under regional granulite facies metamorphism which started at ~1200 Ma. Two of the main lithologies of the GT with a magmatic origin, namely the Eendoorn and Witwater gneisses were emplaced as the result of anatexic melting of the supracrustals (Blouputs Formation, Appendix D). The dominant macroscopic scale structures of the GT in the study area are the sheath fold complexes contained within the larger Riemvasmaak-Kenhardt Mega Sheath Fold (RK-MS).

Three out of the four domains in the GT (Domains 2, 3 and 5) consist of supracrustals intruded by younger syn-tectonic granites with the one exception being the Vaaldrift Sheath fold (Domain 4) which only consist of the Omdraai Formation. Domains 4 and 5 have a close relationship with the largest of the sheet intrusive (Harpersputs gneiss). The Harpersputs gneiss has also been folded with the two domains. The Augrabies sheath fold (Domain 3) contains only one supracrustal sequence (Koekoepkop Formation) along the southern boundary which is an imbricate thrust sheet of the Waterval thrust system. The rest of domain

3 consist of plutonic rocks that intruded during the last stages of terrane accretion as sheet granites. In the second domain the granulites of the Blouputs Formation have undergone two phases of anatectic melting which resulted in the Eendoorn gneiss and the Witwater gneiss, respectively. The Eendoorn gneiss has a close association with the other domains as it forms the footwall sequence of the Waterval thrust system and wraps around the RK-MS in the northwest. Both of the melts in domain 2 can be traced in excess of 100 km across the Namaqua Province.

Domains 2 to 5 are dominated by well-developed, penetrative, north-east dipping S1 and S2 foliations, except in the south eastern part where Domain 3 and 4 are folded by a younger open fold (D4F2; Table 4-3) and the foliations are rotated eastwards. S1 and S2 are co-planar to the axial planes of folds along the long limbs and can only be separated in the fold closures where S1 is folded and S2 forms the axial-planar foliations (Figure 4-1). The same minerals which define the S1 foliation are also defining S2, which is an indication that the metamorphic conditions (temperature and pressure) during the two fabric forming events stayed constant, with no new mineral growth between S1 and S2. The dip of the foliations across the domains is controlled by the later shear events that is superimposed across the study area. The shear effects are intensified in close proximity to the domain boundaries where pre-existing intra-terrane thrusts (Waterval, Kliprug and Neusberg thrusts) have been reactivated as transpressional shears. The regional foliation, if the shear events are eliminated, have a constant dip of 35° towards the north-north east; once affected by the sub-vertical shears the foliation is rotated towards the vertical. The degree of foliation development is controlled by the rheology and composition of lithologies.

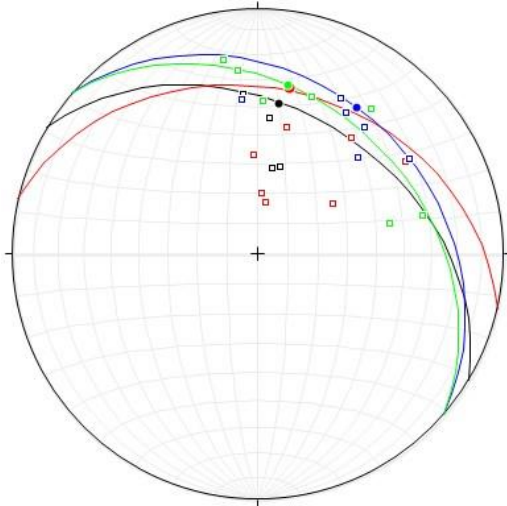


Figure 4-1: Synthesis stereonet combining the regional S (S0, S1 and S2) and L (macroscopic fold axes and mineral stretching lineations) fabrics across Domains 2 (black; 00838, n= 101), Domain 3 (red; 01132, n= 180), Domain 4 (blue; 03429, n= 122), Domain 5 (green; 01031, n= 122). The dots represent the regional mineral stretching lineations and the lines the regional S2 foliation. The squares represent the macroscopic D1(b)F1 and F2 fold axes orientations (steeper plunges are due to D4 shearing). The effects of the D4F2 fold are eliminated. There is a strong co-planar and co-linear relationship between the S and L fabrics across the 4 domains.

The regional mineral stretching lineations within the different domains have a constant north to north-north-east plunge and relate to the main sheath folding event (Figure 4-1). The lineations provide an indication of the tectonic transport direction across the domains and the tectonic transport direction can be estimated to be towards a south-south-westerly direction. The lineations in the south-eastern portion of Domains 2 to 5 are also affected by the late open fold (D4F2; Table 4-3) and the plunges have been rotated towards the east. The younger north-west striking shear zones have rotated the lineations towards vertical plunges. The most dominant mineral stretching lineations across the domains are amphibole needles, quartz-feldspar aggregates, the long axes of megacrysts and augens in the plutonic rocks and quartz pebbles in the quartzites as well as xenoliths. Not many of the supracrustals are aluminous enough for sillimanite needles to form stretched lineations; the only lithologies containing sillimanite in GT are the Blouputs Formation and Witwater gneiss and one of the marker unit (#1) in the Omdraai Formation.

Only one major inter-terrane thrust (terrane bounding thrust) runs through the study area, namely the Hartbees River Thrust (HBRT). The HBRT separates the overlying GT from the underlying BdT. The HBRT contains two thrust sheets as defined by the Putsies Migmatite Complex and Volcanic thrust sheets. The thrust zone is reactivated and rotated towards the

vertical during the last periods of deformation resulting in sub-vertical banding and foliation. The 4 domains within the GT are all separated by intra-terrane thrusts with the Waterval thrust being the sole thrust of the thrust system. Along strike and in depth of the intra-terrane thrusts, thrust sheets cut out (kilometre scale) and lithologies wedge out (metre scale). All of the intra-terrane thrusts strike north-west and dip towards the north-east. Due to younger shears (D4; Table 4-3) superimposed across the domains the intra-terrane thrusts have been reactivated as sub-vertical shear zones. Shear related kinematics indicated that both lateral and vertical shear movement was present during this phase. The thrust zones relate to the latter part of terrane accretion but predate the crustal scale folding that dominates the GT. The intra-terrane thrusts across Domains 2 to 5 are always in contact with at least one sheet granite, which suggests that the thrust planes served as feeder channels for magma during intrusion, similar to “channel flow” reported for the Himalayas (Harris, 2007).

The GT is dominated by sheath folds with lesser amount of Ramsay Type 2 and 3 interference folds. Previously elliptical or “mushroom shaped” structures (e.g. sheath fold 7, Figure 3-2) were interpreted as Ramsay Type 1 or 2 interference folds, however during this study the structures were reinterpreted as refolded sheath folds during a single progressive shear process. The sheath folds in Domain 2, 3, 4, and 5 have major fold closures in the south-east and north-west, their intermediate axes strike north-west (parallel to the regional S2 foliation) with the long axes being sub-parallel to the mineral stretching lineations (north-north-east to north-east). All the relative closures of the sheath folds are co-linear to the regional mineral stretching lineations. Younger folds like the large S-fold along the southern boundary of domain 3 (sub area “e”; Figure 3-8) fold all of the pre-existing S and L fabrics, thrusts and stratigraphy, meaning they are late-tectonic folds not related to the sheath folding event.

The younger, still ductile, shear event (D4; Table 4-3) affected the area to various scales, the Augrabies sheath fold of Domain 3 is highly refolded in the western portion, while the Vaaldrift sheath fold (Domain 4) has been severely deformed in the western and eastern portions by Ramsay type 3 style folding. Sheath fold closures for these two domains have been stretched out and thinned before they are refolded. The eastern portion of the VSF (Domain 4) is a good indication that the thrusting was prior to the folding as the internal decollements and wedging points (branch points) are deformed by the sheaths and shear zones.

The southern boundary of domain 5 (Neusberg shear zone) is a major structural decollement, also serving as a division-line for the style of folding. The effects of the late open fold (D4F2) across domains 1-4 are not present north of this decollement. The sheath folds north of this decollement have more fold phases than the structures south of it. Domain 5 is a much larger area than the underlying domains but contains abundant supplementary smaller sheath folds

in comparison to domains 3-4, which only consist of one large sheath fold. In the western portion of domain 2 (Grünau Terrane) the Nelshoop gneiss sheath folds are structures with variable yz-axis orientations. The two eastern sheath folds have been flattened and stretched while the western sheath folds have been rotated towards the north. This rotation indicates that a macroscopic scale sinistral shear was superimposed on the area.

All five of the domains consist of at least two dominant fold phases related to the D1(b) event. The most dominant fold phase is the D1(b)F1 which trends north-west. The D1(b)F2 has a wider range of orientation but mostly trends sub-parallel to the D1(b)F1 axial traces. Fold phases post-dating the D1(b) event are unique to each domain and cannot be correlated across the entire study area, this resulted in for example that the D2F1's in Domain 3 is not the same D2F1's in Domain 5 (The various fold phases for each domain will be described in the following section 4.3). In sub-area "e" (Figure 3-8) of Domain 3 a macroscopic S-fold is limited to the southern boundary of the domain and cannot be related to any of the major structural events of the study area, however the axial traces of these D4F1 trends are sub-parallel to the D1(b) folds. The most noticeable fold phase post-dating the D1(b) event is the late open north-east trending D4F2 fold present in the Domains 1, 2, 3, 4 and 5 (Map 2). Due to kilometre scale competency differences across the domains various degrees of folding occurred throughout as a result of D4F2, the HBRT being highly folded whereas the Augrabies and Vaaldrift are only folded by large open folds. If the effects of the D2F2 fold is eliminated, an important feature from the remaining fold phases is that the axial traces are all co-planar and trend north-west, apart from being in different domains relating to different structural ages.

Due to the shear process and scale of flow perturbation, model 1 and model 2 folds occur in all 5 of the domains. The two models are recorded in all of the lithologies with rheology controlling the size of the folds, they can range from millimetre intrafolial folds to metre scale S or Z-folds. The model 1 folds range from millimetre scale to metre scale with the largest recorded in the Blouputs Formation of the Domain 2. The model 2 folds occurring over Domains 2-5 are less frequent than the model 1 folds and in the Domain 5 they are rarely seen, while they occur regularly on centimetre scale in other domains. All of the domains are model 1 folds dominated with the most model 2 folds occurring in domain 4, which suggests that the process of layer-normal shear was dominating throughout the domains. Model 1 folds in all domains have fold axes orientated sub-parallel to the regional stretched mineral lineations and major sheath fold closures, whereas model 2 folds form at large angles to the regional L-fabrics.

Along the sub-vertical shear zones, model 1 and model 2 folds are deformed by the shears. Younger S and/or Z-symmetry folds developed by the shearing are used as kinematic

indicators to determine the sense of shear. In the major shear zones, such as: Duiwelsnek-, Neusberg-, and Cnydas shear zones and the reactivated Waterval thrust, the most kinematic indicators recorded are s-c fabric relationships and grain tail complexes.

Table 4-1: Comparison of structural features present across the 5 domains (DSZ: Duiwelsnek, CSZ: Cnydas, NSZ: Neusberg shear zones).

	Domain 1	Domain 2	Domain 3	Domain 4	Domain 5
Plutonites					
(pre/syn/post)	syn/post	pre/post	syn	-	syn
Supracrustals	x	x	x	x	x
Foliations	S1/S2	S1/S2	S1/S2	S1/S2	S1/S2 + localised S3
Lineations	x	x	x	x	x
Inter-terrane thrust	x	x			
Intra-terrane thrust		x	x	x	x
Sheath folds		x	x	x	x
Refolded sheath folds		x	x	x	x
Isoclinal closures	x	x	x	x	x
Number of fold phases	3	3	5	3	3
Type 2 interference folds		x	x	x	x
Type 3 interference folds	x		x		
Late open fold (D4F2)	x	x	x	x	
Sub-vertical shear zones			x (DSZ)	x (DSZ)	x (CSZ+NSZ)
Model 1 folds	x	x	x	x	x
Model 2 folds		x	x	x	x

4.2 Sheath fold criteria

Sheath folds are defined as fold structures with hinge line curvature greater than 90° within their axial planes (Ramsay & Huber, 1987) which will rotate towards parallelism with the transport direction (Carreras, et al., 1977; Cobbold & Quinquis, 1980; Alsop & Holdsworth, 2004a & 2004b) with progressive deformation and have been described in a wide range of tectonic environments such as midcrustal shear zones, extensional and contractional tectonics. They are scale independent and the size of the sheath fold will be controlled by the size of the active shear zone or ductile zone (Alsop & Holdsworth, 2007). Alsop and Holdsworth (2006, p. 1589) explains that the x, y, and z geometric axes of a sheath fold are orientated sub-parallel to the X, Y, and Z axes of a finite strain ellipsoid. Thus making the X-

axis of the sheath fold sub-parallel to the stretched mineral lineation, which marks the transport direction (flow direction) during intense non-coaxial deformation (Alsop & Holdsworth, op.cit).

Macroscopic sheath folds have been recognised and documented for both the ~2Ga Pofadder Terrane and the ~1.6Ma Aggeneys Terrane, Blignault et al. (1983), Colliston (1983) and Colliston & Schoch (2000) describe macroscopic sheath folds outcropping as the Dabenoris and Pella Mountain respectively. In the Aggeneys Terrane the Aggeneys Mountains consist of a series of stacked sheath folds and Gams Mountain (Gamsberg) represents a single macroscopic sheath fold, which plunges to the north-east. According to Colliston & Schoch (2013) sheath folds form under a compressive simple shear regime associated with south-west accretion of terranes.

It can be a challenging task to identify and classify structures such as the RK-MS and internal sheath fold complexes as kilometre scale sheath folds due to their large size and distribution. Alsop & Holdsworth (1999) suggest that the connection between predicted and observed patterns of vergence, obliquity and facing can be used as techniques to classify sheath folds in less exposed regions or where the younging evidence is not preserved during deformation. Using classification schemes and models of sheath folds from various ductile regimes, a detailed set of criteria for sheath fold classification have been constructed. The criteria can be used to map and classify sheath folds in sub outcrop areas or in areas where sheath folds occur on mega scale:

1. Minor S and Z-folds have a reversal in asymmetry across the strike after crossing major fold axial traces and culmination and depression surfaces (Alsop & Holdsworth, 2004b; Alsop & Holdsworth, 1999). Sense of minor fold facing will display distinct reversals in polarity.
2. The core of a sheath fold, also known as the eye fold sections are bounded by double-vergence geometries (Searle & Alsop, 2007), plunging antiforms connected to plunging synforms (Passchier, et al., 2011).
3. Litho-stratigraphical maps indicating a symmetrical arrangement of lithologies coupled with a change in vergence of minor structures (Alsop, 1994).
4. High shear strains, responsible for the generation of large scale sheath folds, will also result in displacement and tectonic sliding along pre-existing structural discontinuities or lithological contacts displaying a clear competency contrast (Alsop, 1994).
5. Localized reversal in fold obliquity (Alsop & Holdsworth, 1999). Minor fold hinges display sequential rotations towards the transport direction with the angle of obliquity systematically reducing (Alsop & Holdsworth, 2004a)

6. Large scale sheath folds can also contain several smaller sheath folds which reflect the scaling of the precursor folds (in the case of second order sheath folds). The short (Z) axis of a sheath fold is controlled by (1) the size of the precursor fold and (2) the width of the active deformation zone (Alsop, et al., 2007).
7. Within large ductile shear zones, either the antiformal or the synformal elements of sheath folds are difficult to recognize since one of them may be sheared out systematically along low-dipping ductile shears or they are strongly flattened (Flower & Kalioubi, 2002).
8. Sheath folds need not show any special spatial or temporal relationship with one another, however they show elongation in the same direction (regional extension or tectonic transport direction) (Flower & Kalioubi, 2002).
9. Sheath folds will have non-continuous axial planes (Flower & Kalioubi, 2002).
10. Core or “eye” structures are situated in major culmination zones between double verging folds where there is an increase in flow velocity resulting in thickened stratigraphy, whereas depression zones are characterised by co-planar S-fabrics.
11. The thickness of sheath fold limbs can be used as shear-sense indicators and to determine the fold closing direction in a yz plane perpendicular to the flow direction (stretching lineation): if the sheath fold closes away (in depth) from the observer a thinned inverted limb indicates top-towards-observed sense of shear (Figure 4-3 inset; Fossen & Rykkelid, 1990).

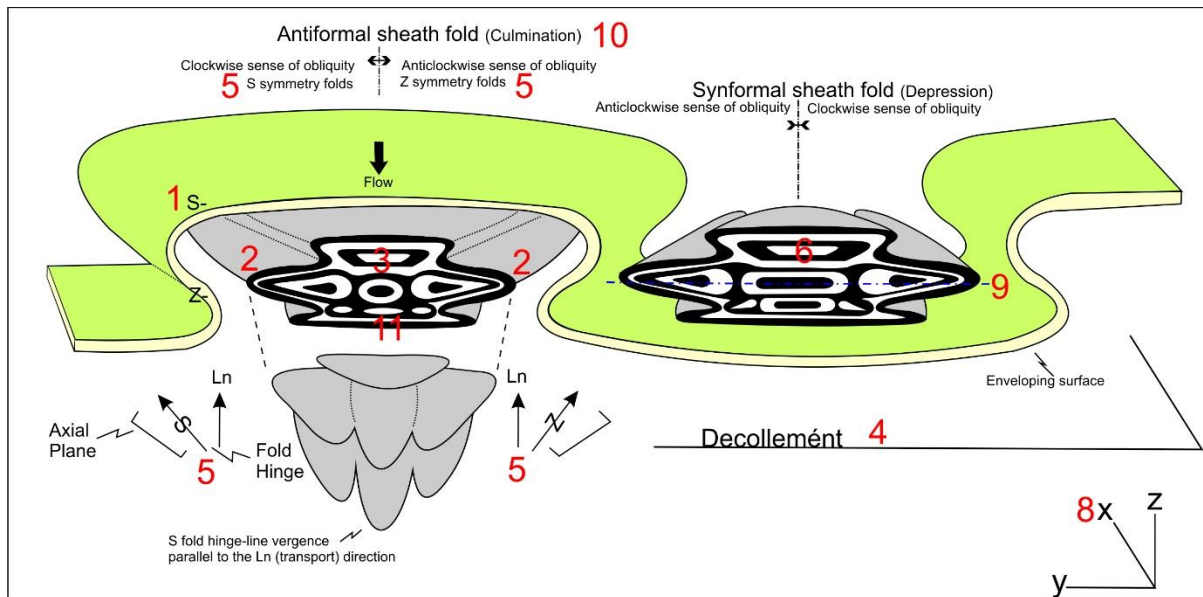


Figure 4-2: Modelled shape of a schematic sheath fold (modified after Alsop and Holdsworth (2004b)); the front face of the model represents the yz plane of the strain ellipsoid, with the stretching direction, “x” into the plane of the page (8). The shape of the sheath fold is referred to as an omega (Ω) type. The numbers 1-11 (red; see text) represent the sheath fold criteria needed to classify a structure as a sheath fold.

1. Minor S and Z-folds have a reversal in asymmetry across the strike after crossing major fold axial traces.
2. The eyes of the structure are bound by double-vergence geometries.
3. Symmetrical arrangement of lithologies (elliptical shapes).
4. Displacement and tectonic sliding along pre-existing structural discontinuities.
5. Localized reversal in fold obliquity (rotation in horizontal).
6. Large scale sheath folds may be composed of several smaller subsidiary sheath folds.
7. Cannot be displayed on this model.
8. Sheath folds show elongation in the same direction (co-linear x-axis).
9. Sheath folds will have non-continuous axial planes. 10. The core or eye structures are situated in culmination zones.
11. Thickness of the sheath fold's limbs indicate flow direction and overturned limb.

4.2.1 Vaaldrift sheath fold is used as an example of listed criteria (section 4.2)

The Vaaldrift sheath fold can be classified as a sheath fold according to the 10 point criteria (Figure 4-3). (refer to numbers on Figure 4-3) There is a reversal in the asymmetry of the minor folds along strike of the axial trace (1), in the central part of the structure (long limb), the minor S- and Z-folds occur along strike on the same structural and stratigraphic level. (2) In the western part the #4 sequence is a double-plunging elliptical shaped core or eye structure with the north-western synform connected to south-eastern antiform with a reversal in facing along strike of the axial trace. (3) The 5 sequences of the Omdraai Formation form a symmetrical alignment around the VSF, although #1, #2 and #5 wedge out along decolleménts. (4) A competency contrast exists between the two plutonic rocks overlying (Harpersputs gneiss) and underlying (Rooipad gneiss) the VSF and the contacts represent pre-existing intra-terrene thrusts and have served as decolleménts along which displacement

and tectonic sliding occurred. (5) A reversal in minor fold hinge obliquity along the strike of the VDSF indicates zones of increased flow velocity and or zones with slugging flow velocities.

(6) The VSF is a smaller sheath fold within the mega RK-MS and forms part of a series of stacked sheath fold complexes. Smaller centimetre to metre scale sheath folds occur throughout the VSF in all 6 sequences. (7) The VSF represents a synformal sheath fold, the antiformal component is not present in the study area. (8) The intermediate axis (Y-axis) of the VSF trends north-west south-east with the long axis (x-axis) orientated sub-parallel to the regional stretched mineral lineation direction, this direction is defined as the tectonic transport direction by Alsop and Holdsworth (2006). This X-axis orientation is sub-parallel to the other sheath fold complexes of the RK-MS. (9) The F1 fold axial trace of the VSF is highly folded and stretches for kilometres but it is not continuous as the sheath fold has major fold closures in the north-west and south-east. (10) The western sub-domain of the VSF can be classified as a culmination zone and the central and eastern sub-domains as a depression zone. (11) In the western sub-domain, the north-eastern limb of the VSF is thinner than the south-western limb (length of blue arrows indicates limb thickness). Using the method of Fossen & Rykkelid (1990) the overturned limb could be established; the difference in thickness indicates that the north-eastern limb is the overturned limb and the VSF closes in depth (synformal sheath fold).

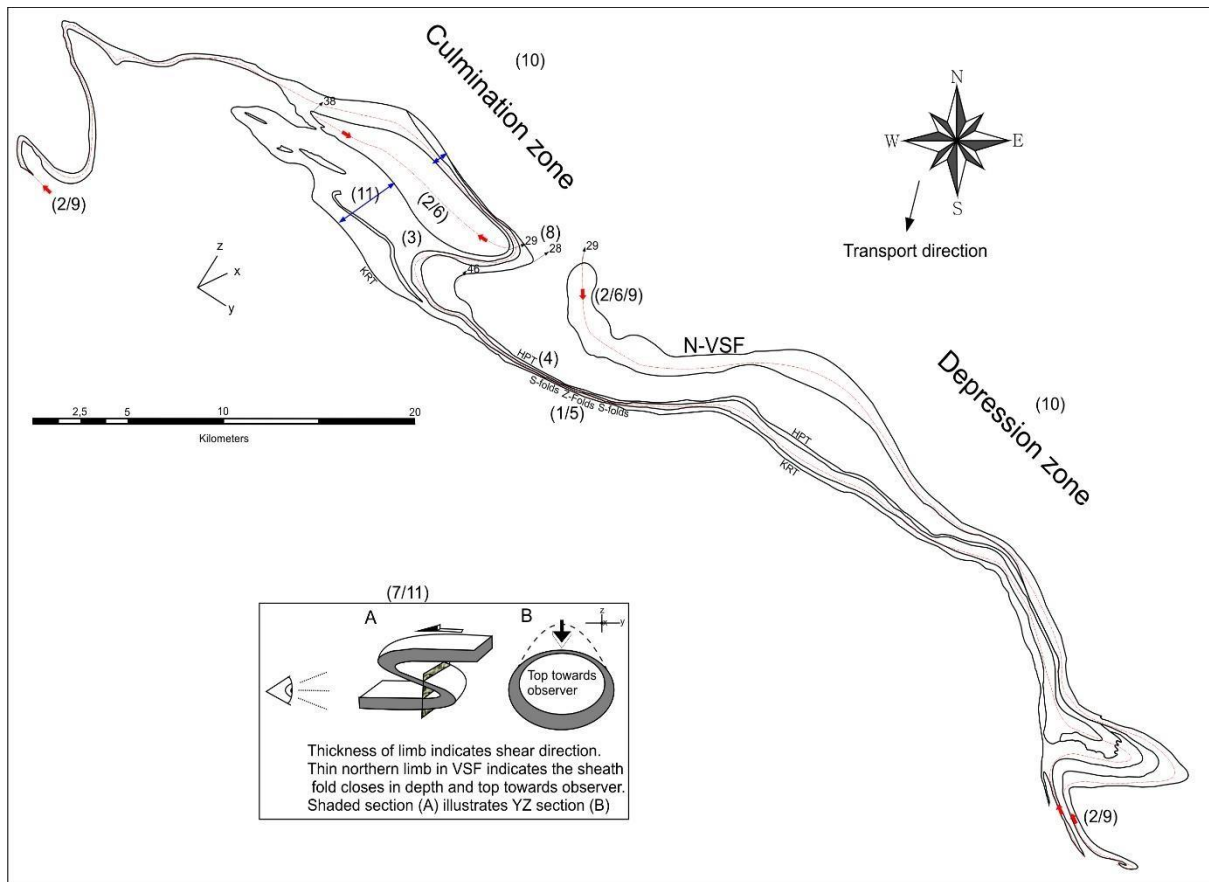


Figure 4-3: Vaaldrift sheath fold as an example for the 10 point sheath fold criteria. Numbers (1-10) relates to the 10 points discussed in the previous section.

1. Minor S and Z-folds display a reversal in asymmetry along strike of the D1(b)F1 axial trace of the Vaaldrift sheath fold.
2. The core of the VSF contains an elliptically shaped lithological unit with a reversal in facing along strike.
3. Symmetrical arrangement of the first, second, third and fourth stratigraphic sequences.
4. Displacement and tectonic sliding along the Harpersputs (HPT) and Kliprug (KRT) thrusts (tectonic transport to south-west).
5. Localized reversal in fold obliquity of the minor folds.
6. The VSF consists of a single core and a supplementary northern (N-VSF) co-planar sheath fold.
7. The VSF is a synformal sheath fold, with closure in depth (northwards).
8. All of the subsidiary sheath folds have co-linear long axes parallel to the stretching direction of the regional strain ellipsoid (x-direction) and sub-parallel to the south-south-westerly tectonic transport direction.
9. All of the above mentioned subsidiary sheath folds have non-continuous axial planes that are co-planar to the regional S-fabrics.
10. The elliptical core of the VSF is situated in a culmination zone between doubly verging folds, whereas the long limb represents a depression zone.
11. The north-eastern limb of the VSF is thinner than the south-western limb (length of blue arrows indicates limb thickness). The difference in thickness indicates that the north-eastern limb is the overturned limb and the VSF closes in depth (synformal sheath fold), refer to the insert for a schematic model from an observer's point of view.

With the example of the VSF, it can be concluded that the sheath fold criteria can be used as a tool in ductile deformation regimes to classify unidentified structures as sheath folds with a high degree of confidence and accuracy. However, fair amount of detailed field mapping of stratigraphy and structural detail will be needed.

4.3 Tectonic Framework of Domains 2 to 5

Four main deformation events have been identified for the north-western half of the RK-MS as part of the deformation undergone by the Grünau Terrane. Previously the different events in the Namaqua Province have been divided into 6 deformation events (Joubert, 1971). During the current research a new model of the deformation events for the eastern part of the Namaqua Province is proposed: progressive deformation from D1 to D3 followed by D4. The D_n , D_{n+1} , D_{n+2} ..., nomenclature will still be used to explain the period of deformation. From D2 the structural events will be discussed separately for each domain as the deformation events differ from this phase. As a summary a regional tectonic framework for the study area is proposed as part of Table 4-3.

Van Bever Donker (1980) describes three main deformation phases; “D1” is recorded as isoclinal intrafolial folding forming the regional foliation. The second event, “D2”, is the main event forming the major plunging inclined structures. The final deformation event, “D3”, yielded only a small amount of deformation and was recorded by Van Bever Donker (1980) as the event forming the localised domal structures in the area. He however suggested that “D1” and “D2” followed shortly after each other with more or less a continuous process, which can be reinterpreted as progressive deformation.

4.3.1 D1

The D1 event is the oldest recorded event during the deformation history of the Namaqua Province and have been identified across the entire mobile belt. It is referred to as the Namaquan (Grenvillian) Orogeny (Colliston, et al., 2014). The D1 in the eastern Namaqua Province has been divided into a D1(a) and a D1(b) events based on field relationships of structures and published geochronological data. The D1 event is the only simultaneous event recorded for all 5 domains (Table 4-2).

The D1(a) is the terrane amalgamation event recorded and described by Blignault, et al. (1983), Stowe (1983), Colliston & Schoch (2013), and Colliston, et al. (2015). D1(a) is recognised by the crustal scale inter-terrane thrusts that links the tectonostratigraphic terranes across the Namaqua Province. In the study area there is only one such a structure – the HBRT which forms the boundary between the Grünau and Bladgrond Terranes. The age of terrane amalgamation is described by Cornell & Pettersson (2007) on detrital zircon aged at 1197 ± 5 Ma and metamorphic rims at 1194 ± 23 Ma (also dated by Fransson (2008) at 1190 ± 15 Ma and Nordin (2009) at 1204 ± 13 Ma). During this time the Grünau Terrane underwent the first stage of melting and the Eendoorn gneiss emplaced between 1192 and 1205 Ma (Nordin,

2009) while Bial, et al. (2015a) suggested an emplacement age of 1197 ± 11 Ma. Peak granulite metamorphism in the GT was dated by Bial, et al. (2016) to be between 1201-1180 Ma at 800-850°C and 4-4,5 kbar. Thus the combined ages of metamorphism and emplacement of the Eendoorn gneiss suggest that the D1(a) event, formation of the HBRT formed at approximately 1200 Ma. This event also served as the activation of the progressive shear system that will continue throughout the D1-D2; model 1 and model 2 folds are formed in the oldest of the plutonic rocks, i.e. Eendoorn gneiss.

The D1(b) event is recognised in all of the intra-terrane thrusts described in the domain descriptions (chapter 3) such as the Waterval thrust system and the Neusberg thrust. The formation of intra-terrane thrusts coincided with the intrusion of the sheet granites of domains 3 and 5. The intra-terrane thrusts served as decollements along which the magma could intrude. The plutonic rocks intruded into a shear regime and simultaneously formed the S1 shear fabric. Model 1 and 2 folds developed and define the S1 fabric. The Augrabies gneiss is dated at 1168 ± 6 Ma (Colliston, et al., 2015) and the Rooipad gneiss at 1155 ± 7 Ma (same age of the equivalent Riemvasmaak gneiss of Pettersson (2008) at 1151 ± 14 Ma). This gives a maximum bracket of 26 Ma years for D1(b), during which the intra-terrane (sub-terrane) developed and the sheet granites intruded. D1(b) also served as the main fabric forming event imprinted over all of the plutonic and supracrustal rocks. The progressive shear model is still active with model 1 and model 2 folds (observed in granites and meta-sediments) formed by the process of flow perturbation. This process will lead to the development of the macroscopic sheath folds towards the latter part of D1(b).

The earliest macroscopic sheath folds are recorded as D1(b)F1 structures which are refolded by a second phase of sheath folding and resulted in D1(b)F2 structures. A characteristic of the D1(b)F1 isoclinal folds is the folding of the pre-existing S0/S1 foliations. The hinges of these folds are transposed and contain the regional S2 foliation, along the limbs of the structures the S0/S1 has a co-planar relationship with the S2 foliation. During the D1(b) event the regional lineation, L1, developed sub-parallel to the regional stretching direction which is co-linear to the D1(b)F1 fold axes of the various sheath folds. D1(b)F1 and F2 folds are recorded in all five of the domains.

4.3.2 D2

The D2 event is recognised as localised tight to isoclinal folding of the D1(b)F1 and F2 sheath folds (Table 4-2). In Domain 2 the D2 event is recognised as the refolding of sheath fold 7 (Figure 3-2) resulting in the mushroom shape. The D2F1 folds in the Augrabies sheath fold (Domain 3) is limited to the Oranjekom Complex sheath fold. The F1 axial trace of the

Oranjekom Complex sheath fold refolds the D1(b)F1 of the Augrabies gneiss core structure. The Oranjekom Complex being a sheath fold gives an indication that sheath folds still developed during D2 as part of progressive deformation. D2F1 folds in Domain 4 are limited to the north-western sub-domain and refold the isoclinal hinge of the Vaaldrift sheath fold (same folds as the D2F2 fold of Domain 3). In domain 5 the D2 event relates to open as well as isoclinal folding in the Neusberg sub-domain, however the isoclinal folds are interpreted as the result of the Friersdale Charnockite intrusion.

The D2 event can be placed in a bracket between 1155 ± 7 to ~ 1100 Ma. With 1155 ± 7 Ma being the emplacement age of the youngest granite (Rooipad gneiss) and ~ 1100 Ma the emplacement age of the Oranjekom Complex (Kruger, et al., 2000). The Witwater gneiss was emplaced at 1123 ± 6 Ma (Diener, et al., 2013) and marks the second melting phase of the Grünau Terrane and it intruded the Nelshoop gneiss which is deformed during D2 (mushroom structure mentioned above). The D2F1 folds are characterised by folding of the co-planar S0/S1 and S2 regional foliation. During progressive shear a slight shift in the tectonic transport direction causes the pre-existing sheath folds to be refolded by younger syn D2 sheath folds and other associated folds. The progressive shear model is now coming to an end.

In summary the D2 event can be described as the localised refolding of pre-existing sheath folds as well as the further development of the progressive shear deformation giving rise to further sheath folding.

4.3.3 Terrane stitching

The late tectonic Karama'am Augen granite gneiss at 1107 ± 6 Ma postdates the D2 event and crosscuts the Hartbees River Thrust stitching the Grünau and Bladgrond Terranes together. It has a weakly defined foliation which is a contrast to the highly deformed country rocks.

4.3.4 D3

The D3 event is recognised by the intrusion of the Friersdale Charnockite (Table 4-2). The charnockite only intruded Domains 2 and 5. The Friersdale Charnockite having an emplacement age of 1080 ± 13 Ma (Cornell, et al., 2012) occurs in the hinge zones of the pre-existing sheath folds. The fabric in the charnockite is weakly defined and no model 1 and model 2 folds were recognised which suggest that the progressive flow perturbation processes that dominated during the D1 to D2 episodes were not active anymore.

4.3.5 D4

D4 is the last recorded event and is defined as the reactivation of the Namaqua Province (Colliston & Schoch, 2013; Colliston, et al., 2015) by transpressional shearing and two phases of folding, caused by oblique collision between the Kalahari Craton and Laurentia. The D4F1 S-fold is only present in Domains 2 and 3 as it is situated on the boundary between the two domains. The open fold (D4F2) that deforms Domain 2, 3 and 4 is a late stage effect and causes the rotation of the regional foliation and mesoscopic structures towards the east. In the western Namaqua Province the open folding of structures is more pronounced than in the east (Colliston, et al., 2014). The D4 folding is not present north of the Vaaldrift sheath fold (Domain 4).

This collision resulted in the reactivation of pre-existing thrust zones and the formation of north-west trending sub-vertical shear zones (Table 4-2). The Waterval thrust was reactivated as a sinistral shear zone, the Neusberg thrust was reactivated as the dextral Neusberg shear zone and the Kliprug intra-terrane thrust was reactivated as the Duiwelsnek shear zone. The sinistral Cnydas shear zone is a north-west striking sub-vertical shear that formed on the limb of the Biesje Poort sheath fold and involves the western closures. The D4 shear events rotated the axial traces of pre-existing sheath folds towards a north-west striking orientation and rotated axial planes and the regional foliation towards the vertical. The shear event is associated with the last metamorphic episode that is superimposed over all 5 domains at 1018 ± 11 Ma to 1024 ± 14 Ma (Colliston, et al., 2015). Bial (2015b) recorded this event as isobaric cooling ($580-660^\circ\text{C}$ at 5.9kbar) of the Grünau Terrane from 1040 Ma to 1020 Ma.

Table 4-2: Structural framework for Domain 2 to 5.

Deformation event	D1a	D1b			D2		D3	D4		
Structural event	Model 1 (F1) and 2 (F1') folds	Intra-terrane thrusting	F1	F2	F1	F2	Charnockite	F1	F2	NW shear zones
Domain 2: Grünau Terrane	x	x	x	x	x		x	x	x	x
Domain 3: Augrabies sheath fold	x	x	x	x	x	x		x	x	x
Domain 4: Vaaldrift sheath fold	x	x	x	x	x				x	x
Domain 5: Puntst/Goede Hoop domain	x	x	x	x	x		x			x

Table 4-3: Tectonic Framework of the study area (GT: Grünau Terrane, HBRT: Hartbees River Thrust, WVT: Waterval, NBT: Neusberg, KRT: Kliprug, HPT: Harpersputs thrusts). Ages: a: Colliston et al. (2015); b: Kruger et al. (2000); c: Cornell et al. (2012); d: Diener et al. (2014); e: Bial et al. (2016).

Deformation Event	Published event	Age (Ma)	Characteristic	Magmatism (Emplacement)	Metamorphism	Structures	Fabric	Progressive shear
D1(a)	D1	~1200	Terrane amalgamation	1st melting of GT; emplacement of Eendoorn gneiss	^d First: 800-850°C at 4-4,5kbar	Inter-terrane thrust (HBRT), Model 1 and 2 folds		Activation of progressive shear model
D1(b)	D2	1168±6 ^a to 1155±7 ^a	Sheet intrusives D1(b)F1/F2 sheath folds	Emplacement of all the sheet intrusives (e.g. Rooipad and Augrabies gneiss)		Intra-terrane thrust (WVT, NBT, KRT, HPT)	S1= shear fabric S2= regional fabric	Progressive flow perturbation continuing
D2	D3	1155±7 to 1100 ^b	Localised refolding of D1(b) folds together with the 2 nd series of sheath folds.	2nd melting of GT; Witwater gneiss emplaced at 1123±6 Ma. Oranjekom Complex(1100Ma)		D2F1 sheath folds, D2F2 folds		Peak of the progressive shear model
Terrane stitching	The Karama'am Augen gneiss intruded the HBRT at 1107±6 Ma and stitches the Bladgrond and Grünau Terranes together.							
D3	D4	1080 ±13 ^c	Friersdale charnockite	Friersdale charnockite into pre-existing (D1b) fold hinges			Folds all pre-existing S fabrics	Progressive shear model terminated
D4	D5/6	1018 ± 11 ^a to 1024 ± 14 ^a	NW shear zones, D4F1 S-fold, D4F2 open folds		^e Isobaric cooling: 580-660 at 5,8±0,5kbar	Reactivation of thrust (intra and inter), formation of NW-trending sub-vertical shear zones	Deforms all pre-existing structures	Activation of transpressional shear model

5 Summary and conclusion

1. The bulk of the area near Kakamas and environs consists of a host of supracrustals intruded by sheet granites in the period from 1200 to 1080Ma. The plutonic rocks in domains 3-5 represent sheet intrusives, while in domain 2 the plutonites are characteristic of anatectic sheet melts from the pre-existing rocks. The high amphibolite to low granulite grade metamorphism superimposed on the supracrustals is a result of heat transfer from the sheet granites.
2. The supracrustal sequences are confined to packages in sheath fold complexes from north to south; the complexes define the 5 domains. The stratigraphy of each domain is separated by regional décollements, either inter-terrane thrusts (Hartbees River Thrust) or intra-terrane thrusts (Waterval, Kliprug, Harpersputs and Neusberg thrusts). The décollements form natural domain boundaries.
3. Domains 3 to 5 form part of the stacked sheath fold complexes (Augrabies, Vaaldrift, Rondekop, Biesje Poort and Neusberg sheath folds) forming the internal structures of a mega scale sheath fold (Riemvasmaak-Kenhardt Mega Sheath Fold). The sheath folds deformed the stratigraphy, the thrust planes and S1 fabric. Within domain 1 smaller sheath folds occur that are unrelated structurally to the RK-MS.
4. Sheath folds were formed by the process of flow perturbation folding under ductile progressive general shear.
5. The macroscopic sheath folds are formed and refolded during the D1(b) deformation event. The isoclinal hinges of the sheath folds are transposed, characterised by an axial planar cleavage which becomes the regional S2 foliation.
6. The Oranjekom Complex intruded at ~1100 Ma and is defined as a macroscopic sheath fold which suggests that the sheath fold developed from D1(b) to D2 during progressive deformation.
7. S1 formed co-planar to S0 during the intrusion of the granite gneisses. The regional S2 is co-planar to the S0/S1 and axial planes of sheath folds.
8. The regional north-west trending lineations formed during D1(b) co-linear to the long axis of the regional strain ellipsoid and long-axes (x-axes) of sheath folds.
9. Stretched mineral lineations and fold axes orientation of model 1 and 2 folds indicate that overthrusting of the Grünau Terrane over the Bladgrond Terrane in a south-west

to a south-south-west direction. This orientation indicates that the sheath folds developed during a south-westerly tectonic transport direction.

10. Two metamorphic events are recorded for the area by previous authors: the first event was during terrane amalgamation at ~1200Ma and the second event during the last stages of deformation (1018±11 to 1024±14Ma; D4 north-west shear event).
11. The Karama'am augen gneiss intruded between major deformational periods and stitched the Grünau and Bladgrond Terranes at 1107±6 Ma, indicating the end of terrane accretion.
12. The Friersdale charnockite intruded the pre-existing D1(b) sheath fold hinges during D3.
13. The thrust faults were reactivated as sub-vertical shear zones during a later transpressional shear phase (D4) superimposed over all of the domains. During this stage the Duiwelsnek shear zone formed along the length of the Biesje Poort sheath fold.
14. The different sheath fold complexes are classified as such using published characteristics compiled for sheath folds across the ductile regimes of the world.
15. Previously researchers tried to correlate deformation phases from the western and central Namaqua Province to the fold phases seen in the eastern part, often leading to confusion. The recognition of crustal scale thrust faults changed the correlating of deformation events over the entire Namaqua Province. Each terrane has its own set of deformation events with accompanying fold phases.
16. A new progressive ductile shear deformation model is proposed (D1a+b to D4) for the deformational events. Previous models indicated separate events and not a progressive deformation (Stowe, et al., 1984). This is based on the fact that the domains deformed simultaneously and continuously, model 1 and model 2 folds formed from D1a+b to D2 as a progressive flow perturbation process.

6 Acknowledgements

Firstly I would like to extend my gratitude to my supervisor Professor W.P. Colliston and although he is not a direct supervisor Professor A.E. Schoch, for the mentorship during this study and the guidance along a challenging learning curve. I appreciate the timeless discussions and field excursions in which my passion and knowledge for structural geology developed. I would also like to extend my gratefulness and appreciation towards my family and friends for the moral and spiritual support during this study. A special thanks go to my parents for the years of financial support.

The field study was enhanced by the superb friendships I cultivated among the farmers of this region and their gracious hospitality. A special word of thanks to David and Jannie Spangenberg and Hannes Buys of the farms Krismar and Zwart Boois Berg.

Permission to do research in the Augrabies Falls National Park (SANParks) and excellent collaboration with management and staff is greatly appreciated. Park manager Frans Van Rooyen is thanked for the accommodation and Nardus du Plessis (head of conservation) for the discussions on this interesting ecosystem in the park area.

Lastly I would like to acknowledge the University of the Free State and the National Research Foundation for the funding they provided during this time.

7 References

Allmendinger, R., Cardozo, N. & Fisher, D., 2013. Structural Geology Algorithms: Vectors & Tensors. Cambridge, England: Cambridge University Press, 289pp.

Alsop, G., 1994. Relationships between distributed and localized shear in the tectonic evolution of a Caledonian fold and thrust zone, northwest Ireland. *Geological Magazine*, 131(1), 123-136.

Alsop, G. & Holdsworth, R., 1999. Vergence and facing patterns in large-scale sheath folds. *Journal of Structural Geology*, 21, 1335-1349.

Alsop, G. & Holdsworth, R., 2002. The geometry and kinematics of flow perturbation folds. *Tectonophysics*, 350, 99-125.

Alsop, G. & Holdsworth, R., 2004a. Shear zone folds: Records of flow perturbation or structural inheritance. *Geological Society London Special Publications*, 224, 177-199.

Alsop, G. & Holdsworth, R., 2004b. The geometry and topology of natural sheath folds: a new tool for structural analysis. *Journal of Structural Geology*, 26, 1561-1589.

Alsop, G. & Holdsworth, R., 2006. Sheath folds as discriminators of bulk strain type. *Journal of Structural Geology*, 28, 1588-1606.

Alsop, G. & Holdsworth, R., 2007. Flow perturbation folding in shear zones. In: A. Ries, R. Butler & R. Graham, eds. *Deformation of the Continental Crust: the Legacy of Mike Coward*. London: The Geological Society, 77-103.

Alsop, G., Holdsworth, R. & McCaffrey, K., 2007. Scale invariant sheath folds in salt, sediments and shear zones. *Journal of Structural Geology*, 29, 1585-1604.

Alsop, G. & Holdsworth, R., 2004b. The geometry and topology of natural sheath folds: a new tool for structural analysis. *Journal of Structural Geology*, 26, 1561-1589.

Beukes, G. J., 1973. 'n Geologies ondersoek van die gebied suid van Warmbad, SuidwesAfrika, met spesiale verwysing na die metamorf-magmatiese assosiasies van die voorkambriese gesteentes, Bloemfontein, 333pp.

Bial, J., Buttner, S. & Appel, P., 2016. Timing and conditions of regional metamorphism and crustal shearing in the granulite facies basement of south Namibia: Implications for the crustal

evolution of the Namaqualand metamorphic basement in the Mesoproterozoic. *Journal of African Earth Sciences*, 123, 145-176.

Bial, J., Buttner, S. & Frei, D., 2015a. Formation and emplacement of two contrasting late Mesoproterozoic magma types in the central Namaqua Metamorphic Complex (South Africa, Namibia): Evidence from geochemistry and geochronology. *Lithos*, 224-225, 272-294.

Bial, J., Büttner, S., Schenk, V., & Appel, P., 2015b. The long-term high-temperature history of the central Namaqua Metamorphic Complex: Evidence for a Mesoproterozoic continental back-arc in southern Africa. *Precambrian Research*, 268, 243-278.

Blignault, H., 1977. Structural-Metamorphic imprint on part of the Namaqua Mobile Belt in South West Africa, Cape Town: Precambrian research unit, Bulletin 23, Department of Geology, University of Cape Town, p.197.

Blignault, H., van Aswegen, G., van der Merwe, S. & Colliston, W., 1983. The Namaqualand Geotraverse and environs: part of the Proterozoic Namaqua mobile belt. In: B. Botha (Ed.). *Namaqualand Metamorphic Complex. Special Publication*, Geological Society of South Africa, 1-29.

Boyer, S. & Elliott, D., 1982. Thrust systems. *The American Association of Petroleum Geologists Bulletin*, 66(9), 1196-1230.

Cardozo, N. & Allmendinger, R. W., 2013. Spherical projections with OSXStereonet. *Computers & Geosciences*, 51, 193-205.

Carreras, J., Estrada, A. & White, S., 1977. The effects of folding on the c-axis fabrics of a quartz-mylonite. *Tectonophysics*, 39, 3-24.

Cobbold, P. & Quinquis, H., 1980. Development of sheath folds in shear regimes. *Journal of Structural Geology*, 2(1/2), 119-126.

Colliston, W., 1983. Stratigraphic and depositional aspects of the Proterozoic metasediments of the Aggeneys Subgroup at Pella and Dabenoris, 101-110. In: B. Botha, (Ed.). *Namaqualand Metamorphic Complex, Special Publication 10*, Geological Society of South Africa, p.198.

Colliston, W., 1990. A stratigraphic and structural investigation of part of the Namaqua Mobile Belt between Dabenoris and Steyerkraal, South Africa, Bloemfontein, 259pp.

Colliston, W., Cornell, D., Schoch, A. & Praekelt, H., 2015. Geochronological constraints on the Hartbees River Thrust and Augrabies Nappe: New insights into the assembly of the Mesoproterozoic Namaqua-Natal Province of Southern Africa. *Precambrian Research*, 265, 150-165.

Colliston, W., Praekelt, H. & Schoch, A., 1991. A progressive ductile shear model for the Proterozoic Aggeneys terrane, Namaqua mobile belt. *Precambrian Research*, 49, 205-215.

Colliston, W. & Schoch, A., 2000. Mid-Proterozoic tectonic evolution along the Orange River on the border between South African and Namibia. *Communs geological survey of Namibia*, 12, 53-62.

Colliston, W. & Schoch, A., 2002. The structural development of the Aggeneys Hills, Namaqua Metamorphic Complex. *South African Journal of Geology*, 105,301-324.

Colliston, W. & Schoch, A., 2006. The distribution and diagnostic features of deformed plutonic rocks in two terranes of the Namaqua mobile belt along the Orange (Gariiep) River, South Africa. *South African Journal of Geology*, 109, 369-392.

Colliston, W. & Schoch, A., 2013. Wrench-shearing during the Namaqua Orogenesis–Mesoproterozoic late stage deformation effects during Rodinia assembly. *Precambrian Research*, 223, 44-58.

Colliston, W., Schoch, A. & Cole, J., 2014. The Grenvillian Namaqua-Natal fold belt adjacent to the Kaapvaal Craton: 1 Distribution of Mesoproterozoic collisional terranes deduced from results of regional surveys and selected profiles in the western and southern parts of the folds belt. *Journal of African Earth Sciences*, 100, 7-19.

Colliston, W., Schoch, A. & Praekelt, H., 2012. Stratigraphy of the Mesoproterozoic Aggeneys Terrane, Western Namaqua Mobile Belt, South Africa. *South African Journal of Geology*, 115(4), 449-464.

Coney, P., Jones, D. & Monger, J., 1980. Cordilleran suspect terranes. *Nature*, 288, 329-333.

Cornell, D. & Pettersson, A., 2007. Ion probe zircon dating of metasediments from the Areachap and Kakamas Terranes, Namaqua-Natal Province and the stratigraphic integrity of the Areachap Group. *South African Journal of Geology*, 110, 169-178.

Cornell, D., Pettersson, A. & Simonsen, S., 2012. Zircon U-Pb emplacement and Nd-Hf crustal residence ages of the Straussburg granite and the Friersdale charnockite in the Namaqua Natal Province, South Africa. *South African Journal of Geology*, 115(4), 465-484.

Cornell, D.H., Thomas, R.J., Moen, H.F.G., Reid, D.L., Moore, J.M., Gibson, R.L., 2006. Namaqua-Natal Province. In: M. Johnson, C. Anhaessler & R. Thomas, eds. *Geology of South Africa*. Pretoria: Geological Society of South Africa and Council of Geoscience, 325-379.

Coward, M. & Potgieter, R., 1983. Thrust zones and shear zones of the margin of the Namaqua and Kheis Mobile Belts, South Africa. *Precambrian Research*, 21, 39-54.

Coward, M. & Potts, G., 1983. Complex strain patterns developed at the frontal and lateral tips to shear zone and thrust zones. *Journal of Structural Geology*, 5(3/4), 383-399.

Dewey, J., Robb, L. & Van Schalkwyk, L., 2006. Did Bushmanland extensionally unroof Namaqualand?. *Precambrian Research*, 150, 173-182.

Diener, J., 2014. Low-P-high-T metamorphism of the Aggeneys Terrane, Namaqua Metamorphic Complex, South Africa. *South African Journal of Geology*, 117(1), 31-44.

Diener, J. et al., 2013. Clockwise, low-P metamorphism of the Aus granulite terrain, southern Namibia, during the Mesoproterozoic Namaqua Orogeny. *Precambrian Research*, 224, 629-652.

Du Plessis, G., 1979. 'n Metamorfe-Magmatiese studie van 'n gedeelte van die Namakwalandse Matamorfe Kompleks langs die Ornajerivier oos van Onseepkans, Bloemfontein, University of the Free State, 139pp.

Eglinton, B., 2006. Evolution of the Namaqua-Natal Belt, southern Africa – A geochronological and isotope geochemical review. *Journal of African Earth Sciences*, 46, 93-111.

Fleuty, M., 1964. The description of folds. London: Proceedings of the Geologists' Association 75, 461–492.

Flower, A. & Kalioubi, B., 2002. The Migif–Hafafit gneissic complex of the Egyptian Eastern Desert: fold interference patterns involving multiply deformed sheath folds. *Tectonophysics*, 346, 247-275.

Fossen, H. & Rykkelid, E., 1990. Shear zone structures in the Oygarden area, West Norway. *Tectonophysics*, 174, 385-397.

Fransson, M., 2008. U–Pb zircon dating of metasedimentary rocks in the Areachap, Kakamas and Bushmanland Terranes in Namaqua Province, South Africa, University of Gothenburg: BSc thesis B54, 44 pp.

Geringer, G., 1973. Die geologie van die Argiese gesteentes en jongere formasies in die gebied wes van Upington met spesiale verwysing na die verskillende granietvoorkomste, Bloemfontein: University of the Free State, 203pp.

Geringer, G., Praekelt, H., Schoch, A. & Botha, B., 1990. The Oranjekom Complex, a layered metamorphosed anorthosite-gabbro suite along the eastern margin of the Namaqua Mobile Belt, South Africa. *South Africa Journal of Geology*, 93(2), 400-411.

Haker, A., 1909. The natural history of igneous rocks. London: Methuen & Co, 348pp

Harris, N., 2007. Channel flow and the Himalayan–Tibetan origin: a critical review. *Journal of the Geological Society*, 164, 511-523.

Hartandy, C., Joubert, P. & Stowe, C., 1985. Proterozoic crustal evolution in South-western Africa. *Episodes*, 8(4), 236-244.

Havenga, A., 1992. Petrologiese en geochemiese aspekte van die Oranjekom Kompleks langs die oostelike rand van die Namakwalandse Moebiele Gordel, Bloemfontein, University of the Free State, 146pp.

Hossack, J., 1968. Pebble deformation and thrusting in the Bygdin Area (southern Norway). *Tectonophysics*, 5, 315-339.

Hsu, T., 1966. The characteristics of coaxial and non-coaxial strain paths. *Journal of Strain Analysis*, 1(3), 216-222.

Jackson, M., 1976. High-grade metamorphism and migmatization of the Namaqua metamorphic complex around Aus in the southern Namib Desert, South West Africa. *Bulletin of the Precambrian Research Unit 18*, University of Cape Town, 299pp.

Jacobs, J., Pisarevsky, S., Thomas, R. & T., B., 2008. The Kalahari Craton during the assembly and dispersal of Rodinia. *Precambrian Research*, 160, 142-158.

Jankowitz, J., 1986. 'n Petrochemiese ondersoek van die Cnydasbatoliet, Wes van Upington, Bloemfontein: University of the Free State, 205pp.

Joubert, P., 1971. The regional tectonism of the gneisses of part of Namaqualand, Precambrian research unit, Bulletin 10, Department of Geology, University of Cape Town, 220pp.

Joubert, P., 1986. The Namaqualand Complex - a model of Proterozoic accretion?. Transactions of the Geological Society of South Africa, 89, 79-96.

Kalpakiotis, P., 2016. The Mapping and Structural Analysis of the Putsies Migmatite (honours dissertation), Bloemfontein: University of the Free State 59pp.

Kruger, F., Geringer, G. & Havenga, A., 2000. The geology, petrology, geochronology and source region character of the layered gabbro-noritic Oranjekom Complex in the Kibaran Namaqua Mobile Belt, South Africa. Journal of African Earth Sciences, 30(3), 675-687.

Lisle, R., 1979. Strain analysis using deformed pebbles: The influence of initial pebble shape. Tectonophysics, 60, 263-277.

Lister, G. & Williams, P., 1983. The partitioning of deformation in flowing rock masses. Tectonophysics, 92, 1-33.

Mathee, H., Colliston, W. & Schoch, A., 2016. Structural analysis of the Riemvasmaak Kenhardt Mega Sheath Fold situated in the Grünau Terrane of the Namaqua Mobile Belt. 4104. Abstract 35th International Geological Congress, Cape Town, South Africa. (<http://www.americangeosciences.org/information/igc>).

McClay, K., 1991a. Glossary of thrust tectonics terms. In: McClay, K.R. (Ed.), Thrust tectonics. London: Chapman & Hall, 419-433.

McClay, K., 1991b. The Mapping of Geological Structures. Chichester, United Kingdom: Geological Society of London Handbook, John Wiley and Sons Ltd, 161pp.

Miller, R., 2012. Review of Mesoproterozoic magmatism, sedimentation and terrane amalgamation in South-western Africa. South African Journal of Geology, 115(4), 417-448.

Moen, H., 2007. The Geology of the Upington area (Explanation: sheet 2820, Scale: 1:250 000). Pretoria: Council of Geoscience, 160pp.

Moen, H. & Armstrong, R., 2008. New age constraints on the tectogenesis of the Kheis Subprovince and the evolution of the eastern Namaqua Province. *South African Journal of Geology*, 111, 79-88.

Moen, H. & Toogood, D.J., 2007. The geology of the Onseepkans area: explanation: sheet 2818, scale: 1: 250 000. Pretoria: Council for Geoscience.

Mookerjee, M. & Peek, S., 2014. Evaluating the effectiveness of Flinn's k-value versus Lode's ratio. *Journal of Structural Geology*, 68, pp. 33-43.

Nordin, F., 2009. U Pb dating, Lu Hf isotopic analysis and geothermobarometry of rocks in the Grünau Terrane and Richtersveld Subprovince, Namaqua Sector, Southern Africa, Göteborg University: Department of Earth Sciences; *Geology*, 52pp.

Passchier, C., Trouw, R., Coelho, S., de Kemp, E., & Schmitt, R., 2011. Key-ring structure gradients and sheath folds in the Goantagab Domain of NW Namibia. *Journal of Structural Geology*, 33, 280-291.

Pettersson, A., 2008. Mesoproterozoic crustal evolution in southern Africa., Sweden: Gothenburg University, (Includes 7 publications).

Praekelt, H., 1984. Die geologie van die gebied rondom Augrabies (2820 C), Bloemfontein, 80pp.

Praekelt, H., Botha, B. & Malherbe, S., 1986. Diskrete korsfragmente in die sentrale gedeelte van die Namakwagordel in die omgewing van Augrabies. *Annals Geological Survey South Africa*, 20, 25-40.

Price, R., 1986. The southern Canadian Cordillera: thrust faulting, tectonic wedging, and delamination of the lithosphere. *Journal of Structural Geology*, 8(3/4), 239-254.

Ramsay, J., 1967. *Folding and fracturing of rocks*. New York: McGraw-Hill. 568pp.

Ramsay, J. & Huber, M., 1987. *The Techniques of Modern Structural Geology. Volume 2: Folds and Fractures*. London: Academic Press, 392pp.

Reineck, H.E. & Singh, I., 1980. *Depositional Sedimentary Environments; with reference to terrigenous clastics*. 2nd. ed. Berlin Heidelberg New York: Springer-Verlag, 549pp.

Robinson, S. & Fyson, W., 1976. Fold structures, southern Stoke Mountain area, Eastern Townships, Québec: Taconic or Acadian?. *Canadian Journal of Earth Science*, 13, 66-74.

Saad, A., 1987. A petrological study of the Tin- Tungsten deposit at Renosterkop, Augrabies, Northern Cape Province, Potchefstroom: North-West University, 165pp.

Samskog, P., 2009. U-Pb, Lu-Hf zircon dating and source magma determination of magmatic rocks in the Richtersveld and Kakamas terrane, Namaqua Province, southern Africa, Gothenburg University: Department of Earth Sciences, 47pp.

Schmid, R., Fettes, D., Harte, B., Davis, E. Desmons, J., 2007. How to name metamorphic rocks. [Online] Available at: www.bgs.ac.uk/scmr/home.html [Accessed 16-03-2017].

Searle, M. & Alsop, G., 2007. Eye-to-eye with a mega–sheath fold: A case study from Wadi Mayh, northern Oman Mountains. *Geology*, 35(11), 1043-1046.

Shackleton, R. M., 1958. Downward Facing Structures of the Highland Border. *Journal of the Geological Society of London*, 113, 361-392.

Steyn, J., 1988. 2820 Upington; 1:250 000 Geological Series. Pretoria: Geological Survey.

Stowe, C., 1983. The Upington geotraverse and its implications for craton margin tectonics. In: B. Botha (Ed.). *Namaqualand Metamorphic Complex*, Special Publication 10, Geological Society of South Africa, 147-171.

Stowe, C., Hartnady, C. & Joubert, P., 1984. Proterozoic Tectonic Provinces of Southern Africa. *Precambrian Research*, 25, 119-123.

Stowe, C.W., 1986. Synthesis and interpretation of structures along the north-eastern boundary of the Namaqua Tectonic Province, South Africa. *Transactions of the Geological Society of South Africa*. 89, 185–198.

Strydom, D. & Visser, J., 1986. Nappe Structures in the highly deformed Proterozoic metasedimentary, Aggeneys-type sequence of Western Bushmanland, South Africa. *Precambrian Research*, 33, 171-187.

Tankard, A., Jackson, M., Eriksson, K., Hobday, P., Hunter, D., Minter, W., 1982. Crustal evolution of Southern Africa, 3.8 Billion years of Earth history. Berlin: Springer Verlag. 423pp.

Thomas, R., Cornell, D., Moore, J. & Jacobs, J., 1994. Crustal evolution of the Namaqua-Natal metamorphic province, Southern Africa. *South African Journal of Geology*, 97, 8-14.

Van Bever Donker, J., 1980. Structural and metamorphic evolution of an area around Kakamas and Keimoes, Cape Province, South Africa. Bulletin 28, Cape Town: Precambrian Research Unit, 165pp.

Vernon, R., 1986. K-feldspar Megacrysts in Granites Phenocrysts, not Porphyroblasts. Earth Science Reviews, 23, 1-63.

Vollmer, F., 2015. Orient 3: a new integrated software program for orientation data analysis, kinematic analysis, spherical projections, and Schmidt plots. Geological Society of America Abstracts with Programs, 47(7), 49pp.

Von Backström, J., 1964. The geology of an area around Keimoes, Cape Province, with special reference to phacoliths of charnokitic adamellite-porphyry. Pretoria: Memoir Geological Survey, 53, 218pp.

Von Backström, J., 1967. The geology and mineral deposits of the Riemvasmaak Area, Northwest Cape Province. Annals of the Geological Survey, 6, 43-54.

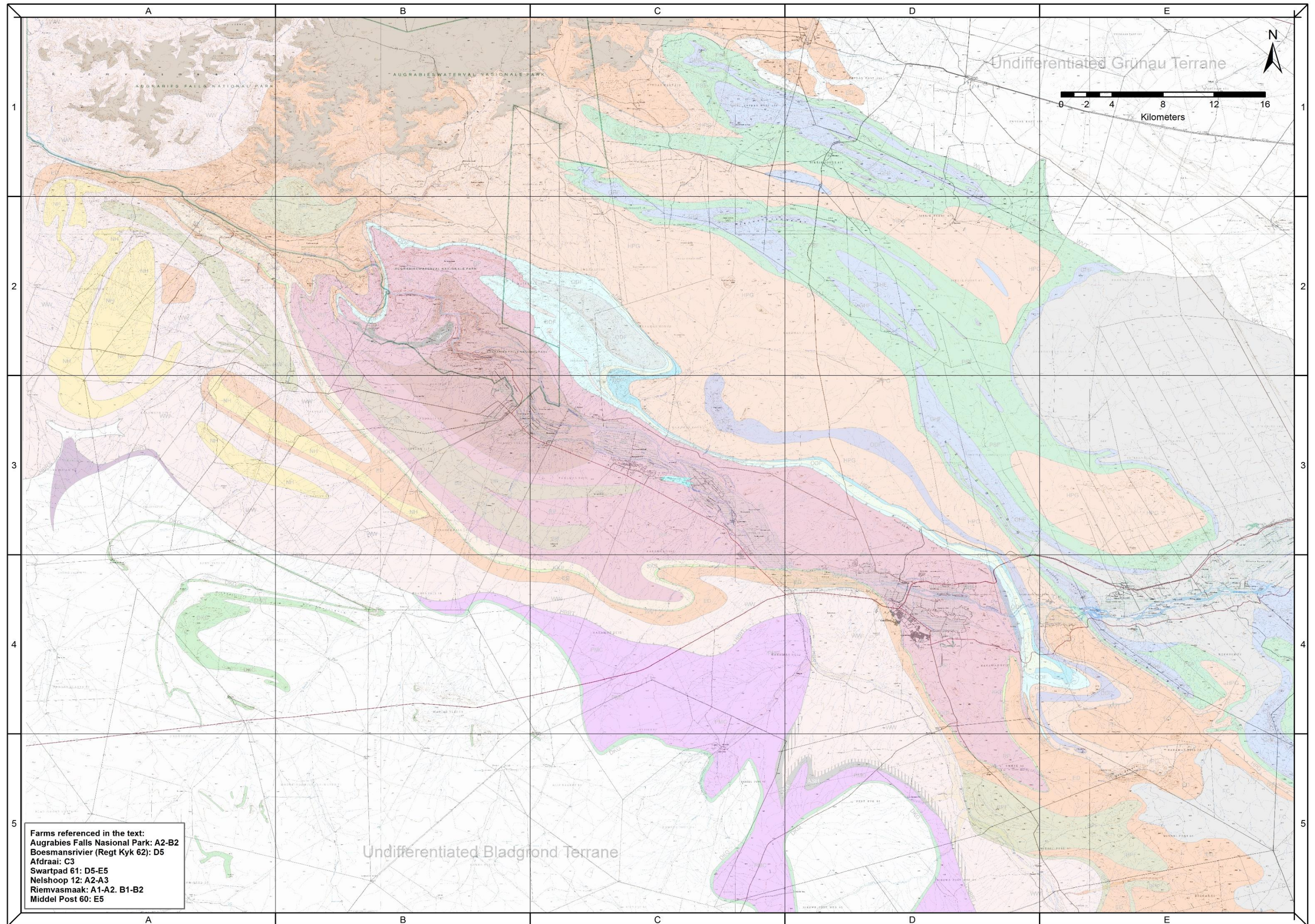
Waters, D., 1986. Metamorphic zonation and thermal history of pelitic gneisses from western Namaqualand, South Africa. Transactions of the Geological Society of South Africa, 89, 97102.

8 Appendices

Appendix A: Geographic coordinates of relative figures.

Figures	Geographic coordinates	
Figure 2-4	28°44'35.39"S	20°32'54.75"E
Figure 3-7A	28°33'41.94"S	20°13'8.48"E
Figure 3-7B	28°52'31.32"S	20°37'22.93"E
Figure 3-7C	28°53'36.18"S	20°37'7.09"E
Figure 3-13	28°33'41.94"S	20°13'8.48"E
Figure 3-14	28°34'45.89"S	20°17'1.03"E
Figure 3-20A	28°44'35.39"S	20°32'54.75"E
Figure 3-20B	28°53'13.03"S	20°41'19.19"E
Figure 3-20C	28°31'5.72"S	20°17'27.74"E
Figure 3-20D	28°44'35.39"S	20°32'54.75"E
Figure 3-21	28°36'5.26"S	20°18'51.43"E
Figure 3-22A	28°36'5.26"S	20°18'51.43"E
Figure 3-22B	28°49'31.76"S	20°37'59.23"E
Figure 3-22C	28°49'31.76"S	20°37'59.23"E
Figure 3-22D	28°44'35.39"S	20°32'54.75"E
Figure 3-27A	28°36'13.26"S	20°27'4.40"E
Figure 3-27B	28°36'16.92"S	20°24'30.58"E
Figure 3-27C	28°47'10.74"S	20°42'42.28"E
Figure 3-27D	28°35'7.60"S	20°24'0.74"E
Figure 3-63A	28°44'32.92"S	20°42'33.92"E
Figure 3-63B	28°44'45.05"S	20°43'7.61"E
Figure 3-63C	28°39'20.41"S	20°39'46.77"E
Figure 3-63D	28°43'52.95"S	20°42'23.34"E
Figure 3-63E	28°43'52.95"S	20°42'23.34"E
Figure 3-37A	28°34'53.84"S	20°37'32.06"E
Figure 3-37B	28°34'53.84"S	20°37'32.06"E
Figure 3-37C	28°34'51.18"S	20°37'27.58"E
Figure 3-37D	28°32'58.66"S	20°34'44.99"E

Appendix B: Topographic map of the study area superimposed on the geological map. Refer to text box (lower left corner) for place names used in the text.



Appendix C: Stratigraphic nomenclature of previous research conducted in the study area

Current Study	Von Backström ('64)	Geringer ('73)	Van Bever Donker ('80)	Stowe ('83; 86)	Praekelt ('84)	Jankowitz ('86)	Moen ('07)
Supracrustals							
Koekoepkop Formation	Dark-weathering quartz-rich granulite	-	Marais River Amphibolite	Marais River Formation	Marais River Formation	-	Koekoepkop Formation
Omdraai Formation	Quartz-plagioclase schist and quartz-tourmaline schist's of the Kaaien Series	Riemvasmaak Formation	Marais River Amphibolite and Micaceous quartz-feldspar schist	Wolfskop Formation	Omdraai Formation	-	Omdraai Formation
Renosterkop Rocks	-	-	-	-	Topaz-bearing rocks	-	Renosterkop gneiss
Goede Hoop Formation	Quartzite and quartz-sericite schist	Goede Hoop Formation	Neuspoort Member and Zwart Boois Berg Member	Neusberg Quartzite	Goede Hoop Formation	Goede Hoop Formation	Goede Hoop Formation
Puntsit Formation	Granulite containing lenses of calcsilicate rocks	Biesje Poort Formation	Baviaanskrantz Calcsilicate rich quartzite	Baviaanskrantz Calcsilicate	-	Biesje Poort Formation	Puntsit Formation
Blouputs Formation	Gabbro, norite, ortho-amphibolite, picrite, peridotite	Toeslaan Formation	Middlepost Mafic Rocks	Amphibolite, Meta-pyroxenite, Serpentinite	Blouputs Formation	Toeslaan Formation	Vyfbeker Metamorphic Suite and Kourop Migmatites
Driekop Group	Pink gneiss	-	Marais River Amphibolite	Wolfskop Formation	Driekop Group	-	Droëboom Group and Arribees Group
Plutonic Rocks							
Augrabies gneiss	Pink gneiss	-	-	-	Augrabies granite	-	Augrabies gneiss
Rooipad gneiss	Pink gneiss	Riemvasmaak Formation	Wolfskop gneiss	Grey gneissic granite	Rooipad granite	-	Riemvasmaak gneiss
Harpersputs gneiss	Pink gneiss	Riemvasmaak Formation	Wolfskop gneiss	Wolfskop Formation	Rooipad granite	Cnydas East Granodiorite	Riemvasmaak gneiss
Brabees gneiss	Pink gneiss	Riemvasmaak Formation	-	-	Brabees granite	-	Riemvasmaak gneiss
Seekoeisteek gneiss	Pink gneiss	Riemvasmaak Formation	-	-	Seekoeisteek granite	-	Riemvasmaak gneiss
Oranjekom Complex	-	-	-	-	Metagabbro and anorthosite	-	Basic intrusive
Friersdale Charnockite	Charnockitic Adamelite-Porphry	-	Warm Zand Charnockitic Adamelite	Charnockitic Adamelite	-	-	Friersdale Charnockite
Eendoorn gneiss	Porphyroblastic grey gneiss	Bakrivier and Kouroprivier granite	Wolfskop biotite gneiss	Grey gneissic granite	Eendoorn granite	Cnydas East Granodiorite	Eendoorn Suite
Witwater gneiss	Grey gneiss	Mixed with Blouputs Fm.	Wolfskop biotite gneiss	Grey gneissic granite	Witwater granite	Cnydas East Granodiorite	Witwater gneiss and Kenhardt Migmatite
Nelshoop gneiss	-	Riemvasmaak Formation	-	-	Seekoeisteek granite	-	Riemvasmaak gneiss
Putsies Migmatite complex	Porphyroblastic grey gneiss	-	Wolfskop gneiss	Hartbees Formation	Putsies granitoid	-	Putsies gneiss
Karama'am Augen gneiss	-	-	-	-	Droëboom granitoid	-	Banksvlei gneiss

Appendix D: Regional study of the Blouputs Formation (BPF).

Author	Mapped as	Types	Field Characteristics	Petrography			Chemistry	Relationship to ED/WW	Metamorphic Conditions
				Main minerals	Accessory minerals	Mineralogical remarks			
Du Plessis (1980)	Narries Formation	1. Garnet-biotite-gneiss, garnet-sillimanite-cordierite-biotite-gneiss and garnet-quartz-feldspar-gneiss. 2. Calc-silicates and marble		> Garnet, > Sillimanite, > Cordierite (>50%), > Biotite, > Plagioclase, > K-feldspar	> Hypersthene > Zircon, > Apatite	> Garnet = almandine (sillimanite inclusion, cordierite rim) > alternating migmatitic banding > Sillimanite = stretching lineations in the regional fabric	ACF/AFK diagrams (p. 2126)		FeO + MgO relationship indicates at partial melting = migmatization: P: 5,5-7Kbar (8Kbar), T: 620-650°C (800°C)
Prækelt (1984)	Blouputs Formation	1. Biotite Gneiss (60%) 2. Amphibolite 3. Hornblende-gneiss (25%) 4. Biotite-cordierite-sillimanite-garnet-gneiss (15%)	> Intruded by Witwater > Xenoliths of BPF in Witwater > Migmatitic: neosomes can't be distinguished from WW	1. Quartz, plagioclase, biotite 2. Hornblende, plagioclase 3. Garnet (50%), quartz, plagioclase, hornblende, biotite. 4. Biotite, quartz, K-feldspar, plagioclase	1. K-feldspar, sillimanite, cordierite, garnet 2. Quartz, biotite 3. Cordierite, sillimanite, garnet	> Vein Migmatization > garnets are situated in the paleosomes and neosomes		Witwater interpreted as the anatectic product of Blouputs Formation	
Geringer (1973)	Toeslaan Formation	1. Garnet-quartz-feldspar gneiss, garnet-sillimanite-cordierite-biotite gneiss 2. Amphibolites 3. Garnet-hornblende gneiss	> para-amphibolites with graded contacts between it and the metasediments	1. Quartz (17%), microcline (3%), garnet (15%), sillimanite (23%), cordierite (6%), biotite (27%), plagioclase 2. Plagioclase, hornblende	1. Cordierite, sillimanite, biotite, plagioclase 2. Quartz, biotite, garnets, +/- diopside	> Migmatites: banding defined by quartz-feldspar and biotite-sillimanite > Garnets + feldspar gives a porphyroblastic texture > Biotite fabric wraps around porphyroblasts.	ACF/AFK diagrams (p. 47)		
Nordin (2009)	Aluminous Gneiss	Aluminous Gneiss	K-feldspar forms a banding most probably related to migmatization	> Sillimanite, > K-feldspar, > Plagioclase > Garnets > Cordierite		> Garnets are zoned: Mg > cores, Fe > rims, grow as T decrease; Ca (P-dependent) are the same for cores and rims. > Cordierite (inclusions of sillimanite), > Plagioclase forms around the garnets during metamorphism > Garnets have biotite, ilmenite, rutile inclusions			> T: 620-645°C for the rims and 720-760°C for cores > P: 5,3±1Kbar for the rims and 7-8Kbar for the garnet cores > Prograde regional metamorphism peak with 650°C at 5-6Kbar > Granite ages correspond with metamorphic rim ages of the aluminous gneiss (1204±13 and 1197±12Ma)
Beukes (1973)	Arus Formation/ Umeis Formation	<u>Arus Formation:</u> > garnet-sillimanite-cordierite-biotite-gneiss > garnet-granulite > garnet bearing quartz-feldspar-gneiss <u>Umeis Formation:</u> > biotite schist and amphibole gneiss > para-amphibolite > sillimanite- cordierite gneiss/schist > granulite with bands and lenses of calc-silicates and marble > meta-conglomerate	> Arus younger stratigraphic unit overlies the Umeis	> Garnet (0-15%) > Sillimanite > Cordierite (50%) > Biotite > Quartz > Plagioclase > K-feldspar (microcline, 23%)	> Magnetite, > Spinel, > Zircon, > Apatite, > Sphene > Hornblende > Hypersthene, > Diopside	> With increase in garnet there is a decrease in sillimanite and cordierite > Garnet (almandine) contains inclusions of quartz, sillimanite, biotite, spinel > Migmatitic textures (migmatite bands are folded by isoclinal folds) > Garnets porphyroblasts (5cm)	ACF/AFK Diagrams (p. 169)		
Diener (2013)	Garub Sequence	1. Aluminous metapelitic gneiss 2. Aluminous metapsammitic gneiss 3. Mafic granulites (10-200m)	> All 3 have experienced anatexis > All 3 have well developed fabric (biotite) > Leucosomes are commonly present and aligned with the tectonic fabric	1. Garnet-cordierite-biotite-sillimanite-quartz-K-feldspar 2. Quartz-plagioclase-biotite-K-feldspar and garnet 3. Hornblende-plagioclase, orthopyroxene and quartz	>Plagioclase >Ilmenite >Cordierite	>Metapilitic: Well developed fabric (defined by biotite), porphyroblasts of K-feldspar. >Garnet, Cordierite, sillimanite flattened and elongated in the fabric: • Gneissosity: defined by alternating cordierite-sillimanite-garnet-biotite layers with garnet-K-feldspar-quartz-rich layers. • Metapsammitic: medium grained, quartz rich, 10mm porphyroblasts and low proportions of biotite, weak developed fabric. • Gneissosity defined by preferred orientations of isolated biotite grains and in some places 3-55mm wide leucosomes.		> Metapsammitic gneisses are intruded by metre scale leucogranite sheets and dykes	> metamorphosed to amphibolite and granulite facies conditions > Peak metamorphic conditions are estimated at 825 °C and 5.5 kbar, with prograde metamorphism characterised by a clockwise burial-heating path and retrograde metamorphism dominated by isobaric cooling
Blignault (1977)	Aluminous Gneisses	1. Garnet-sillimanite-cordierite gneisses 2. Biotite gneiss 3. Thin (centimetres) metaquartzite and calc-silicate bands	> Intimately associated with large massifs of syn-tectonic granitoid. > Leucosomes are present > Rhythmic banding interpreted as sedimentary layering			Coarse blastic growth of garnet and sillimanite		Intimately associated with large massifs of syntectonic granitoid	

Appendix E: Regional study of the Eendoorn gneiss (ED).

Author	Mapped as	Field Characteristics	Xenoliths	Petrography			Chemistry	ED/WW/BPF relationship	Metamorphism	Age	General Comments
				Main minerals	Accessory minerals	Mineralogical remarks					
Du Plessis (1980)	Eendoorn Granite	> Aplitic veins: leucocratic banding consisting of quartz-microcline-plagioclase-garnet formed parallel to regional S (WW) > Sheared ED have smaller megacrysts > Anastomosing fabric is defined by megacrysts and biotite,	> Garnet bearing biotite gneiss (Narries), enderbite, garnet gneiss > shape: rounded, fabric wraps around xenoliths	> K-feldspar (32%) > Quartz (31%) > Biotite (2-34%) > Plagioclase (18%).	> Zircon, > Sphene, > Apatite, > Almandine > Sillimanite, > Cordierite, > Hornblende	> Garnets have inclusions of quartz > Microcline megacrysts are tabular to elliptical (up to 8cm)	> QAP diagrams classify as a monzo-syeno granite	> Strong association with Witwater, Witwater occurs always with Eendoorn		> Early syn-tectonic (F1 folding phase)	> Tectonic control on the fabric and the banding. > Genesis: no large scale mobilization but rather anatexis of pre-existing rock
Praekelt (1984)	Eendoorn Granite	> Duplication (thickening) towards the north due to folding and thrusting. > Migmatization seen near contacts (leucosomes same as Witwater) > Fabric defined by biotite and wraps around megacrysts	> Quartzites > Amphibolites > Garnet bearing amphibolites > Biotite gneiss	> Quartz >Microcline >Biotite	> Plagioclase > Garnet > Sillimanite > Zircon > Apatite	> Megacrysts (microcline) up to 10cm					>Intrusive Origin
Geringer (1973)	Bakrivier Granite and Kouroprivier Granites	> sharp contacts with garnet gneiss and quartz-feldspar gneiss (Toeslaan Formation) > lit-par-lit intrusive relationship	> Toeslaan Formation (BPF) > Mafic lenses (lenses are orientated parallel to the regional S): finer grained, same composition as granite and graded contacts	> Quartz > Plagioclase > Microcline > Biotite	> Hornblende > Zircon > Apatite	> Kouroprivier contains pyroxene (only difference between Bakrivier and Kourop)				Katazone; syn-tectonic granite	> "Illusive contacts" indicates metasediments was at a high temperature when granite was emplaced > Little in situ granitization have taken place, granite body is product of magmatic intrusion > 600°C/3.5Kbar = right temperature for metasediments to melt (these melts mobilized and intruded the metasediments)
Nordin (2009)	Megacrystic Granite	> Intruded into the aluminous gneiss	> aluminous gneiss xenoliths	> K-feldspar > Biotite > Plagioclase > Quartz	> Sillimanite				P/T: 422-470, 343-397 °C	> Zircon xenocrysts core: 1827 ±39 Ma (reflects crustal material older/underlying the ED) > 1205-1192Ma formation age (emplacement age coincides with metamorphic age (1204-1197Ma) of the Aluminous gneiss > 1376-1344 Ma zircon cores: first magmatic augmentation of the Grünau Terrane	

Beukes (1973)	Eendoorn Granite	<ul style="list-style-type: none"> > Concordant contacts with the Arus Formation > migmatitic contacts > Bands of leucocratic leptite near the contact with the country rocks, parallel to the region fabric; coarse migmatites (Witwater "dykes" also seen by other authors) > lit-par-lit contact with Umeis Formation > Where ED is homogenous: total anatexis melt. > Where ED is heterogeneous: partial anatexis and granitization > fabric defined by biotite and megacrysts 	<ul style="list-style-type: none"> > Mafic xenoliths > Banded gneiss and migmatites > Garnet gneiss > Xenoliths are remnants of the migmatitic rocks (metasediments) ED intruded into. 	<ul style="list-style-type: none"> > Quartz (31%), > K-feldspar (Microcline, 33%), > Biotite (18%), > Plagioclase (18%) 	<ul style="list-style-type: none"> > Zircon, > Sphene, > Apatite, > Magnetite, > Ilmenite, > Almandine, > Sillimanite, > Cordierite, > Hornblende 	<ul style="list-style-type: none"> > K-feldspar megacrysts are not a primary feature but developed during metamorphism > Megacrysts are up to 8cm 	<ul style="list-style-type: none"> > ED is classified as an alkali granite > Groundmass of the ED indicates characteristics of a granodiorite and resemble the composition of the protolith. 			<p>Syn-tectonic granite based on:</p> <ol style="list-style-type: none"> 1. Concordant and graded contacts 2. ED is deformed with the metasediments (same fabric in both) 3. Migmatites are found in the ED 4. ED is a gneiss (orthogneiss) 5. ED is intrusive into rocks of amphibolite facie metamorphism 6. Coarse grained granite and porphyroblastic 7. Mafic inclusions parallel to the fabric 	<ul style="list-style-type: none"> > The plagioclase/K-feldspar relationship in the matrix of ED indicates that the syn-tectonic granite developed from a pre-occurring granodiorite because of the potassium-metasomatism (p.220).
Diener (2013)	Tsirub Gneiss	<ul style="list-style-type: none"> > Migmatized, garnet-bearing tonalitic to granodioritic augen gneiss. > Intruded into the Garub sequence. > Sharp contact with the Garub sequence, parallel to the regional fabric > Well-developed gneissic fabric defined by aligned hornblende and biotite and fine-scale leucosomes. 	<ul style="list-style-type: none"> > Metasedimentary xenoliths 	<ul style="list-style-type: none"> > Garnets (5-10mm) situated in a medium to coarse grained matrix of: > Hornblende, > Biotite, > Plagioclase > Quartz > K-feldspar 					<ul style="list-style-type: none"> > Granulite metamorphism and anatexis. > Peak metamorphic conditions are estimated at 825 °C and 5.5 kbar, with prograde metamorphism characterised by a clockwise burial-heating path and retrograde metamorphism dominated by isobaric cooling 	<ul style="list-style-type: none"> > Tsirub Gneiss being emplaced at 1085± 4 Ma > Oldest igneous suite, pre-tectonic origin, never truncates a fabric of the Garub Sequence 	
Blignault (1977)	Megacrystic Granite	<ul style="list-style-type: none"> > The intrusive nature of the megacrystic granite is evident from the many inclusions and contact relationships. > Lit-par-lit nature of the contact zone. > Foliation defined by quartz, feldspar and biotite, this is a primary flow fabric along which a tectonic foliation developed (alignment of the K-feldspar megacrysts after the crystallization of the magma) 	<ul style="list-style-type: none"> > Xenoliths of paragneiss, aluminous and biotite-rich enclaves > granulite inclusions 	<ul style="list-style-type: none"> > Orthoclase, microcline (An27-33) > Biotite > Quartz Table 2.9, p. 58 	<ul style="list-style-type: none"> > Garnets > Cordierite > Sillimanite 	<ul style="list-style-type: none"> > Contaminated by alumina and contains appreciable amounts of biotite, cordierite, garnet and sillimanite. > K-feldspar phenocrysts laths shorter than 5cm 	QAP diagrams (p. 55)	<ul style="list-style-type: none"> > Pegmatitic pockets and concordant leucocratic veins, without mafic rims, and up to 1 m in width, were observed locally. > The formation of the concordant leucosomes is thought to be contemporaneous with that of the granite 		>Syn-tectonic	

Appendix F: Regional study of the Witwater gneiss (WW).

Author	Mapped as	Field Characteristics	Xenoliths	Petrography			Chemistry	ED/WW/BPF relationship	Metamorphism	Age	General Comments
				Main minerals	Accessory minerals	Mineralogical remarks					
Du Plessis (1979)	Witwater granite	> Medium to coarse grained leucocratic pegmatitic granite >Leucocratic bands (1cm - >10m) found in the Narries Formation > Fabric defined by alignment of Kfeldspar and quartz	Eendoorn granite	> Microcline (45%) > Quartz (43%) > Plagioclase (12%)	> Garnet > Biotite > Sillimanite > Apatite > Zircon > Cordierite > Muscovite	> Garnet (almandine) contains inclusion of quartz and feldspar	QAP-diagram classified it as a syeno-granite and a alkali granite	Formed from melting of the Eendoorn gneiss and Narries			> The presence of garnet and the absence of biotite indicates a melt with a high viscosity (a dry magma)
Praekelt (1984)	Witwater Granite		Eendoorn granite	> Microcline > Quartz	> Plagioclase > Biotite >Sillimanite >Apatite >Zircon >Garnet			Anatectic product of Blouputs Formation			> Migmatic character defined by "pinch and swell structures "
Beukes (1973)	Warmbad Granite	> Weak foliation > Intrusive into the Umeis Formation > Cross cutting veins runs that out of the main WB granite body are post-tectonic: no deformation > Warmbad granite occurs as cross cutting dikes and sills and never as massive bodies	Xenoliths of the Umeis Formation	> Quartz (34%), > K-feldspar (microcline) (40%) > plagioclase (19%)	> Muscovite (4%) > Biotite (4%), > Zircon, > Apatite, > Sphene	> Biotite is the only dark mineral > Foliation can only be seen near the contacts	QAP-diagram (Fig. 50, 51, p. 194) classifies the granite as a alkali granite	Warmbad granite is the product of selective melting of sedimentary (Umeis Fm) rocks	Mesozone granite: 7-17km depth of formation at 350-500°C	Late tectonic granite due to: 1. Massive and unfoliated 2. Discordant contacts: intruded after folding 3. Contacts are sharp and migmatization is seen in the country rocks 4. Fine to medium grained: aplitic character 5. Leucocratic alkali granite, low dark mineral content, muscovite indicates a young granite, Kfeldspar = microcline 6. Xenoliths of the country rocks	
Diener (2013)	Kubub Gneiss/ Aus Gneiss	> Aus Gneiss: coarse grained K-feldspar megacrystic leucogranites > Kubub Gneiss: leucocratic, medium-grained granite that occurs as isolated bodies surrounded by leucosome-rich migmatite > Fabric defined by alignment of Kfeldspar		Kubub: > Garnet > K-feldspar, > Quartz	Kubub: > Plagioclase > Biotite			Contact with Garub is abrupt and parallel to S1		> Kubub Gneiss having an emplacement age of 1123±6Ma	